Harper Adams University

A Thesis Submitted for the Degree of Doctor of Philosophy at

Harper Adams University

Copyright and moral rights for this thesis and, where applicable, any accompanying data are retained by the author and/or other copyright owners. A copy can be downloaded for personal non-commercial research or study, without prior permission or charge.

This thesis and the accompanying data cannot be reproduced or quoted extensively from without first obtaining permission in writing from the copyright holder/s. The content of the thesis and accompanying research data (where applicable) must not be changed in any way or sold commercially in any format or medium without the formal permission of the copyright holder/s.

When referring to this thesis and any accompanying data, full bibliographic details including the author, title, awarding institution and date of the thesis must be given.

The control of agricultural tractors carrying out draught cultivations

JAMES LINDSEY WARD

BEng (Hons) Agricultural Engineering

Thesis submitted in partial fulfilment of the requirements of Harper Adams University for the award of the degree of Doctor of Philosophy

19th October 2016

Harper Adams University, Edgmond, Newport, Shropshire, TF10 8NB.

United Kingdom

DECLARATION

I declare that the content of this thesis is composed entirely by myself and has not been submitted or accepted for any previous application for a degree. The research of which this thesis is a record has been conducted entirely by myself. Any material used as a source of reference material is clearly acknowledged within this thesis.

The entire subject matter created by this study is subject to discussions regarding intellectual property protection and therefore must not be distributed or reproduced in any way.

James Lindsey Ward

ABSTRACT

The subject area of tractor automation, tractive efficiency and traction is well researched with numerous papers and concept vehicles developed worldwide. Current in-tractor systems display performance attributes such as work rate and pass-to-pass accuracy but not factors such as cultivation quality, consistency of operation and utilisation of power. The significant research in this area relies on quasi-static systems using field calibrations or static mathematical models. Dynamically, tillage causes variation in implement depth and wheel power. Little research exists in this area and forms the basis of the study here within.

In this study, three point linkage force resolution and tractor dynamic kinematic models were developed and integrated with an instrumentation system to measure the force and positional parameters required. This allowed the resolution of draught and vertical forces acting on the tractor, prediction of implement tillage depth and tractor pitching and field energy performance calculations. Initial field and laboratory experiments concluded that existing linkage control systems are too complex to achieve a consistently energy efficient field operation. The models developed were integrated into a three point linkage position controlling algorithm based on three selectable work modes: field work rate; tractor and fuel efficiency; consistent cultivation depth and quality; whilst displaying real-time field performance to the tractor operator. The study demonstrates an improvement in energy usage of 3.5 % is achievable through accurately controlled tillage depth in real-time.

The study contributes significantly to knowledge through the novel integration of the developed models and instrumentation system into a control algorithm which has significant future potential. A commercialised version of the system can be retrofitted to tractors as an add-on or through manufacturer integration. Recommendations are made for further work and how the system could be utilised for field mapping and spraying and fertiliser application consistency and rate monitoring in real-time.

ACKNOWLEDGEMENTS

I would like to thank the following:

The Douglas Bomford Trust, Harper Adams University Development Trust and AGCO Corporation for funding this research work and AGCO for the loan of the Massey Ferguson 8480 research tractor.

My supervisory team past and present; Professor Dick Godwin, David White, David Clare, Dr. Alex Keen and the late Professor David Crolla and Eur Ing Geoffrey Wakeham for all of their support, advice, encouragement, ideas and help over the last 7 years.

Harper Adams University Engineering Department particularly Tim Dicker, Tom Lucas, Maurice Smith and David Vickers for their help, support, skill, advice and encouragement.

Finally my family, my wife Vicki, daughters Daisy, Alice and Emily and Mum and Ray for supporting me over the last 7 years in the quest to complete this work and supporting me through the tougher times.

TABLE OF CONTENTS

LIST OF FIGURES

LIST OF TABLES

LIST OFABBREVIATIONS

δAID	Change in implement tillage depth (mm)
EORT	Extended Octagonal Ring Transducer
δFAH	Nominal change in height of the front axle centreline above the undisturbed ground (mm)
δFx	Additional front tyre deflection due to δZR (mm)
δRAH	Nominal change in height of the rear axle centreline above the undisturbed ground (mm)
δRPH	Nominal change in height differential between front and rear axles above the undisturbed ground (mm)
δRPS	Nominal change in height of the tractor horizontal reference plane, at the centre point between front and rear axles, above the undisturbed ground (mm)
δRx	Additional rear tyre deflection due to δZR (mm)
δZF	Change in front axle ground reaction force (kN)
δZR	Change in rear axle ground reaction force (kN)
Cos	Trigonometric mathematical function
CI	Soil Cone Index (N mm^{-2} or Pa)
DBP	Drawbar Power (kW)
DLRF	Dynamic loaded radius of the tractor front wheels (m)
DLRR	Dynamic loaded radius of the tractor rear wheels (m)
ELP	Linkage positional measurement (V)
FAH	Front axle height from the undisturbed ground surface (mm)
FC	Fuel consumption (l h^{-1})
FLR	Summed measured axial force component of LLR and RLR (kN)

FTL	Measured axial force in the top link (kN)
Frk	Front tyre stiffness constant, (N mm^{-1});
Fx	Summed horizontal three point linkage forces acting on the tractor (kN)
Fx1	Resolved horizontal force component of FTL (kN)
Fx2	Summed measured horizontal force component of LLP and RLP (kN)
Fx3	Resolved horizontal force component of FLR (kN)
Fy	Summed vertical three point linkage forces acting on the tractor (kN)
Fy1	Resolved vertical force component of FTL (kN)
Fy2	Calculated resultant vertical force component of Fx2 (kN)
Fy3	Resolved vertical force component of FLR (kN)
GPS	Global Positioning System
GTR	Gross Traction Ratio (%)
h1	Vertical distance between tyre contact and top link attachment point (mm)
h2	Vertical distance between tyre contact and lower lift arm attachment point (mm)
h3	Vertical distance between tyre contact and lift arm / lift rod pin joint (mm)
IID	Quasi-static prediction of implement cultivation depth (mm)
11	Horizontal distance between rear axle centre and top link attachment point (mm)
l2	Horizontal distance between rear axle centre and lower lift arm attachment point (mm)
l3	Horizontal distance between rear axle centre and lift arm / lift rod pin joint (mm)
LLA	Lower Lift Arm
LLP	Measured horizontal force in the nearside (left) lower lift arm (kN)

LLR	Measured axial force in the nearside (left) lift rod (kN)
LVDT	Linear Variable Differential Transformer
Lwb	Horizontal distance between front and rear axle centre lines (mm)
MF8480	Massey Ferguson 8480 research tractor
mg	The mass of the tractor implement combination multiplied by gravity (kN)
NTR	Net Traction Ratio (%)
OSR	Oil Seed Rape
PDE	Power delivery efficiency (Ratio)
RAH	Rear axle height from the undisturbed ground surface (mm)
RLP	Measured horizontal force in the offside (right) lower lift arm (kN)
RLR	Measured axial force in the offside (right) lift rod (kN)
Rrk	Rear tyre stiffness constant (N mm^{-1})
RTK	Real Time Kinematic
Sin	Trigonometric mathematical function
SOG	True forward speed (m s^{-1} or km h^{-1})
TE	Tractive efficiency of a wheel (Ratio)
TLP	Electro-hydraulic linkage control valve control Voltage (V)
TRR	Travel Reduction Ratio (dimensionless)
Va	Actual travel speed (m s^{-1})
Vt	Theoretical wheel speed (m s^{-1})
ZF	Nominal static front axle ground reaction force (kN)
ZR	Nominal static rear axle ground reaction force (kN)

LIST OF SYMBOLS

β	Angular displacement between lower lift arm and corresponding lift rod (°)
δ	Difference between values (dimensionless)
γ	Angular displacement of lift arm with respect to the tractor horizontal reference plane (°)
μ	Angular displacement of the lower lift arms from the longitudinal vertical tractor reference plane (°)
ρ	Angular displacement of the lift rods from the longitudinal vertical tractor reference plane (°)
σ	Tractor attitude change in relation to the undisturbed ground surface, (°)
θ	Angular displacement of top link with respect to the tractor horizontal reference plane (°)
ω	Angular velocity of the wheel (rad s^{-1})
F	Applied force to spring element (tyre) or generated spring force from compression (kN)
k	Spring constant (N mm^{-1})
r	Rolling radius of the wheel on a hard surface (m)
S	Wheel slip (numeric value)
x	Compressive or extensive linear deformation of spring element (mm)

CHAPTER 1 - Introduction

1.1 Background

The concept of utilising a tool to complete a task has been around as long as the human race itself. An extract of the definition of a tool is:

> *'An implement, such as a hammer, saw, or spade, that is used by hand';*
>
> *'A power-driven instrument; machine tool'.*
>
> (Collins English Dictionary, 2015)

Early tillage used hand tools similar to those used today in small scale domestic gardening. As the human race has evolved, means of soil tillage have changed. Right from the early tillage operations ways of mechanisation have been used from simple hand tools to early animal drawn implements. The key aspect to all forms of tillage is the means by which the tool or implement is worked through the soil. Any work done requires energy which in the case of tillage has gone through the stages of human to animal to machine. Prior to the first machines large animals were and still are used to pull tillage implements.

Early agricultural tractors, as shown in Figure 1, were driven by steam and used in either a stationary form for threshing cereal crops or in the field for tillage using a pulley system whereby the tractor pulled the tillage implement across the field using a series of ropes/chains and pulleys.

Figure 1: Early stationary tractor ploughing

(Source: http://www.reading.ac.uk)

With the advent of the internal combustion engine the base form of the tractors used today was developed with an early example shown in Figure 2. As with early forms of tillage using animals, weight of the *tractor* is important. As the implement is pulled through the soil it provides resistance to motion due to its working action whether this be turning, loosening or tilling soil in preparation of a seedbed. The *tractor* therefore must be able to pull the implement and to summarise Newton's Third Law of Motion:

'For every action there is an equal and opposite reaction'

(Isaac Newton, 1687)

The tractor must be able to provide a pull force equivalent to that created by the implement and more if the implement is to move forwards as failing to do so will result in a stationary operation. No surface has zero frictional loss and therefore there will be losses in the tillage

system. The pull is defined as the *drawbar pull* and is usually expressed in terms of *force.* Wong (2008) summarises that the drawbar pull available is the tractive force available at the tractor drawbar and is the difference between the tractive effort developed by the tractor and the resistance to its motion. The resistances to motion are the force required to pull the implement (draught force), frictional losses due to surface type (rolling resistance) and wheel slip losses. Surface to surface contacts results in a non-perfect energy transfer causing frictional losses; in this context it is referred to as *wheel slip*. Wheel slip is dependent on a number of factors which will be discussed in subsequent chapters.

Figure 2: An early internal combustion engine tractor

(Source: http://www.aghistoryproject.org/)

The means by which the tillage implement is attached to the tractor has developed from the early trailed method to a more complex multi-point linkage. Massey Ferguson developed the automatic Draught Control three point linkage consisting of three points of attachment between the implement and the tractor as shown in Harry Fergusons *black tractor* from 1933

in Figure 3. This is the result of many years of development by Harry Ferguson. Ferguson recognised that by having a third point of attachment the pull or draught generated by the implements tillage action could be utilised to add weight to the main rear driving wheels effectively turning the implement attachment into a closed loop system. This had several advantages, which will be discussed later but primarily it improved the drawbar pull of the tractor. The rear wheels are generally larger than the front wheels on most conventional tractors and have greater contact with the ground, thus by ensuring the wheels push against the ground the tyres will grip more efficiently.

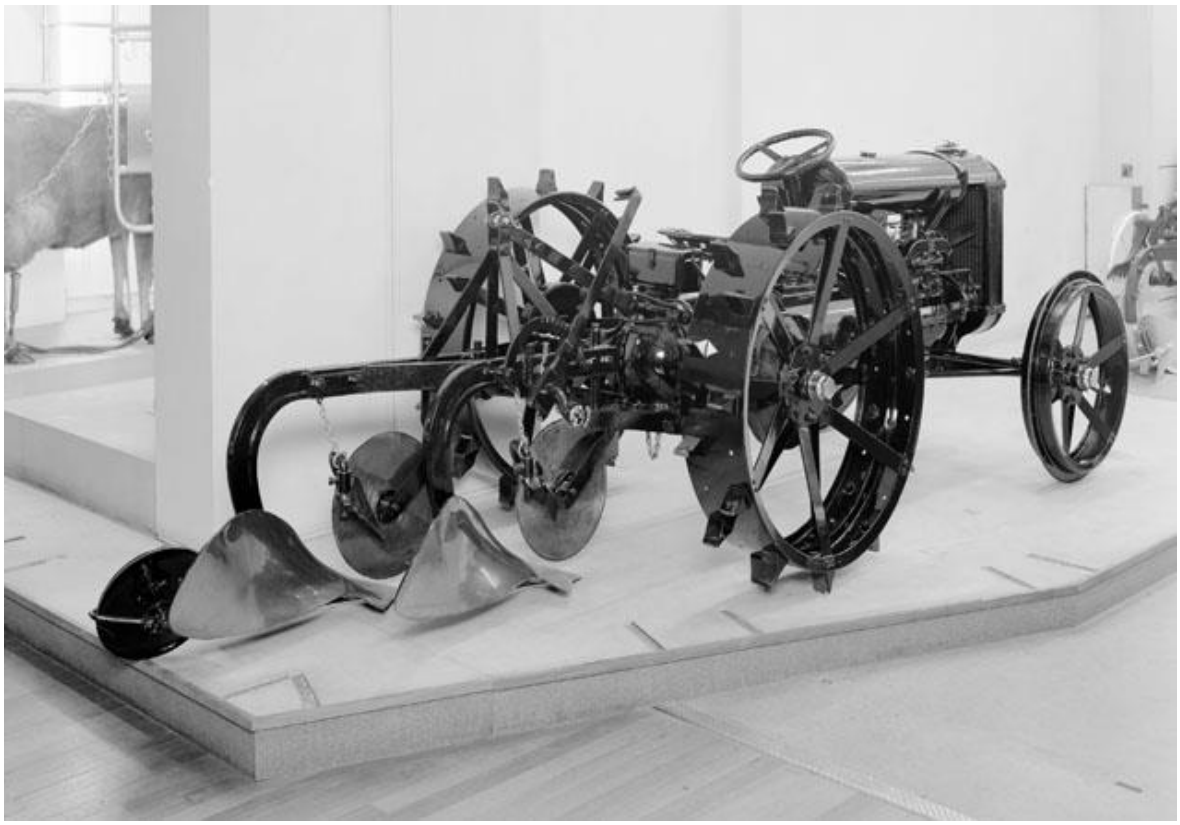

Figure 3: Early Ferguson *black tractor* with three point linkage

(Source: http://www.nationalmediamuseum.org.uk)

As tractors have developed over the last century the basic layout and principle over at least the last 70 years has remained largely unchanged. The only major changes have been to how the functionality is controlled from a largely mechanical system (Culpin, 1992) to an

electronically controlled system utilising hydraulic and electronic components and actuators. These changes have largely mirrored technology changes within the world itself and are largely attributable to the development of the silicon microchip.

Through the application of this technology higher control fidelity is possible over the basic tractor functions and, more importantly today, the efficiency of field operations. The fossil fuels (diesel fuel) that are used by tractors and other vehicles are being used at a high rate globally and there is only a finite resource available. The use of bio fuels, such as bio-diesel, is contributing to a reduction in this burden, however the usage is still high. Over the last three decades, but particularly the last two, there has been a drive to improve the efficiency of fuel usage and reduce emissions. Improvements in accuracy of crop sowing and field trafficking have been made and are being adopted more and more. The *efficiency* of field operations is largely seen as work rate, minimal trafficking and optimum seed usage for a given yield i.e., productivity or quantitative based. Coupled with more efficient engines and larger tractor implement combinations these factors do improve efficiency and profit margins. However, little emphasis has been placed on the efficiency of actual field tillage operations. Deep tillage in particular requires high levels of power and therefore what may seem as small improvements in accuracy could see more tangible benefits in reduced fuel usage. Modern high horsepower tractors can use fuel at a rate of between 20 litres to in excess of 100 litres of diesel fuel per hour ($l\ h^{-1}$). Over a typical eight hour working day could equate to in the order of 600 litres of fuel used, therefore even a 5% reduction in fuel usage over a year could significantly reduce costs and fuel usage.

The increased levels of electronic systems in the modern tractor, excluding field mapping, are tailored to suit the productivity emphasis rather than field work efficiency. Whilst existing linkage control systems offer a great degree of flexibility little or no feedback is available to the operator about the efficiency of tillage operations. Most operators know how

to set up a tractor implement combination for a specific field task and how to adjust in the field mitigating the more pronounced performance losses. However, the smaller dynamic changes that operators are unaware of are a potential source of energy loss. In a deep tillage environment such as sub-soiling requiring high power, (Spoor and Godwin, 1978) proved a relationship between draught force and implement depth (Godwin, 1974); where, as an approximation, doubling the depth of tillage results in a quadrupled draught force requirement. It stands to reason that a small depth changes result in larger energy fluctuations and hence fuel usage. Therefore through accurate depth control it may be possible to reduce fuel usage and improve work rate and efficiency.

Most research already conducted has centred on the creation of mathematical models for implement behaviour in soils, tractor/implement combination selection and tractive efficiency with little further development on real time measurement and control. Most commercial products now incorporate Draught control, slip control, position guidance, work-rate and fuel consumption monitoring systems. However, the settings and response to these systems is largely down to the tractor operator. Tractor operators vary considerably in skill level and, of all the systems available, only fuel consumption measurement gives a very basic measure of efficiency. Often, common practice is to complete the tillage job as quickly as possible, driven by weather windows, but there may be efficiency gains that can be made even through the unseen dynamic changes. For example, by utilising smart implement technology such as variable width, more accurate depth control and correct utilisation and application of tractor power greater efficiency gains could be made such as more even tillage leading to increased yield, reduced fuel consumption and potentially reduced operator time (Keen *et al.*, 2009).

To conclude technology has advanced significantly since the creation of the typical agriculture tractor in commonplace usage today. Electronic systems have improved the

usability of the equipment but little emphasis has been placed on efficiency of the tillage operation at the working point and the main focus has been on higher level efficiency gains such as field mapping, reduction of field traffic and field preparation accuracy through application of guidance systems.

1.2 Research Aim

'To develop a control algorithm for agricultural tractors conducting draught cultivation operations with the aim of optimising tractor efficiency thereby minimizing fuel usage and operator time'.

1.3 Research Objectives

The objectives of this study are:

1. To develop a real-time computer based model to evaluate the critical soil/vehicle/implement parameters to efficiently control the tractor based upon the operator's preferred work modes of field work rate, tractor and fuel efficiency or consistent tillage depth and quality;
2. To create and develop an instrumentation system for the collection of the relevant parameters for the control algorithm and validate the performance of the control algorithm;
3. Develop an operator information interface to allow selection of work mode and display real time tractor/implement performance.

1.4 Hypothesis

By developing and integrating real-time tractor force and kinematic models with a measurement system it is possible to adequately measure and automatically control the functions of the three point linkage to maintain a controlled tillage depth within limits whilst optimising tractor energy use efficiency.

1.5 Outline Methodology

In order to achieve the above objectives the following methodology was adopted:

1. Review the literature in the subject area of tractor control and establish a need for real time performance monitoring of efficiency. From this the relevant parameters required to effect control can be established;
2. Investigate the types of relevant instrumentation and measurement systems that would be applicable to a control system to monitor performance;
3. Develop a novel, versatile kinematic model to calculate three point linkage forces, weight transfer, tractor attitude, tractor sinkage and tyre deflection. This to be based on the research tractor (MF8480) provided by Massey Ferguson pictured in Figure 4 below;
4. Develop an instrumentation system to measure the relevant parameters to provide input data to a control and performance monitoring algorithm;
5. Conduct a series of initial field experiments evaluated standard three point linkage performance in the field using standard tractor controls. These were used to briefly evaluate the energy savings possible;
6. Conduct a series of laboratory experiments to evaluate the control functionality of the standard linkage control system;

7. Develop a performance monitoring control algorithm to monitor tractor performance in real-time and control the three point linkage.

Figure 4: Massey Ferguson 8480 research tractor used in this study

CHAPTER 2 - Review of Literature

2.1 Introduction to Three Point Linkages and Tractor Performance

The subject area of the effects on tractor implement combination performance is not new but according to Ward *et al.*, (2011) has languished since the late 1970's and early 1980's. The control systems have developed little since the introduction of Ferguson's Draught Control except that the systems are electro-hydraulically rather than mechanically actuated (Culpin, 1992; Ward *et al.*, 2011). There was substantial interest by Crolla in 1975 (Ward *et al*., 2011) where a substantial review took place of the subject area. It was noted that substantial contributions had been made by Cowell *et al.*, Crolla, Dwyer *et al.*, Hesse, McKeon, Seifert and Skalweit (Ward *et al.*, 2011).
Scarlett (2001) completed a more recent comprehensive review of the status of tractor control and potential developments and was a summary of the work reviewed in part 2.2.3.

In the late 1970's and early 1980's the agricultural engineering industry was interested in several key areas:

1. The relative merits of depth vs Draught control;
2. The relationship between the implement forces and the forces transmitted to the three point linkage;
3. The relative merits of top vs lower link sensing;
4. The dynamic behaviour of the implement;
5. The dynamic behaviour of the tractor-implement combination (Crolla, 1975).

(Ward *et al.*, 2011)

The subject area of the three point linkage control system and its suitability today has largely been unchallenged for many years with current systems being a development of Harry Fergusons original design. The effects of the current control systems on overall dynamic performance of the tractor/implement combination has been little researched (Ward *et al.*, 2011) since.

Research in the early 1980's Cowell and Herbert (1988) looked primarily at the concept of automated top link length adjustment and sensing. The primary aims of the research were to improve the quality of ploughing depth by changing the geometry of the linkage connection between tractor and implement to take into consideration ground undulations. Another approach was adopted by Simalenga and Kofeod (1992) with a variable geometry three point linkage system adjusting tillage depth based on measured draught forces. Hu *et al*. (2015) developed a control system to compensate for tractor roll automatically adjusting the linkage lift rams to compensate in real-time. Lee *et al.* (1998) developed a system for controlling tillage depth of rotary cultivators based on tractor attitude. However this was purely a tillage depth based system with no apparent monitoring of tractor performance, consideration of energy usage or traction performance of driving wheels. Since the inception of this study in 2009 Xie *et al*. (2013) has developed a three point linkage control system to control tillage depth with a comparison to traditional *fifth wheel* implement depth control methods. This system though is purely designed to control tillage depth rather than a whole coherent tractor performance monitoring and control performance.

A significant body of work exists in the area of linkage instrumentation systems for direct and indirect force measurement; the main aims of most of this work were to look at the forces acting on the implement. A significant number alter the linkage geometry such as the load frame (Alimadarni *et al.*, 2008) and this subject area is covered in Chapter 4. Use of the three point linkage as a weighing system to monitor application rates has also been successfully used (Aeurnhammer, 1988) through the inclusion of load cells within the lift rams and forward speed measurement; There are multiple advantages to this inclusion when considering control and monitoring of spray or fertiliser application rates.

Performance monitoring of tractors has also formed a significant contribution to research such as the work by Summers (1986). Much of the work was conducted some years ago with lower technology computers and more recently in autonomous tractors from a pure functionality viewpoint. Yahya *et.al*. (2009) developed a Global Positioning System (GPS) tractor performance and field mapping system to produce computer based field plots of field parameters including terrain, tractor traction and implement force parameters, however this is a passive (i.e., non-controlling) system with the primary aim of field mapping to reduce field inputs. Zoz and Grisso (2003) also developed a computer based prediction software to match implements to tractors on a power basis to optimise the potential field operations. However this system did not operate in real-time or take into account field or weather variations. Scarlett (2001) investigated and patented various tractor automation technologies. However the systems developed by Scarlett rely on field passes to calibrate the system; therefore the tractor is always set up based on recorded soil parameters from at least one cultivation width displacement in the field. Section 2 contains a detailed analysis of the relevant filed patents.

2.2 Review of Patents

Attempts at tractor automation, rather than fully robotic tractors have been tried in the past but the patents reviewed here are the most recent work. Most tractors now as standard feature display information on factors such as work rate, fuel consumption along with speed control and guidance systems and also incorporate draught, depth and slip controls.

It became apparent during this work that Dr A J Scarlett claimed to have published work in the subject area of this study and that work was protected through patents filed by Case New Holland. The contents of the patents are briefly summarised by Scarlett (2001) and therefore

a thorough review of the patents was completed on an individual document basis to ensure that the context of this study was still valid.

2.2.1 European Patent Specification – EP 0 838 141 B1 (2003) – A Vehicle Control Apparatus and Method. CNH UK Ltd

This patent was filed in 1997 and was last updated in 2003. The main content of the patent details a system for automatically controlling the functions of an agricultural tractor with the aim of improving efficiency during almost all operations. The system is not exclusively for tillage implements such as ploughs or tined cultivators but also includes all implements that may be attached to a tractor including semi-trailed and also combination implements with items mounted on the front and rear linkages. The vehicle system as a whole comprises of the tractor and implement(s).

The document gives some history of most previous attempts at automated tractor control. Most previous attempts at automatic control have been largely unsuccessful and this is given as the rationale for developing the system within in the patent document. It also details work conducted and Patented by Massey Ferguson (EP A 0070833) but this prior system only maximised tractor performance based on operator dictated inputs such as maximum work-rate or minimum fuel consumption; it was not based around measured field variables in the prevailing conditions and could not be considered fully automatic. Also, other work conducted is discussed but the system described within this Patent resolves areas and issues that others have failed to address so far.

The idea behind the system is to measure variables, within the whole tractor system whilst working, such as soil resistance (which is used to estimate draught force), percentage wheel slip, the pull (force) measurable at the implement hitch (which is more commonly known as drawbar pull) and the forward speed of the vehicle. The idea is by taking these measurements

they can be used to affect changes to the tractor system such as engine speed/governor setting, transmission ratio, implement hitch height and also implement specific adjustments such as width to maintain efficiencies as required.

The control system consists of a main control system programmable controller including vehicle reference model data, slave controllers on the vehicle sub-systems (throttle, gear setting, implement settings etc), various sensors connected to the main controller to monitor sub-system performance and a comparator that will compare sub-system sensor data with an updateable steady state reference model. Depending on the output of the comparator the main controller is able to sanction automatic change settings through the sub-system controllers, in effect a closed loop control system. The system is advanced enough so that the operator only needs to steer the tractor and deactivate the system at the end of the run to turn by several means but typically lifting the implement at the end of the run with control being returned when the implement is lowered again.

The system is fully automatic but can be calibrated with a field pass in each direction to teach the system the requirements of the operator and create boundaries with which the system should work within i.e. the operator has specific requirements which may not be within the bounds of the reference model but these requirements need to be adhered to whilst the system maintains them as efficiently as possible.

The steady state reference model referred to in the system incorporates physical parameters of the tractor/implement system, such as mass and moments of inertia are taken to be constant but it is mentioned that these will vary during operation. The model also incorporates data on all variations and combinations of engine performance, transmission/engine performance data, vehicle tractive efficiency data, driveline losses and data on setting the implement. By the system working in this way it does not include the dynamic effects of weight transfer including wheel load variation, tractor attitude due to

weight transfer and tractor sinkage effects (which affects overall implement depth as the system calculates implement depth in relation to the tractor. These are critical to accurate calculation of tractor efficiency.

The tractive efficiency data within the steady state reference model includes data on various wheel tyre combinations on various surface types; however this does not really allow for real-time control or variations in set-up by the farmer without further data input. The system would be much improved if it could measure tractive efficiency from live real-time field data. A further issue is that within this system the tractive efficiency data is for the entire tractor system but does not differentiate between front and rear driven wheels, hence not taking into account tractor attitude, tractor sinkage and weight transfer.

The control system is a *bus* based system in that all controllers and sensors are linked to the main controller, however there is provision for the system to be either retrofitted to a tractor or incorporated in to a CANBus equipped tractor. The system incorporates a display interface with the operator and effectively only controls engine output, transmission ratio, implement width and occasionally depth. The system records real time data during a field pass and deactivates at the headland and also is smart enough, from measurement of plough orientation, to recognise the direction of travel and also records data on the second pass. The initial settings of the performance parameters are made by the operator. The system then compares the requirements with optimum settings dictated by the steady state reference model and suggests changes which the operator can accept or override. If the operator chooses to override the system the system will operate as efficiently as possible within the boundaries set by the operator although this may not be optimum. During the field passes in each direction the system monitors conditions and adjusts throttle and gear settings and width (though this is preferred at headland turns while the implement turns over) throughout to maintain efficiency within the required parameters during the field pass. The system then

compares the data stored on each pass so that the next pass in that direction will use data from the subsequent pass for initial set-up.

In conclusion, although the system is described as a real-time system, it uses many updateable steady state models. The system is designed to operate within operator selected work modes such as work-rate, minimum fuel consumption or wheel slip data which is included within the steady state reference model. It does exhibit real-time control but uses these models and ideal performance characteristics to dictate initial settings. The ultimate system would require less manual inputs from the operator and be smart enough to complete any operation efficiently without needing data on tyre characteristics, soil surface, rolling resistance, etc. The main omissions are real-time measurements of weight transfer and how this affects the tractive performance of front and rear axles and hence power distribution and therefore tractive efficiency. Tractive efficiency is treated as a complete steady state system depending on tyre and surface types with no provision for weight transfer effects.

2.2.2 European Patent Specification – EP 1 169 902 B1 (2007) – A Method and Apparatus for Controlling a Tractor/Implement Combination. CNH UK Ltd

The patent was filed in 2001 and last updated in 2007. The patent details a system for controlling a tractor/implement system and is related to EP 0 838 141 B1 (2003). The system itself is similar to that in EP 0 838 141 B1 (2003) however the system details are more sparse but described in detail is how engine output torque can be related to draught force and used within a system for controlling tractor performance for any given ground engaging implement.

The system consists of a series of micro controllers and sensors that control and measure the variables of transmission ratio, implement working depth (depth is constant within the system but provision is made for variation) and width, tractor engine governor and tractor

engine power output (it is assumed that power output can be varied via the engine control unit in isolation of the throttle opening i.e., if engine speed reduces under heavy load at wide open throttle the governor system can interact and alter engine parameters to create more power, using more fuel and allowing extra turbo boost pressure).

The system requires calibration and this is completed by conducting a pass across the field in the desired tillage direction and reverse direction (i.e., to simulate a ploughing cycle) with the implement raised from the ground in a desired gear and also usually at full throttle. The torque at the engine flywheel is then recorded in each direction and an average value calculated. The calibration process is then repeated whilst engaging the implement with ground at the desired depth. The calibration should be conducted on level ground but an inclinometer is included in the system to factor in the dynamic changes due to sloping ground. Whilst this calibration process is conducted the micro controllers and sensors records the relevant settings and magnitude of their variables. The system then calculates the increase in flywheel torque due to the additional forces from the tillage operation and corrects it for driveline losses between the ground/wheel interface and also the rolling radius of the tyres using historical data. Then, using a formula defined in the patent, the implement draught force is calculated. This information is then used to update a steady state reference model. However there is no limit on the number of calibration cycles that can be completed and there is no restriction on gear ratio or throttle setting. It is not clear if within the patent whether the system can store data from more than one field calibration in the field; it may be simply a case of trial and error until the desired settings are achieved by the operator to complete the tillage operation.

The system is depth control based and once calibrated the system uses the stored draught force within the steady state reference model. The system will then maintain the implement depth; using the stored calibration data in the steady state model and also live data real-time

comparisons can be made (this is implied within the patent) and changes made to transmission ratio, implement working width, tractor engine governor and tractor engine power output whilst maximising work-rate.

In conclusion the system is simple and favours draught force estimation/measurement using flywheel torque. Whilst there is some logic to this system it relies on large quantities of historical information on tyre deflections, transmission and driveline losses in all gears and speeds; it would be more sensible to measure implement draught force in real time from the three point linkage interface as this removes potentially large errors in system calculations. The system relies on a field calibration in both directions to obtain engine torque difference when cultivating.

The main problem with this whole system is that it effectively assumes the soil type is fairly constant and draught forces should remain within certain boundaries. The system is based around work rate rather than overall efficiencies and again does not take into account varying weight transfer and hence tractive efficiency; arguably by calibrating the system in the field this would be included in the overall measurements but not separately or accurately measured.

2.2.3 European Patent Specification – EP 0 838 139 B1 (2003) – Improvements in or Relating to Tillage. CNH UK Ltd

The subject area this patent is similar to EP 0 838 141 B1 (2003) and EP 1 169 902 B1 (2007) in that it details a system for controlling and improving operational efficiency when conducting tillage operations; however this system is based around altering the width of an plough based on draught force magnitude. The system is, again, based around working modes such as maximum work rate and minimum fuel consumption and allows adjustment via micro controllers, either independently or via a CANBus system, of implement width

and also optionally other parameters such as transmission ratio, throttle opening, or wheel slip to maintain working depth and operate within the working mode parameters.

The system requires calibration in two directions (similar to EP 1 169 902 B1) in that a device will measure the force indicative of the draught force between the tractor and the plough. No mention is made of what the device consists of but assumes that it exists. The calibration consists of a static draught measurement and then a run in each opposing directions within the field (simulating a ploughing cycle) recording draught force data and monitoring vehicle performance (sensors for implement depth and width may also be incorporated). Then by using the formula in the dynamic draught force addition is used to calculate soil strength values along the length of each run. The system also compares real performance data with a steady state model and allows adjustments as necessary to maintain working depth within the parameters defined in working mode selected. The steady state reference model is based around historical recorded data from the tractor sensors whilst carrying out tillage with the same implement in a variety of field conditions and also mechanical parameters of the combination such as tractive efficiency, weight and other physical dimensions. This model is updatable using collected data, however some mechanical parameters of the combination will be fixed independent of prevailing conditions.

The system is smart in that it knows which direction the tractor is going with use of micro switches on the plough (these are also used in conjunction with a movable mounting in EP 0 857 408 B1 (2003)). In direction 1 when recording data the system logs the draught force data against the direction indicated by the micro switch and when turning the plough at the headland the system repeats this process for the opposite direction. The data recorded in direction 1 will be used to adjust the width of the plough prior to completing the next pass in the same direction and vice versa this continuing throughout the field. Dynamic changes

in the plough width are not permitted during the cultivation pass, but occur as the system disengages at the headland through lifting the implement. This could not be described as a real time system in that the data stored from the previous run in the same direction is used to set up the next run in this direction. If a large plough or cultivator is being used there could be 10 metres between parallel runs. Soil properties could easily change within this area. Again the system is look up table based in that the soil strength (calculated) data is stored within the system for comparison purposes on the next run.

The system has the facility for the operator to override the system if necessary and will search the steady state model and performance curves held within the system to establish if their settings are within acceptable limits. If they are the system will run as normal, if a performance curve cannot be found it will warn the operator, if overridden again the system will optimise settings as best as possible. The data is also stored to provide an approximate soil map for the field which can be stored on removable discs for future usage.

In conclusion the system is only partially real-time as previous pass field data is used for set-up purposes but a degree of real time control is used. The system uses soil strength (calculated) data to set-up the plough for the next pass in the same direction but using calculations made by the steady state reference model allows changes in transmission/engine settings during the field pass but only plough width changes at the end of the run depending on collected data. This system could be problematic to work properly as the system must log data in reference to either a start finish time base for the run or in line with a GPS position; the reason for this is that the system uses data from the previous run in the same direction for set up of the entire system including plough width on the current run, the problems arise when a tree/obstacle is in line with the field pass where the plough would need to be lifted, hence deactivating the system. The system would then reactivate as the plough is lowered to the ground again after clearing the tree using data collected from the

first part of the same run; therefore soil changes that occur along the length of the previous full run would not be used.

Again weight transfer is little considered and its effects on traction but mechanical both fixed and variable tractor properties are integrated into a steady state reference model which is updatable and used for comparison and control purposes. Little extra information is given on sensors and their usage.

2.2.4 European Patent Specification – EP 0 857 408 B1 (2003) – A Gravity Actuated, Moveable Mounting. CNH UK Ltd

Although not specifically relevant to real time control this patent details a device that can be used for measuring implement depth through the use of one sensor only. The sensor is allowed to pivot via a counterbalanced shaft that has an over centre action so that the sensor remains in the same orientation as the plough is turned over, the over centre action allowing for the lateral tractor angle during ploughing. The sensor locks via the over centre action in position so and via micro switches can give an indication of the orientation of the plough as used in EP 0 838 139 B1 (2003). The document also details a calibration procedure, but the depth sensor only measures implement depth in relation to the ground and not tractor sinkage. The system used within this project measures four point tractor sinkage and therefore implement depth, thus giving true implement depth.

2.2.5 European Patent Specification – EP 1 153 538 B1 (2007) – Method and Apparatus for Controlling a Tractor/Baler Combination. CNH UK Ltd

Originally filed in 2001, this patent details a system for optimising a tractor baler performance, where the baler is of the large square type. The system again offers some degree of real time control but as characterised by other patents from the same authors large emphasis is placed on *look up table* information that is used to compare against live data.

The invention presented is the monitoring of biological mass flow through a baler so that the speed of the pulling tractor can be controlled to maintain optimum flow rate within boundary limits and maximise efficiency. Sensors are used to monitor the engine torque, gear selected, torque of the tractor PTO shaft, inclinometer, the baler packer or rotary feeder driveshaft torque (strain gauges), the baler packer fork con-rod force and the positioning of a sensor door in a pre-compression chamber to monitor flow rate. The system monitors all sensors over the baler plunger (or packer) cycle but particularly takes average values of the senor door position, engine torque and PTO shaft torque. The programmable controlling and comparing processor contains information of all tractor engine/gear data, PTO torque data, baler parameters such as packer drive torque and optimum flow rates; it can also predict and compare performance using a steady state reference model containing parameters such as gear selected, swath density data, inclination of the tractor and the effects this has.

The system calculates whether by increasing or decreasing speed through gear changes only (constant engine speed required for rated PTO speed) if flow rate will fall to within ideal levels to maintain bale density consistency and overall efficiency without blocking or slowing any functions of the baler such as cutter knives. Before sanctioning any gear changes the system predicts if the increase in torque on the engine is within acceptable levels and whether the speed increase will optimise the flow rate; should all predicted results be acceptable the gear change will be sanctioned. However the flow rate is monitored over time and only if levels are consistently different from optimum will the gear change be sanctioned. Gear changes are timed to a point on the baler plunger cycle, presumably to avoid any potential blockages or to reduce torque pulses within the system due to gear changes. The system via a swath heap sensor is smart so that if a swath heap is encountered the tractor/baler will slow down through gear changes; this could be difficult as slowing down may be quite abrupt.

In conclusion, of all the patents reviewed so far this one has the greatest degree of real time control, although theoretically one factor is being altered (gear ratio). Again there is a large dependency on historical information but there is a greater usage of live data such as flow rate, various drive shaft torques and bale production. The system uses programmable controllers and can be integrated to a CANBus system.

2.3 Tractor Efficiency

Tractive efficiency of a wheel by definition is the efficiency by which wheel input power is converted into wheel output power (Wismer *et al.*, 1974). It is in effect tractive inefficiency as defined by Zoz and Grisson (2003) and is a measure of velocity losses (i.e. wheel slip) and pull losses (such as differing soil types or weight distribution changing causing rolling resistance increases) where motion resistance reduces the amount of traction available. Single wheel tractive efficiency (TE) is defined by Wismer *et al.* (1974) as:

$$\text{Tractive Efficiency} = \frac{\text{Wheel Output Power (kW)}}{\text{Wheel Input Power (kW)}} \text{ (Ratio)}$$

Equation 2.1

Zoz and Grisso (2003) also defines tractive efficiency (TE) as:

$$\text{TE} = \text{Pull Ratio x Velocity Ratio} = \frac{\text{NTR}}{\text{GTR}} \text{ x } \frac{\text{Va}}{\text{Vt}} \text{ (Ratio)}$$

Equation 2.2

Where,

NTR = Net Traction Ratio (%);

GTR = Gross Traction Ratio (%);

Va = Actual travel speed (m s^{-1});

Vt = Theoretical wheel speed (m s^{-1}).

The magnitude of tractive efficiency depends on the pull, torque and slip characteristics of the wheel (Wismer *et al.,* 1974). However the Wismer *et al.* (1974) approach is for a single wheel but subtle change is required within the definition to incorporate the tractive efficiency of a complete vehicle.

Brixius (1987) defines tractive efficiency (TE) as:

$$\text{TE} = \frac{\text{Output Power or Drawbar Power (kW)}}{\text{Input Power to Drive Wheels (kW)}} \text{ (Ratio)}$$

Equation 2.3

Wong (2009) also defines tractive efficiency as the ratio of drawbar power to the power delivered by the engine; where engine power can be expressed as wheel input power including the relevant transmission losses.

Keen et al. (2009) also defined tractive efficiency of a wheel as:

$$\text{TE} = \frac{\text{Drawbar Pull (kN) x Rolling Radius (m) x (1 - Wheel Slip)}}{\text{Wheel Input Torque (Nm)}} \text{ (Ratio)}$$

Equation 2.4

An alternative method of calculating tractor efficiency, power deliver efficiency (PDE), is defined by Zoz and Grisso (2003):

$$\text{Power Delivery Efficiency} = \frac{\text{Drawbar Power (kW)}}{\text{Engine Power (kW)}} \text{ (Ratio)}$$

Equation 2.5

Power delivery efficiency (PDE) is a more overall measure of how efficiently power is used by the tractor implement combination and neglects the specifics of wheel slip, however the losses associated are indirectly included.

The torque and slip characteristics of a wheel are linked to the cohesion available between the wheel tyre and the soil surface and also the drawbar pull. Tractive efficiency is linked to wheel slip where maximum tractive efficiency is commonly where wheel slip is at a minimum for a given soil/surface type and conversely minimum tractive efficiency is where slip is at its greatest (Wismer *et al.*, 1974).

Wheel slip is defined as (Wismer *et al.*, 1974):

$$S = \frac{1 - Va}{Vt} \text{ (Numeric value)}$$

Equation 2.6

Where,

S = Wheel slip (numeric value);

Va = Actual travel speed (m s^{-1});

Vt = Theoretical wheel speed, r. ω, (m s^{-1});

r = Rolling radius of the wheel on a hard surface (m);

ω = Angular velocity of the wheel (rad s^{-1}).

Wheel slip is a measure of motion loss through development of soil strains during traction (Wismer *et al.*, 1974) occurring between the wheels and the ground surface; where the forward speed of the vehicle is less than the forward speed indicated by wheel rotations.

Equation 2.6 calculates wheel slip as a decimal but it is usually expressed as a percentage (multiply S by 100) (Wismer *et al.*, 1974). An alternative definition used by Zoz and Grisso (2003) is that of travel reduction ratio (TRR) and is defined as:

$$\text{Travel Reduction Ratio (TRR)} = \frac{1 - \text{Actual Velocity (m s}^{-1})}{\text{Theoretical Velocity (m s}^{-1})} \text{ (Ratio)}$$

Equation 2.7

Keen *et al.* (2009) showed that through correct matching of implement size to available engine power, through the number of tines, tractive efficiency can be maintained whilst increasing work rate. Therefore, through accurate control of wheel input power, drawbar power and wheel slip tractive efficiency can be accurately controlled. It is not necessary to know the absolute behaviour of the implement through the soil or the soil properties to control tractive efficiency within a given field situation.

2.4 Field Dynamic Effects

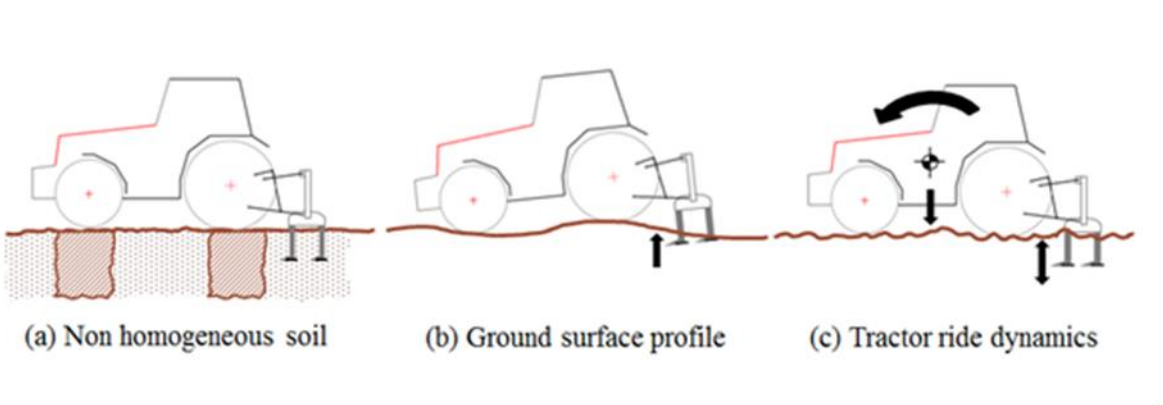

Figure 5: Field effects on implement depth control

(Source: Ward *et al.*, 2011)

Ward *et al.* (2011) hypothesised to the effects of tractor dynamic behavior. To expand on this work the surface *roughness* and homogeneity of a field can have a significant impact on how well implement depth is controlled through the dynamic undulations and causing a shift in the centre of gravity of the tractor implement combination. Ward *et al.* (2011) hypothesised that three main field variables could disturb the accuracy of implement depth control as shown in Figure 5 above.

1) Non homogeneous soil

Varying soil conditions and levels of compaction either through natural variation or trafficking will result in weight transfer causing tractor attitude changes. An implement operating with a form of depth control, such as depth wheels or packer-rollers will result in broadly consistent soil tillage depth but fluctuating draught forces generated. Depending on the tractor linkage control strategy selected this will have differing effects. If the tractor is operated in Draught control the draught force applied to the tractor will fluctuate but soil tillage depth will vary; if operated in Position control implement depth and draught force will vary furthering the effect on tillage depth through increased weight transfer (Ward *et al.*, 2011).

2) Ground surface profile

Uneven surfaces will cause the tractor to pitch fore and aft as the tractor tries to follow the ground contours. The effects of this will be variable depending on the weight of the tractor and the field soil conditions; that is to say there may be some *damping* to these effects through compaction of the undulations. Tyre pressures also are key in this situation as a higher inflation pressure will result in a stiffer tyre transmitting more of the actual undulations to the tractor itself; a lower inflation pressure will result in more *damping* but the tyres will be more likely to follow the profile of the ground surface. The form of linkage control strategy chosen in this situation is very important. Should implement depth wheels be fitted the implement should also broadly follow the contours of the ground however as the implements is mounted well behind the tractors pitch axis the effects are magnified (Ward *et al.*, 2011). This will affect the forces transmitted through the three point linkage to the tractor altering the weight transfer effects and axle loadings. This scenario is most prevalent when operating in Position control as soil

tillage depth will vary significantly as the implement position in relation to the tractor is fixed.

3) Tractor ride dynamics

Ward *et al.* (2011) commented that tractor ride dynamics have a significant effect on axle loads and soil tillage depth fluctuations and this particular area is less well understood. High tyre inflation pressures will tend to magnify the effect whereas lower inflation pressures will tend to dampen the effects. However with a soil engaged implement this may result in lesser effect than first thought but will result in fluctuating axle loads and more cycling of loads through linkage components increasing fatigue degradation of the components and reducing comfort for the operator. (Ward *et al.*, 2011)

2.5 Implement Models and Soil Behaviour

The prime consideration for this research is the field operation of deep sub soiling tillage. Much prior research has been carried out in this subject area but the primary area of interest is the behaviour of winged sub soiling tines. Tractor linkages can be set to change position depending on draught force loads via three normal control modes; Position, draught and a mixture of the former, Intermix. However, as shown by Godwin (1974) there is a relationship between tillage depth and draught force. Current tractor linkage control systems do not take individual implement characteristics into account but rather use a rudimentary draught force measurement to control linkage behaviour.

Godwin (1984) developed a model that predicted horizontal (draught) and vertical forces acting on a tined tillage implement. The initial model did not however take into account the effects of multiple tines and how the soil deformation profile between two parallel tines interacts; Godwin (1984) incorporated into the model a further element to consider spacing of tines (rows and width spacing). The model was developed, as cited in Godwin (2007),

from work by Hettiararchi *et al.* (1966), Godwin and Spoor (1977), McKyes (1985); Godwin (1984) and Wheeler and Godwin (1996). Godwin (2003 and 2007) updated the model to incorporate the effects of speed and multiple tine configurations. In multiple tine configurations interaction of soil disturbance between tines takes place and accounts for additional draught force requirement. The model simply adds the draught forces together for a number of tines in a known configuration and then subtracts the additional draught force required to disturb soil in the interacting deformation zones between tines (effectively losses through incorrect or inappropriate spacing). The model incorporates effects of soil mechanics, the implement size, and speed.

The model defines the forces by:

$$\text{Force} = [(\text{Soil factors } (k\ Nm^{-1}) \times (\text{Implement size } (m)) + \text{Inertia term } (kN)] \times \text{Direction } () \ (kN)$$

Equation 2.8

Forces are resolved in to component vertical and horizontal forces using the *direction* part of Equation 2.8 where the sine and cosine return the component forces. Whilst the models will not necessarily be used in this work it is important to understand what factors affect the forces acting on a tractor transmitted via the three point linkage.

2.6 Background Literature Review Conclusion

Whilst there have been some attempts at improving tractor efficiency through performance recording there has been no significant effort at a real-time system. Work conducted by Scarlett centred on a system that relies on historical previous pass data with its limitations. It can clearly be seen that by minimising tillage depth variation either through tractor ride height control or improved linkage control energy savings can be made. What was apparent in the systems developed by Hu *et al*. (2015), Lee *et al*. (1998) and Bin *et al*. (2013) is that

they are purely based around the control of the three point linkage from a pure tillage depth viewpoint. There were no apparent considerations on the performance aspects of the field operation, the energy used or the mode of work required. Introduction of improved implement depth control could lead to significant savings in energy and improved tillage quality. As will be seen in further Chapters, in-tractor three point linkage cab controls play a significant part in the set up and behaviour of the three point linkage.

Scarlett (2001) hypothesised within research that tractor control could be influenced by a number of work modes but this did not cover the aspect of real-time linkage control and this forms the basis of this research. The effects of improved tractor three point linkage control and the effects on tractor performance form the outcome of the research. It is concluded that the approach taken within the scope of this study is significantly different enough from the reviewed patents for there to be no infringement.

CHAPTER 3 - Tractor Kinematic Models

3.1 Background to Tractor Kinematics

Aside from threshing operations initially tractors were used as just a means of pulling an implement or cultivator through soil with the aim of doing work i.e., tillage. Little emphasis was placed on what effects the work done has on the tractor itself. The pull required to move an implement through soil has already been described as the draught force and this is usually measured in kiloNewtons (kN). The draught force though, has a pronounced effect on the dynamics of the tractor Ward *et al.* (2011) where the rear wheels of the tractor act as a pivot point at the contact point with the ground. The act of attaching an implement to the tractor will alter the weight distribution on the tractor shifting weight (weight transfer) and hence altering the centre of gravity.

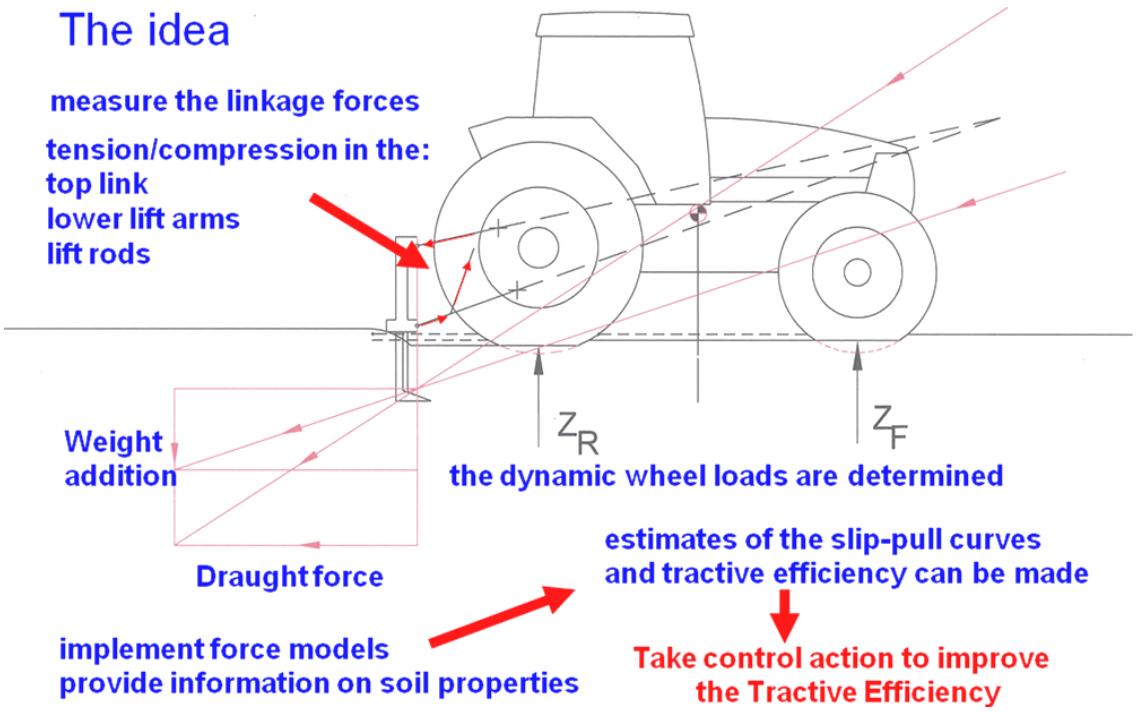

Figure 6: The concept of measuring linkage forces in real-time control

(Source: Keen *et al.*, 2009)

Through modelling of the forces and trigonometric calculations it is possible to quantify the draught force effect on the centre of gravity of the tractor. This in turn allows the weight on each tractor axle to be calculated and therefore the effects on traction of each tractor axle. The theory on the effects of draught force and linkage kinematics on the tractive performance and efficiency of tractors is comprehensively described by Wong (2008), Vantesevich (2010) and Keen *et al.* (2009) however this work is largely over 20 years old (Keen et al, 2009) and was based on earlier tractor designs where electronic systems had a much lesser widespread usage than they do today. More recently Zoz and Grisso (2003), Keen *et al.* (2009), Ward *et al.* (2009), and Scarlett (2001) have reinvigorated research on the effects of tillage on tractive efficiency and the basic principal is shown above in Figure 6.

3.1.2 Implement Force Effects

The effects of force generated by the tractor implement combination doing work have a profound effect on energy usage. The subject matter for this research is that of deep tillage operations i.e., sub-soiling. This field operation generates high draught forces and hence power requirements. The action of lifting the soil as part of the operation to loosen and lift the soil generates a vertical force. Both horizontal draught and vertical forces alter the weight distribution of the tractor which in turn changes axle loads or in simpler terms the weight on each wheel. By changing the amount of push the wheels generate vertically on the soil results in tyre deformation and therefore, increase the contact area between tyre and soil surface (Wong, 2008). By increasing the contact patch there is greater potential for transfer of energy between tyre and soil and therefore increasing the potential draught pull available (Wong, 2008). Generally weight is added to the rear wheels however, this results in weight being taken off the front wheels. Over the last 30 years four wheel drive tractors have become the standard; by reducing the effective traction contribution of the front wheels by removing axle weight a question is raised to the actual suitability of 4WD tractors today. Through

careful ballasting these issues can be compensated for but this increases the weight of the overall tractor implement combination, requiring more energy to overcome rolling resistance. There is an argument that by reducing weight on a front axle the energy required to drive the wheels may be wasted; there is the scope for the driven front wheels in this scenario to scrub or roughen the traction surface for the main rear driving wheels reducing the traction effectiveness and increasing energy requirements.

3.1.2.1 Draught Forces

The action of pulling an implement through soil generates draught force and by attaching the implement rigidly to the tractor it is transferred directly to it. This is through a lever effect; this is shown below in Figure 7.

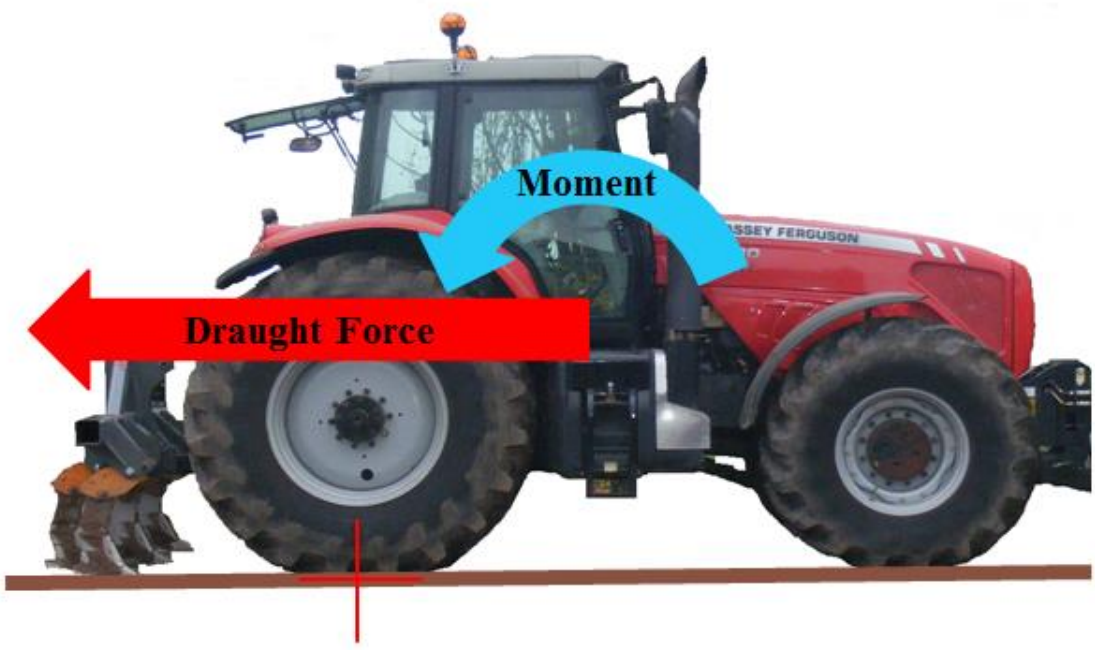

Figure 7: Dynamic effects of draught force on an agricultural tractor

(Source: This study)

This action generates a rotational force about the tractor and this is reacted at the tyre ground contact patch and will not only transfer weight from the front axle to the rear but also add weight to the tractor – weight addition.

3.1.2.2 Vertical Forces

Most tillage operations generate not only horizontal draught forces but also vertical forces (Godwin, 1984). Deep tillage operations, such as sub-soiling, generate substantial vertical forces which have the opposite effect on the tractor to draught forces transferring weight to the front axle of the tractor. The vertical forces are caused by the tractor creating an equal and opposite reaction to the implement *lifting* the soil. This is more pronounced in wing tined sub-soilers that are design not only to shatter the soil but also lift it to generate a more efficient tillage pass (Godwin *et al.*, 1978)

Shown below in Figure 8 is the effect of vertical forces on the tractor.

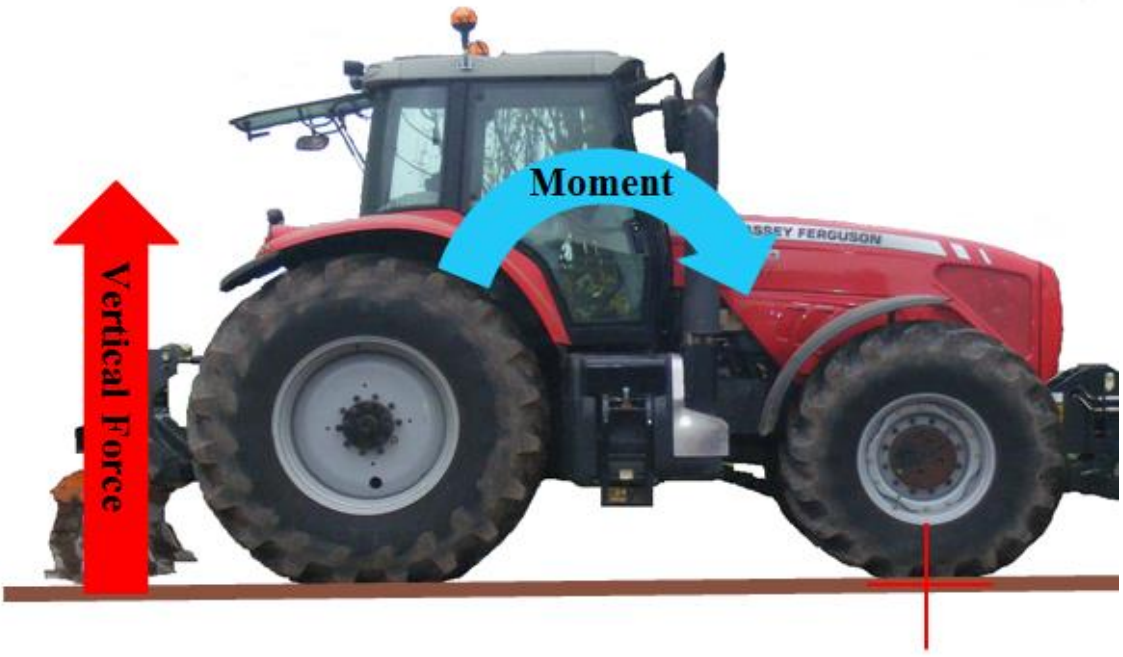

Figure 8: Dynamic effects of vertical force on an agricultural tractor

(Source: This Study)

3.1.3 Three Point Linkage Attachment

Shown in Figure 9 below is a schematic representation of a modern three point linkage.

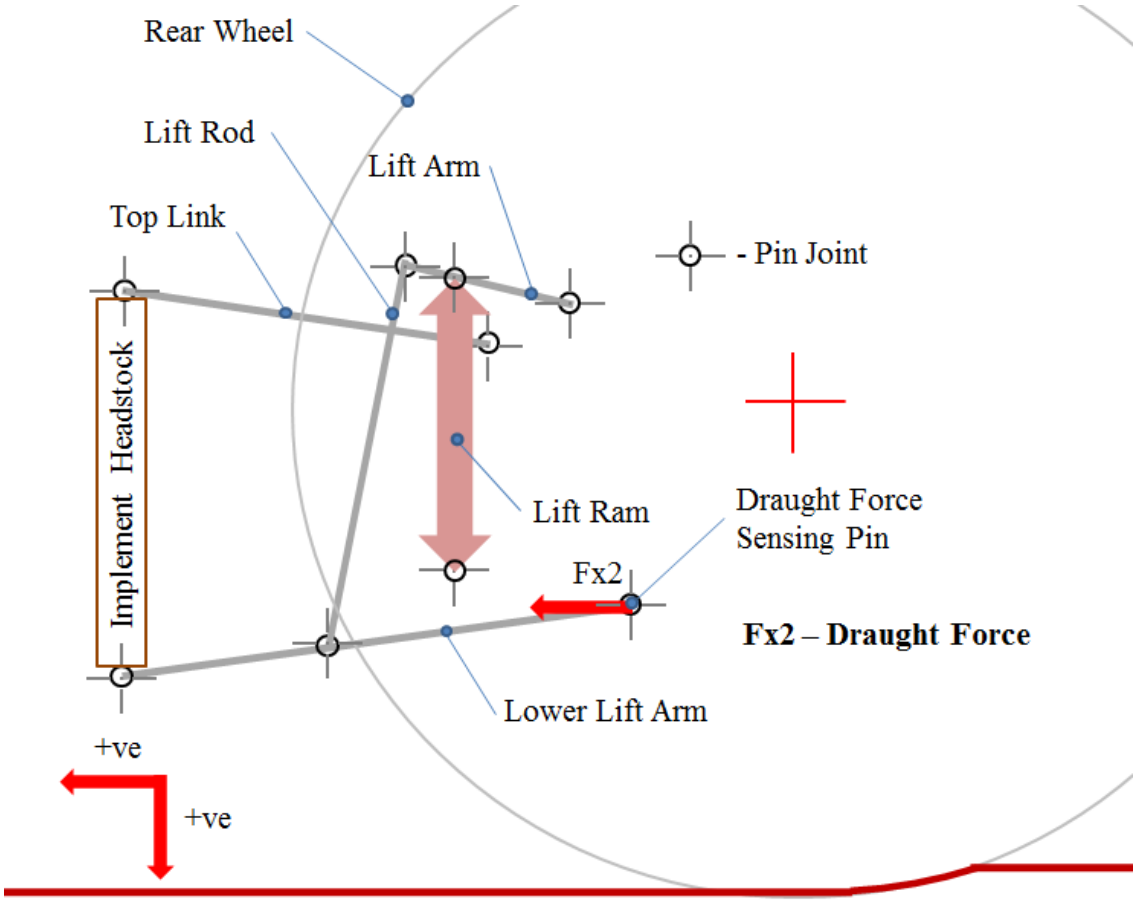

Figure 9: Schematic representation of a modern three point linkage components

(Source: This study)

The three point linkage was developed to allow the effects of implement forces producing weight transfer to be utilised in a positive manner. Whilst even in a trailed implement environment some usage can be made of weight transfer from front to back axles using the lever effect. However, in this application the vertical forces generated are not utilised. Ferguson recognised this by having three points of attachment to the tractor where the vertical force can be used to counteract the effects of draught force. Since the advent and now widespread usage of four wheel drive tractors this has become more relevant. The front wheels do work contributing to the tractive effort of the tractor. Earlier two wheel drive

tractors do not benefit to the same degree as four wheel drive tractors from a traction perspective, however there are stability and control benefits. Therefore front ballast can be reduced and the front wheels are more likely to remain in contact with the ground.

The three point linkage allows positive attachment to the tractor of an implement through the lower lift arms and top link attachment points. The forces seen in each linkage element are directly attributable to the tillage operation or work being conducted by the tractor. The lower lift arms (LLA) are the primary attachment point on the tractor of an implement and generally see tensile forces generated by draught force. The top link (FTL) is a secondary attachment point and allows vertical forces generated by the implement to be transferred to the tractor hence top link forces are generally compressive when operating the tractor linkage in normal control modes. It is possible to see purely tensile forces in the top link depending on the tillage operation and the position of the linkage at working depth. The function of the lift rods is to aid the positioning of the linkage in work which are actuated by the lift arms which in turn are actuated by the lift ram(s). The forces seen in the lift rods can be both tensile and compressive depending on the tillage operation. In general terms the forces in the lift rods are tensile (Keen *et al.*, 2009; Ward *et al.*, 2009; Ward *et al.*, 2011) due to the attachment to the lower lift arm which is usually under draught load (tensile force). However, the tensile element of the lift rod force can be counteracted by large vertical forces due to tillage; the setting of the linkage control system also will affect this particularly in Position control. In certain situations equilibrium can exist where the positive and negative forces in the lift rods cancel resulting in a zero force as seen by Davies (2006) in Figure 10.

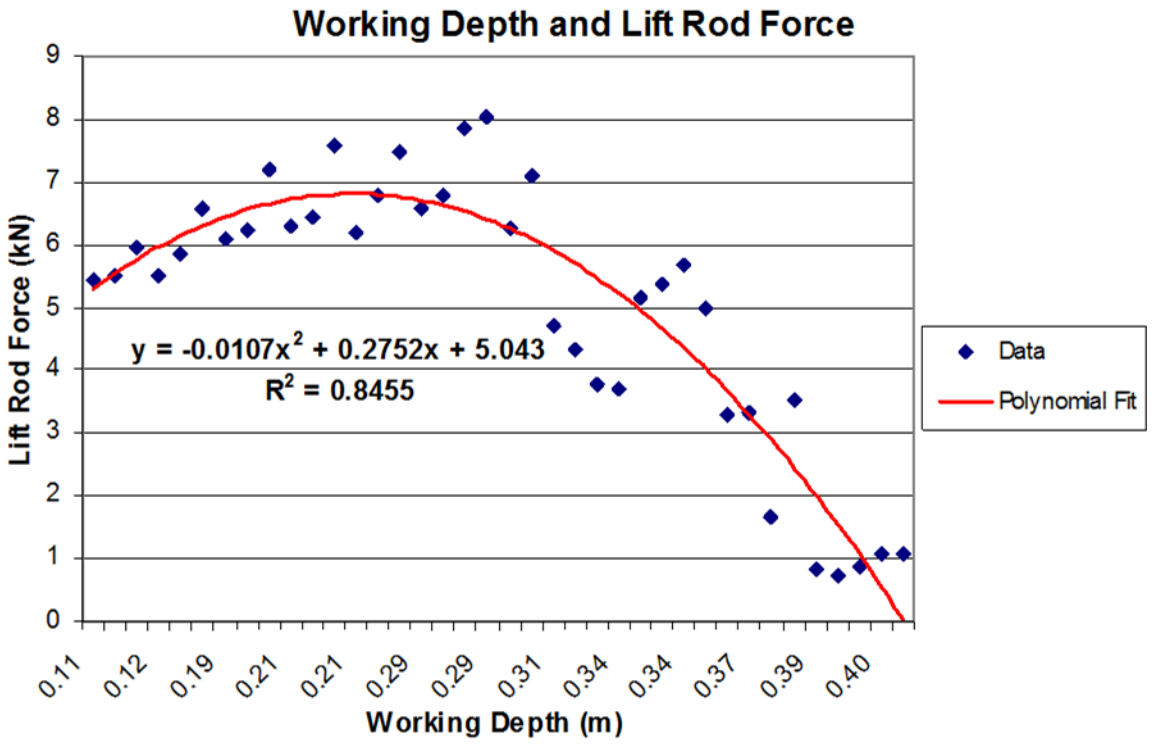

Figure 10: Lift rod forces plotted against working depth in field working experiment

(Source: Davies, 2006)

3.2 Linkage Kinematic Models

Many linkage models have been created in the past by many but more recent notable contributions have been made by Bentaher *et al.* (2008), Keen *et al.* (2009), Ward *et al.* (2009) and many others. According to Keen *et al.* (2009) the models used in existing tractor performance research have generally been of a quasi-static nature (Whitney, 1988; Zoz and Grisso, 2003) relying on force resolution using fixed or semi-fixed kinematic relationships between model elements. Usually accompanying those models were specific instrumentation systems. A unique feature of the models generated in this study is that they can be used on any tractor (provided draught force sensing pins are fitted) and allows it to be tuned to any linkage set up and used in real-time. One of the main issues when creating a kinematic model of a tractor three point linkage is that the working length of linkage components vary with day to day application change. With further work and the addition of top link and lower lift

arm angle sensing the model can be used regardless of implement or linkage configuration (Ward *et al.*, 2011). The model is a significant development of that used by Keen *et al.* (2009) shown in Figure 11 and has been presented by Ward *et al.* (2011) previously. The model relies on the use of the draught force sensing pins rather than strain gauges attached to the lower lift arms.

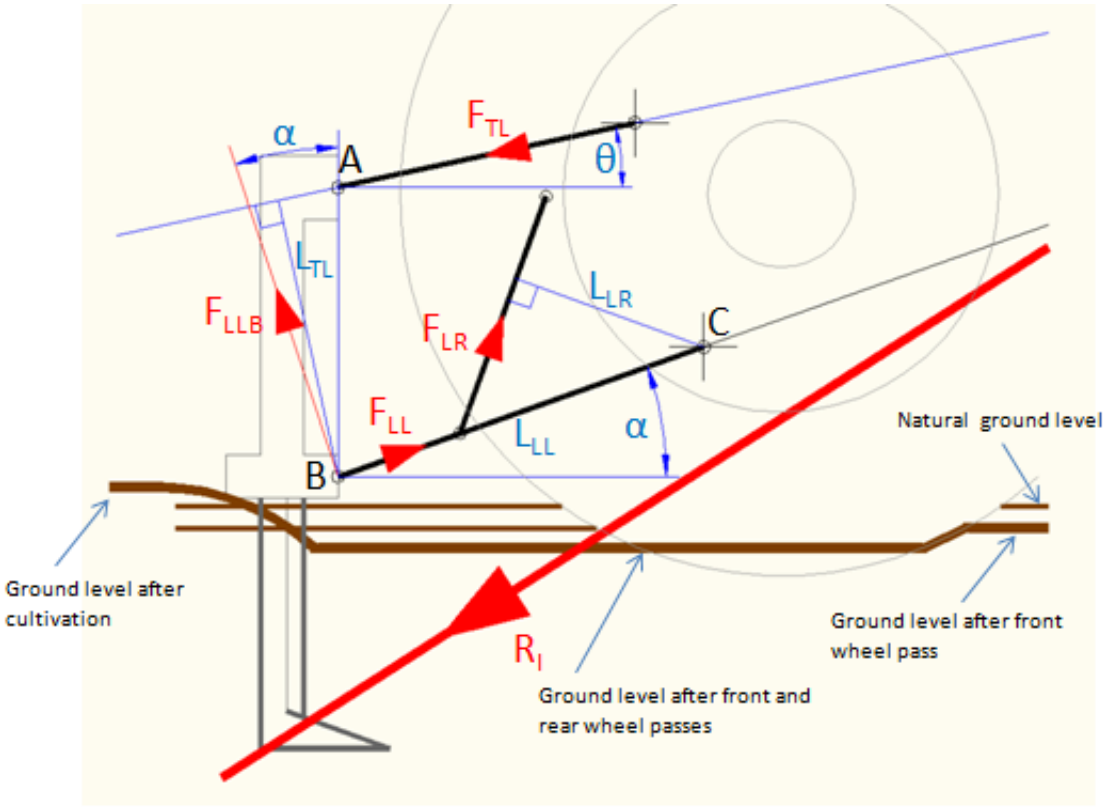

Figure 11: An example of a linkage force resolution model

(Source: Keen *et al.*,2009)

In any control system, that aims to monitor performance of a tractor, resolution of the forces created by work is critical. It allows real-time performance attributes to be calculated as the forces are a measure of the work done and also any possible improvements to the efficiency of the field operation can also be determined.

3.3 The Linkage Force Resolution Model

The linkage force resolution model generated in this study is a significant development of that used by Keen *et al.* (2009), being simpler and more versatile (Ward *et al.*, 2009 and Ward *et al.*, 2011). An additional element to the work presented by (Ward *et al.*, 2009 and Ward *et al.*, 2011) is the inclusion of an overall tractor dynamic kinematic model that incorporates tyre deflection, tractor sinkage and attitude correction factors; allowing implement depth to be measured based on kinematics rather than a physical measurement. The model is based around two reference planes – one horizontal and one vertical. The reference planes are based on fixed tyre pressures of 1.4 Bar front and 1.2 Bar rear and run horizontally and vertically through the tractor passing through the centre point of the rear axle. The planes are theoretical only as a point of reference for kinematic measurements of both the three point linkage and tractor axle centre heights.

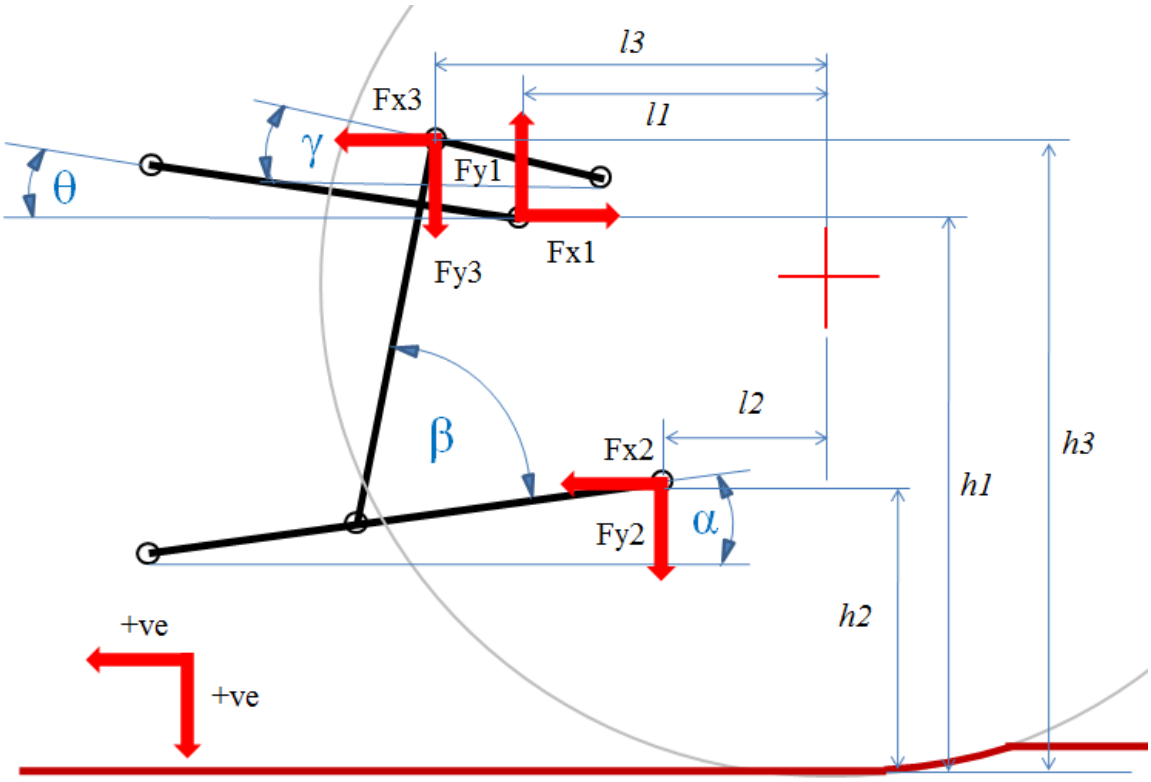

Figure 12: Three point linkage kinematics used in this study

(Source: Ward *et al.*, 2009 and Ward *et al.*, 2011)

Figure 12 shows the required parameters to resolve and evaluate the effects on the tractor draught force (Fx) and vertical forces (Fy) generated through field work. When evaluated the parameters can be used to calculate weight transfer, tractor sinkage, tyre deflection and performance attribute associated with the tillage operation. Forces are measured with a specific linkage instrumentation system.

The linear dimensions shown in Figure 12 were measured in this study using a commercially available laser-level at key three point linkage tractor interface points and axle centres. The laser was used to mark a vertical surface perpendicular to the ground at the various tractor interface points in the vertical plane; horizontal measurements of the points were made using a simple tape measure using the same vertical surface. The data collected are shown in Table 1 below.

Table 1: Massey Ferguson 8480 tractor and three point linkage kinematic linear measurements

Dimension (mm)	
Linkage kinematic position	**Horizontal and vertical measurements**
h1	1224
h2	601
h3	1334*
l1	448
l2	217
l3	608*
Front axle height (FAH)	940**
Rear axle height (RAH)	704**

* - Requires real time correction due to lift arm angle

** - Quasi-static 1.4 Bar Front and 1.2 Bar rear tyre inflation

(Source: This study)

It is assumed that the forces act on the tractor at their attachment point. Using standard mathematical trigonometric functions the following equations were developed during this study to generate the kinematic model.

Resolve axially measured force in the top link, FTL, horizontally:

$$Fx1 = FTL. \cos \theta \text{ (kN)}$$

Equation 3.1

Where,

Fx1 = Resolved horizontal force component of FTL (kN);

FTL = Measured axial force in the top link (kN);

cos = Trigonometric mathematical function;

θ = Angular displacement between top link and horizontal reference plane (^{o}).

The horizontal force component (Fx2) of the lower lift arms is measured:

$$Fx2 = LLP + RLP \text{ (kN)}$$

Equation 3.2

Where,

Fx2 = Summed measured horizontal force component of LLP and RLP (kN);

LLP = Measured horizontal force in the nearside (left) lower lift arm (kN);

RLP = Measured horizontal force in the offside (right) lower lift arm (kN).

Resolve axially measured combined forces in the lift rods, FLR, horizontally:

$$FLR = LLR + RLR \text{ (kN)}$$

Equation 3.3

Where,

FLR = Summed measured axial force component of LLR and RLR (kN);

LLR = Measured axial force in the nearside (left) lift rod (kN);

RLR = Measured axial force in the offside (right) lift rod (kN).

Therefore:

$$Fx3 = FLR. \cos(\alpha+\beta) \text{ (kN)}$$

Equation 3.4

Where,

Fx3 = Resolved horizontal force component of FLR (kN);

cos = Trigonometric mathematical function;

α = Angular displacement between lower lift arm and horizontal reference plane (^{o});

β = Angular displacement between lower lift arm and lift rod (^{o}).

Resolve axially measured force in the top link, FTL, vertically:

$$Fy1 = FTL. \sin\theta \text{ (kN)}$$

Equation 3.5

Where,

Fy1 = Resolved vertical force component of FTL (kN).

Calculate the vertical force component acting on the lower lift arms:

$$Fy2 = Fx2. \tan \alpha \text{ (kN)}$$

Equation 3.6

Where,

Fy2 = Calculated resultant vertical force component of Fx2 (kN).

Resolve axially measured combined forces in the lift rods, FLR, vertically

$$Fy3 = FLR. \sin (\alpha+\beta) \text{ (kN)}$$

Equation 3.7

Where,

Fy3 = Resolved vertical force component of FLR (kN).

The component draught forces can be summed into a total draught force:

$$Fx = Fx1 + Fx2 + Fx3 \text{ (kN)}$$

Equation 3.8

Where,

Fx = Summed horizontal three point linkage forces acting on the tractor (kN).

The component vertical forces can be summed into a total vertical force:

$$Fy = Fy1 + Fy2 + Fy3 \text{ (kN)}$$

Equation 3.9

Where,

Fy = Summed vertical three point linkage forces acting on the tractor (kN).

Using the resolved linkage force data, weight of the tractor and the tractor wheelbase, quasi-static weight transfer is calculated by first and calculating the change in normal front axle ground reaction force by taking moments:

$$\delta ZF = \frac{(Fx1 - Fx2 - Fx3) + (Fy1 - Fy2 - Fy3)}{Lwb} \text{ (kN)}$$

Equation 3.10

Where,

δZF = Change in front axle ground reaction force (kN);

Lwb = Horizontal distance between front and rear axle centerlines (mm).

Using the calculated value of δZF above the change in rear axle ground reaction force can be calculated using the following:

$$\delta ZR = (mg - \delta ZF - ZF - ZR) + Fy1 + Fy2 + Fy3 \text{ (kN)}$$

Equation 3.11

Where,

δZR = Change in rear axle ground reaction force (kN);

mg = The mass of the tractor implement combination multiplied by gravity (kN);

δZF = Change in front axle ground reaction force (kN);

ZF = Nominal static front axle ground reaction force (kN);

ZR = Nominal static rear axle ground reaction force (kN).

Weight transfer equations 3.10 and 3.11 are for a quasi-static system where ZF and ZR are known and a quasi-static linkage position is known. However to make the model more versatile where perhaps ZF and ZR are not known δZF and δZR can be calculated using moments theory about the rear tyre contact patch with the ground surface. Therefore using

data from Table 1 and resolved forces Fx1, Fx2, Fx3, Fy1, Fy2 and Fy3 the following equations can be used to calculate weight transfer/addition to front and rear tractor axles using simple moment's theory. It is important to note that dimensions h3 and l3 vary with linkage position as the transmission to the tractor chassis is via the lift arm and therefore require correction. Therefore:

$$\delta ZF = \frac{(Fx1.h1 - Fx2.h2 - Fx3.(h3 - (\gamma.\cos 355)))}{Lwb} + \frac{(Fy1.l1 - Fy2.l2 - Fy3.(l3 - (\gamma.\sin 355)))}{Lwb} \text{ (kN)}$$

Equation 3.12

Where,

δZF = Dynamic change in front axle ground reaction force (kN);

h1 = Vertical distance between tyre contact and top link attachment point (mm);

h2 = Vertical distance between tyre contact and lower lift arm attachment point (mm);

h3 = Vertical distance between tyre contact and lift arm / lift rod pin joint (mm);

11 = Horizontal distance between rear axle centre and top link attachment point (mm);

l2 = Horizontal distance between rear axle centre and lower lift arm attachment point (mm);

l3 = Horizontal distance between rear axle centre and lift arm / lift rod pin joint (mm);

Lwb = Horizontal distance between front and rear axle centerlines (mm).

Therefore using simple force equilibrium:

$$\delta ZR = Fy1 + Fy2 + Fy3 - \delta ZF \text{ (kN)}$$

Equation 3.13

Where,

δZR = Dynamic change in rear axle ground reaction force (kN).

The model does take into account tyre deflection through variation of vertical kinematic measurements h1, h2 and h3 and as tractor attitude angle changes are likely to be relatively small can be used without correction. For example to correct for a tractor attitude change of 10 ° the cosine of the angle is 0.9848 resulting in a 1.512 % error factor which is well within the limits of experimental and measurement error.

3.3.1 Practical Usage of the Linkage Force Resolution Model

The linkage force resolution model is based on measured force data and positional measurement of the linkage components. Angular displacement is based on a singular positional measurement of the linkage as described by Ward *et al.* (2011). Shown in Figure 13 is the two dimensional model of the Massey Ferguson three point linkage that was developed in computer aided design software for this study. The model relies on fixed linkage component lengths for a given implement headstock design and a singular angular positional measurement on the lift arm assembly. The purpose of the fully articulating model was so that the linkage could be articulated as installed on the tractor with the angles β, γ and θ, measured for a given α angular input with reference to the tractor horizontal reference plane. The measured data is used to derive a series of equations to calculate the relationship of β, γ and θ with respect to α to avoid the use of look up tables. Combining the measured attributes and the linkage kinematics allows full force resolution into Fx and Fy either statically or in real time through the logging of measurement data using equations presented in Section 3.3.

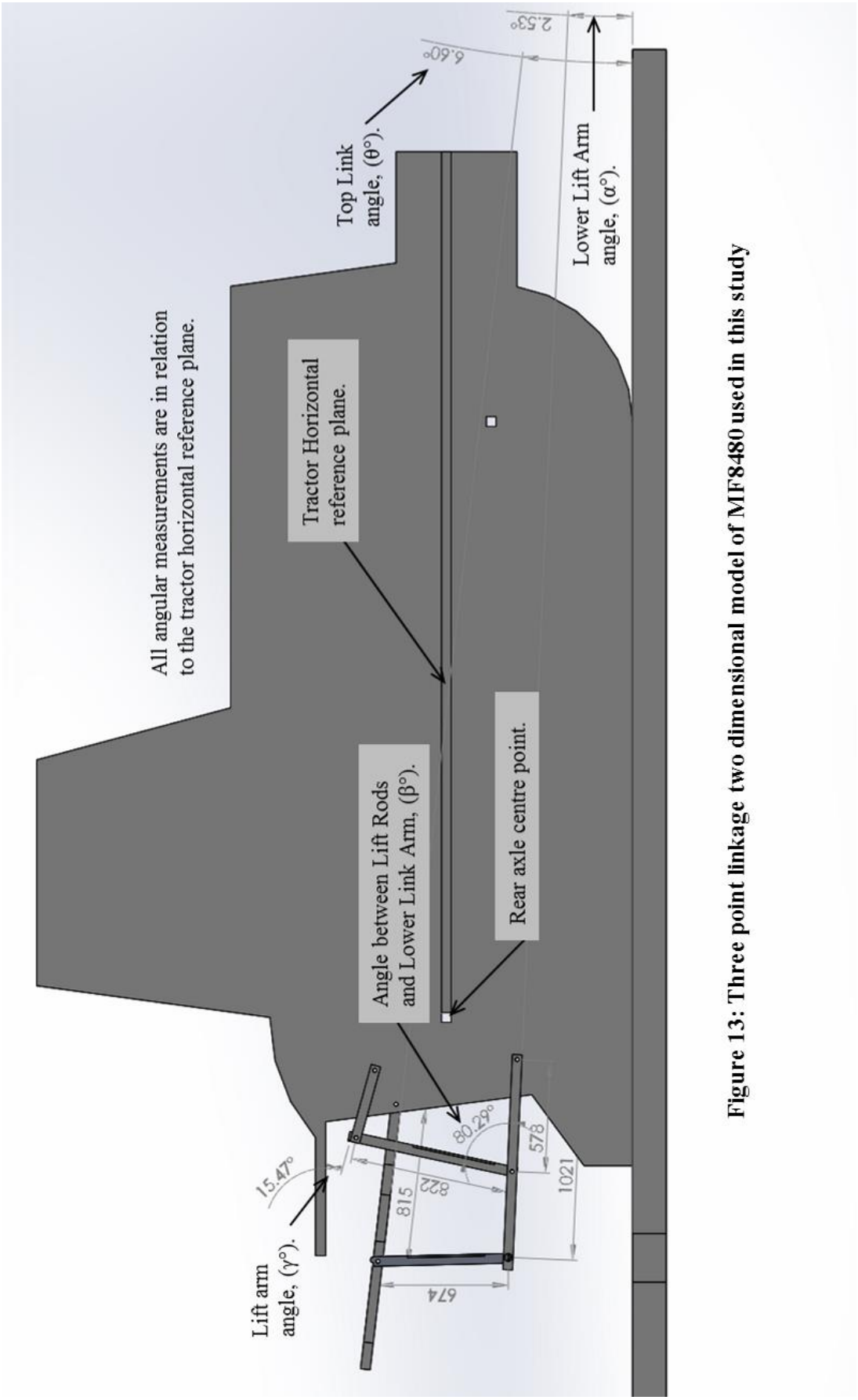

Figure 13: Three point linkage two dimensional model of MF8480 used in this study

Through articulation of the linkage model data were created to generate the necessary values for creation of the kinematic equations and is presented in Table 2 below.

Table 2: Kinematic links between the three point linkage components of the MF8480

Lower Lift Arm Distance to Ground (mm) *	Predicted Implement Tillage Depth (IID) (mm) **	α (°)	β (°)	γ (°)	θ (°)
200	562	22.76	56.82	24.26	25.16
250	512	19.75	59.86	19.39	21.34
300	462	16.8	62.77	14.7	17.62
350	412	13.89	65.56	10.14	13.97
400	362	11.01	68.27	5.66	10.37
450	312	8.17	70.89	1.24	6.81
500	262	5.34	73.45	-3.15	3.28
550	212	2.53	75.94	-7.53	-0.25
600	162	-0.28	78.38	-11.92	-3.77
650	112	-3.09	80.76	-16.36	-7.31
700	62	-5.9	83.09	-20.86	-10.88
750	12	-8.73	85.37	-25.45	-14.49
800	-38	-11.58	87.59	-30.16	-18.16
850	-88	-14.47	89.76	-35.03	-21.9
900	-138	-17.38	91.86	-40.1	-25.74
950	-188	-20.35	93.8	-45.42	-29.7
1000	-238	-23.37	95.8	-51.08	-33.8

* - From the centre line of lower lift arm attachment ball

** - Implement set up used in this study is 762 mm tine tip to lower lift arm attachment centre with the depth as an indication only in a static condition

(Source: This study)

Shown below in Figures 14 to 17 are graphical representations of the mathematical relationships between the kinematic parameters; quasi-static predicted implement tillage depth (IID), β, γ, θ and α presented in Table 2 above. The angular displacement of the lower lift arm, α , was chosen as the reference variable for all angular measurements as lower lift arms are generally of fixed length geometry related to a tractor type or model; lift rods, top links and implement headstocks are of a variable nature. The generation of the equations allows positional measurement to take place in multiple locations on the linkage.

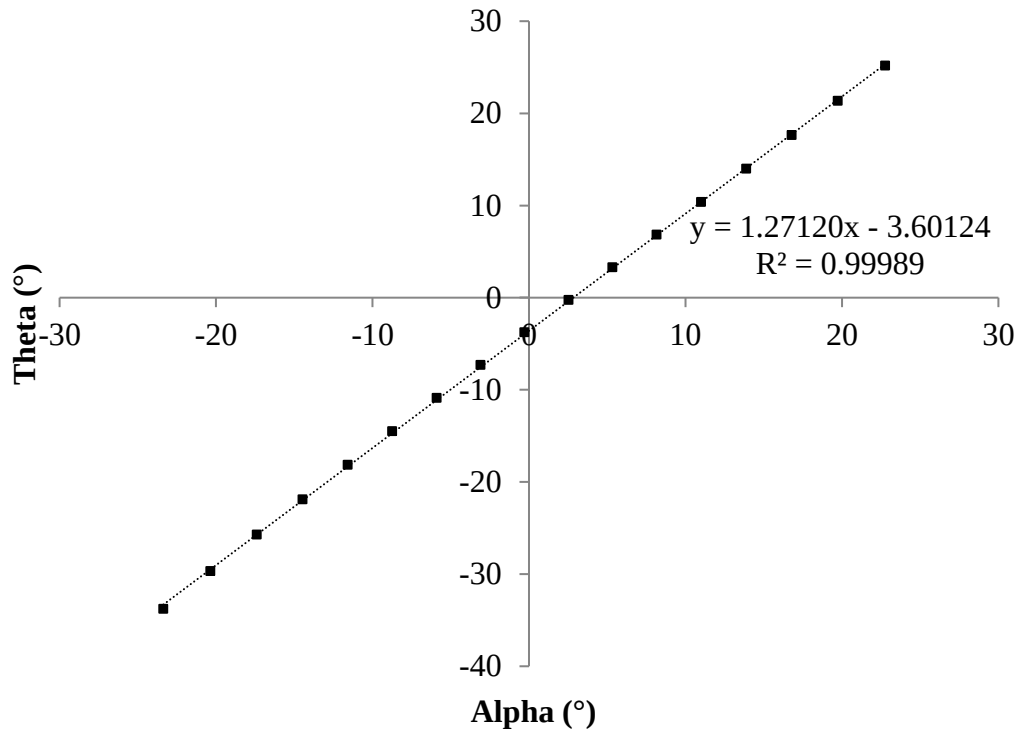

Figure 14: Calculated kinematic relationship between theta (θ) and alpha (α)

(Source: This study)

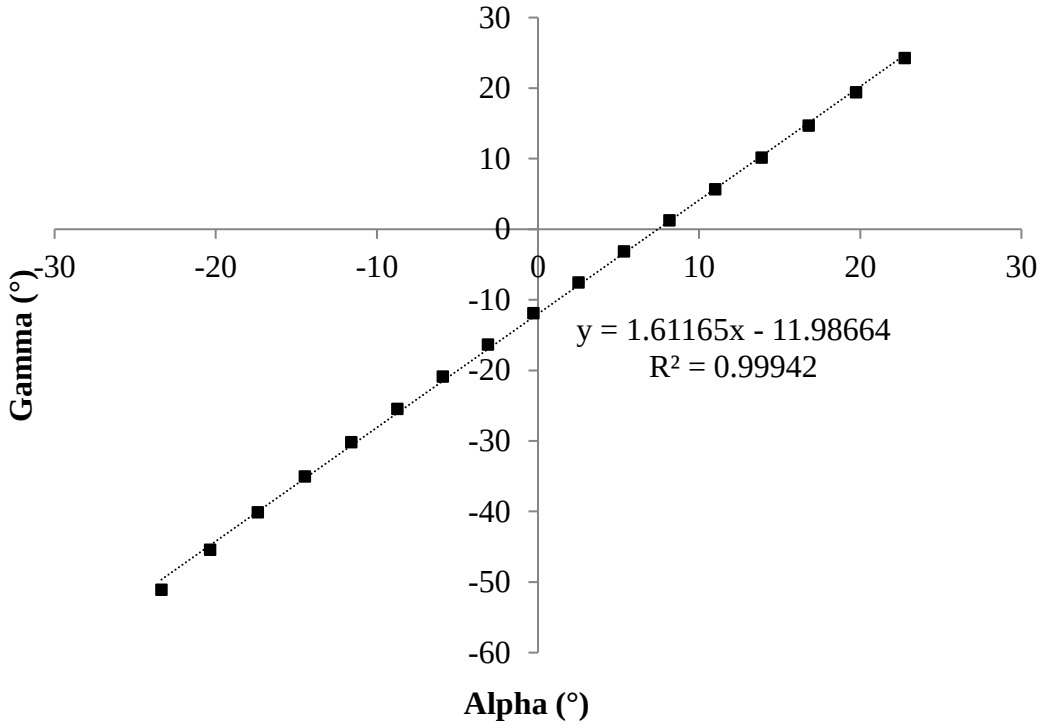

Figure 15: Calculated kinematic relationship between gamma (γ) and alpha (α)

(Source: This study)

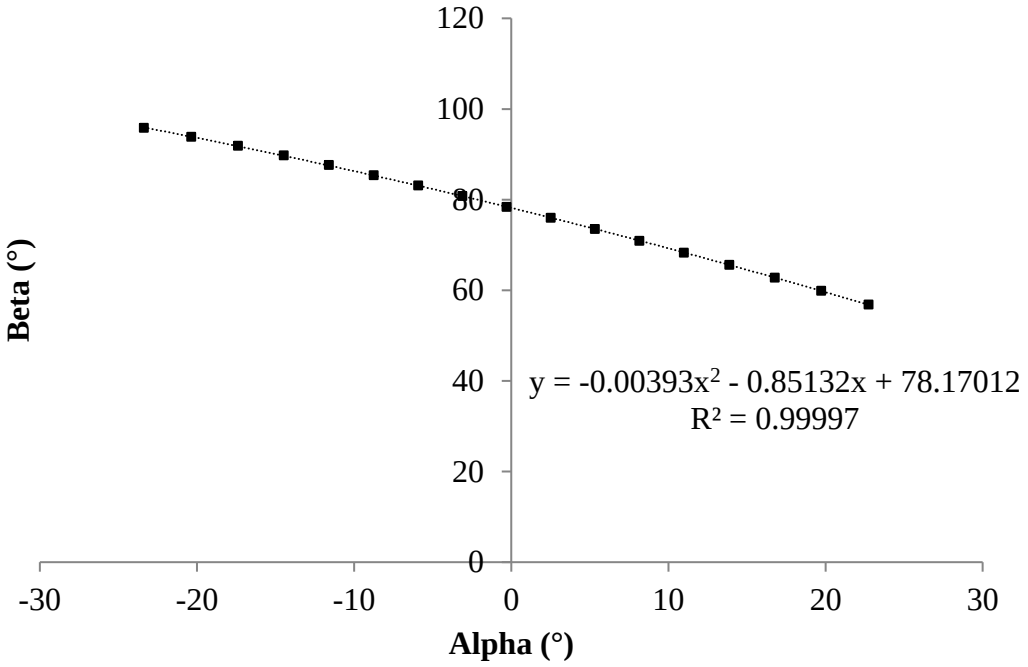

Figure 16: Calculated kinematic relationship between beta (β) and alpha (α)

(Source: This study)

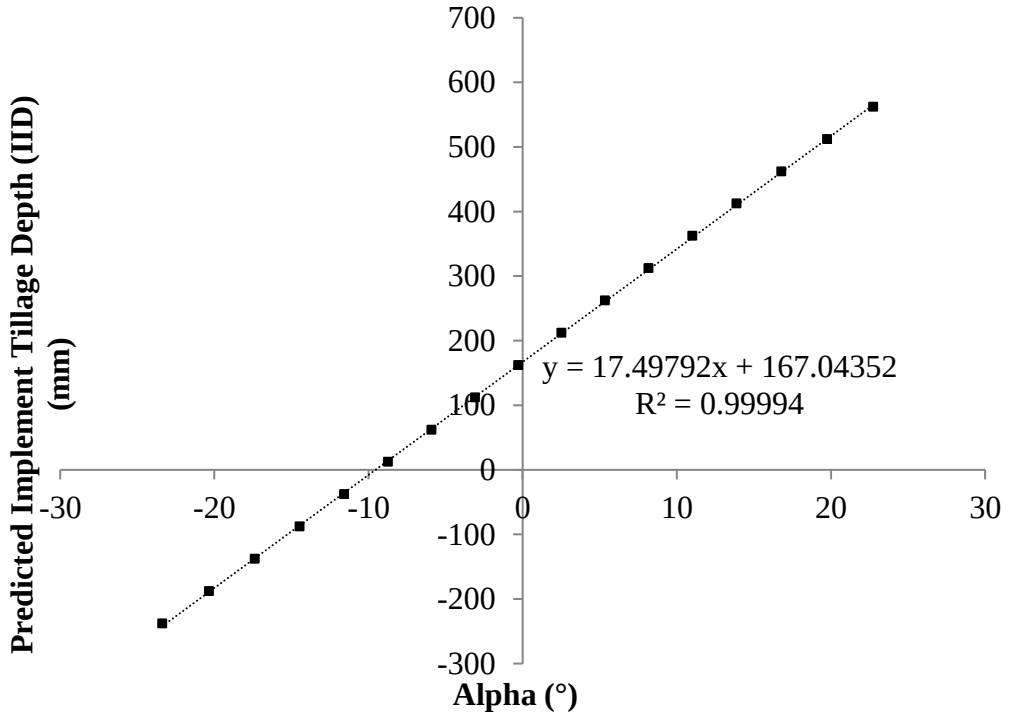

Figure 17: Calculate kinematic relationship between predicted implement tillage depth (IID) and alpha (α)

(Source: This study)

It can be seen from the equations of best fit lines in Figures 14 to 17 that R^2 values for the data sets are 0.99989, 0.99942, 0.99997 and 0.99994. This gives confidence in the accuracy of the data collection and as the model is computer based indicates that the data were collected in an accurate way.

Using trend line equations given in Figures 14 to 17, with greater numeric precision than that displayed, equations generated for the linkage angular displacement parameters are calculated as follows:

$$\beta = -0.00392890.\ \alpha^2 - 0.85132316.\ \alpha + 78.17011829\ (^o)$$

Equation 3.14

Where;

α = Angular displacement of lower lift arm with respect to the tractor horizontal reference plane (°);

β = Angular displacement between lower lift arm and corresponding lift rod (°).

$$\gamma = 1.61165350.\ \alpha - 11.98664105\ (^o)$$

Equation 3.15

Where;

γ = Angular displacement of lift arm with respect to the tractor horizontal reference plane (°).

$$\theta = 1.27119507.\ \alpha - 3.60124377\ (^{o})$$

Equation 3.16

Where;

θ = Angular displacement of top link with respect to the tractor horizontal reference plane (°).

$$IID = 17.49792047.\ \alpha + 167.04351825\ (mm)$$

Equation 3.17

Where;

IID = Quasi-static prediction of implement tillage depth (mm).

Substituting the derived Equations, 3.14 to 3.1, of the relationships between β, γ, θ and α, into equations 3.1, 3.3 to 3.5, 3.7 and 3.12 the final set of linkage force resolution model equations are generated. Therefore:

Substitute equation 3.16 into equation 3.1 to resolve the axially measured force in the top link, FTL, horizontally:

$$Fx1 = FTL.\ \cos\theta\ (kN)$$

Equation 3.18

Substitute Equation 3.14 into Equation 3.4 to resolve the axially measured combined forces in the lift rods, FLR, horizontally:

$$Fx1 = FTL.\ \cos(1.27119507.\ \alpha - 3.60124377)\ (kN)$$

Equation 3.19

Substitute Equation 3.16 into Equation 3.5 to resolve the axially measured force in the top link, FTL, vertically:

$$Fx3 = FLR.\cos(\alpha + (-0.00392890.\alpha^2 - 0.85132316.\alpha + 78.17011829))\ (kN)$$

Equation 3.20

Substituting Equation 3.14 into Equation 3.7 to resolve the axially measured combined forces in the lift rods, FLR, horizontally:

$$Fy1 = FTL.\sin(1.27119507.\alpha - 3.60124377)\ (kN)$$

Equation 3.21

Substitute equation 3.15 into Equation 3.12 to calculate change in front axle load, δZF:

$$\delta ZF = \frac{(Fx1.h1 - Fx2.h2 - Fx3.(h3 - ((1.61165350.\alpha - 11.98664105).\cos(355))))}{Lwb}$$

$$+ \frac{(Fy1.l1 - Fy2.l2 - Fy3.(l3-((1.61165350.\alpha - 11.98664105).\sin(355))))}{Lwb}\ (kN)$$

Equation 3.22

Note: Lower lift arm angle, α, is defined later in this research in Chapter 4 as it is a numeric value that is directly related to an electronic positional measurement.

The above model allows the kinematic parameters to be defined and used in the control algorithm that forms the basis of this work. Whilst there are limitation the model goes some way towards a system that could be incorporated on a commercial product as well as be highly suitable for research purposes. However there are further corrections that need description, although small in value the effects on precision of any system are important.

3.4 Linkage Force Resolution Model Correction Factors

The linkage force resolution model created assumes all components of the three point are acting in one vertical, longitudinal plane. However, in reality this is not the case and therefore corrections should be made to ensure force calculations are as accurate as possible. Figure 18 schematically demonstrates the scale of the corrections required.

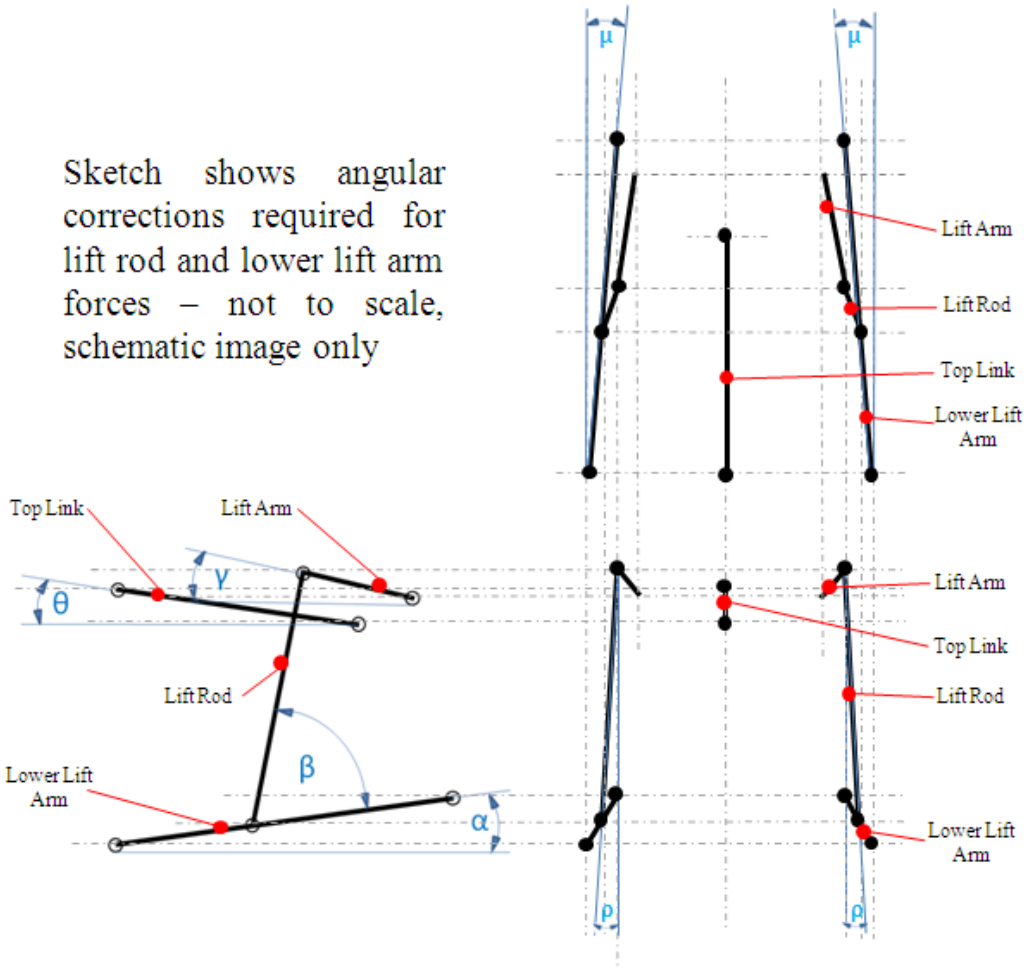

Figure 18: Linkage force resolution model correction factors

(Source: Ward *et al.*, 2009)

The linkage force resolution model is based on the use of the standard tractor draught force sensing pins. Therefore correction factor shown in Figure 18, μ is not required as the draught force sensing pins measure the draught force acting at the lower lift arm tractor attachment point. However when resolving lift rod forces, LLR and RLR, it is necessary to further

resolve the measured forces by an angular factor shown in Figure 18, ρ. The angular displacement values, ρ, are usually within the range of 5 ° to 10 ° and therefore the error is small. However to enable a system to be as accurate as possible this correction should be incorporated where possible.

Generally lift arms are cranked, however no correction is required as the lift arm has no swivel-pin joint attached at the tractor attachment point and is directly linked to the cross shaft.

3.5 Tractor Dynamic Kinematic Model

The linkage force resolution model is based on quasi-static vertical dimensions h1 to h3. To ensure all dynamic variations in these dimensions are corrected a tractor dynamic kinematic model was generated to apply correctional factors. The corrections consist of tractor sinkage, attitude change and tyre deflection. The subject of tractor or vehicle attitude/pitch is not new and has been covered by many in the past and has a direct effect on tillage depth and weight transfer calculation. During the creation of the linkage force resolution model a calculation proposal was made of a predicted implement tillage depth (IID). One of the elements of this study is to improve tractor efficiency through more accurate tillage depth control and therefore accurate tillage depth prediction (IID) is critical where a measured implement tillage depth (AID) is not available.

Therefore to generate the required correctional factor equations an additional two dimensional model was built in three dimensional computer aided design software to replicate the tractor axle heights, wheelbase and lower lift arm. The model is shown in Figure 19 below with the aim of establishing the effects of axle height position on actual implement tillage depth through tractor sinkage and tractor attitude change, σ.

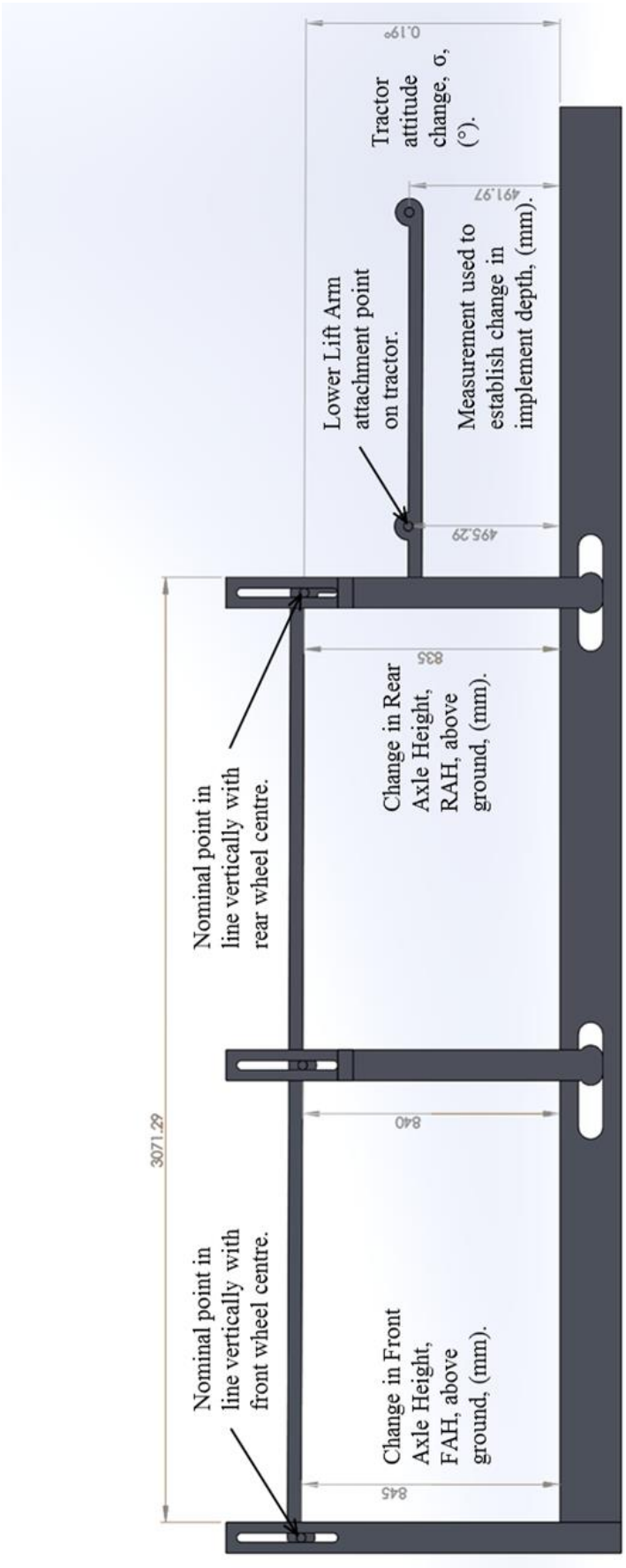

Figure 19: Tractor axle height dynamic kinematic corrections model

(Source: This study)

The purposes of the calculations are that with known implement characteristics, tyre stiffness properties, linkage kinematics and weight transfer it is possible to automatically calculate a predicted implement tillage depth (IID) without directly measuring it.

The model was constructed using a nominal centre point between the front and rear axles as a sinkage measurement point; this point is not at the tractor implement combination centre of gravity as this will shift with weight transfer. From a linkage to ground positional relationship the tractor does not pivot around this nominal midpoint but has three degrees of freedom; front tyre deformation, rear tyre deformation and overall sinkage. The model was constructed to allow the effective tractor wheel base (Lwb) to change with tractor attitude change (σ).

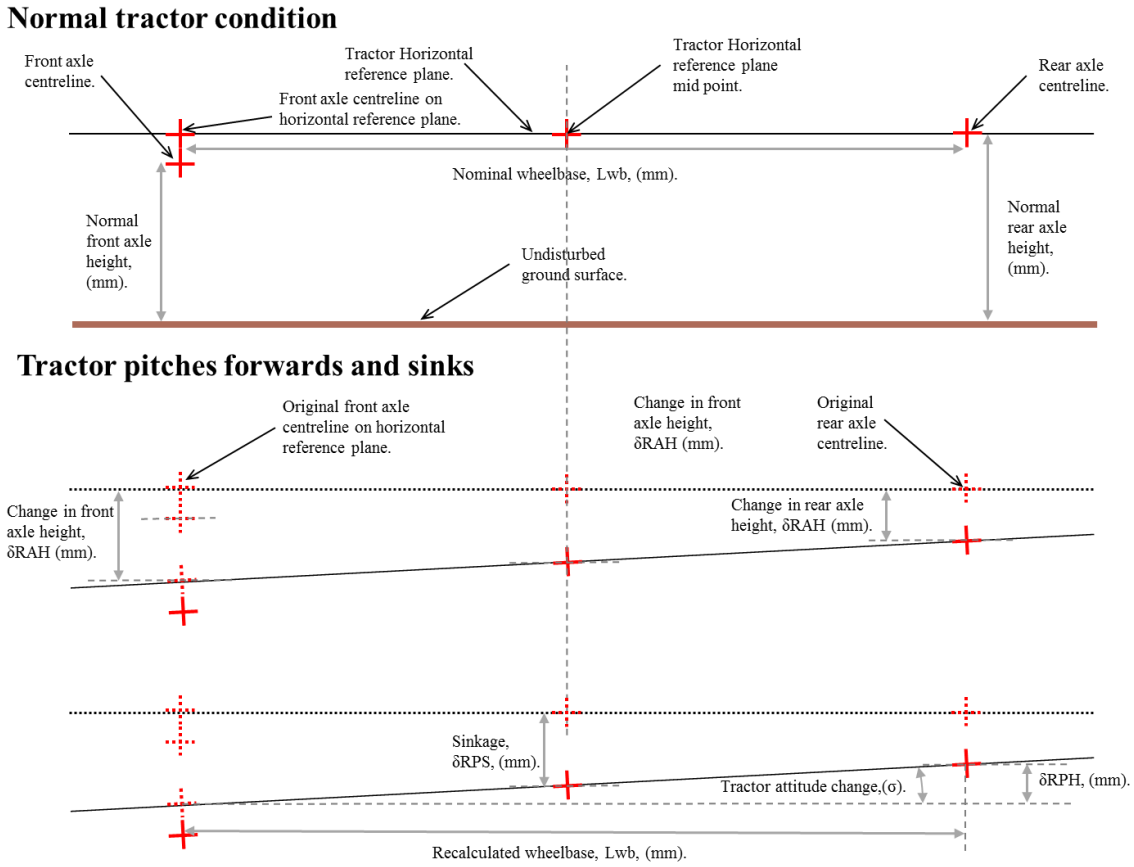

Figure 20: Graphical image of tractor dynamic kinematic model equation parameters

(Source: This study)

Shown graphically in Figure 20 is the first part of the process in defining how the relationship between front axle height (δFAH) and rear axle height (δRAH) changes by a nominal height.

This relationship for the purposes of this model is defined as δRPH:

$$\delta RPH = \delta RAH - \delta FAH \text{ (mm)}$$

Equation 3.23

Where,

δRPH = Nominal change in height differential between front and rear axles above the undisturbed ground (mm);

δRAH = Nominal change in height of the rear axle centreline above the undisturbed ground (mm);

δFAH = Nominal change in height of the front axle centreline above the undisturbed ground (mm).

By measuring the axle height changes in relation to the tyre and ground surface contact patch, tyre deflection can therefore be discounted in this method of calculating tractor attitude; it is relevant though for the purposes of force resolution. The convention used for this very simple formula is an increase in front axle height (δFAH) is positive and an increase in rear axle height (δRAH) is negative. This is necessitated by the need to understand whether the tractor is pitching forwards (σ is -ve) or rearwards (σ is +ve) as this can then related directly to the change in implement tillage depth caused.

Tractor attitude change, σ, is defined as:

$$\sigma = (\delta RPH / Lwb). \sin^{-1} (^{o})$$

Equation 3.24

Where,

σ = Tractor attitude change in relation to the undisturbed ground surface (°);

Lwb = Horizontal distance between front and rear axle centre lines (mm).

Overall tractor reference plane height change, which could be described as tractor sinkage (δRPS) is defined below.

$$\delta RPS = \delta FAH + \delta RAH \text{ (mm)}$$

Equation 3.25

Where,

δRPS = Nominal change in height of the tractor horizontal reference plane, at the centre point between front and rear axles, above the undisturbed ground (mm).

Whilst equations 3.23 and 3.25 are similar, they must not be confused, both have an effect on the tillage depth when using the tractor in a Position Control mode or where the implement is position is fixed in relation to the tractor. As can be seen the effects on implement tillage depth can automatically be calculated if the change in front and rear axle heights is known. Data collected from the three dimensional computer model were manipulated as shown in Tables 3 and 4 and Figure 21 to describe the tillage depth change through tractor attitude change only.

Note: all dimensions are based on a quasi-static instance neglecting tyre deflection at this stage and in relation to the ground using tractor parameters presented earlier in Table 2.

Table 3: Data generated from the tractor dynamic kinematic model for negative attitude/pitch changes (pitching forwards)

Change in RPH (mm)	Change in σ (°)	Change in Lwb (mm)	Change in h2 (mm) due to σ	Change in AID*(mm) due to σ
-200	-3.73	3064.80	-114.80	-181.44
-190	-3.55	3065.43	-109.03	-172.16
-180	-3.36	3066.03	-103.27	-163.08
-170	-3.17	3066.60	-97.51	-154.00
-160	-2.99	3067.14	-91.75	-144.92
-150	-2.80	3067.65	-85.99	-135.84
-140	-2.61	3068.12	-80.24	-126.77
-130	-2.43	3068.56	-74.49	-117.69
-120	-2.24	3068.96	-68.74	-108.62
-110	-2.05	3069.34	-62.99	-99.55
-100	-1.87	3069.68	-57.25	-90.49
-90	-1.68	3069.99	-51.51	-81.43
-80	-1.49	3070.27	-45.77	-72.37
-70	-1.31	3070.51	-40.04	-63.31
-60	-1.12	3070.72	-34.31	-54.26
-50	-0.93	3070.90	-28.58	-45.21
-40	-0.75	3071.05	-22.86	-36.16
-30	-0.56	3071.16	-17.14	-27.11
-20	-0.37	3071.24	-11.42	-18.07
-10	-0.19	3071.29	-5.71	-9.03
0	0.00	3071.31	0.00	0.00

* - Measured implement tillage depth (AID)

(Source: This study)

Table 4: Data generated from the tractor dynamic kinematic model for negative attitude/pitch changes (pitching rearwards)

Change in RPH (mm)	Change in σ (°)	Change in Lwb (mm)	Change in h2 (mm) due to σ	Change in AID (mm) due to σ
0	0.00	3071.31	0.00	0.00
10	0.19	3071.29	5.71	9.03
20	0.37	3071.24	11.41	18.06
30	0.56	3071.16	17.11	27.08
40	0.75	3071.05	22.80	36.10
50	0.93	3070.90	28.49	45.12
60	1.12	3070.72	34.18	54.13
70	1.31	3070.51	39.86	63.13
80	1.49	3070.27	45.54	72.14
90	1.68	3069.99	51.22	81.14
100	1.87	3069.68	56.89	90.13
110	2.05	3069.34	62.56	99.12
120	2.24	3068.96	68.22	108.10
130	2.43	3068.56	73.88	117.09
140	2.61	3068.12	79.53	126.06
150	2.80	3067.65	85.18	135.03
160	2.99	3067.14	90.83	144.00
170	3.17	3066.60	96.47	152.96
180	3.36	3066.03	102.10	161.96
190	3.55	3065.43	107.73	170.86
200	3.73	3064.80	113.36	179.81

* - Measured implement tillage depth (AID)

(Source: This study)

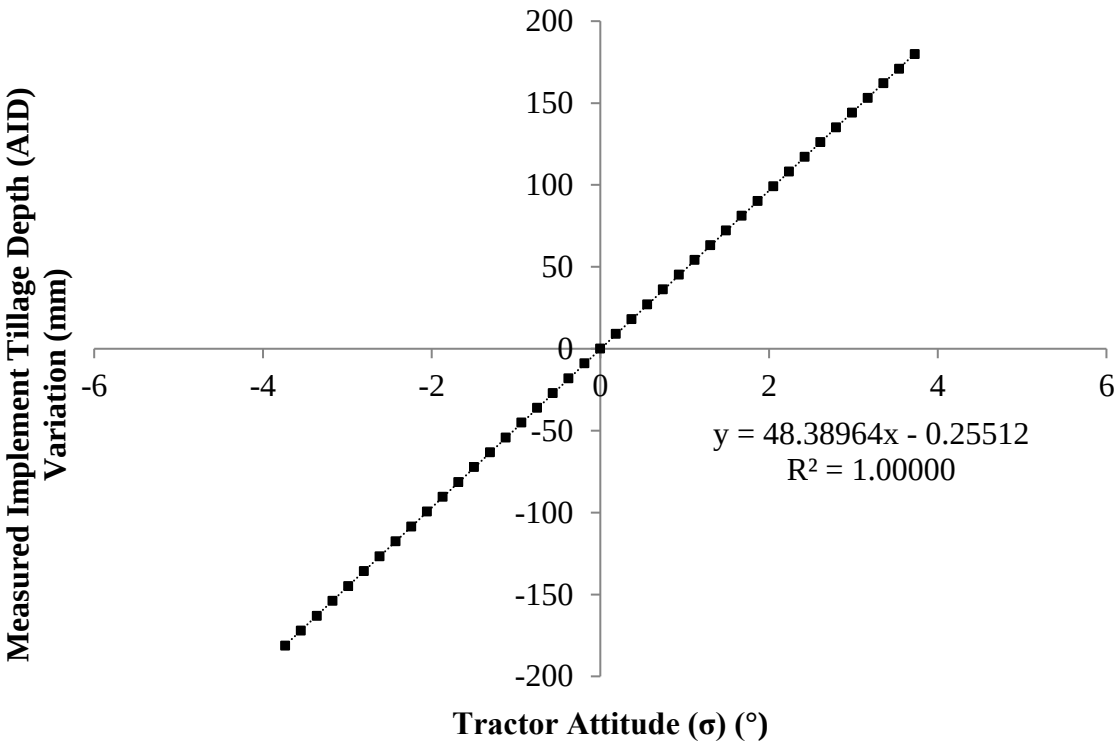

Figure 21: Effect on measured implement tillage depth (AID) due to tractor attitude changes (σ)

(Source: This study)

The final corrective action required from a tractor kinematics viewpoint is that of tyre deflection. Tyres are manufactured from an elastomeric rubber compounds with various stiffening materials. The apparent stiffness of a tyre is defined usually by its load rating i.e., the higher the load rating the stiffer the tyre. However this is not always the case as large tyres can have apparent high load ratings but this is due to the physical size rather than any special construction techniques. Inflation pressure also bears a huge significance on the load carrying ability of a tyre and hence stiffness (Dwyer, 1982).

The effects of load on tyre dimensions can be described using a simple spring rate formula; effectively the tyre is a spring that deforms under load or expands through load reduction.

$$F = k.\ x\ (kN)$$

Equation 3.26

Where,

F = Applied force to spring element (tyre) or generated spring force from compression (kN);

k = Spring constant (N mm^{-1});

x = Compressive or extensive linear deformation of spring element (mm).

Equation 3.26 can be rearranged in terms of x:

$$x = F / k\ (mm)$$

Equation 3.27

Using equation 3.27 it is possible to calculate the tyre deflections in real-time. By substituting *F* with the changes in front and rear axle loads (δZF and δZR) calculated in equations 3.13 and 3.22.

Therefore for the front tyres:

$$\delta Fx = \delta ZF / Frk\ (kN)$$

Equation 3.28

δZF = Change in front axle ground reaction force (kN);

Frk = Front tyre stiffness constant (N mm^{-1});

δFx = Additional front tyre deflection due to δZF (mm).

Therefore for the rear tyres:

$$\delta Rx = \delta RF / Rrk \text{ (kN)}$$

Equation 3.29

δZR = Change in rear axle ground reaction force (kN);

Rrk = Rear tyre stiffness constant (N mm^{-1});

δRx = Additional rear tyre deflection due to δZR (mm).

3.6 Kinematic Models Conclusion

The linkage force resolution and tractor dynamic kinematic models and equations generated within this chapter are both versatile and simplistic in nature and develop more recent research conducted by Keen *et al.* (2009), Ward *et al.* (2009) and Ward *et al.* (2011). Previously models used have been quasi-static in nature whereas the models presented here can be used in real time taking into account geometric and field variations. The linkage force resolution model allows forces generated through tillage to be resolved and used in performance, weight transfer and tyre deflection calculations. The tractor dynamic kinematic model integrated with the tractor dynamic kinematic model, allow tractor sinkage, attitude and weight transfer to be calculated through two simple dynamic axle height measurements in real-time. The follow on from this is that with known implement and dynamic linkage kinematics it is possible to predict implement tillage depth in real-time without actual measurement. The models lend themselves to incorporation into an implement tillage depth control algorithm and a real-time performance monitor. Previous attempts at performance related monitoring and control systems have required in-field calibration or previous-pass data to effect control of the next pass. The system developed in this study overcomes these constraints by the mathematical models operating dynamically in real-time with live data.

CHAPTER 4 – Control System Measured Parameter Requirements and System

4.1 Background

A key part of any system to control tractor performance is the three point linkage itself. It has been seen in Chapter 2 that there are several factors that affect the fuel usage of a tractor. These are:

- The efficiency of the engine converting the fuel energy by combustion into kinetic energy;
- The energy losses through the driveline of the tractor;
- The losses through the tyre ground interaction conditions- slip;
- The energy required to do work behind the tractor – its primary purpose.

Throughout the scope of this work it was not possible to improve the engine and transmission losses it is apparent that by reducing losses through increased efficiency of work that fuel savings can be made.

As was seen in Section 3.4 tillage depth has a pronounced effect on the draught force required to pull an implement through soil. The relationship as defined by Godwin (1974) is approximately squared whereby a factorial increase in depth of two will result in approximately four times the force required to do work. Through accurate measurement of draught force, wheel slip of the tyre ground interaction, tractor sinkage, tillage depth it is possible to predict with reasonable confidence where energy is used and also lost.

Measurement of the work done during draught tillage operations is simply defined by the following equations:

$$\text{Work Done} = \text{Force (N)} \times \text{Distance (m)} \text{ (Nm)}$$

Equation 4.1

$$\text{Drawbar Power} = \text{Draught Force (kN)} \times \text{Forward Speed (m s}^{-1}\text{)} \text{ (kW)}$$

Equation 4.2

As can be seen by measuring a few simple parameters it is possible to determine the energy required through drawbar work.

The following parts of this Chapter appraise previously used three point linkage measurement systems appropriate to this study.

4.2 Linkage Force Measurement Systems

4.2.1 Instrumented Load Frames

Many types of linkage force measurement systems have been developed for research and commercial purposes and one of the most common is the instrumented load frame. The frames consist of a manufactured metal framework that interconnects between tractor and implement and has been used extensively for research by Reece (1961), Reid *et al.* (1985), Clark and Adsit (1985), Chaplin *et al.* (1987), Palmer (1992), Godwin *et al.* (1993), McLaughlin *et al.* (1993), Al-Jalil *et al.* (2001) and Alimadarni *et al.* (2008). A typical example of an instrumented load frame is shown in Figure 22 below.

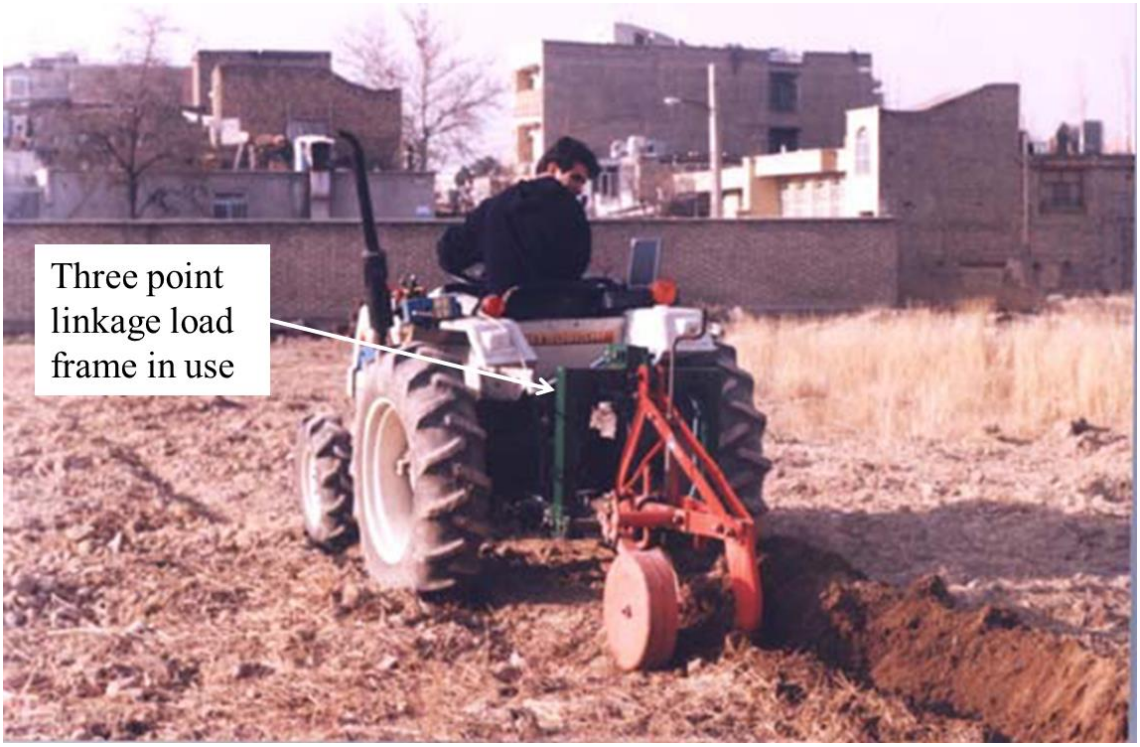

Figure 22: A typical linkage mounted load frame in use

(Source: Alimadarni *et al.*, 2008)

The instrumentation component of the frames has many guises such as the use of standard load cells, direct mounting of strain gauges or the use of load pins in the pin joints between either tractor and load frame or implement and load frame.

In some respects the instrumented load frame is an elegant simple solution. There are no issues with varying linkage element dimensional parameters or the resolution of forces within the linkage components; the instrumented load frame can be calibrated as a single instrument in horizontal and vertical planes and can be transferred from tractor to tractor. However, there are a number of limiting factors that curtail the usage in a commercial tractor application.

1. Due to positioning the implement further away from the tractor three point linkage the kinematics of the tractor implement combination are changed (Kirisci *et al.*, 1993) and become unrealistic;

2. Whilst the weight of the load frame can be taken into consideration during a system calibration the physical weight will alter the dynamic effects of vertical plane and any rotational forces. These will be inaccurately measured as the frame relocates the implement further away from the tractor;
3. Whilst transferability from tractor to tractor is possible generally the frames designed for a particular tractor implement combination and should be treated as a laboratory instrument;
4. The specific nature of the load frame and susceptibility to working environment damage render their suitability to commercial applications as unfeasible.

In conclusion the instrumented load frame is suitable as a research tool only with the limitations outlined above.

4.2.2 Linkage Dynamometers Mounted on the Linkage Elements

The disadvantages of the instrumented load frame led to the development of the Extended Octagonal Ring Transducer (EORT) (Kirisci *et al.*, 1993; Godwin *et al.*, 1993; Al-Janobi, 2000). These are precision manufactured instruments (Kirisci *et al.*, 1993) that are primarily used between the interfaces or are incorporated directly as part of the linkage elements. A distinct advantage of these instruments is that they are much lighter than the load frames but can still alter the kinematics of the tractor implement system. A typical example of a drawbar type EORT is shown in Figure 23 below.

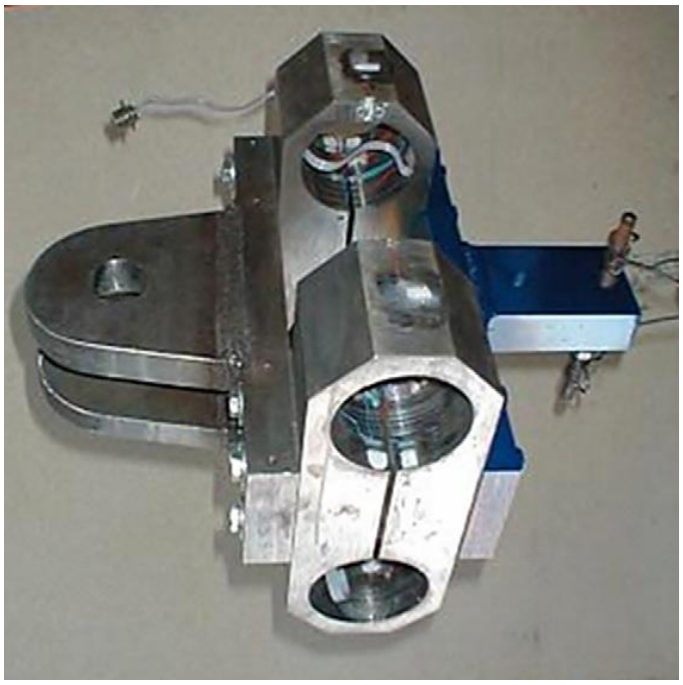

Figure 23: A drawbar type Extended Octagonal Ring Transducer (EORT)

(Source: Chen *et al.*, 2007)

The instruments measure force by the discreet application of strain gauges to the instrument to measure strain within the instrument through the application of force. It is a direct measurement system but generally costly to produce.

Strain gauges are not without limitations particularly durability and achieving the correct level of sensitivity through careful instrument design. In any commercial application strain gauges are not a truly viable solution. Although they are firmly attached to the instrument and can be protected, the day to day usage of the linkage and its environment may easily cause damage. A further disadvantage through the use of strain gauges is that they are prone to variation in sensitivity through temperature change and therefore must be used in a Wheatstone Bridge Circuit with additional non sensing gauges for temperature compensation. It is, however, a reliable method of direct force measurement.

4.2.3 Direct Application of Strain Gauges to Linkage Elements

A common research approach to linkage force measurement is the direct application of strain gauges or load cells to the linkage elements themselves as shown in Figure 24 below.

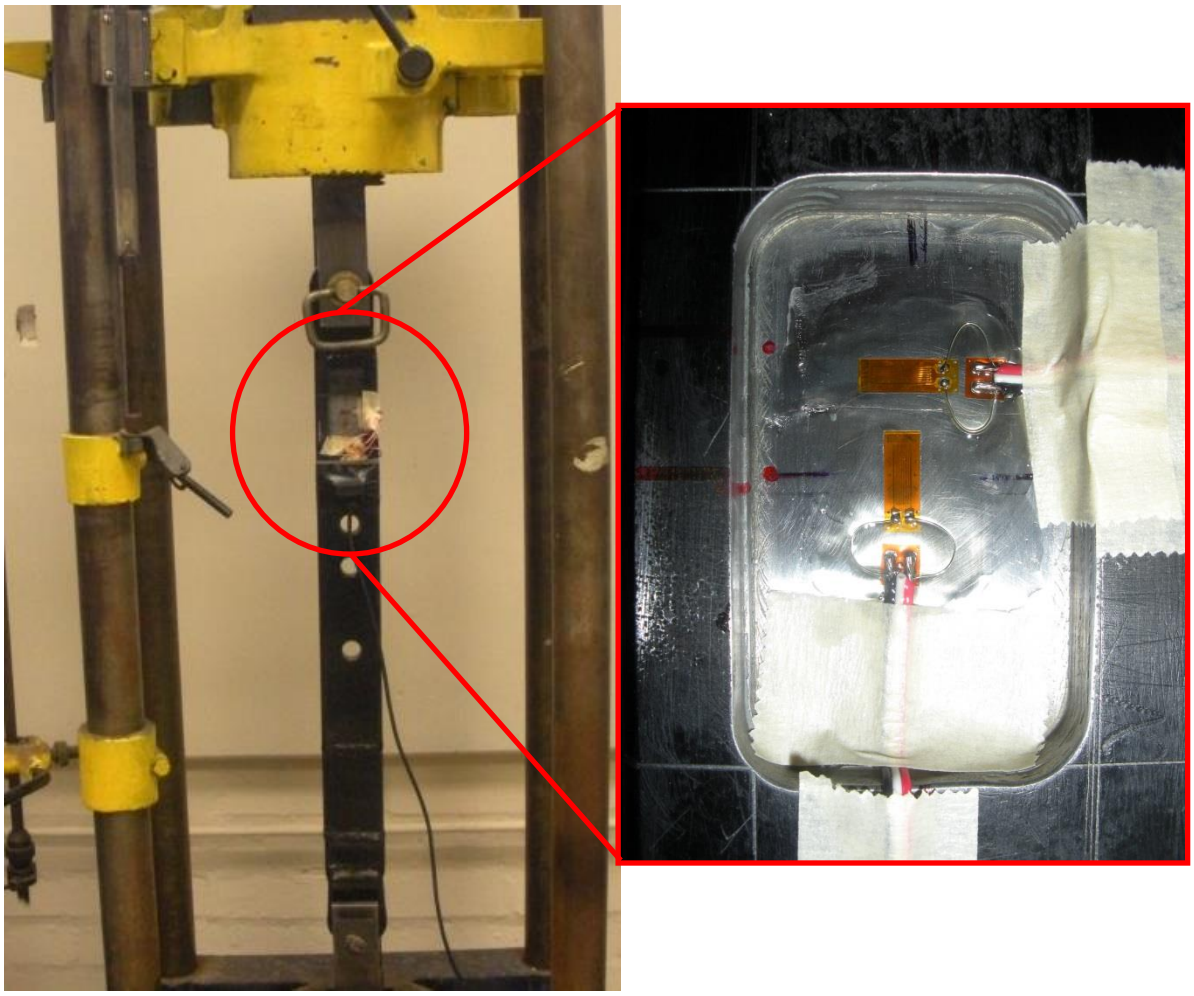

Figure 24: Calibration of directly applied strain gauges to a lower lift arm

(Source: Ward *et al.*, 2009)

The technique consists of applying strain gauges to the linkage elements on their neutral axes to measure direct strain. Benetaher *et al.*(2008) concluded that the resolution of the forces in the lower link arms (tension, compression and bending) may be difficult to execute and therefore omitted application of strain gauges to these components; but the method used by them is complex. Lower link arm forces were calculated based on complex mathematics using known linkage geometry kinematics.

Whilst this approach is non-invasive to the linkage elements geometry and physical characteristics it does not account for a free linkage situation. This was observed by Davies (2006) and Bachche (2009) where the forces in the lift rods can be zero in certain situations.

To accurately measure linkage forces, the tension/compression in all linkage elements is required. Bentaher's concerns over the complexity of total linkage force measurement was proven to be a relatively straightforward process (Keen *et al.,* 2009; Gholkar *et al.*, 2009; Ward *et al.,* 2009; Davies, 2006). This involved the direct strain gauging (Upadhyaya *et al.,* 1985; Kirisci *et al.,* 1993; Khan *et al.,* 2006; Keen *et al.,* 2009, Gholkar *et al.,* 2009; Ward *et al.,* 2009) of all linkage elements to measure tension/compression on or close to the neutral axis. The approach is only suitable for research applications as it requires modification of the linkage components and would render replacement in a commercial application difficult. This accompanied by a kinematic force resolution method as used by Keen *et al.* (2009) and Ward *et al.* (2009) allows directly measured forces to be converted to horizontal and vertical component forces.

However no solution to linkage measurement is without limitation and Reece (1961), Godwin (1975) and Khan *et al.* (2006) noted that a problem can exist with direct linkage mounted strain gauges. Bending can exist in the lower link arm elements due to the restraint provided by the lift rod attachment, causing cross-sensitivity between lift rod forces and lower link arm force measurement. A solution to this was to apply strain gauges to the upper and lower edges of the lower link arm (Godwin *et al.,* 1975) to measure direct tension and by comparing force measurement between upper and lower gauge sets a measure of the bending and hence cross-sensitivity can be determined.

Although improved accuracy is implied it is not necessarily the case. The accurate mounting of the strain gauges on upper and lower surfaces is imperative as should they not be in line inaccuracies will occur.

It can be argued that by measuring accurately the forces exerted on the lift rods the bending applied to the lower link arms is actually measured directly as an increase or decrease in tension in the lift rods

4.2.4 Load Sensing Pins as Part of a Draught Control System.

Prior to incorporation of electronic draught force sensing many had used the idea of a force sensing pin. The idea behind a force sensing pin is that it replaces a natural pivoting pin within an assembly and directly measures the force linkage between the two components. Reece (1961) developed single axis force sensing load pins by applying strain gauges to the pin. Force sensing pins are commercially used on agricultural tractors as part of the linkage control system and form the draught force sensing element. The application of draught force sensing pins to tractors consists of replacing the lower lift arm inboard pivot pin with a draught force sensing version. Commercially used draught force sensing pins are generally single directional axis measuring (http://www.boschrexroth.com/) devices and therefore if oriented as such only measure pure draught force. This measurement is usually parallel to a reference plane on the tractor itself and therefore does not measure draught force parallel to the ground surface. Tractor fore aft angular changes are relatively small, however this does generate an error in the measurement system.

Several versions of the draught force sensing pin have been developed and the first types seen were electro-mechanical. Later types of draught sensing pins were piezoelectric and magnetic induction based the latter being the version in use currently.

The electro-mechanical type was originally developed by Robert Bosch (1988) and is the subject of patent US 4,721,001. The construction of an electro-mechanical type of load pin is shown in Figure 25 below.

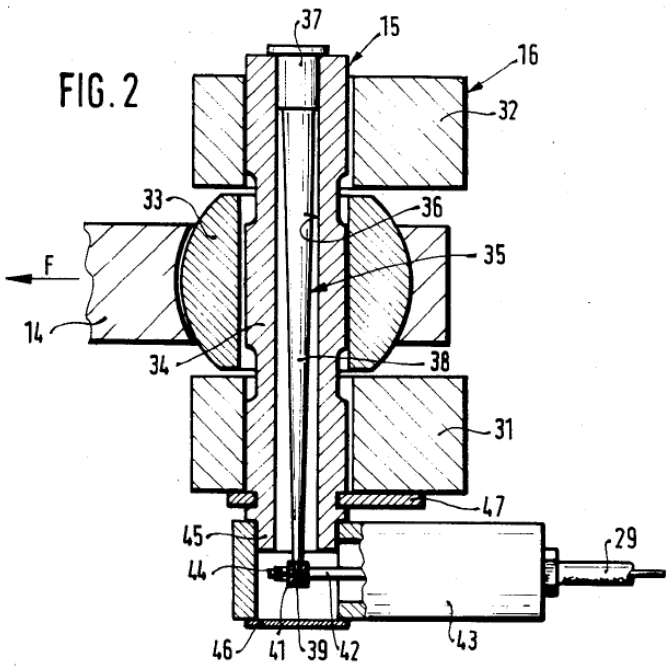

Figure 25: Bosch draught force sensing pin

(Source: Bosch, 1988)

Referring to Figure 25, mounted to the small diameter end of the conical centre portion (38) is a displacement transducer (43) which is in turn fixed to the outer portion (45) of the load pin assembly. When the load is applied to the assembly the outer portion (45) of the pin deflects leaving the conical centre pin (38) un-deformed and the displacement is measured by the displacement transducer (43) (by the outer of the transducer moving over the fixed centre) (Bosch, 1988). This design of draught force sensing pin would have been very expensive to manufacture as the tolerances required to achieve accurate measurement would have been extremely fine; the deflection of the conical centre pin (35) would be small even under high loading leading to a very high precision displacement transducer being required (43). Another limitation due to the high precision mechanical nature of this design is that it is likely to suffer damage easily and be susceptible to frequency induced vibration.

The latter electromagnetic type of draught force sensing pin is that currently used in most tractor electro hydraulic linkage control systems, including the MF8480 research tractor and an image is shown in Figure 26 below of a typical form.

Figure 26: Bosch Rexroth draught force sensing pin

(Source: http://www.boschrexroth.com/)

The pin is inserted into the linkage assembly in exactly the same manner as the electromechanical type shown in Figure 24. The principle of operation is that shearing stresses occur on the pin in two planes perpendicular to the axis of the pin (highlighted in points 3 and 4 in Figure 27 below, http://www.boschrexroth.com/).

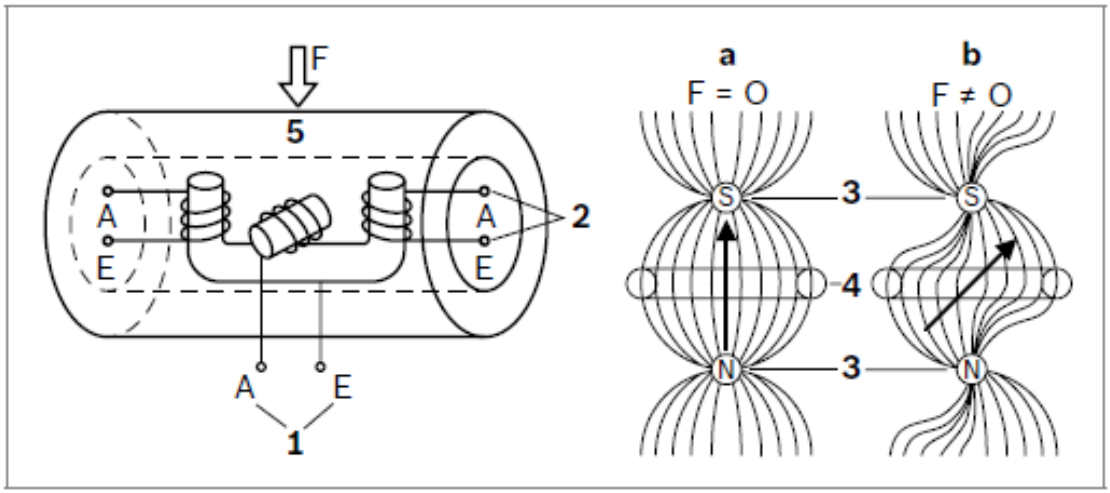

1 Primary coil
2 Secondary coil
3 Primary pole surface
4 Secondary pole surface
5 Steel sleeve
a Symmetrical magnetic field
b Asymmetrical magnetic field

Figure 27: Bosch Rexroth draught force sensing pin functionality

(Source: http://www.boschrexroth.com/)

Within the pin are two magnetic coils as shown in Figure 27 above. In an unloaded state the magnetic field generated by the primary coil is symmetrical (http://www.boschrexroth.com/). As shearing force is applied the core material of the primary coil is deflected altering its electromagnetic properties the magnetic field induced is no longer symmetrical and induces a voltage within the secondary coil. This current is proportional to the amount of draught force applied and with amplification and signal conditioning provides a proportional voltage output (http://www.boschrexroth.com/).

As already discussed these types of draught force sensing pins is that they only measure the magnitude of the force in one direction parallel to a tractor axis. This is achieved by locating the pins accurately on the tractor using the square section included on the pin. This limits the

use of the pin in a complete linkage force measurement system but as will be seen later on through careful calibration and known kinematics the draught force sensing pins are eminently suitable.

4.3 Positional Measurement Techniques

Positional measurement techniques are generally simpler than force measurement. Most components of a three point linkage have limited movement, less than 90°, and generally rotate about points geometrically fixed to the tractor chassis. Therefore for simple angular measurements potentiometers or positional hall-effect encoders/sensors can be used. This approach is simple and has multiple possibilities for incorporation into a real time tractor instrumentation system.

4.3.1 Kinematic Measurements

Tractors are generally now fitted with radar or GPS based speed measurement systems. However there can be some inaccuracies in these systems, and as an indication of tractor sinkage is required to correctly calculate implement depth and tractor attitude, the data wheel was conceived and constructed similar in concept to Mouazen *et al.* (2004).

The idea behind the swinging arm wheel concept used by Ward *et al.* (2009) and Ward *et al.* (2011) was to mount a wheel to a swinging arm and locate this on the tractor so that the wheel can track on undisturbed land – an example is shown in Figure 28 below. By measuring the angle of the swinging arm (via a calibrated potentiometer) it is possible to estimate tractor undulations. Also with the addition of a shaft encoder attached to the wheel accurate forward speed measurement can take place. In addition to the individual wheel speed measurements an accurate estimation of individual wheel slip can be made.

Figure 28: A swinging arm depth wheel suitable for measuring axle vertical displacement and forward speed

(Source: This study)

4.3.2 Speed Measurement

Imou *et al.* (2001) proposed the use of high resolution ultrasonic Doppler speed sensor previously developed by them for speed measurement in forward and reverse directions and low speeds; the system was particularly developed for agricultural vehicles. Imou *et al.* (2001) mounted a conventional ultrasonic Doppler sensor with the transmitter at an angle α (to the horizontal) and similarly the receiver at angle β – see Figure 29.

Imou *et al.* (2001) states that the transmitter sends an amplified signal (F_0) to the ground surface and due to the nature of forward speed and surface roughness the sound signal is diffused and only a few weaker signals are received by the receiver. The Doppler effect causes a shift in frequency and this is taken into account in the calculations presented by Imou *et al.* (2001). The forward speed calculation takes into account the speed of sound in air, C_S, and uses basic trigonometry to resolve the frequencies so that the frequency out of

the sensor is approximately proportional to transmission frequency and the absolute value of vehicle velocity (Imou *et al.*, 2001). A disadvantage of this system is that it cannot determine velocity direction and that it is not very accurate at measuring low forward speeds and further work would be required to establish the suitability in this research. The velocity is calculated using trigonometry and there is no reason that with simple modifications to the calculations depth could not be measured. A schematic is of Imou *et al.* (2001) system is shown below in Figure 29.

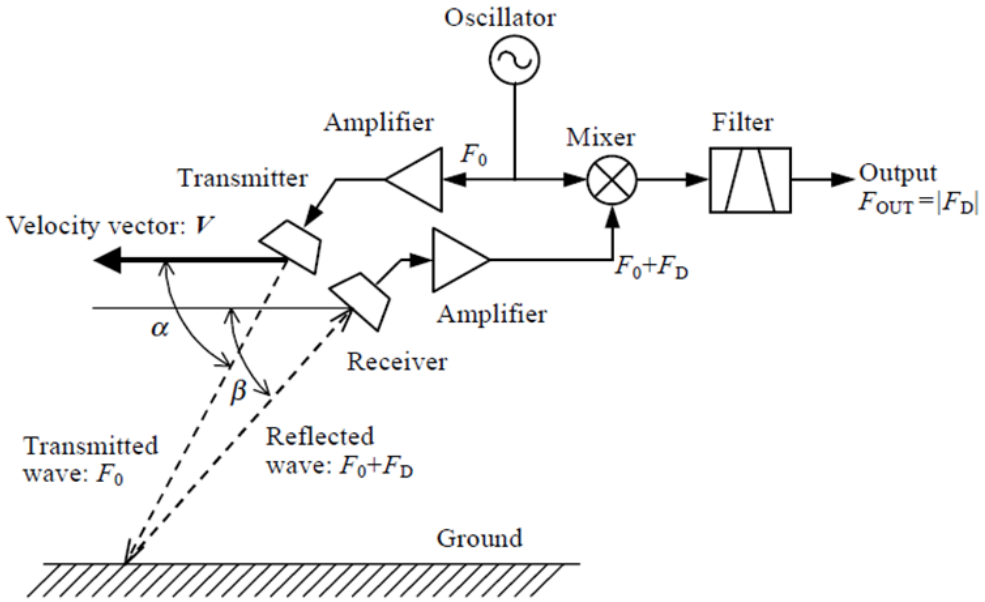

Figure 29: Block diagram of a conventional ultrasonic Doppler speed sensor

(Source: Imou *et al.*, 2001)

Scarlett (2001) also proposed the use of ultrasonic transducers for measuring implement depth. Combining the approach described by Imou *et al.* (2001) and Scarlett (2001) a proposed similar set–up to Imou *et al.* (2001) and Yahya *et al*. (2009) could be used for determining tractor attitude and sinkage; by using an ultrasonic transducer at a prescribed angle to the horizontal plane in four places (2 front and 2 rear) on the tractor axles/chassis to measure depth only. From this, data measurements of tractor height from the working surface

and therefore tractor attitude and sinkage could be made. Tractor attitude and sinkage measurements are key inputs to this study and this sensor type may be applicable

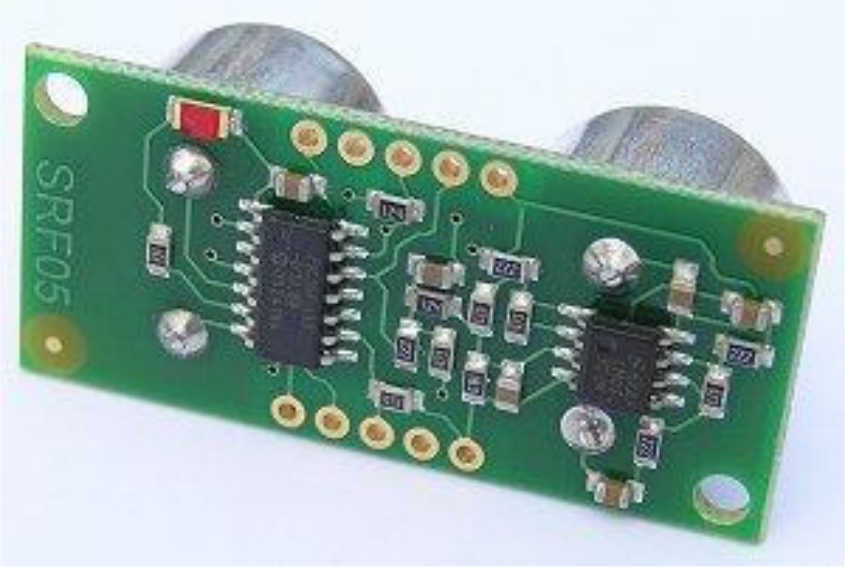

Figure 30: SRF05 – Ultrasonic ranger

(Source: http://www.rapidonline.com/)

4.5 Fuel Usage Measurements

The fuel consumption measurement system on the MF8480 tractor used in this study is typical of modern day tractors; based on the engine map using the CANBus electrical network. Fuel use is measured based on engine speed and load through the engine ECU with no physical measurement taking place.

Commercial third party fuel measurement systems exist in the market place such as those manufactured by JPS Engineering. The main measuring element of these systems is the Oval Model LSF41 fuel meter (Figure 31) which has a max flow rate of 100 l h^{-1} (litres per hour) and accurate to within 1 %. The systems are therefore suitable for tractor research purposes.

Figure 31: Oval Model LSF41 fuel meter

(Source: http://www.icenta.co.uk/)

CHAPTER 5 - Tractor Measurement System

In order to provide the input parameters to the linkage force resolution and tractor dynamic kinematic models, developed in Chapter 3, a specific instrumentation system was developed similar to Keen *et al.* (2009), Ward *et al.* (2009) and Ward *et al.* (2011). In addition to the input parameters additional measurements are required to measure fuel consumption, independent wheel speeds and true forward speed. The additional measured parameters are required to allow real-time tractor field performance to be calculated. Whilst not concerned specifically with tractive efficiency it is important for the operator to be aware of the amount of fuel being used in the field as well as wheel slip – both are indicators of tractor power usage. Wheel slip is optimised between 10 and 15% for draught tillage operations therefore the tractor operator needs to be aware so that measures can be taken to improve performance such as adjusting tyre pressures.

There are four streams to the instrumentation systems:

1. Force measurements;
2. Positional measurement;
3. Wheel speed measurement;
4. Fuel consumption measurement.

The data logging equipment selected for the final algorithm verification was based around a National Instruments cRIO – 9014 Embedded Controller (Compact Rio). The Compact Rio has the ability to both log data and also provide control signals to various sensors.

The following modules were incorporated into the chassis for the purposes of data logging final experiments and development of the system:

- NI9237 4 Channel 24 Bit Bridge Analogue Input Module;
- NI9201 8 Channel 12 Bit Analogue Input Module;
- NI9219 4 Channel 24 Bit Universal Analogue Input Module;
- NI9263 4 Channel 16 Bit Analogue Output Module.

Shown in Figure 32 below is an image of the prototype National Instruments Compact Rio set up used in this study.

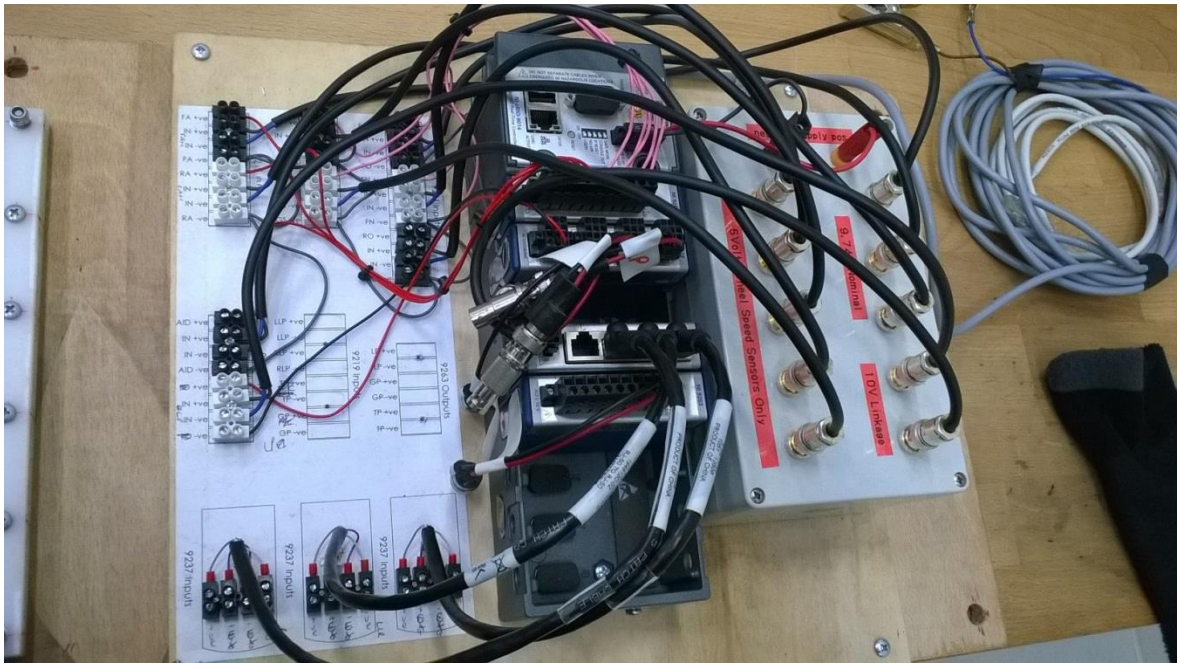

Figure 32: Prototype National Instruments Compact Rio data logging apparatus

(Source: This study)

The following sections briefly detail the instrumentation and the most recent calibrations used in this study. Calibration Equations are generated with each measurement sensor with a precision of five decimal places for clarity; the control algorithm uses higher levels of precision in these Equations to aid accuracy.

5.1 Positional Measurement

5.1.1 Measured Implement Tillage Depth

Tillage depth is measured using a simple linear depth wheel as shown in Figure 33 below. The depth variation is measured using a Celesco SP1 – 50 string potentiometer. Linear vertical movements are encompassed by a sliding tube within a tube arrangement, with the moving part of the string potentiometer attached to the moving depth wheel as shown in Figure 33 below.

Figure 33: Measured implement tillage depth (AID) measurement wheel used

(Source: This study)

A calibration curve for the measured implement tillage depth wheel is shown in Figure 34 below.

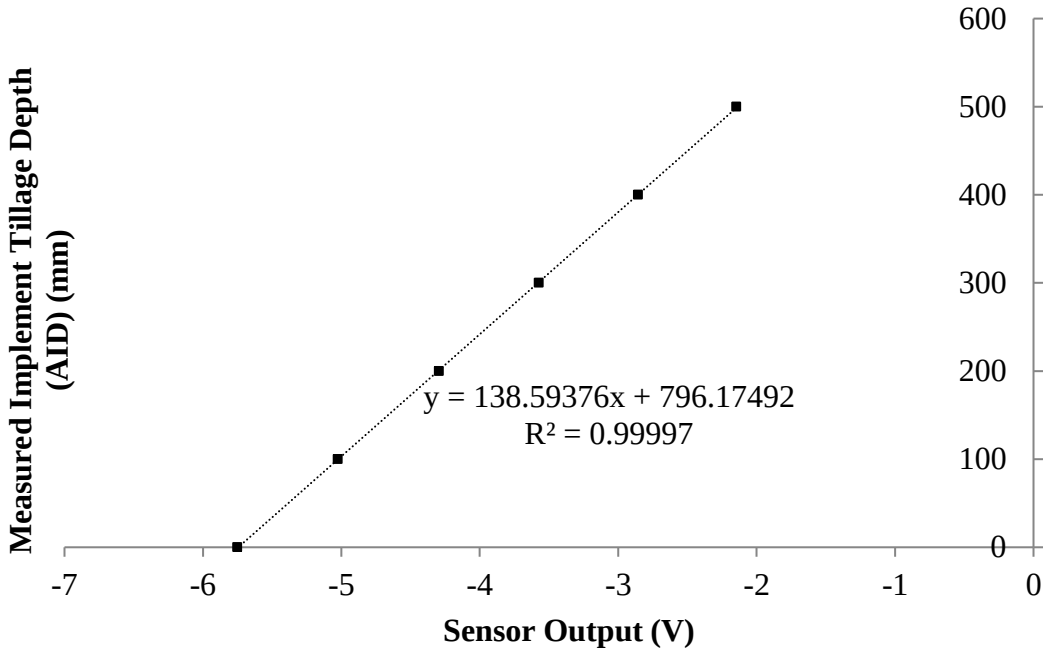

Figure 34: Measured implement tillage depth (AID) wheel calibration

(Source: This study)

5.1.2 Linkage Position

Linkage positional measurement (ELP) is simply a 10 kΩ (kOhm) rotary potentiometer attached to the three point linkage cross shaft with a nominal excitation voltage 10 V (Volts) with no amplification gain applied to the sensor output. A suitable fixture was manufactured to house the body of the sensor with a coupling connecting the rotating part of the sensor to the cross shaft. The linkage positional sensor was calibrated two times by simply lifting and lowering the tractor linkage with the tractor situated on a hard level surface. The implement tines were removed and representative weights added to ensure maximum linkage travel and accurate weight distribution. As the linkage was articulated in raising and lowering conditions, in Position control mode the following parameters were recorded at intervals during the cycle:

1. The distance in mm between the lower lift arm implement ball attachment point centre and the ground;

2. The voltage output from the linkage positional measurement sensor (ELP);

3. The measured implement tillage depth as a voltage output from the measurement wheel – which was then converted into measured implement tillage depth (AID) using the calibration presented in Figure 34;

4. The tractor linkage actuation electro-hydraulic valve control signal voltage from the cab mounted depth control dial (TLP).

Using the models presented in Chapter 3 the data collected in 1 to 4 above were then processed to generate a relationship to lower lift arm angle, α, in all cases.

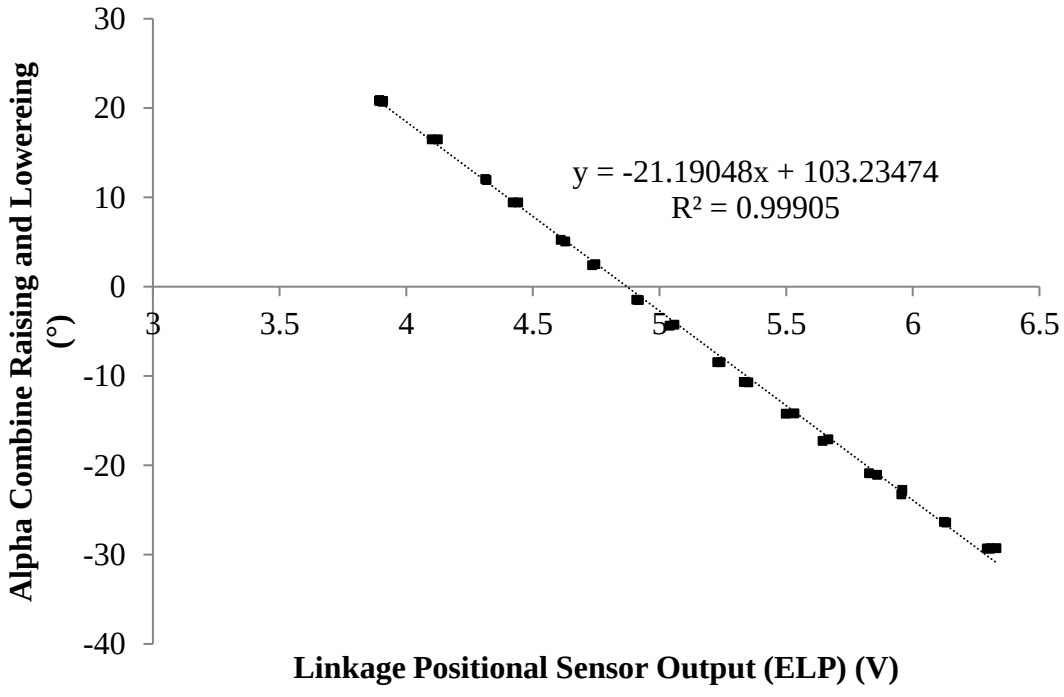

Figure 35: Linkage positional measurement sensor (α) calibration graph showing combined raising and lowering operation data

(Source: This study)

A calibration graph and equation are presented in Figure 35 above for the relationship between angular displacement of the lower lift arm, α, and the linkage positional measurement sensor voltage output. Data collected from the measured implement tillage depth (AID) measurement wheel were manipulated to provide the change in tillage depth due to an angular displacement of the lower lift arm, α. The relationship is presented in Figure 36 below; it is a kinematic relationship and non-dependent on the linkage control.

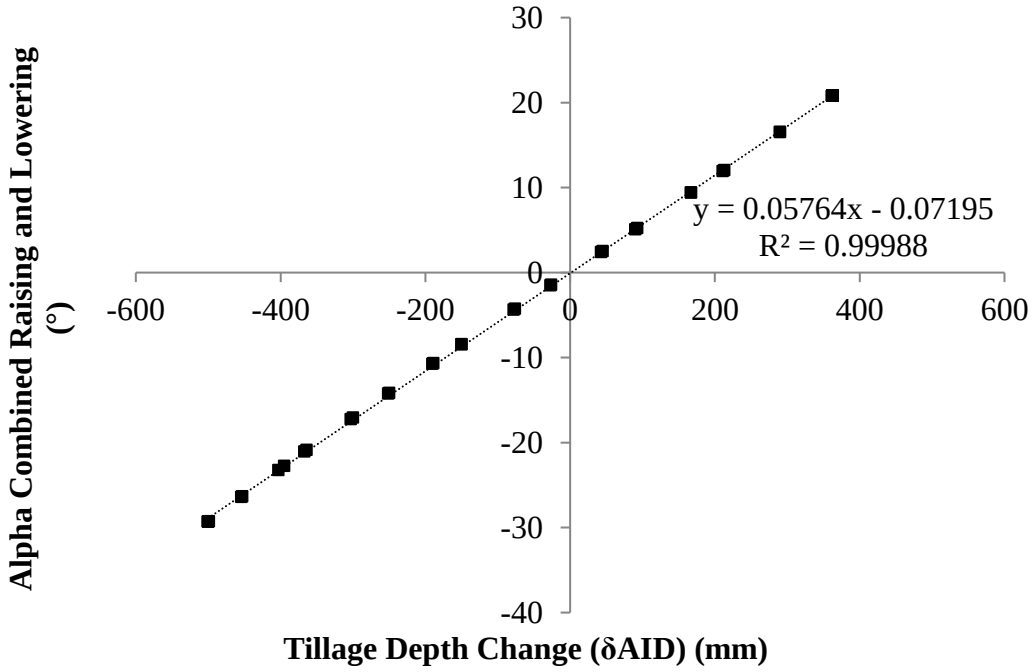

Figure 36: Tillage depth change (δAID) due to linkage movement (α) calibration graph showing combined raising and lowering data

(Source: This study)

Voltage data collected from the cab mounted depth control dial (TLP) were manipulated to provide the change in tillage depth due to an angular displacement of the lower lift arm, α. It is particularly important that data for this relationship is manipulated in both raising and lowering conditions to capture any difference in extension or retraction characteristics of the linkage hydraulic lift rams and are presented below in Figures 37 and 38 respectively.

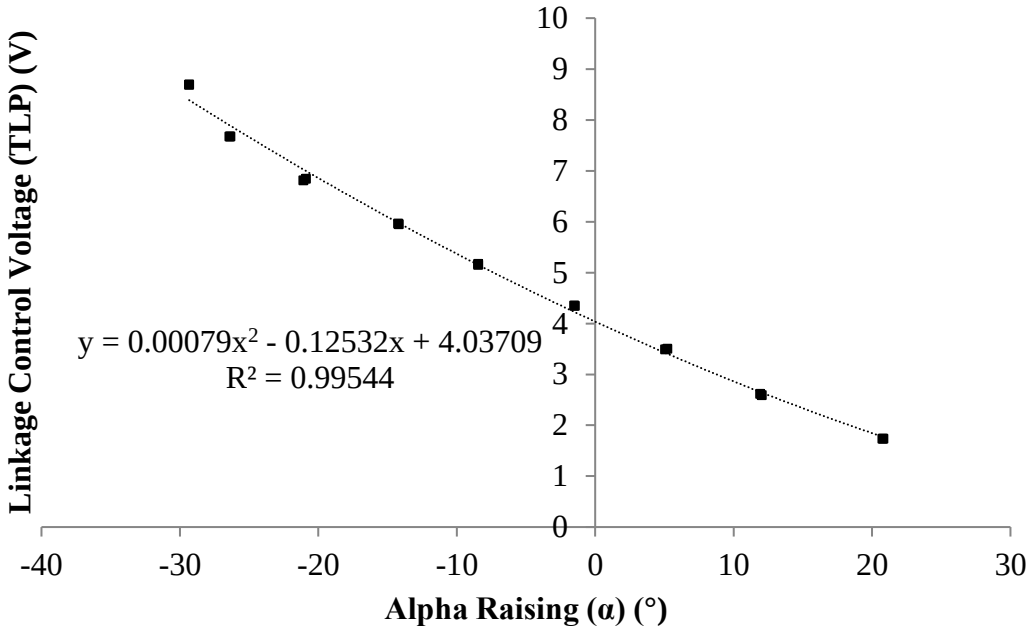

Figure 37: Linkage electro-hydraulic control valve voltage (TLP) for a given raising linkage movement (α)

(Source: This study)

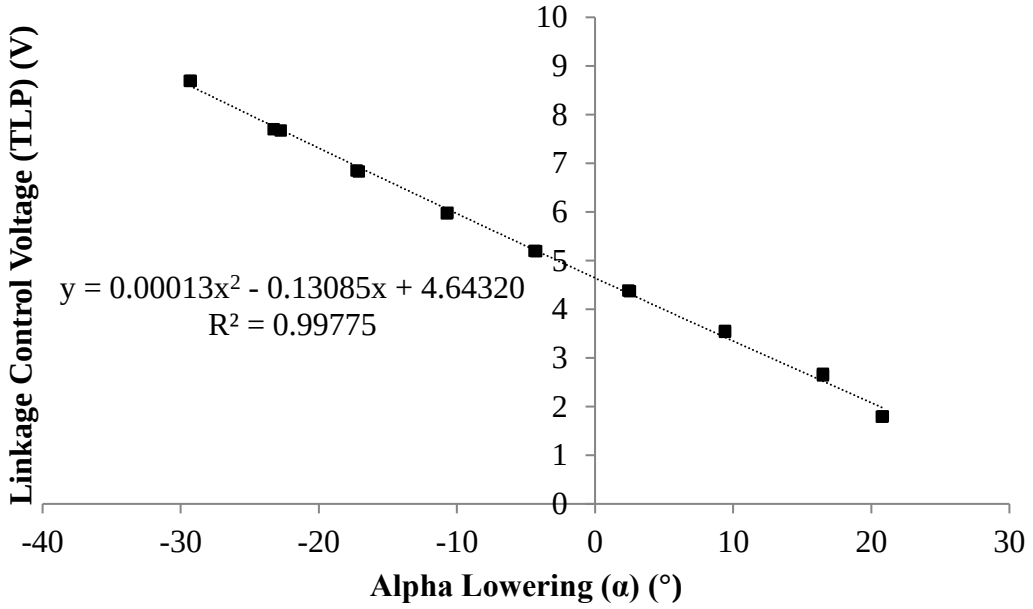

Figure 38: Linkage electro-hydraulic control valve voltage (TLP) for a given lowering linkage movement (α)

(Source: This study)

5.1.3 Axle Height Measurement

Similar to the swinging arm depth wheel shown in Figure 28 in Chapter 4, swinging arm depth wheels were developed to measure axle heights above the undisturbed ground surface in real-time. Axle height change (δFAH and δRAH) is measured using a 10 kΩ rotary potentiometer where the body of the sensor is attached to the swing arm with the centre portion remaining fixed to the retaining assembly. The swinging arm depth wheels are located on the centreline of the tractor chassis running longitudinally between the tractor wheels. An image of the front axle swinging arm depth wheel is shown in Figure 39 below.

Figure 39: Image of the front axle height sensor fitted to the MF8480 research tractor

(Source: This study)

The front axle swinging arm wheel is also equipped with a 128 bit end encoder as shown later in Figure 49 to measured true forward ground speed (SOG). The swinging arm axle height sensors fitted to both the front and rear axles were calibrated using slip gauges to a nominal 196 mm deflection; simulating the ground surface rising in relation to the tractor. Calibration data are shown in Figures 40 and 41 for the front and rear axle height sensors respectively.

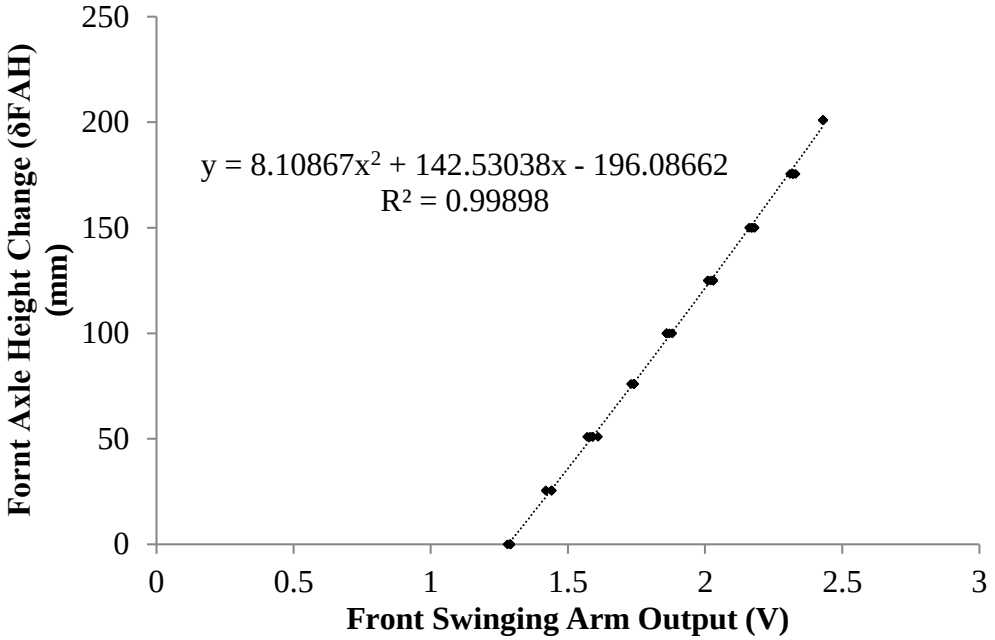

Figure 40: Front axle height (δFAH) sensor calibration graph showing combined raising and lowering data

(Source: This study)

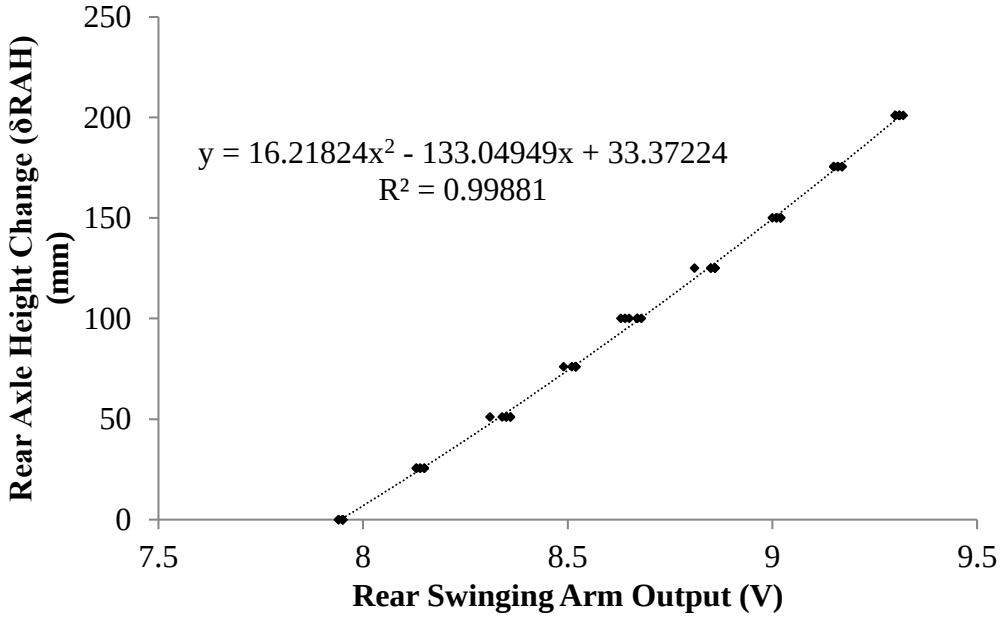

Figure 41: Rear axle height (FAH) sensor calibration graph showing combined raising and lowering data

(Source: This study)

5.2 Linkage Force Measurement

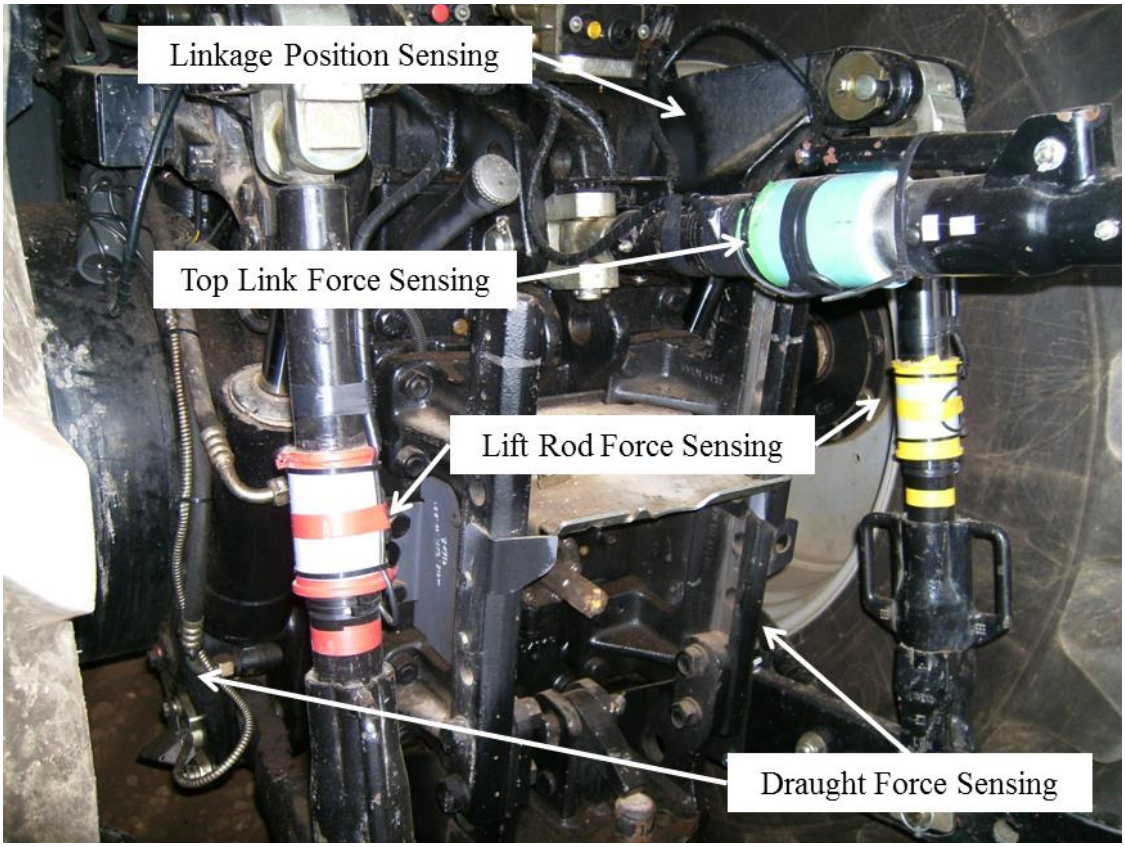

Figure 42: Layout of the three point linkage force measurement instrumentation

(Source: This study)

Shown in Figure 42 above are the force measuring components of the tractor measurement system and consists of the standard tractor fitment draught force sensing pins, Bosch Model No. KMB 090 10 3 A / 30 - 15 (see Appendix A for a data sheet), and full strain gauge Wheatstone Bridges (see Figure 43 below) applied to the top link and lift rods. All elements of the system were calibrated in loading and unloading conditions.

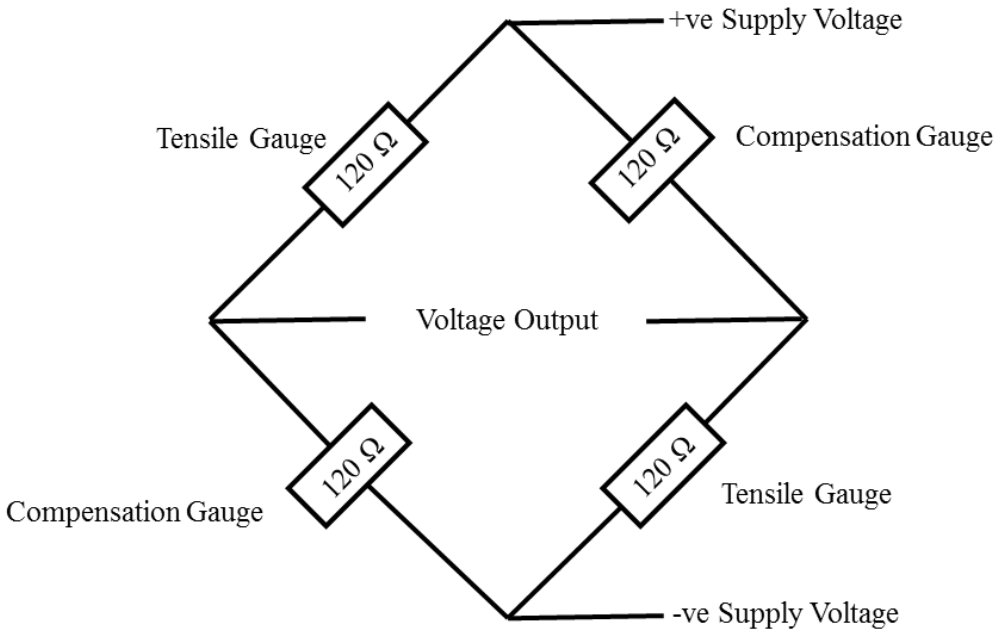

Figure 43: Schematic of Wheatstone Bridge used on top link and lift rod for measuring longitudinal forces in this study

(Source: This study)

5.2.1 Top Link

Strain gauges were applied in a Wheatstone bridge format as shown in Figure 42 above with two gauges in tension applied to either side of the top link centre tube. The reasoning behind the orientation of the gauges in the bridge with the tensile gauges diagonally opposite is to increase signal output from the bridge. The gauges used were single axis 120 Ω (Ohm) +/- 0.3 % standard strain gauges available from VISHAY.

The top link (FTL) was calibrated in an Avery Dennison tensile testing machine in loading and unloading conditions using an excitation of nominally 10 Volts and an output signal gain of 1000. The process was similar to that shown in Figure 24 in Part 4.2.3. The calibration graph is presented in Figure 44 below.

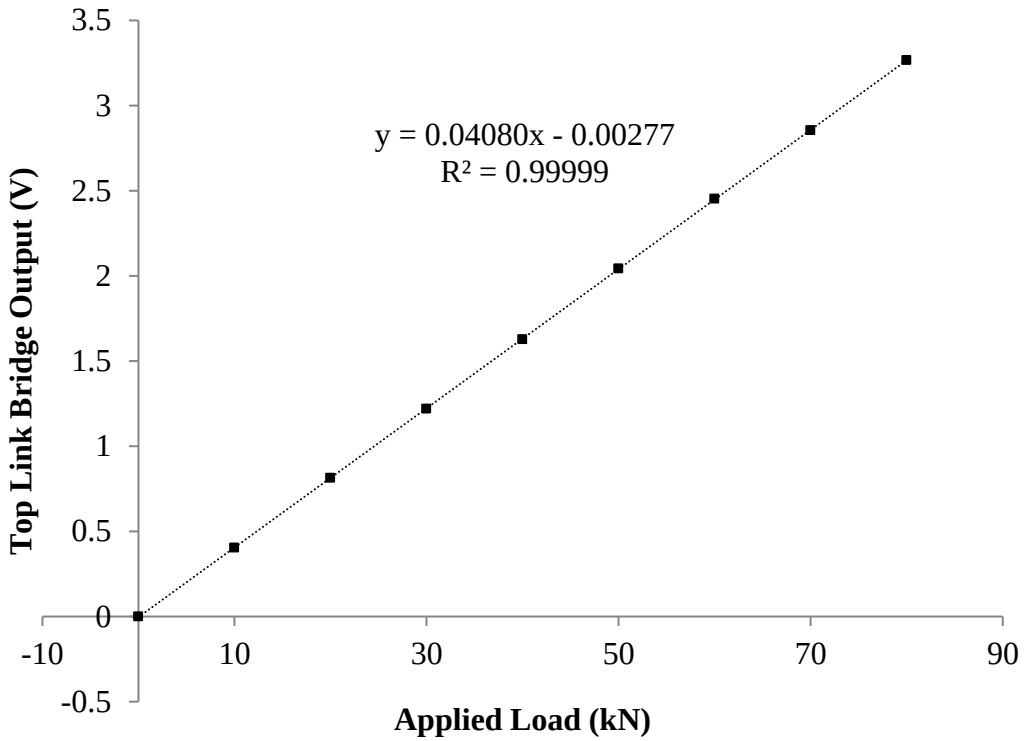

Figure 44: Calibration graph for the instrumented top link (FTL) showing combined loading and unloading data

(Source: This study)

5.2.2 Lift Rods

The strain gauge application and calibration procedure for the lift rods is exactly as per that of the top link. Calibration curves are presented in Figures 45 and 46 below for the left lift rod (LLR) and right lift rod (RLR) respectively.

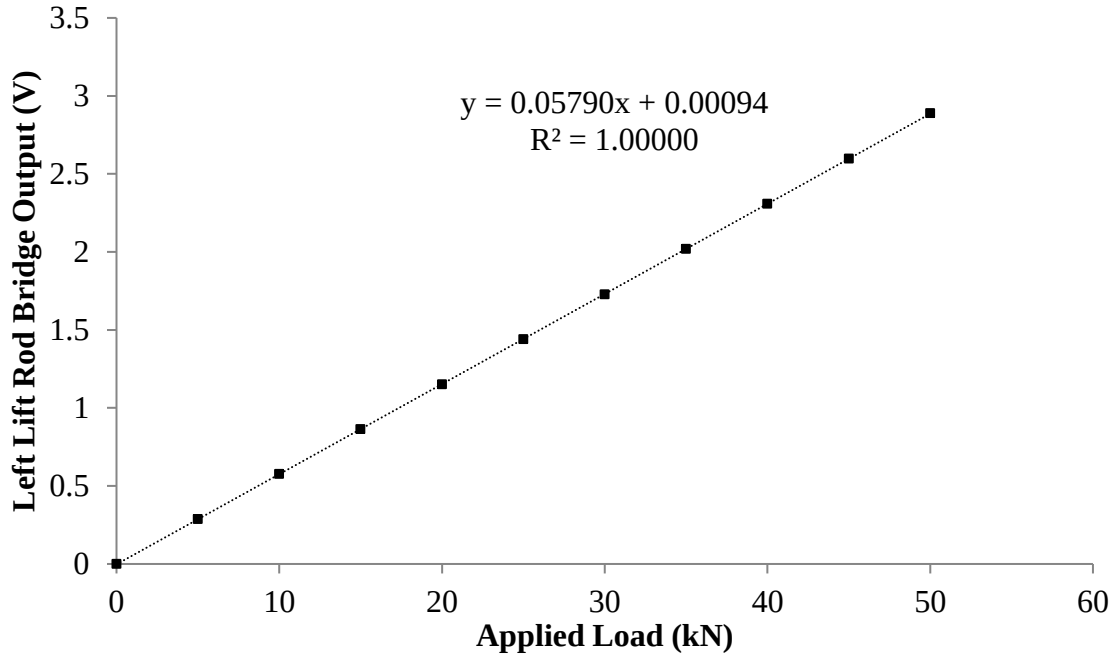

Figure 45: Calibration curve for the instrumented left lift rod (LLR) showing combined loading and unloading data

(Source: This study)

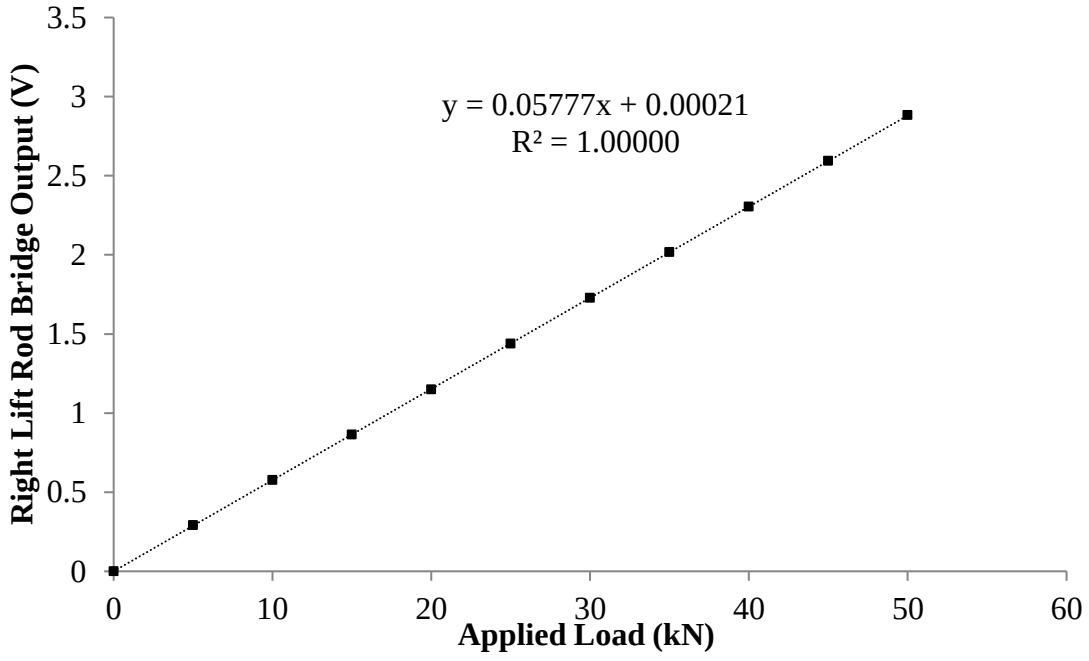

Figure 46: Calibration curve for the instrumented right lift rod (RLR) showing combined loading and unloading data

(Source: This study)

5.2.3 Draught Force Sensing Pins

The standard Bosch Model No. KMB 090 10 3 A / 30 – 15 draught force sensing pins fitted to the tractor were used as part of the linkage force measurement system. The pins are able to measure up to +/-90 kN individually and a data sheet is presented in Appendix A. The draught force sensing pins were calibrated in situ on the tractor using a substitute lower lift arm a proprietary 5 Tonne load cell to measure the applied load. The load was applied using a telescopic handler boom attached to the load cell via a strop with increased load applied by retraction of the boom. The calibration was completed on level ground with a spirit level attached to the substitute lower lift arm to ensure a parallel load was applied. Presented in Figures 47 and 48 below are the calibration graphs and equations for both draught force sensing pins, LLP and RLP, respectively.

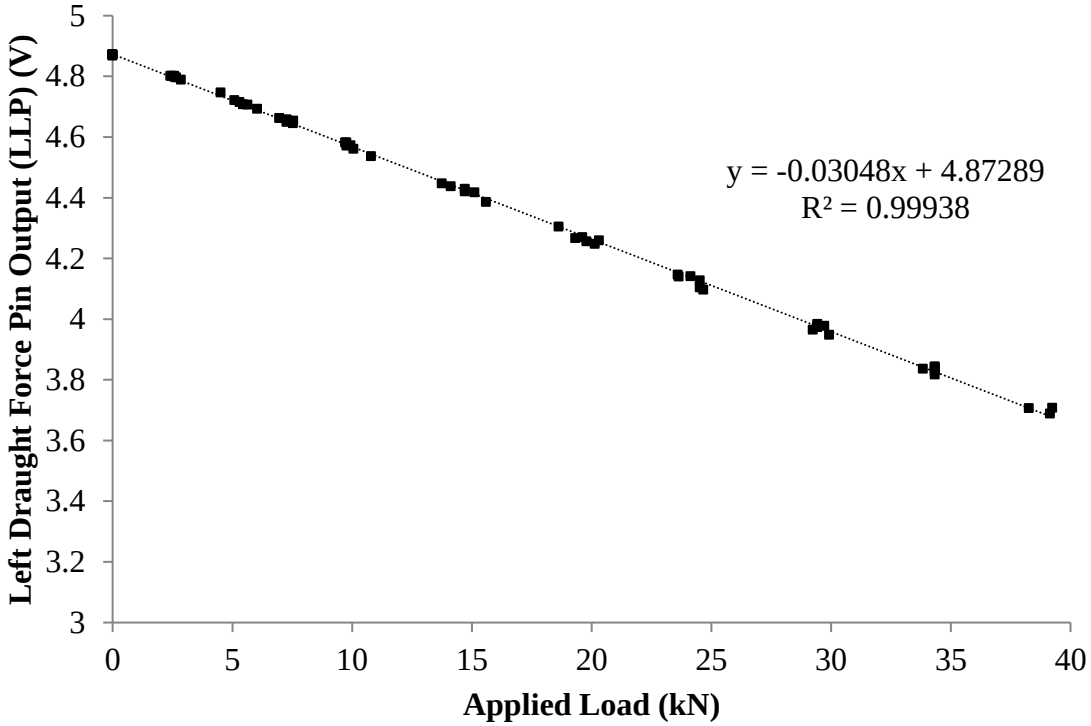

Figure 47: Calibration curve for the left draught force sensing pin (LLP) showing data from three calibration replicates

(Source: This study)

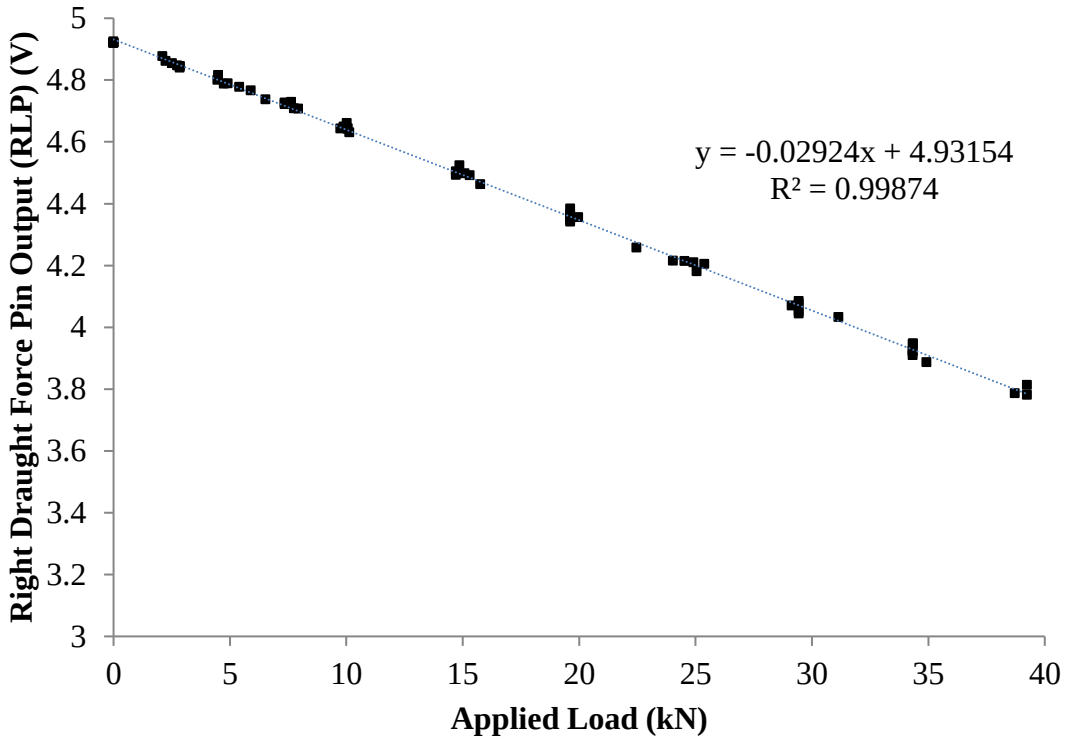

Figure 48: Calibration curve for the right draught force sensing pin (RLP) showing data from three calibration replicates

(Source: This study)

5.3 Wheel Speed Measurement

The individual wheel speeds on the tractor measurement instrumentation system were measured using 128 bit (128 pulses/revolution) optical end encoders (Model Bourns: EMA1J – B20) shown in Figure 49.

Figure 49: Bourns EMA1J-B20 optical end encoder used in this study

The encoders are attached to the centre line of each wheel as shown in Figure 50 below. The encoders are housed in a self-supporting assembly attached to the wheel hub. The outer portion of the casing only has to be prevented from rotating to measure wheel speed.

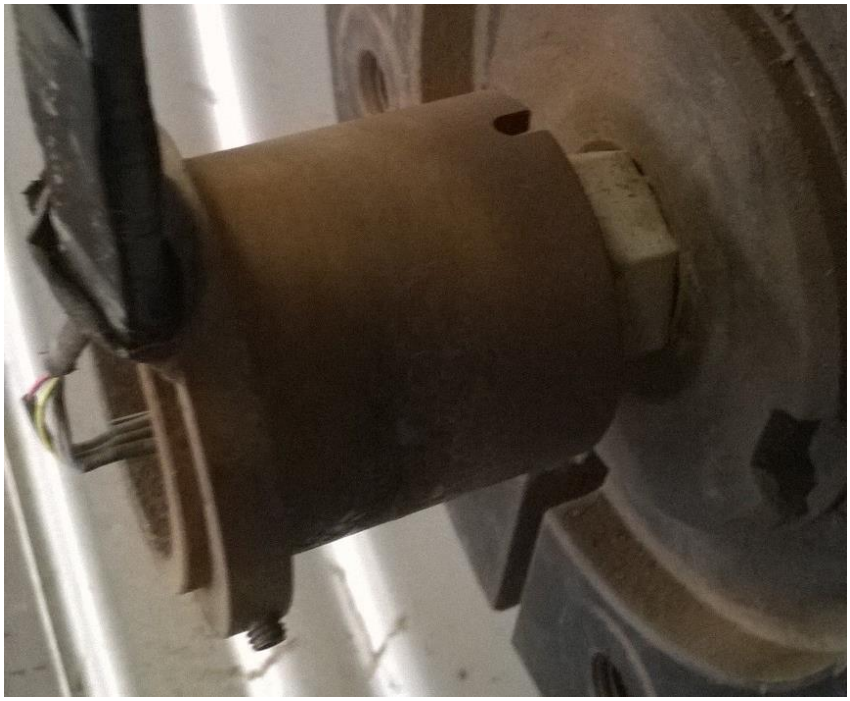

Figure 50: Wheel speed sensor assembly fitted to the front wheel of the MF8480 research tractor

(Source: This study)

Shown in Figure 51 below is an exploded 3D rendering of the design model for this assembly. One off each of these assemblies is fitted to the MF8480 research tractor wheels; a further sensor is fitted to the front axle height swing wheel to measure forward speed.

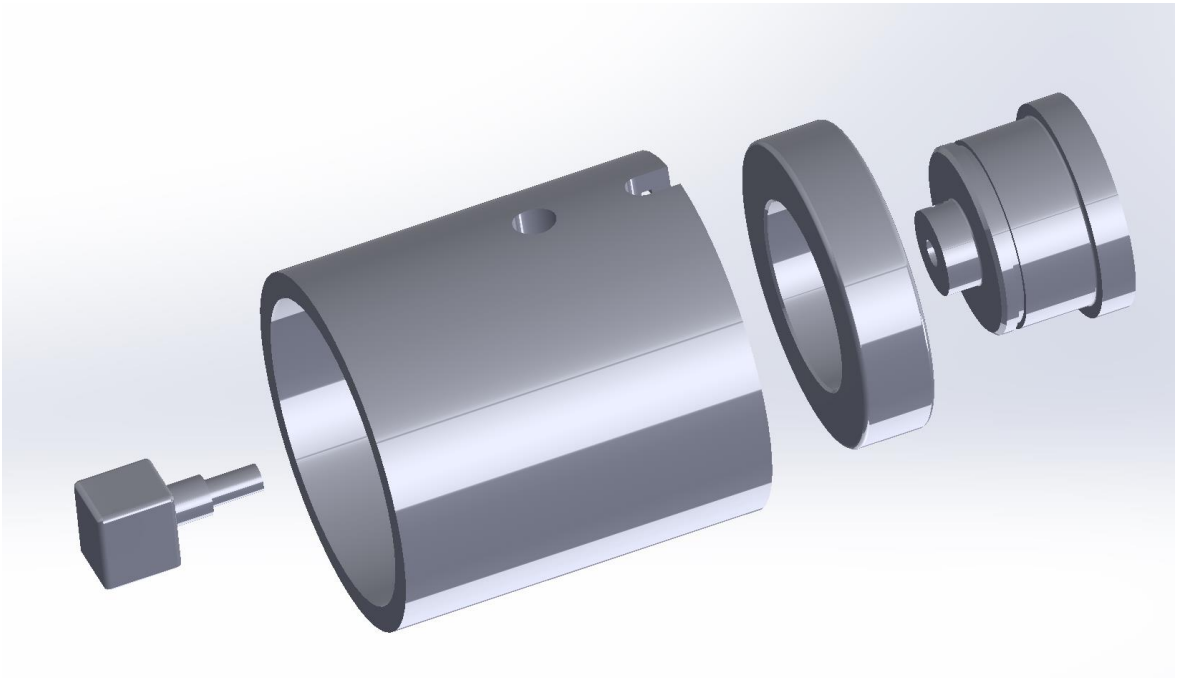

Figure 51: Design rendering of wheel speed sensor components designed in this study

5.4 Fuel Consumption Measurement

A standard fuel measuring system was selected to measure fuel consumption of the Massey Ferguson and manufactured by JPS Engineering, Model No. FMS MK4. The system works by maintaining a constant fuel head in the supply tank (part of the system). The fuel supply is connected to a fuel pump internally which supplies fuel to the supply tank via an Oval Model LSF41 metering unit capable of measuring up to 100 l h^{-1} and accurate to within 1 %. Fuel for the engine is taken from the supply tank, with the engine return line also connected to the supply tank; the internal pump then ensures the constant head of fuel is maintained with only the fuel added, i.e., used, measured. An image of the unit fitted to the MF8480 research tractor is shown in Figure 52 below.

Figure 52: JPS Engineering FMS MK4 fuel measuring system fitted to the MF8480 research tractor

(Source: This study)

CHAPTER 6 - Preliminary Linkage Performance Experiments

6.1 Background

The aim of a tractor and implement combination, performing draught tillage is to do work. Lacking in current tractor operator information systems are feedback on how efficiently the field operation is being conducted. The end users are constrained by weather and therefore there is always the desire to complete the field work as quickly as possible. This has become even more the case with the large rise in the number of farms using external farm based sub-contractors; the investment required in new equipment dictates it is utilised as much as possible.

What is lacking in this scenario is an emphasis on efficiency rather than high work rate. Working at maximum tractive efficiency of a wheel implies three factors:

1) Maximum conversion of fuel energy into work done;
2) Working at the maximum rate for the given power/torque input to the driving wheels but not necessarily the maximum possible;
3) Wheel slip is optimised for the given tractor/implement combination.

Whilst systems have been developed for optimising tractor implement complementation such as that developed by Zoz and Grisso (2003) this excludes the possible set up options available to the operator. The MF8480 used in this study is fairly typical of a modern day tractor incorporating a generic linkage control system with Position, Draught and Intermix controls. An experienced operator will have preferences in how to set up the linkage control system. However, current information display systems in tractors only show simple performance parametric such as fuel consumption and work rate leading to no energy efficiency information being available to the operator and manager of equipment – this now being transmittable to a farm base using GPS and RTK based management systems.

Three point linkage movement, and hence tillage depth, in relation to the ground is dictated by the following factors:

- **Ground undulations** - pitching fore and aft can lead to the implement going deeper and shallower in relation to the ground – most prevalent in Position Control;
- **The linkage control strategy chosen** – Position Control fixing the linkage in relation to the tractor; Draught Control maintain a predetermined draught force through linkage movement;
- **Weight transfer** – leading to rear tyre deflection and in a Position Control mode allowing the implement to pull in further in respect of a winged tine sub soiler.

Deep cultivation equipment may occasionally be fitted with depth control wheels or a packer roller. SOYL have developed a control system that will actively lift and lower a packer roller in the field to adjust tillage depth based on field properties. This system, however, is passive in that it references a soil map responding to cropping and soil tillage requirements minimising over tillage. The system therefore relies on the linkage control strategy being set in either Draught or float control mode. There is no real- time element that responds to current traction conditions or monitoring of drawbar power usage and therefore efficiency. By inference this system will reduce overall energy requirements through minimising tillage however it does not allow the tractor to respond to areas where minimal tillage is required resulting in unused power and therefore not maximising efficiency.

As was seen in Chapter 2 and demonstrated by Godwin *et al.* (1974) the relationship between draught force and depth of a wing tined sub-soiler in a homogeneous soil is non-linear; the relationship in fact is broadly a squared one where a doubled tillage depth results in four times the draught force generated.

Using a winged tined sub-soiler example where 40 kN of draught force is generated at a depth of 400 mm a table of nominal values was created, using the squared relationship, and data is presented in Table 5 and graphically in Figure 53 below.

Table 5: Nominal draught force and implement tillage depth data

Draught Force (kN)	Depth (mm)
0	0
0.15625	25
0.625	50
2.5	100
10	200
40	400
160	800

(Source: This study)

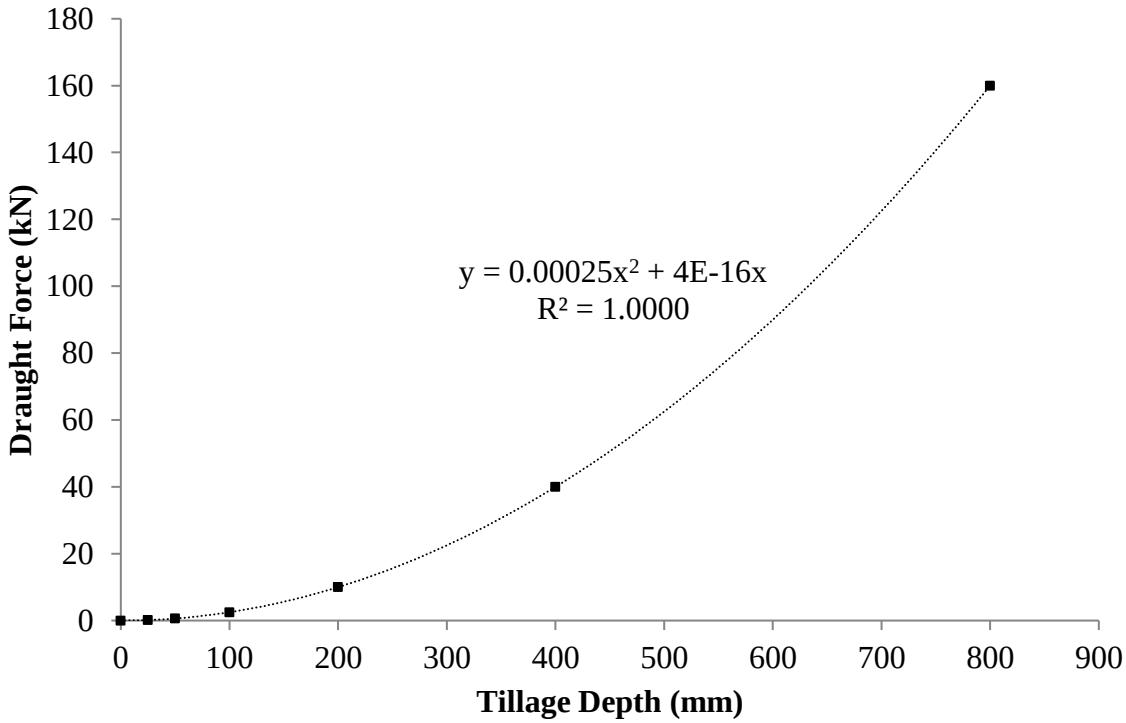

Figure 53: Predicted tillage depth and draught force relationship

(Source: This study)

Drawbar power or draught power was defined in Equation 4.1. In conjunction with Figure 53 above, tillage depth has a direct effect on drawbar power which is derived from fuel energy conversion in the tractor engine. Using Figure 53 as a guide, for a given constant forward speed a 50 mm variation on a nominal 400 mm depth, resulting 40 kN draught force, will have the following approximate effect on drawbar power:

1. 350 mm results in a draught force of approximately 31 kN – a 22.5 % reduction in drawbar power;
2. 450 mm results in a draught force of approximately 50 kN – a 25 % increase in drawbar power.

As can be seen a relatively small change of 50 mm can result in large changes in the required power from the wheels and hence engine. A reduction in draught force through more accurate depth control will result in a reduction in wheel slip and therefore energy losses. This *extra* energy could be used to increase forward speed, utilise a wider implement or reduce load on the engine and therefore fuel consumption.

To conclude this analysis resulted in a need to establish a series of controlled experiments to establish the baseline performance for existing typical tractor linkage control systems both in the field and laboratory and prove the instrumentation system described in Chapter 5. Therefore in the field, for a given set of forward speed and tillage depth, what effects do field conditions and linkage control strategies have on tillage depth and therefore drawbar power and fuel required. As draught force is not a perfect running constant, to further enhance understanding of linkage control system performance a series of experiments in the laboratory using simulated draught forces were devised.

6.1.1 Generic Tractor Linkage Controls

The aim of this section is to describe in detail the typical components of a modern tractor three point linkage control system. The current three point linkage is a modern interpretation of that developed by Harry Ferguson in the early twentieth century. The functionality of *Ferguson's Draught Control* is largely unchanged however its execution is now by electrohydraulic rather the mechanical-hydraulic means.

6.1.1.1 Normal Components of a Tractor Linkage control system

Most modern tractor linkage control systems have a similar functionality despite differing iterations of in cab visible controls. Most of these systems are manufactured by Bosch or licensed production with internal parameters being either standard or particular to a specific manufacturer or machine.

The basic functions of a linkage control system include Draught Control, Position Control and Intermix Control (a mixture of both Draught and Position Control settings), linkage lift height and linkage lift speed. As can be determined there are a multitude of possible linkage settings without any real feedback to the performance and efficiency characteristics in the field. The only feedback mechanism is the tractor operator or more obvious physical indicators such as forward speed reduction or increases in wheel slip – but little actual live feedback data.

Shown below in Figure 54 is a typical set of three point linkage control panel.

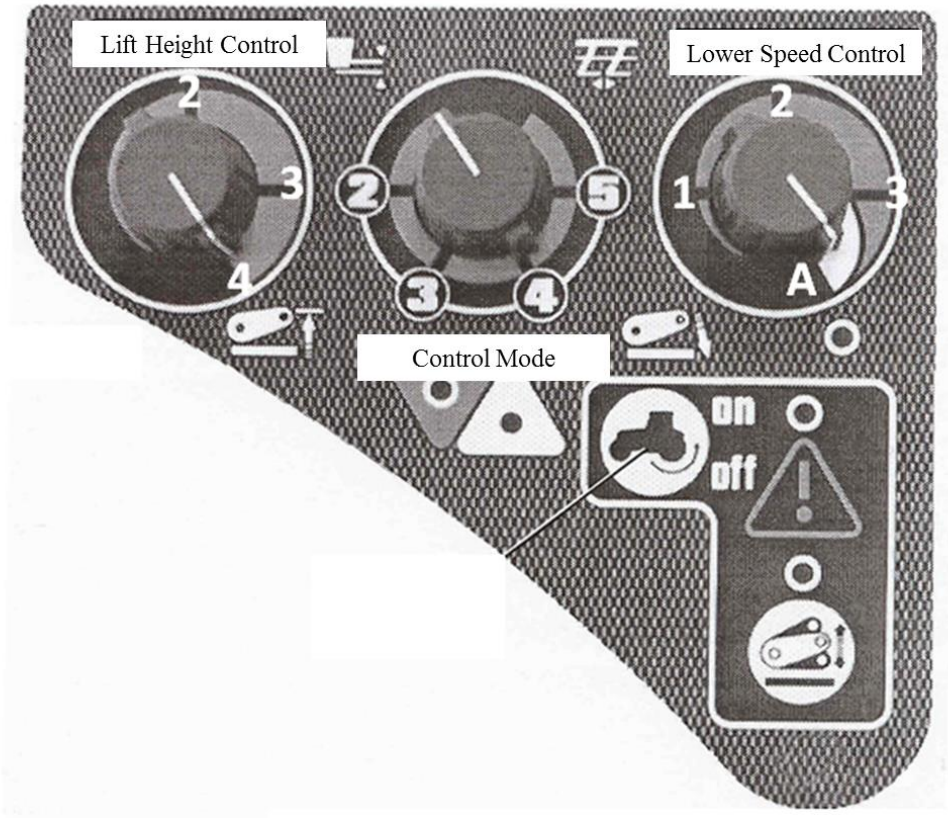

Figure 54: Typical three point linkage in cab controls

(Source: This study)

6.1.1.2 Functional Modes

Tractor linkage control systems have many settable attributes that determine the function and performance of the tractor implement combination in terms of efficiency, speed and quality of work done. The remainder of this section will discuss these parameter options and also their limitations.

6.1.1.2.1 Draught Control

Draught control is designed to limit the amount of draught force (F_x) exerted on the tractor due to a tillage process. On the MF8480 research tractor the draught force limit is setting using the depth control dial on the seat armrest. The lift height can also be adjusted using the dial shown in Figure 54. It is therefore very difficult to adjust the parameters accurately with

no feedback on performance attributes. This system is typical of most generic tractor linkage control systems. The feedback from the linkage to control this system is via three electrical sensors; two off draught force measuring pins on the lower lift arm (LLA) tractor attachment point measuring pure draught, and a positional sensor usually located on the cross shaft connecting both lift arms – Figure 42 in Chapter 5. The functionality of Draught control is executed by the tractor linkage control system lifting the linkage when the draught force exceeds the limit set to the predetermined lift height. Therefore the more compacted field areas are less cultivated than required. It is impossible to know with current systems what the limit set actually is and how much draught force is being generated by the tractor implement combination.

6.1.1.2.2 Position Control

Of the two main linkage control parameters Position Control is the most simplistic. By selecting Position Control (for the MF8480) as shown in Figure 54 the linkage position in relation to the tractor is fixed using the depth control wheel. The feedback from the linkage to control this system is from the cross shaft located positional sensor. Operating in this mode there is no form of draught force limitation with linkage in effect fixed in a position relative to the tractor. It can be determined, from previous chapters, that by fixing the linkage position the weight transfer effect on the tractor is increased. This is due to the now fixed pin joint between tractor chassis and lower lift arm. Some linkages are allowed to *float* whereby the upward motion of the linkage is not restricted whereas the downward motion is. Whilst this can be useful in allowing implements to *ride* over underground obstacles, during deep tillage operations using winged tines this has little or no benefit as the tines are designed to lift the ground by pulling into the ground (downwards motion). As has already been seen weight transfer causes tyre deformations (usually at the rear) and increased tractor sinkage due to increased ground pressures – allowing the implement to pull in further and

require more energy. It has already been seen in this work that draught force increases exponentially with depth therefore energy is almost certainly being wasted through poor linkage control.

6.1.1.2.3 Intermix Control

As shown in Figure 54 it is possible to adjust the linkage control mode dial to a combination of both Position and Draught control. Complex algorithms within the control system allow the selection of varying degrees of Draught and Position control modes. Depending on the position selected the control strategy deployed will be biased either towards Position control with a degree of Draught control override or vice versa. However what is not known due to intellectual property restrictions is the logic and processes behind the linkage control strategy fitted within the MF8480 research tractor.

6.2 Field Experiment Introduction

The main purpose of the field experiments was to evaluate whether there was any perceivable difference in how tillage depth varies in relation to which linkage control strategy is applied. These experiments formed the basis of Ward *et al.* (2011). No information was available from Massey Ferguson on the internal control algorithms of the fitted linkage control system as it was a proprietary controller. Therefore a series of laboratory experiments were also devised to understand how the linkage controller functionally works rather than understand the mathematical code within it.

6.2.1 Experimental Method

Presented in Table 6 below is a summary of the treatments adopted during the field experiments.

Table 6: Initial field experiments treatments summary

Treatment	Nominal Tillage Depth (mm)	Linkage Control
1	200	Draught
2	200	Position
3	200	Intermix
4	400	Draught
5	400	Position
6	400	Intermix

(Source: This study)

6.2.1.1 Nominal Tillage Depth

As has already been seen implement depth has a profound effect on draught force and therefore drawbar power. Two nominal depths were chosen to be able to ensure the implement developed for this study conformed to the nominal depth draught relationship described in section 6.1. Therefore the depths chosen had a factorial relationship of two, being nominally 200 mm and 400 mm, where 400 mm would be considered a deep sub soiling operation;

6.2.1.2 Three Point Linkage Control Strategy

As described in section 6.1.1 typical three point linkages have many features which result in an almost infinite number of possible settings. The following three linkage control treatments to the nominal tillage depths for this experiment:

1) Pure Draught control – the linkage control dial set in Draught Control only mode;
2) Pure Position control – the linkage control dial set in Position Control only mode;
3) Intermix control – the linkage control dial set mid-way between Draught Control and Position Control indicating an equal mix of both strategies.

6.2.1.3 Field Plan

The field used for the experiments had previously been cropped with Oilseed Rape (OSR) and had a light covering of herbage and residual OSR plant stems. The soil type is a Sandy Loam through a texturing analysis conducted in the field. Each treatment was to be replicated three times to ensure data validity and utilising a random number table the field plan in Table 7 was generated.

Table 7: Field based linkage performance experimental plan

Block	Plot	Treatment	Nominal Tillage Depth (mm)	Control Strategy
1	1	6	400	Intermix
1	2	5	400	Position
1	3	4	400	Draught
1	4	3	200	Intermix
1	5	2	200	Position
1	6	1	200	Draught
2	1	4	400	Draught
2	2	6	400	Intermix
2	3	1	200	Draught
2	4	3	200	Intermix
2	5	5	400	Position
2	6	2	200	Position
3	1	6	400	Intermix
3	2	1	200	Draught
3	3	5	400	Position
3	4	2	200	Position
3	5	4	400	Draught
3	6	3	200	Intermix

(Source: This study)

6.2.1.4 Field Measurements

The field test area was marked out with individual plots measuring 4.0 m x 24.0 m (dictated by tramlines). The experiment was concerned solely with the performance of the tractor linkage control system therefore for the success of the experiment the field test area had to be reasonably homogeneous and the listed field measurements were taken.

1. Cone Index readings were taken using an Eijkelkamp Recording Cone Index Penetrometer in five locations in each plot in a typical W formation ensuring even distribution within and between plots.
2. Bulk density samples were taken at the depth to be cultivated at as presented in Table 7 above. These were taken using a 1000 cm^3 bulk density sample ring in five locations and the sampling was such that it was within 0.5 m radius of the CI reading location. The five samples were then bulked, mixed and then $1/5^{th}$ of the sample weight was dried in an oven at 104 °C for a minimum of 24 h thereafter being weighed regularly until weight loss ceased. A simple calculation of the weight lost determines the Moisture Content of the samples analysed as shown in Equation 6.1 below:

Moisture Content = ((Fresh Weight (g) – Dry Weight (g)) / Dry Weight (g)) x 100 (%)

Equation 6.1

6.2.1.5 Tractor and Implement Combination Setup

The tractor used for these experiments was the MF8480 in combination with the sub-soiler developed for this study by the author and is based upon the winged tines and tine holders of a Simba DTX3000. The sub-soiler attached to the tractor is shown in Figure 55 below. and is based upon the winged tines and tine holders of a Simba DTX3000. The sub-soiler can operate with one, two, three or five tines. A design consideration behind the implement was that it may be possible to automate the number of tines that interact with the ground to enable draught force to match the available tractor wheel power in the prevailing field conditions.

Figure 55: Wing tined 1, 2, 3, or 5 leg sub-soiler developed for this study

(Source: This study)

The tractor and sub-soiler were set up for field use in a typical manner with the linkage set up so that the implement headstock and tines remained as close as possible to the tractor vertical reference plane; this will not be truly perpendicular to the ground as undulations and weight transfer effects will alter this relationship due to dynamic attitude changes.

The following comprised the general set up of the tractor used in the field experiment:

- Differential Locks – All activated
- 4WD – Activated
- Tyre Pressures – 1.4 Bar front and 1.2 Bar rear
- Lift Rod Length – 822 mm
- Top Link Length – 815 mm

- Tractor Speed – 5 km h^{-1}
- Lift Height Control – Position 4
- Lower Speed Control – Position 3

6.2.1.6 Instrumentation System and Measured Parameters

The experiment was designed to establish tillage depth in relation to which linkage control strategy is applied. Whilst other factors such as tractor sinkage, wheel slip and fuel consumption will be more important later on in this study they are not relevant at this stage. Therefore a simple linkage force measurement, linkage position and tillage depth system described in Chapter 5 was required to measure the required parameters.

Parameters measured during the experiment:

- Linkage element forces (lower lift arms, lift rods, top link);
- Tillage depth;
- Linkage position.

The instrumentation was calibrated as described in Chapter 5 with the calibrations summarised in Table 8 below.

Table 8: Instrumentation calibration summary used in initial field experiments

Component	Excitation	Gain	Calibration	R^2
Left Draught Pin (LLP)	-	10	64mV kN^{-1}	0.999
Right Draught Pin (RLP)	-	10	65mV kN^{-1}	0.999
Left Lift Rod (LLR)	5V	1000	30.46mV kN^{-1}	1
Right Lift Rod (RLR)	5V	1000	31.57mV kN^{-1}	1
Top Link (FTL)	5V	1000	24.81mV kN^{-1}	1
Depth Wheel (AID)	10V	1	12.79mV mm^{-1}	0.999
Lower Lift Arm Angle (α)	5V	1	Equation	0.991

(Source: Ward *et al.*, 2011)

6.2.1.7 Data Logging and Instrumentation Set Up

Shown below in Figure 56 is a schematic of the data logging set up used in this experiment. The main components were the measurement transducers, strain gauge amplifier, National Instruments USB6008 data logger and a host computer.

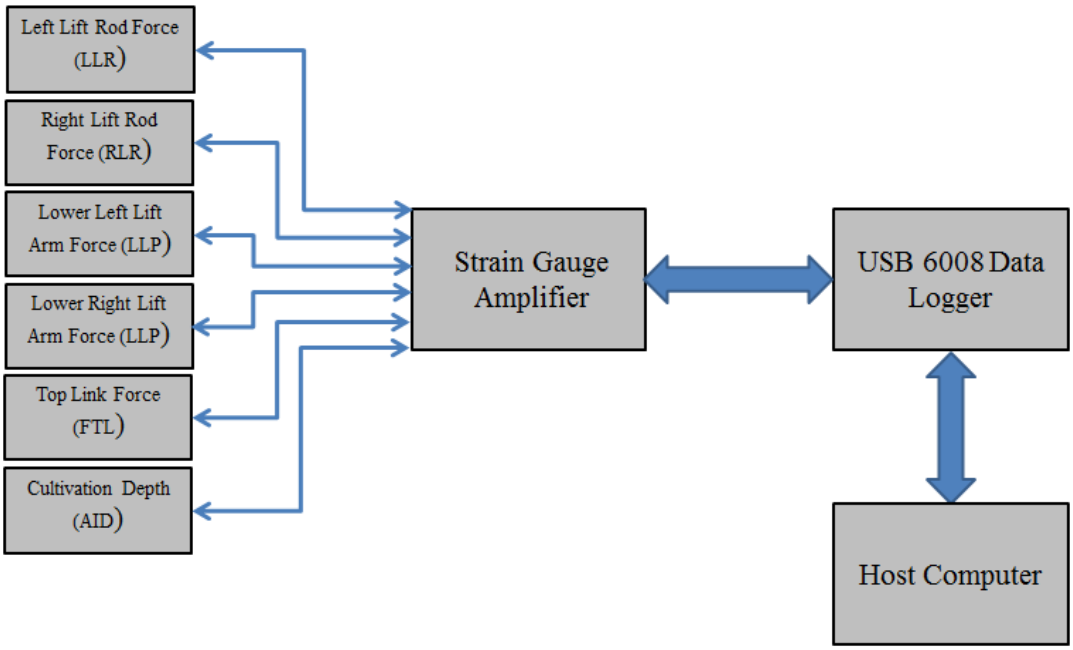

Figure 56: Data acquisition schematic used within the initial field experiments

(Source: This study)

The following parameters were logged during the field experiments:

- Left Lift Rod Force (LLR) – Tensile/compressive forces measured in the tractor nearside lift rod;
- Right Lift Rod Force (RLR) – Tensile/compressive forces measured in the tractor offside lift rod;
- Lower Left Lift Arm Force (LLP) – Tensile/compressive forces measured in the tractor nearside lower lift arm;

- Lower Right Lift Arm Force (RLP) – Tensile/compressive forces measured in the tractor offside lower lift arm;
- Top Link Force (FTL) – Tensile/compressive forces measured in the tractor top link;
- Measured Implement Tillage Depth (AID) – tillage depth of the sub-soiling implement.

A sampling frequency of 500 Hertz (Hz) was chosen for these initial field evaluation experiments. A high frequency was chosen to ensure all data were captured and to investigate the frequency that force data and tillage depth fluctuated. The purpose of this was to establish the level of response from a control system that may be required to adjust linkage position in real-time and to evaluate how much 'noise' was generated within the recorded data and how homogeneity of the field is translated into force measurement.

6.2.2 Field Experiment Results

The following sections summarise the data recorded as part of the field experiments.

6.2.2.1 Field Property Measurements

Table 9 below presents a summary of the field data collected prior to the experiments being conducted. As can be seen from the results Table 9 above there was some variation in the CI readings at comparable depths between plots. This would indicate the presence of stones and clods within the field test area skewed results; this may be an indicator of inconsistent field preparation prior to the sowing of the previous OSR crop. However, bulk density values were more consistent throughout the field test area with a standard deviation 6.2 % of the mean. Moisture content varied by 5.4 % of the mean, across both tillage depths and the field test site. With this in mind there is some confidence in the drying process used and the

homogeneity of the field test site. Full graphical data of CI readings are presented in Appendix B.

Table 9: Initial field experiment field soil properties

Block	Plot	Moisture (%)	Wet Bulk Density (kg m^{-3})	Dry Bulk Density (kg m^{-3})	Mean CI at Tillage Depth (Pa)	Tillage Depth (mm)
Block 1	1	13.7	1580.9	1363.7	4907.6	400
	2	13.7	1439.2	1242.6	4598.4	400
	3	13.1	1588.9	1381.4	4006.8	400
	4	14.3	1756.3	1505.5	1887.7	200
	5	13.8	1609.0	1386.4	2097.5	200
	6	15.3	1584.5	1342.6	2145.9	200
Block 2	1	13.9	1803.2	1553.3	4039.0	400
	2	13.1	1730.1	1503.0	4369.8	400
	3	13.6	1626.1	1405.2	2108.3	200
	4	14.8	1580.8	1346.4	2199.7	200
	5	13.9	1507.5	1297.5	3233.6	400
	6	14.1	1552.3	1333.7	2737.5	200
Block 3	1	12.1	1550.5	1362.9	4147.9	400
	2	13.4	1635.7	1416.5	1656.5	200
	3	12.8	1546.1	1348.4	3533.5	400
	4	14.0	1560.3	1341.4	3834.7	200
	5	13.2	1677.2	1456.4	5168.5	400
	6	13.2	1810.2	1571.0	1963.0	200
Mean		**13.7**	**1618.8**	**1397.7**		
Std. Deviation		**0.7**	**100.9**	**88.4**		
Std. Deviation Error		**5.4 %**	**6.2 %**	**6.3 %**		

(Source: This study)

6.2.2.2 Implement Depth Field Performance

Data were recorded during the experiments at a rate of 500 Hz. It is important to note that an earlier linkage positional sensor was used in these experiments located at the lower lift

arm; the remainder of the process, whereby the linkage kinematic angular measurements were calculated from this one positional measurement is still utilised.

A mathematical worksheet was created to process the raw tractor data. The worksheet was developed to calculate primarily resolution of linkage forces, a quasi-static estimate of weight transfer, implement depth. An earlier version of the linkage force resolution model developed in Chapter 3 was included that calculated weight transfer using known static axle loads ZF and ZR was. Figure 57 below shows where the calculated parameters act on the tractor.

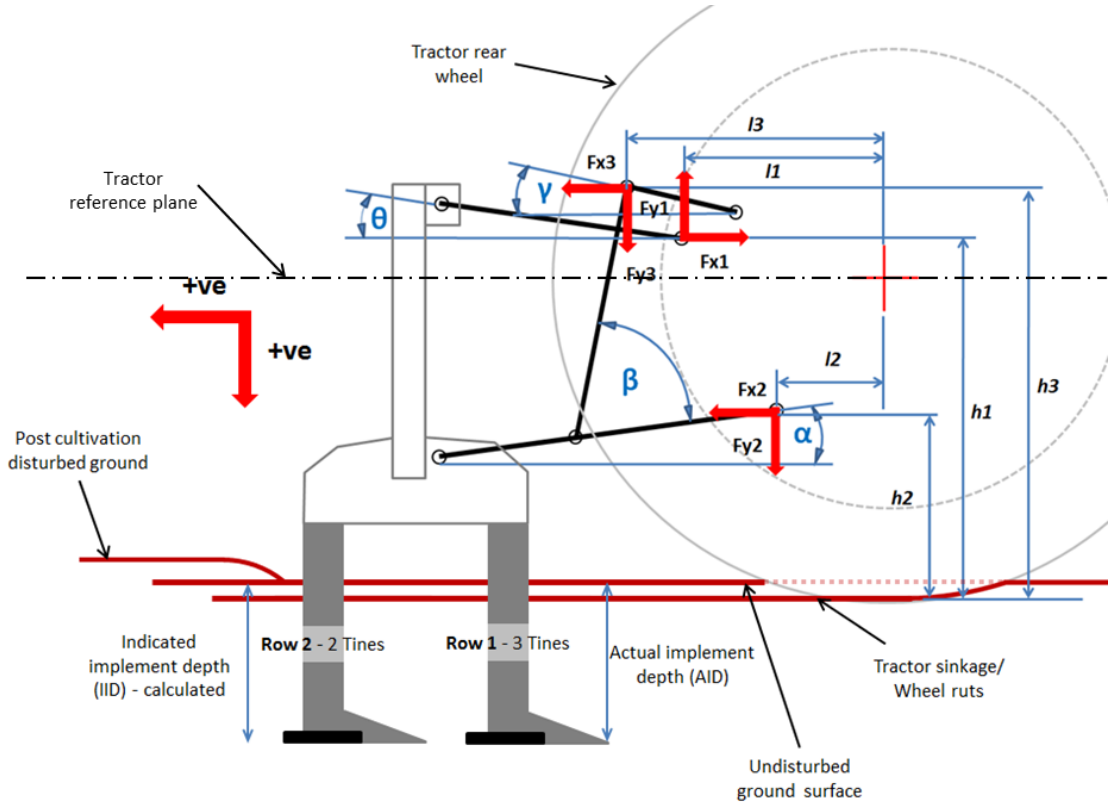

Figure 57: Linkage kinematics during initial field experiments

(Source: This study)

A complete summary table of the recorded data is presented in Appendix D. A summary of the combined data from three replicates recorded during experiments of Treatments 1 to 3 is presented in Tables 10 and 11 and Figures 57 and 58 below.

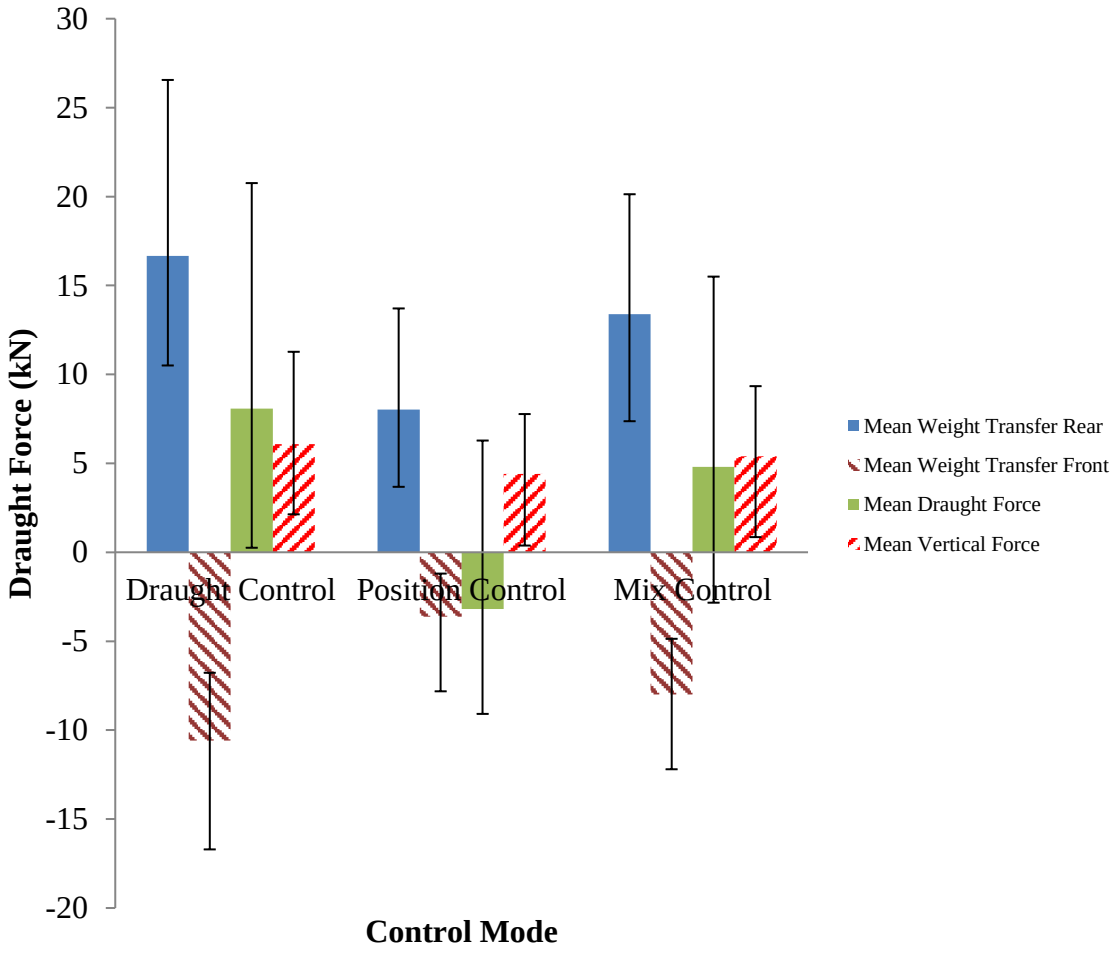

Figure 58: Mean force data recorded during 200 mm depth initial experiments with error bars

(Source: This study)

Draught force (Fx) values shown for maximum and minimum in Table 10 below represent the maximum and minimum variation on the mean values recorded during the experiment. It can be seen that there was significant variation in both Draught and Intermix Control modes selected with minimum Fx values of 7.83 kN and 7.64 kN reduction on the mean

recorded and maximum Fx values recorded of 12.67 kN and 10.69 kN increase on the mean. This is a significant variation whereas data for Position Control showed a reduction to a maximum of 9.46 kN and minimum of 5.91 kN variation on the mean. This leads to a conclusion that at shallower depths weight transfer is less pronounced therefore tillage depth is better controlled. It is interesting to note that a negative mean draught force -3.18 kN is recorded during the Position Control experiments – this may be attributable to the fact that the implement is heavier than the vertical forces generated during the tillage when resolved cancel out the draught force required to pull the implement.

Table 10: Mean force data recorded during 200 mm depth initial experiments

Parameter	Draught Control	Position Control	Intermix Control
Mean δZR (kN)	16.66	8.02	13.38
Max. δZR (kN)	9.89	5.69	6.75
Min. δZR (kN)	6.16	4.34	6.01
Mean δZF (kN)	-10.60	-3.62	-7.99
Max. δZF (kN)	3.82	2.43	3.13
Min. δZF (kN)	6.11	4.19	4.21
Mean Fx (kN)	8.09	-3.18	4.81
Max. Fx (kN)	12.67	9.46	10.69
Min. Fx (kN)	7.83	5.91	7.64
Mean Fy (kN)	6.07	4.40	5.39
Max. Fy (kN)	5.20	3.37	3.95
Min. Fy (kN)	3.94	4.02	4.54

(Source: This study)

Tillage depth variations are large as presented in Figure 59 and Table 11 below with a typically circa. +/-50 mm variation on the measured implement tillage depth (AID) – measured with the measurement wheel. At this depth, 200 mm, from the recorded data it is not possible to draw any real conclusions as to the consistency of tillage depth. This could be attributed to the tread bars on the tyres having a significant effect on tractor ride dynamics

as weight transfer is relatively low the tyres will be less likely to ‘dig in’ to the soil making the ride more oscillatory.

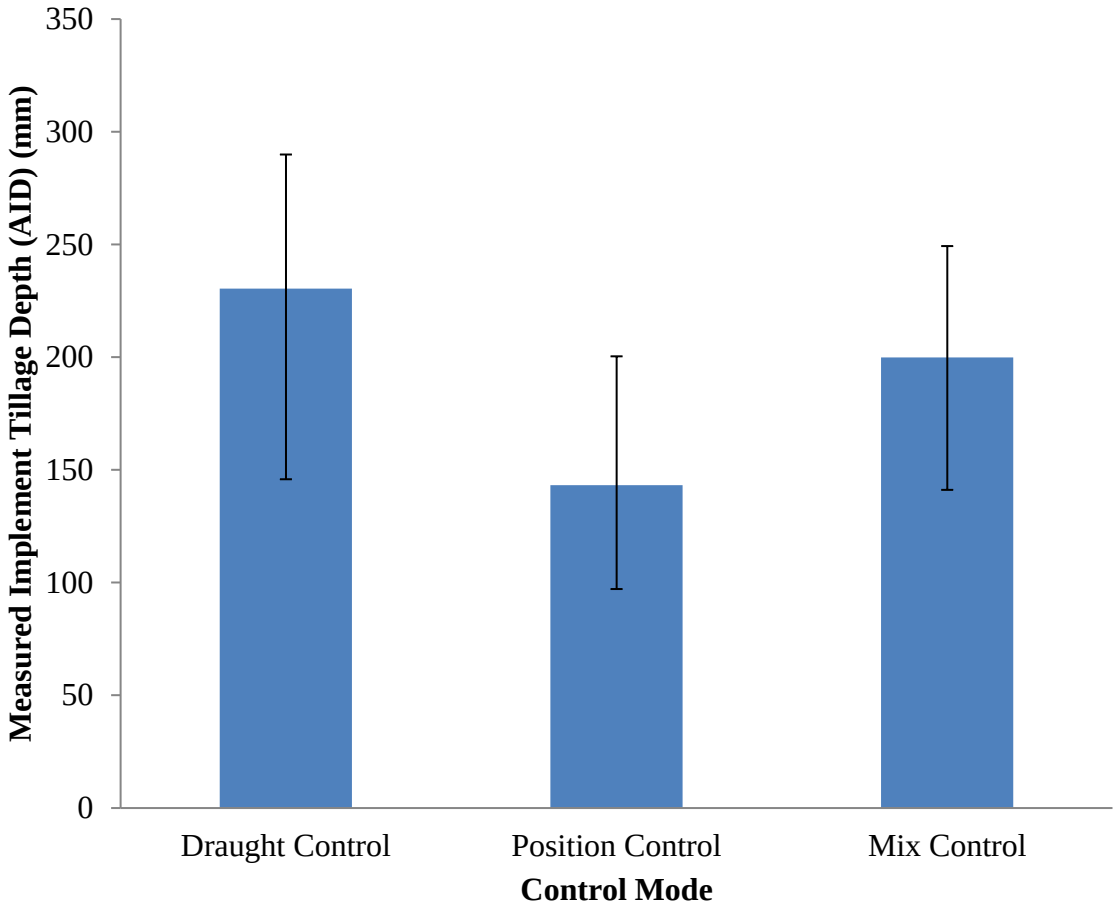

Figure 59: Tillage depth measured during 200 mm depth initial experiments with error bars

(Source: This study)

Table 11: Tillage depth recorded during 200 mm depth initial experiments

Parameter	Draught Control	Position Control	Intermix Control
Mean AID (mm)	230.47	143.17	199.92
Max. AID (mm)	59.45	57.22	49.39
Min. AID (mm)	84.61	46.00	58.77

(Source: This study)

A summary of the combined data from three replicates recorded during experiments of Treatments 4 to 6 is presented in Tables 12 and 13 and Figures 60 and 61 below.

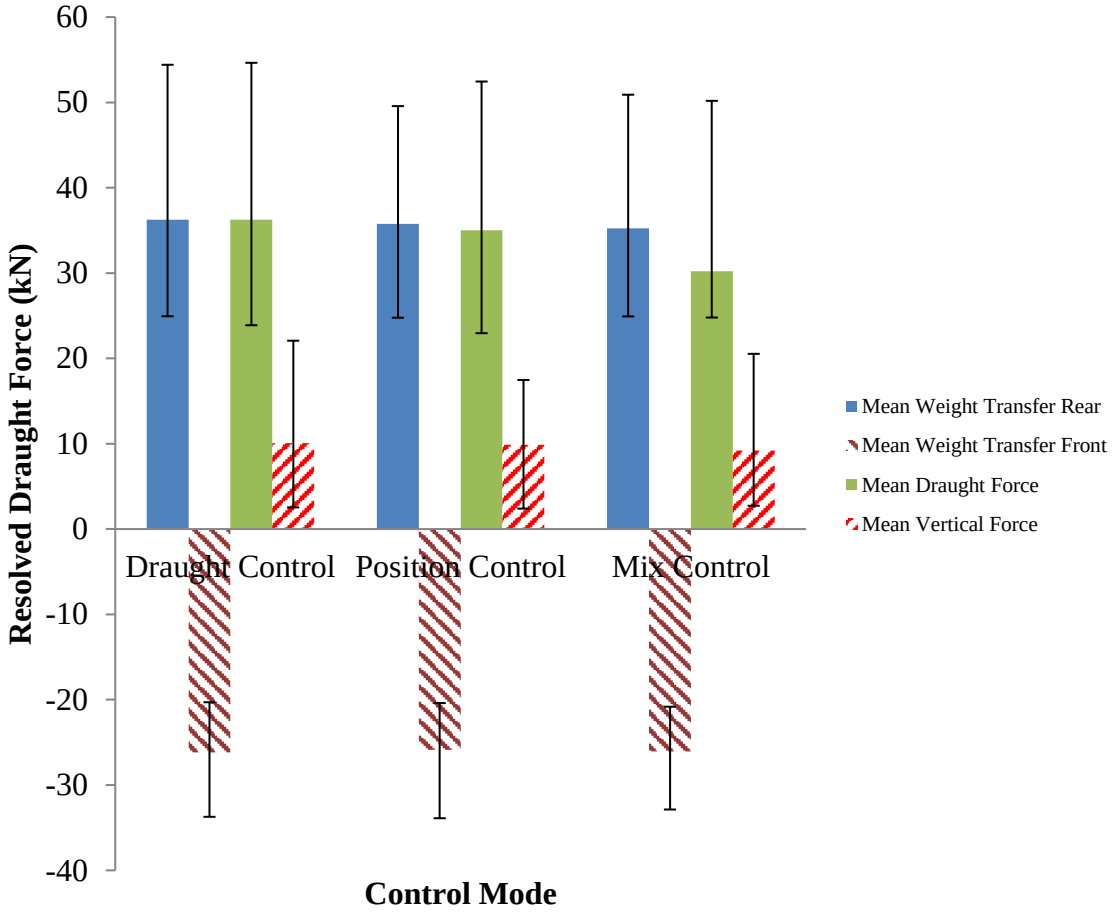

Figure 60: Mean force data recorded during 400 mm depth initial experiments with error bars

(Source: Ward *et al.*, 2011)

Draught force (Fx) values shown for maximum and minimum in Table 12 below represent the maximum and minimum variation on the mean values recorded during the experiment. It can be seen that there was significant variation in draught force throughout all control modes with increases above the mean ranging from 17.45 kN to 19.96 kN and reductions ranging from 5.43 kN to 12.35 kN. Based on a mean Fx values ranging from 30.22 kN to 36.23 kN this is significant and could be attributed to variations in field conditions or control

mode corrective actions. It can also be seen from Table 12 below that weight transfer is relatively uniform across all control modes.

Table 12: Mean force data recorded during 400 mm depth initial experiments

Parameter	Draught Control	Position Control	Intermix Control
Mean δZR (kN)	36.27	35.76	35.24
Max. δZR (kN)	18.14	13.81	15.66
Min. δZR (kN)	11.33	10.99	10.32
Mean δZF (kN)	-26.19	-25.88	-26.05
Max. δZF (kN)	5.89	5.48	5.23
Min. δZF (kN)	7.53	8.01	6.82
Mean Fx (kN)	36.23	35.00	30.22
Max, Fx (kN)	18.41	17.45	19.96
Min. Fx (kN)	12.35	12.05	5.43
Mean Fy (kN)	10.08	9.89	9.21
Max. Fy (kN)	11.99	7.58	11.32
Min. Fy (kN)	7.55	7.50	6.49

(Source: Ward *et al.*, 2011)

It can be seen in Figure 59 and Table 12 that measured implement tillage depth (AID) variations were between 34.72 mm and 49.61 mm above the mean and 39.92 mm and 49.21 mm below the mean. It can be seen that the greatest increases above the mean 49.61 mm were experienced in the Intermix Control mode which is significantly different to values recorded for Draught and Position Control modes, 38.02 mm and 34.72 mm respectively. It was noted at the time of the test that during intermix replicates that the speed governor control on the tractor struggled to maintain forward speed accurately with significant changes in engine note indicating fluctuating loads. This gave the impression that there may be some instability in the control mode selected. A further observation from Table 10 and Table 12 is that within the Draught Control experiments at both 200 mm and 400 mm nominal tillage depth the draught mean draught forces recorded over 3 replicates of each

treatment were 8.09 kN and 36.23 kN respectively. This broadly matches Godwin (1974) predicted relationship between draught force and tillage depth where a doubled depth results in approximately a quadrupled draught force. This gives some confidence in the experimental data presented here and the quality of the experiment.

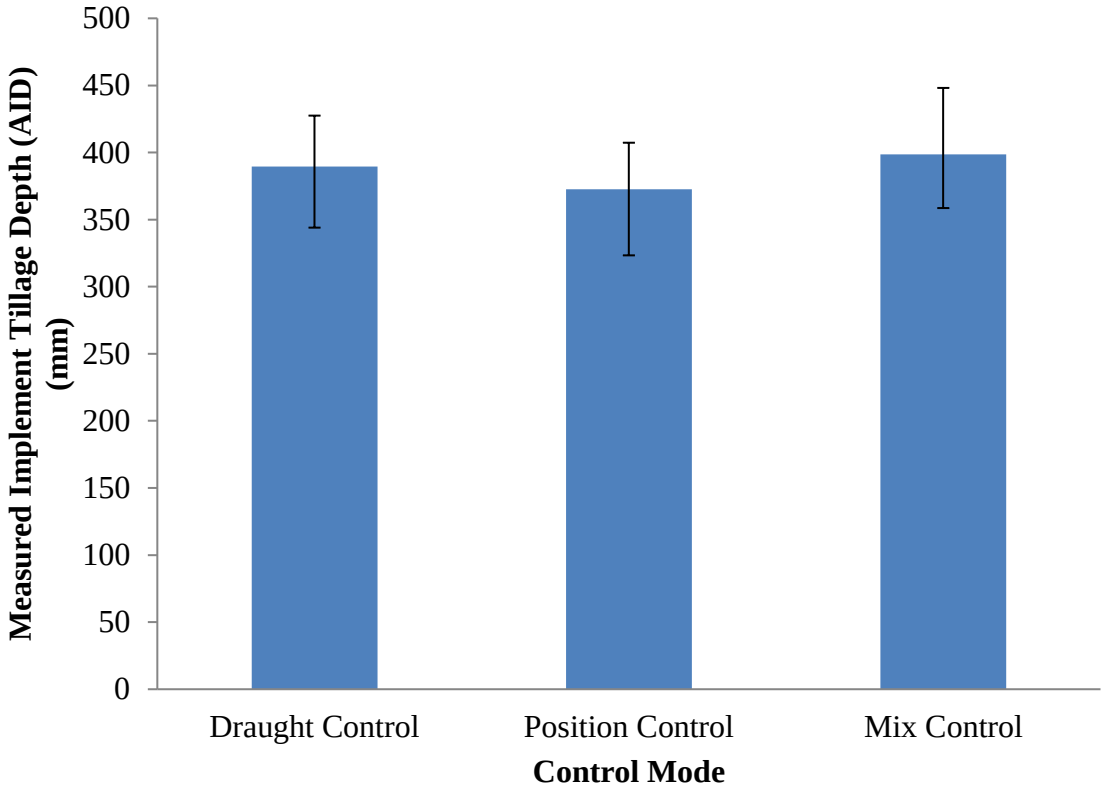

Figure 61: Tillage depth measured during 400 mm depth initial experiments with error bars.

(Source: Ward *et al.*, 2011)

Table 13: Tillage depth recorded during 400 mm depth initial experiments

Parameter	Draught Control	Position Control	Intermix Control
Mean AID (mm)	389.46	372.57	398.51
Max. AID (mm)	38.02	34.72	49.61
Min. AID (mm)	45.46	49.21	39.92

(Source: Ward *et al.*, 2011)

6.2.2.3 Implement Depth Field Experiment Analysis

Using a singular dataset, from the summary table in Appendix C, recorded from the initial field experiments it is possible to investigate the potential efficiency gains through more effective tillage depth control. The data set chosen was from Treatment 4 (Block 1, Plot3, 400 mm depth in Draught Control) as the mean tillage depth was as near to the nominal 400 mm as possible within the data collected. This exhibited significant undulations in tillage depth – mean depth 407.13 mm (draught force Fx – 36.896 kN) with a maximum variation to 453.513 mm and a minimum variation to 360.61 mm. Based on a nominal depth of 400 mm, the mean tillage depth increase was 7.13 mm. Using the relationship predicted by Godwin (1974) Table 14 was generated below, using the mean draught force (Fx) of 36.896 kN and mean implement tillage depth (AID), and is represented graphically in Figure 62.

Table 14: Manipulated tillage depth and draught data from Block 1, Plot 3, Treatment 4

Draught Force (Fx) (kN)	Tillage Depth (AID) (mm)
0.00	3.18
0.01	6.36
0.04	12.72
0.14	25.45
0.58	50.89
2.31	101.78
9.22	203.57
36.896 *	**407.13 ***
147.58	814.26

* - Mean recorded data

(Source: This study)

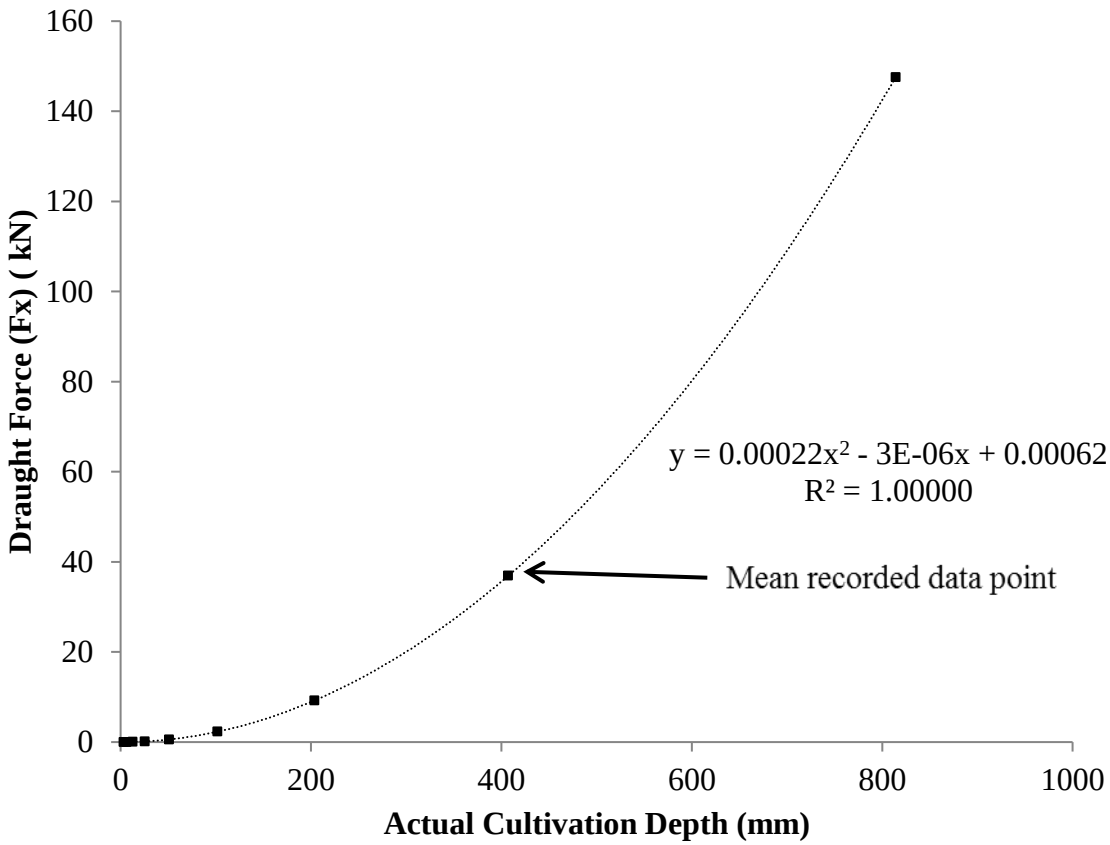

Figure 62: Manipulated tillage depth and draught data from Block 1, Plot 3, Treatment 4

(Source: This study)

Utilising the trend line equation from Figure 62 it can be calculated that for a correct depth of 400 mm the draught force requirement would be 35.61 kN which is approximately a 3.5 % reduction in draught force and for a given constant speed would result in the same reduction in power required assuming wheel slip was also consistent. This is calculated for a specific dataset, however it does practically demonstrate that a relatively small increase in depth has a more significant effect on energy used.

6.2.2.4 Implement Depth Field Experiment Conclusions

It was found through the experiments that implement tillage depth and draught forces vary significantly about the mean points. Particularly during the 400 mm depth experiment tillage

depth varied by as much as 49.61 mm above the mean value of 398.51 mm in Intermix Control experiments. Whilst this may not appear significantly high, when considering the depth draught force relationship described earlier this could lead to significant amounts of energy being wasted when tillage is not required at to the increased depth.

What is also important is the ability to set the tillage depth as required. This involves setting the linkage based on a physical field measurement, however what is not known is how the linkage control strategy changes depending on linkage position. Whilst the general functionality of Draught, Position and Intermix Controls are relatively well known the only means of adjusting linkage position is using the depth control wheel in the tractor cab. However, the effects of doing this on the control strategy in use during the field operation are not so well known.

It was also found during Draught Control experiments at nominally 200 mm and 400 mm tillage depths the mean draught forces across the three replicates were 8.09 kN and 36.23 kN respectively. This accurately matches Godwin's (1974) prediction. An example based on this prediction was presented and due to a 7.13 mm increase in tillage depth a 3.5% increase in energy or drawbar power would be required. This highlights that with even greater variations in tillage depth from what is required will result in wasted energy. Therefore, there is merit in development of a revised three point linkage controller to mitigate energy usage inefficiency.

6.3 MF8480 Linkage Control Performance

Initial experiments evaluated the field performance of the tractor implement combination in the field. However, to develop an understanding of how the existing linkage control system functions depending on the tillage depth, a further experiment was conducted. The manufacturer of the MF8480 tractor were asked to provide this information, however this

information was not forthcoming, therefore this experiment was devised to characterise the functional performance of the standard linkage control system algorithms. This key understanding was necessary to develop an alternative control methodology. The experiment is performed with the research sub-soiler frame with tines removed and substitute weights added. This allows the linkage to move freely with the correct weight added for this work. This was done to ensure should there be a weight control element to the three point linkage controller the results of the experiment are consistent and applicable throughout this research. Shown below in Figure 63 is the implement set up. The instrumentation used in this experiment are the depth wheel and original lower lift arm angle sensor as used in the initial field experiments using historical calibrations. Only basic graphical data obtained from this experiment is presented to protect any intellectual property rights

Figure 63: Linkage control evaluation experiment test set up

(Source: This study)

6.3.1 Linkage Control Evaluation Experiment

To complete the experiment a simple draught sensing pin simulator was developed to input known draught loads based the calibration data from Bosch (Appendix A). The manufacturer calibration, rather than the calibration from this study was used as it excludes any mechanical friction or looseness present in the lower lift arm. The device consisted of a number of variable resistors that could be adjusted to allow a known voltage input to be applied to the tractor electrical system simulating a draught force input. A schematic of the circuit diagram is shown in Figure 64 below.

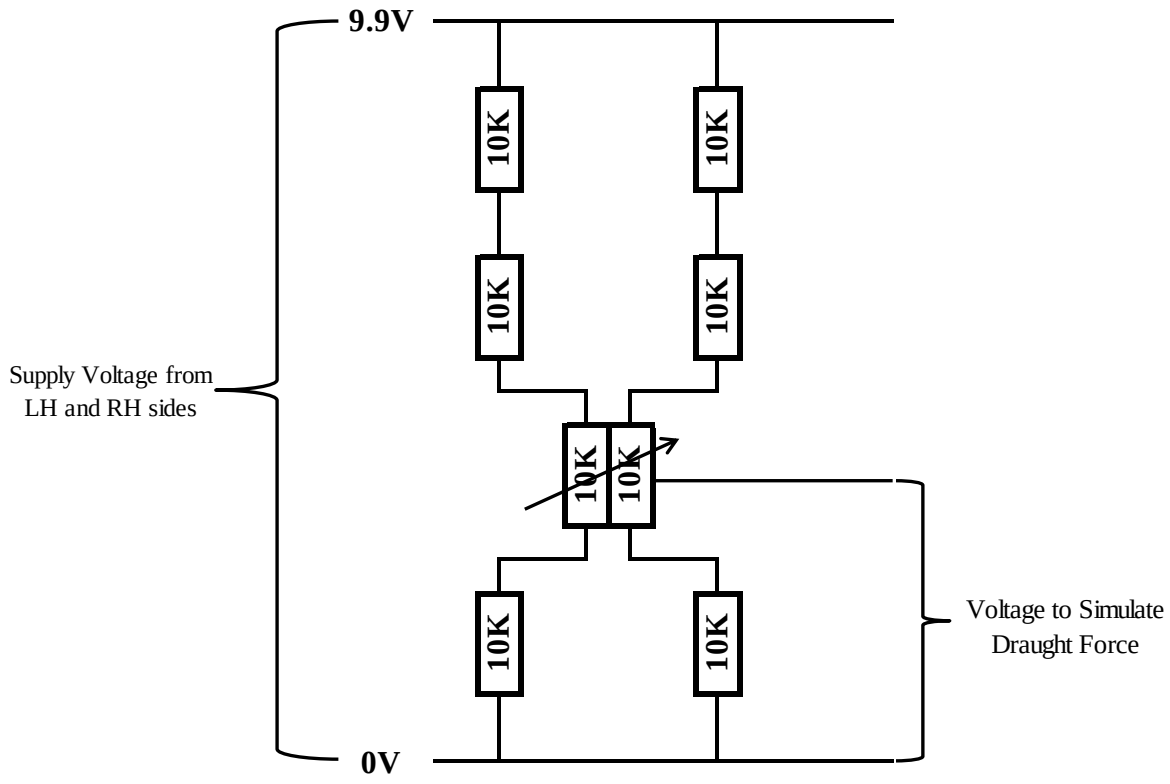

Figure 64: Circuit diagram of the draught force simulator

(Source: This study)

6.3.1.2 Linkage Control Evaluation Experiment Plan

The experiment consisted of establishing the movement characteristics of the linkage during work. Data logged during the experiment consisted of measured implement tillage depth (AID) using the implement tillage depth measurement wheel and lower lift arm angle (α) using the original linkage positional measurement sensor. A typical engine operating speed was selected based on an initial evaluation of linkage speeds as a function of engine speed under no load.

The experiment consisted of the following variables:

1. Control mode selection: Position, 2, 3, 4, 5, Draught;
2. Depth control dial – Depth 1 to 9;
3. Lift height control - 4;
4. Lower speed control – 3;
5. Engine speed – 2000 min^{-1} (typical tillage engine speed);

Using the draught force simulator the following steps were completed for all combinations of the control mode and depth control variables in the list above (items 1 and 2):

- Using the draught force simulator establish for each permutation what the load required to generate linkage movement by applying a ramped load input using the draught force simulator;
- Once the linkage motion start and stop loads were established by evaluating the graphical data step load inputs were chosen to establish the exact response at a given set of control variables.

The measured data was logged using a National Instruments USB6009 data logging card and host computer at a rate of 250 Hz. A relatively low sampling frequency was used as only linkage movement was observed rather than high frequency soil disturbance.

6.3.1.3 Linkage Control Evaluation Experimental Data

Data were processed in the context of the study implement and linkage kinematics and therefore any depth data quoted are on this basis. It was found during the experiment that there was no linkage response to depth positions 1, 2, 3 and 9. Presented in Table 15 below are the implement or tillage start positions for all of the experimental permutations. These are also presented graphically in Figure 65 below.

Table 15: Data for implement tillage depth start position during linkage control evaluation experiment

Parameter	Linkage Control Position	Control Mode					
		Position	2	3	4	5	Draught
AID (mm)	4	-13.0	-34.9	-104.1	-424.3	-424.3	-424.3
	5	90.8	120.0	190.6	435.6	436.2	436.1
	6	211.7	248.7	333.6	437.3	437.1	435.4
	7	328.9	371.4	439.2	438.8	439.5	438.2
	8	436.8	436.1	436.1	436.8	436.1	435.4

(Source: This study)

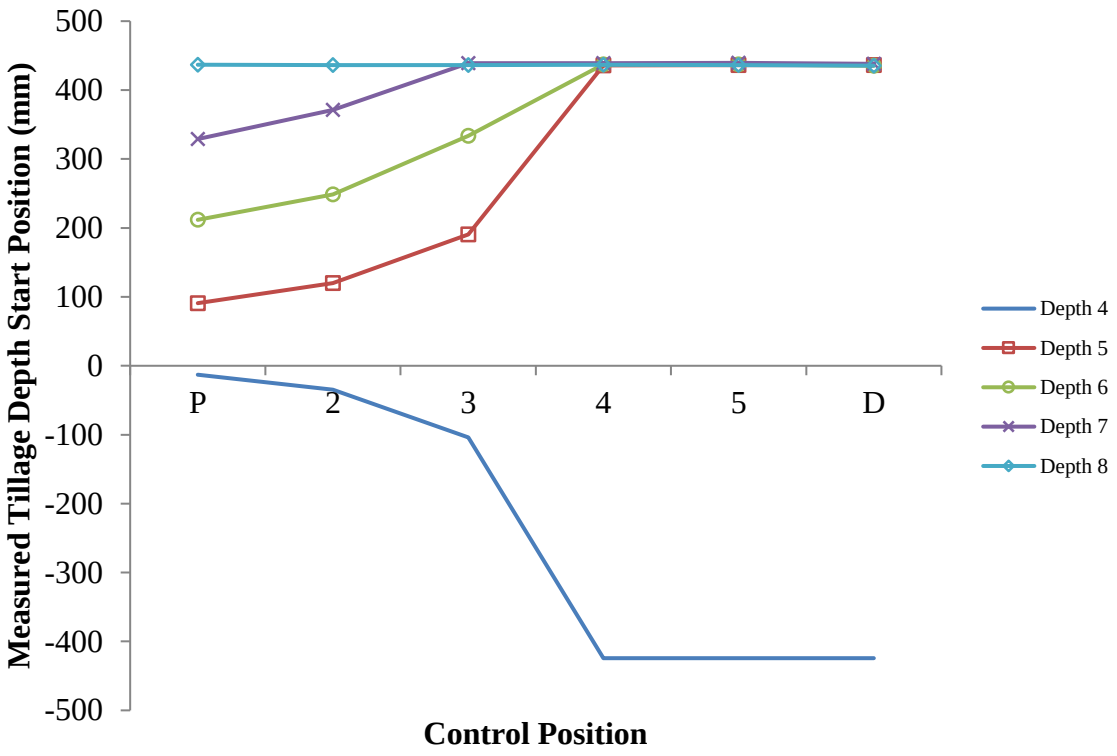

Figure 65: Measured implement tillage depth start positions based on linkage control set up during linkage control evaluation experiment

(Source: This study)

As can be seen from Figure 65, above, for a nominal tillage depth, for example, of 400 mm there are multiple possibilities for tractor set up. Shown in Figure 66 below are the linkage actuation load ranges that were established as part of determining the draught force simulator input voltage during the experiment. Data are show for each of the linkage control permutations tested. Shown also in Figure 66 are the behavioural characteristics of the response to the draught load input and as the control mode selected moves between Position and Draught Control the limits of linkage in response to a step simulated draught force input increase.

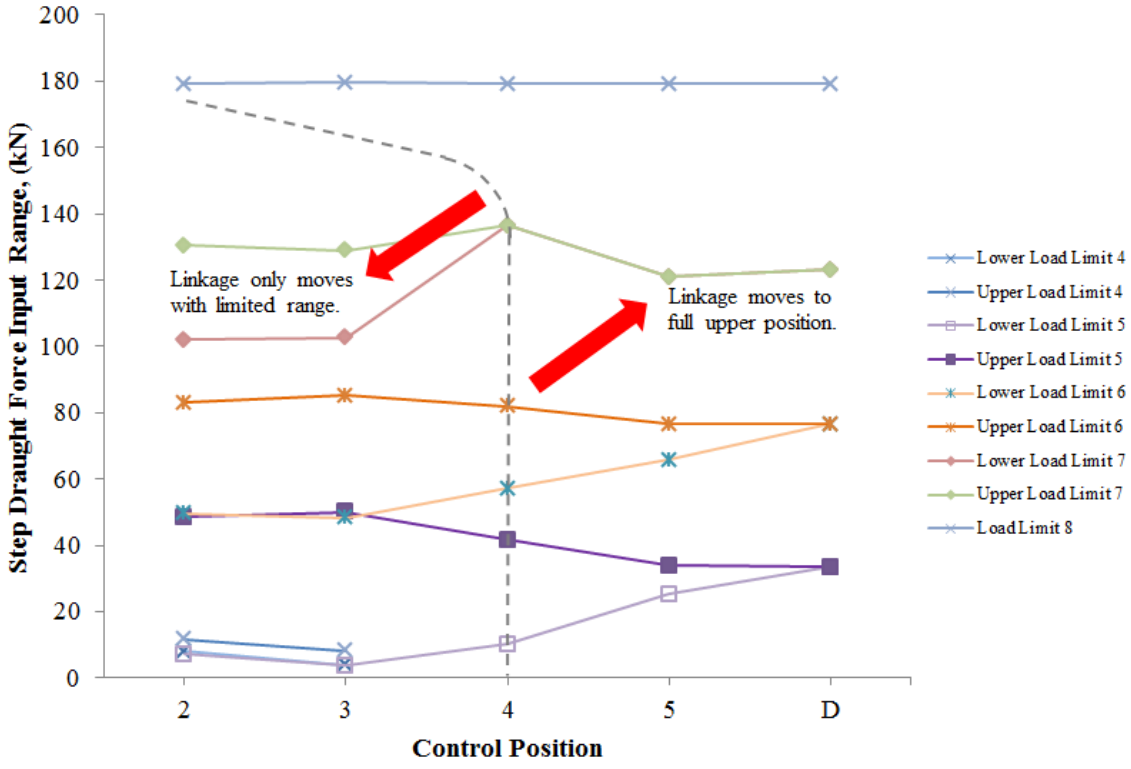

Figure 66: Linkage control system load response ranges recorded during linkage control evaluation experiment

(Source: This study)

These data are presented for information only to understand whether current linkage control systems are easy to set up and use in an efficient. To conclude there are many potential set up possibilities for any given tillage operation.

6.4 Linkage Control Systems Conclusions

It is reasonable to suggest that the operator of a tractor has many potential permutations of linkage set up options consisting of:

- Position, Draught or Intermix Control;
- Lift height settings limiting Draught Control lift height;
- Lift speed to determine the rate of linkage response.

Whilst an experienced operator will be able to set the tractor up to what is believed correct there is no real-time performance feedback on the operation conducted. Whilst physical signs may be obvious such as increased wheel slip, engine note change under excessive load or reduction in forward speed these do not indicate the quality or efficiency of the operation performed. It is also possible by selecting certain parameters to mimic the operation of another; by limiting lift height in Draught Control mode is in effect operating the tractor in Position Control mode. Due to the constantly changing nature of soil conditions within a field it therefore is extremely difficult for an operator to adjust settings to operate efficiently; whilst experience will dictate tractor implement combinations there is no absolute science in the selection process with inefficiencies in the field becoming unknown. Software exists developed by Zoz and Grisso (2003) and Sahu *et.al*. (2008) to match implements to tractors but these do not take into account varying field conditions.

The purpose of conducting the linkage evaluation experiment was to establish what parameters dictate the operation and functionality of the linkage control system. The field and laboratory experiments justify the need for a more intelligent but easier to use linkage control system with real-time implement tillage depth control. Coupled to a performance monitoring system and more accurate tillage depth monitoring and control it can be concluded that potential energy efficiency improvements are feasible.

CHAPTER 7 - Control Algorithms

7.1 Control Algorithm Background

Current agricultural tractor three point linkage control systems were comprehensively covered in Chapter 6. To summarise the systems are largely of a generic physical design and functionality with main features including:

1. Draught force measurement via electronic draught force measurement pins;
2. Positional measurement using a rotational transducer on the linkage lift arm cross shaft;
3. Variation in feedback control through variations between Draught and Position control;
4. A form of lift height control to provide a limit to the mechanical response to feedback control – variation between Draught and Position Control;
5. Response control which controls/limits the speed at which the mechanical response to linkage inputs are attenuated.

What is lacking is the ability to display real-time field performance from an energy usage perspective; with the emphasis on time or usage related performance such as work rate or seed rate. From this basis tractor electronic systems are relatively straightforward in daily use. A series of field and laboratory experiments, presented in Chapter 6, concluded the need for a simple linkage control system that accurately monitors and controls tillage depth in real-time whilst monitoring the energy efficiency of the field operation; leading to potential energy and time gains.

Past research has alluded to the concept of automated tractor control functions (Blackmore *et al.*, 2002) and primarily focussed on the functionality (Scarlett, 2001) of the tractor such

as automatically guided but little work has been conducted in the area of linkage control and field efficiency. More recent research has looked at the effects on tractive efficiency.

The idea of tractor performance monitoring is not new and simple performance monitors for agricultural tractors have been developed such as that by Summers *et al.* (1986). However, knowledge of current performance is useful but there is no instruction to the operator about what changes that could be made to improve performance and better utilise energy available. Tractor implement matching is not a new theory with significant contributions to the subject area made by Zoz and Grisso (2003).

In field use there are number of factors that affect the quality of the tillage operation, field performance and energy usage of an agricultural tractor. To summarise:

1. Soil type and condition variation throughout a field including compacted areas;
2. Seen in Chapters 2 and 6 the draught force (Fx) and tillage depth relationship is exponential;
3. Tillage operation – different tillage operations have varying degrees of set up possibilities as do tractors as described in Chapter 6;
4. Tractor selection – the correct matching of a tractor and implement is imperative to ensure maximum available energy usage (Zoz and Grisso, 2003);
5. Speed of work – speed and draught force (Fx) will affect the wheel slip encountered and therefore energy losses;
6. Field undulations causing tillage depth fluctuations.

Various elements of the control algorithm developed within this study are based on standard mathematical processes and brings previous quasi-static analyses into real-time measurement and control. The system described here operates in real-time in the field whilst work is being done. The system is based around the unique integration of the linkage force resolution and tractor dynamic kinematic models developed in Chapter 3 with the instrumentation system described in Chapter 5 and the conclusions from initial linkage performance evaluation experiments described in Chapter 6.

The control algorithm was designed around the following specification:

1. Simplified three point linkage operator controls – it was seen in Chapter 6 that current systems are too complex to set up accurately;
2. The ability to reduce tillage energy losses through more accurate tillage depth control appropriate to the desired mode of work operation;
3. Real-time performance monitoring such as power usage, fuel consumption, wheel slip and work rate through calculation;
4. Informing the operator of tractor/implement set up changes that could be made to improve the current performance.

7.2 Control Algorithm Overview

The control algorithm, developed in National Instruments LabVIEW, incorporates the linkage force resolution and dynamic kinematic model equations developed in Chapter 3 and instrumentation calibrations and relationships detailed in Figures 34 to 48 in Chapter 5. A schematic representation of the control algorithm overall functionality is shown in Figure 67.

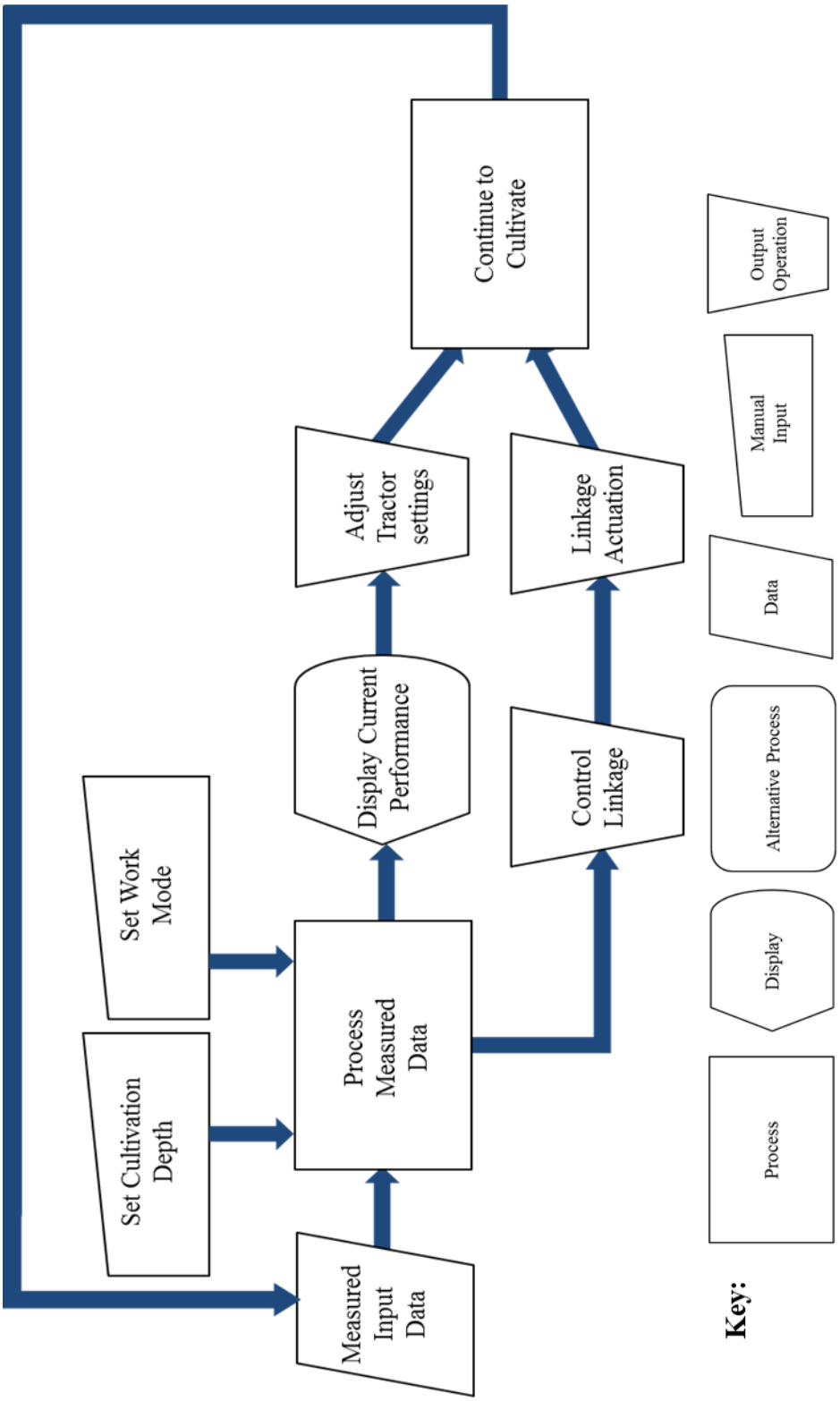

Figure 67: Overview of the control algorithm sub-systems developed in this study

(Source: This study)

The following key features form the basis of the control algorithm:

1) It has three work modes of operation – field work rate, tractor and fuel efficiency and consistent tillage depth and quality. The work modes control the limits of tillage depth monitoring;
2) Measures linkage force data and position;
3) Calculates dynamic forces acting on the tractor through the tillage operation including draught force (Fx), vertical force (Fy) and weight transfer effects. The data is used to predict current performance, tyre deformation and potential improvements that can be made;
4) Measures and calculates forward speed and wheel slip;
5) Measures axle heights and estimates tillage depth through kinematic resolution equations and directly measures implement tillage depth (AID) as verification;
6) Constantly monitors tillage depth in real-time against the nominal value set and depending on the limits of operation set by the selected work mode makes corrections where required to correct the implement tillage depth. All work modes function in this way;
7) Uses recorded data to predict power delivery efficiency in real time and makes suggestions for energy optimisation such as increasing speed or adjusting implement configuration to utilise the power available.

7.3 Control Algorithm Functional Elements and Operation

The algorithm features many standard mathematical processes; these will not be described, as they are covered in the equations generated in Chapter 3 and instrumentation system calibrations detailed in Chapter 5. Screen captures of the control algorithm developed in LabVIEW in this study, using a block diagram based code, are presented in Appendix F.

The algorithm is still at a developmental stage with various verification processes installed to ensure the core mathematical processes work effectively – such as measuring implement tillage depth (AID) to verify the predicted implement tillage depth from the kinematic resolution of axle heights.

Shown in Figure 68 below is a screen capture of the prototype tractor operator algorithm interface.

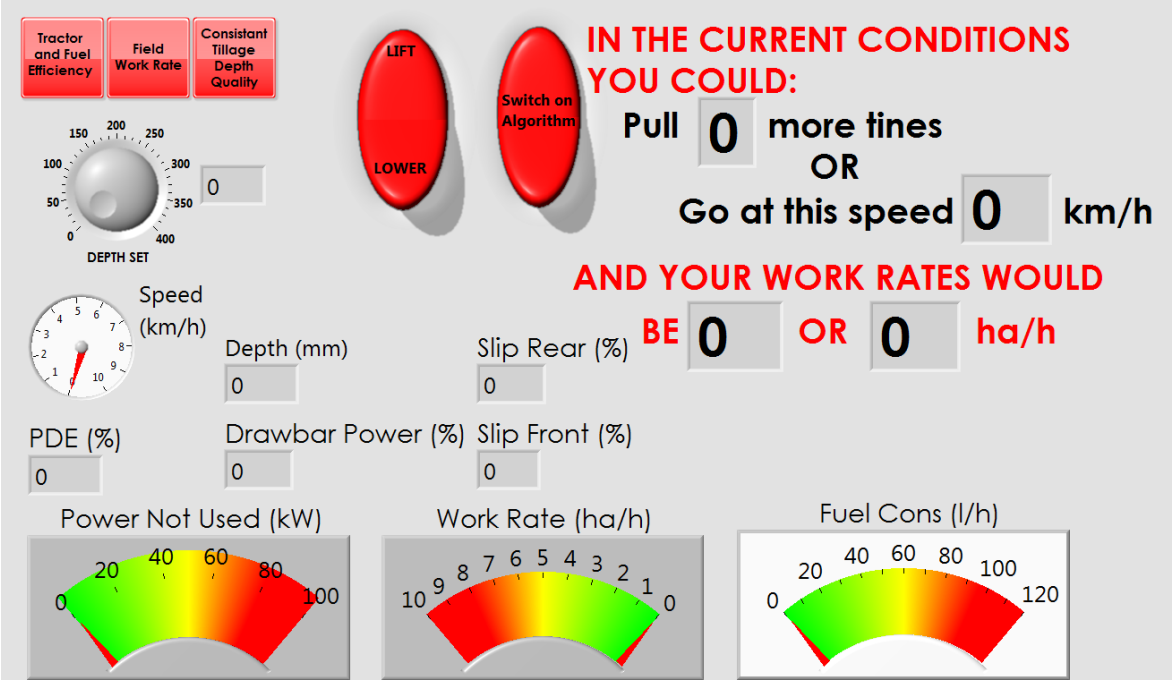

Figure 68: Screen capture of the development operator interface

(Source: This study)

Table 16 below provides a summary of the nomenclature used in the control algorithm screen captures (Appendix F) throughout the remainder of this Chapter.

Table 16: Input data parameters to the control algorithm

Data Input Name	Description
ELP	Linkage positional measurement - linkage kinematics (V)
FAH	Front axle height from the undisturbed ground surface (mm)
RAH	Rear axle height from the undisturbed ground surface (mm)
AID	Measured implement tillage depth (mm)
FOS	Wheel speed front off side (m s^{-1})
FNS	Wheel speed front near side (m s^{-1})
ROS	Wheel speed rear off side (m s^{-1})
RNS	Wheel speed rear near side (m s^{-1})
SOG	True forward speed over ground (m s^{-1})
FTL	Top link force (kN)
LLR	Left lift rod force (kN)
RLR	Right lift rod force (kN)
LLP	Left load pin force (kN)
RLP	Right load pin force (kN)
FC	Measured fuel consumption (l h^{-1})

(Source: This study)

The control algorithm is designed to operate at 1000 Hz, due to certain sensors with a pulsed output, in a constantly iterating loop with all data input, calculations and control in real-time. As the control algorithm is still at a developmental stage, the data is streamed to a host computer to log the performance attributes for off tractor data analysis; which potentially is a feature of the final version.

The following sections detail the constructional elements of the control algorithm, in LabVIEW, and their functionality to achieve the desired algorithm output. The Figures presented of the block diagram code are highlighted in Appendix F.

7.3.1 Work Mode and Desired Tillage Depth and Tolerances Selection

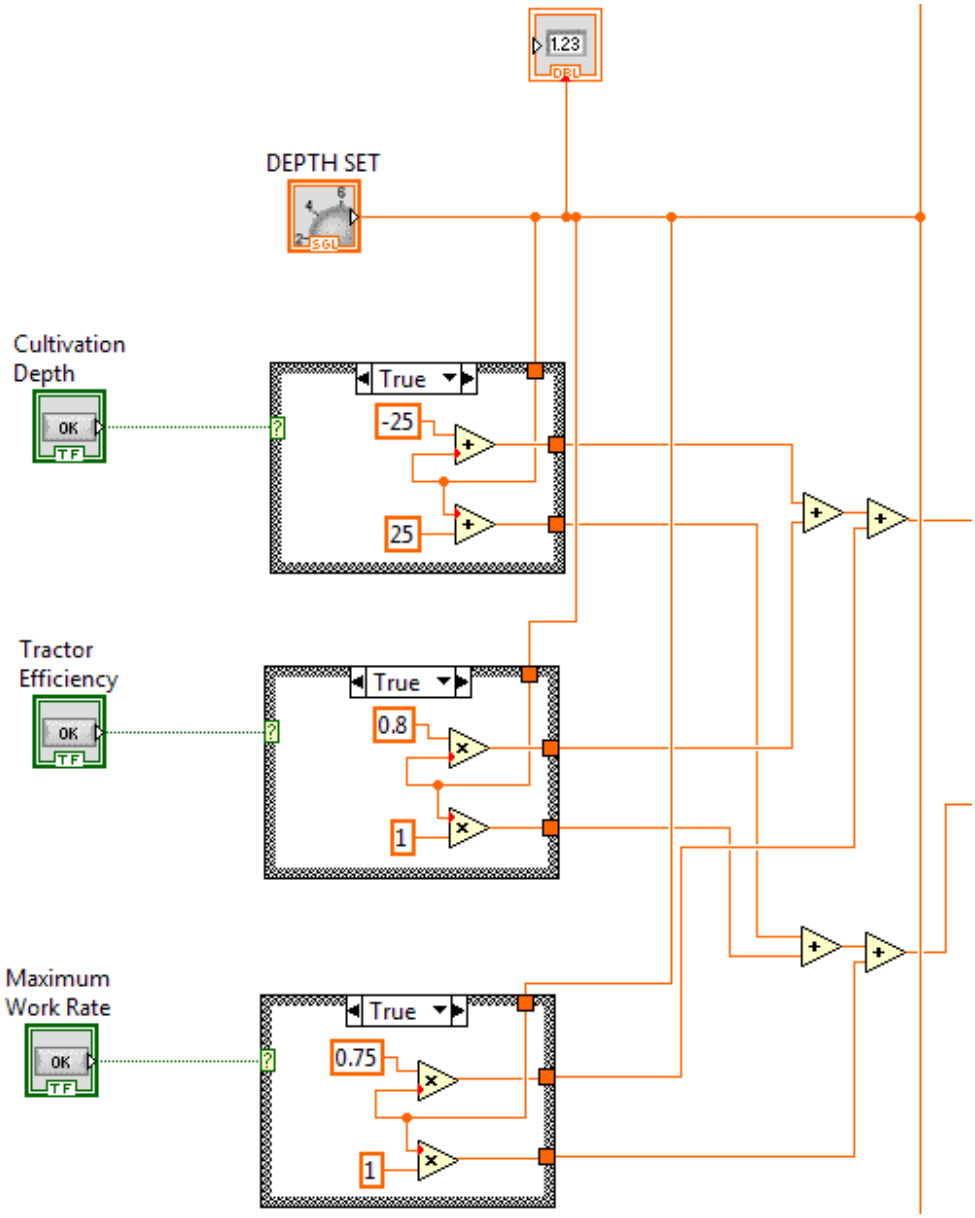

Figure 69: Work mode, implement tillage depth setting and limits block diagram code developed shown in the 'true' condition

(Source: This study)

Figure 69 above shows the relevant block diagram code developed in this study to complete the following functions:

- Set desired tillage depth;

- Choose work mode;
- Provide implement tillage depth limits based on the selected work mode.

The following list describes the series of tasks that take place within the algorithm sector captured in Figure 69 to effect the setting of work mode, tillage depth and tillage depth tolerances:

1. The tractor operator sets the desired work mode on the operator interface which sets the relevant case structure in Figure 70 to the *True* condition;
2. The selection of the work mode then applies limits to the allowable variation in implement tillage depth – the remaining work mode case structures output. The limits are as follows:
    - **Field Work Rate** – Nominally allows tillage depth to increase by 0 % and decrease by up to 25 % therefore minimising draught force loads – designed to reduce load to aid speed of the work but still maintains a certain degree of tillage depth accuracy;
    - **Tractor and Fuel Efficiency** – Nominally allows the tillage depth to increase by 0 % and decrease by up to 20 % - designed not to allow the depth to increase beyond the nominal value set but allow a reduction with a tighter tolerance than achieving high field work rates;
    - **Consistent Tillage Depth and Quality** – Nominally allows only +/- 20 mm tillage depth. A numeric value is used rather than a percentage to allow much finer tuning in the development system being non-dependent on tillage depth. This limit is based on results achieved with a nominal tillage depth of 400 mm in early field experiments (Chapter 6).

3. The tractor operator then selects the desired nominal tillage depth using the operator interface;

4. The algorithm then sums all limits set from each possible work mode selection to generate upper and lower tillage depth tolerance limits – where the non-selected work modes output a zero value through the *False* case structure.

Note: The tillage depth tolerance limits currently applied are and further experimentation is required to provide more accurate tolerance limits.

The desired set tillage depth is then turned into a nominal quasi-static linkage position, α, using trend line equation given in Figure 36 and then into a control voltage (TLP) using the α lowering calibration trend line equation given in Figure 38. The code developed for this function is shown below in Figure 70.

Note: In a linkage lowering situation the lower lift arm angle (α) is positive (+ve).

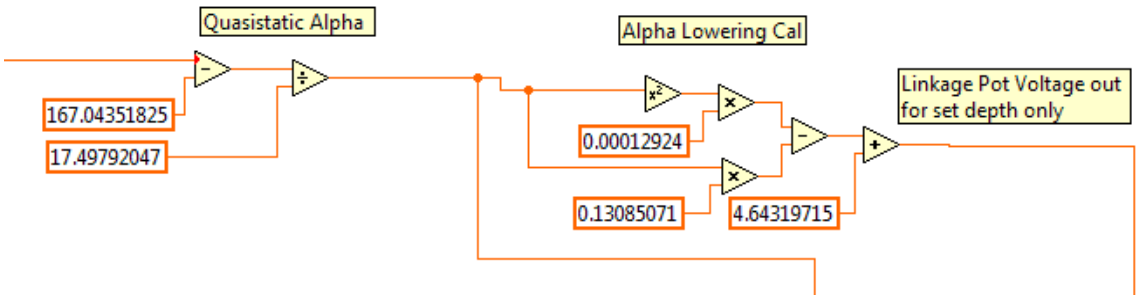

Figure 70: Block diagram code developed to calculate and set linkage position

(Source: This study)

When steps 1 to 4 above and the linkage control voltage has been set the operator can move the tractor forwards using a set engine speed of 1500 min^{-1}. Once moving, the lift / lower switch on the operator interface can be used in the normal manner to engage the implement with the soil. The actuation of the lift / lower switch enables a control voltage to be applied

to the electro-hydraulic valve controlling the linkage lift rams through a simple *True / False* case structure.

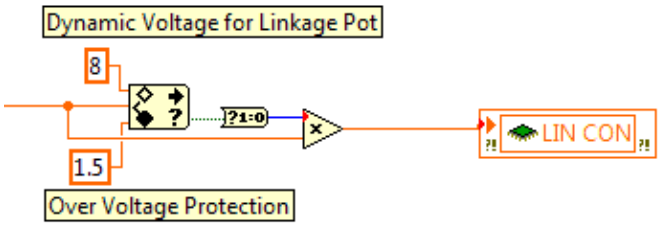

Figure 71: Block diagram code developed for supplying the control voltage to the linkage lift rams electro-hydraulic control valve

(Source: This study)

Shown above in Figure 71 is the block diagram code developed to supply the control voltage to the linkage lift rams electro-hydraulic control valve. The purpose of the code is to ensure the control voltages applied are within the normal tractor control voltage operating limits – which were measured as part of the linkage control evaluation experiment in Section 6.3. The control voltage at this stage also includes any linkage position correction, which at this stage is zero, as the tractor implement combination is operating in a quasi-static manner with no corrective actions applied.

Once all of the above processes are complete the operator can switch on the tillage depth correction function using the appropriate switch on the operator interface (Switch Algorithm On) which allows corrective actions to take place. The set voltage for the linkage dictated by the set depth at the start of the process will continue to apply at all times unless a correction is required due to tillage depth being out of the tolerance limits set.

7.3.2 Implement Tillage Depth Measurement and Corrective Actions

The main part of the algorithm is the tillage depth control function and this forms one of the novel elements of this study. Essentially it is a position control based function with correction based on actual tillage depth in respect of the desired tillage depth. Although no Draught Control is included as a direct function it is implied in that should tillage depth increase beyond the defined work mode limits a corrective action is applied; therefore reducing draught force as discussed in Chapters 2 and 6. The algorithm therefore allows controlled tillage of areas that with current systems may not be done at the correct depth due to the control strategies employed by the operator.

The first element of this function is to measure the actual tillage depth, (AID). Shown below in Figure 72 is the block diagram code developed to complete this unction using data input from the measured actual tillage depth wheel and calibration trend line equation given in Figure 34.

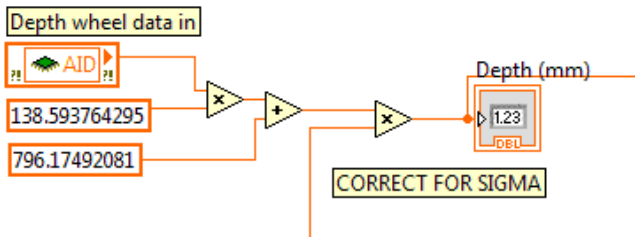

Figure 72: Block diagram code to measure implement tillage depth (AID)

Referring to Figure 72, the code also incorporates a correction factor for tractor attitude, σ^{o}, vide a true tillage depth; the depth wheel was calibrated completely perpendicular to the ground.

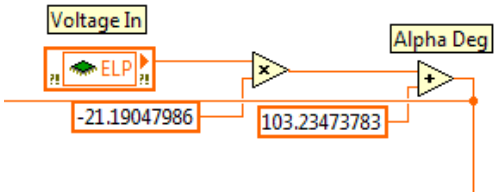

Figure 73: Block diagram code to measure linkage position in relation to the tractor (ELP)

(Source: This study)

The second part of the tillage depth control function is to understand the actual position of the linkage in relation to the tractor; feedback for the set depth required in Section 7.3.1. Referring to Figure 73 above the developed block diagram code incorporates the calibration trend line equation, given in Figure 35, generated for the linkage positional sensor (ELP). The functionality of this part of the overall algorithm is to allow a correction value of the linkage position to be established.

Shown below in Figure 74 is the decision making element of the overall control algorithm.

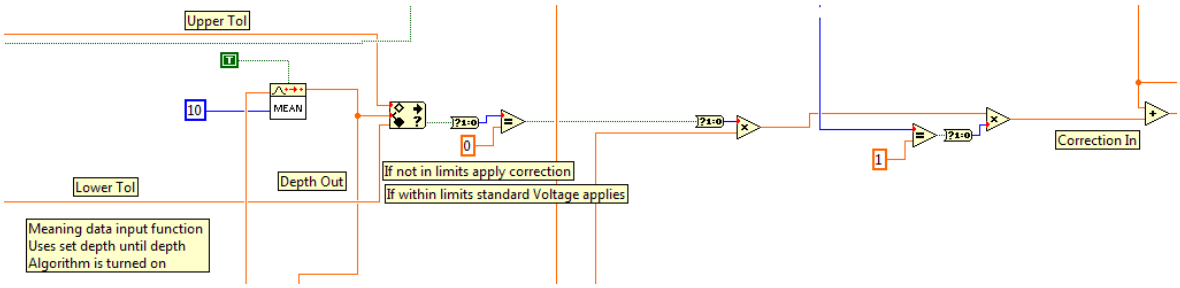

Figure 74: Real-time implement tillage depth correction decision block diagram code

(Source: This study)

The measured implement tillage depth forms the basis of the input data (Figure 72 refers). The following describes the decision making process tasks in Figure 74:

1. Until the tillage depth correction function is switched on the system uses the set depth as the input data to the system. Once the control algorithm is activated the system then uses measured implement tillage depth (AID);

2. The measured implement tillage depth (AID) is smoothed using a meaning function which returns a value every 10 ms (milliseconds);

3. Using a limits function with the upper and lower work mode tolerance limits applied a decision is made if the measured implement tillage depth is within limits or not;

4. Logic functions are used to either apply a correctional factor, shown in Figure 75, to the control voltage supplied to the electro-hydraulic linkage control valve – if no correction is required then the control voltage remains as previously set by the desired tillage depth shown in Figure 70;

Note: Certain mathematical functions are not described above as these are related to achieving the functionality described.

Shown below in Figure 75 is the bock diagram code developed to calculate the linkage positional correction required.

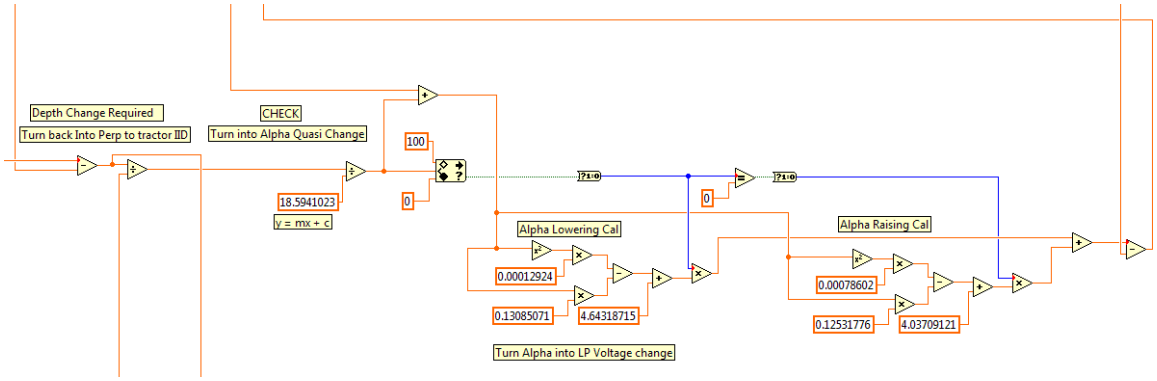

Figure 75: Block diagram code developed to calculate the linkage positional correction required to maintain tillage depth within work mode limits

(Source: This study)

The functional tasks of the code described in Figure 75, working from left to right, are as follows:

1. Using tractor attitude, σ, the corrected measured implement tillage depth (AID) described in Figure 72 is re-corrected to provide the true calibrated value;

2. Once decision has been made on whether a correction of linkage position/tillage depth is required, shown in Figure 74, the difference is simply calculated using the set depth and the measured implement tillage depth (AID);

3. Using a rearrangement of Equation 3.17 the depth correction is converted into a lower lift arm angular positional change (α) which will either a positive or negative numerical value;

4. A limits function is then used again to establish if the value is positive or negative with limits set between 0 and 100. The purpose of these limits is such that if the correctional value of α is negative then it is outside of limits and a zero multiplier is used in the next task – if within limits a multiplier of one is used;

5. The correctional value of α established in task 3 is then converted into the control voltage correction required to supply the linkage electro-hydraulic valve using **both** α, raising and lowering calibrations; using calibration trend line equation given in Figures 37 and 38 respectively.

6. Depending on the multiplier created in task 3 each correctional voltage calculated in task 5 is multiplied as appropriate depending on whether the required correction is positive or negative;

7. The correctional values are then summed and in turn summed with the desired tillage depth electro-hydraulic control voltage calculated in the code shown in Figure 71;

8. The implement tillage depth correction is therefore applied in real-time as the tractor continues to cultivate.

7.3.3 Tractor Dynamic Kinematics

As a major enabler to the functionality of the control algorithm the calculation of the linkage positional kinematics are critical. Shown below in Figure 76 is the block diagram code generated to turn the lower lift arm angular position α, into β, γ and θ.

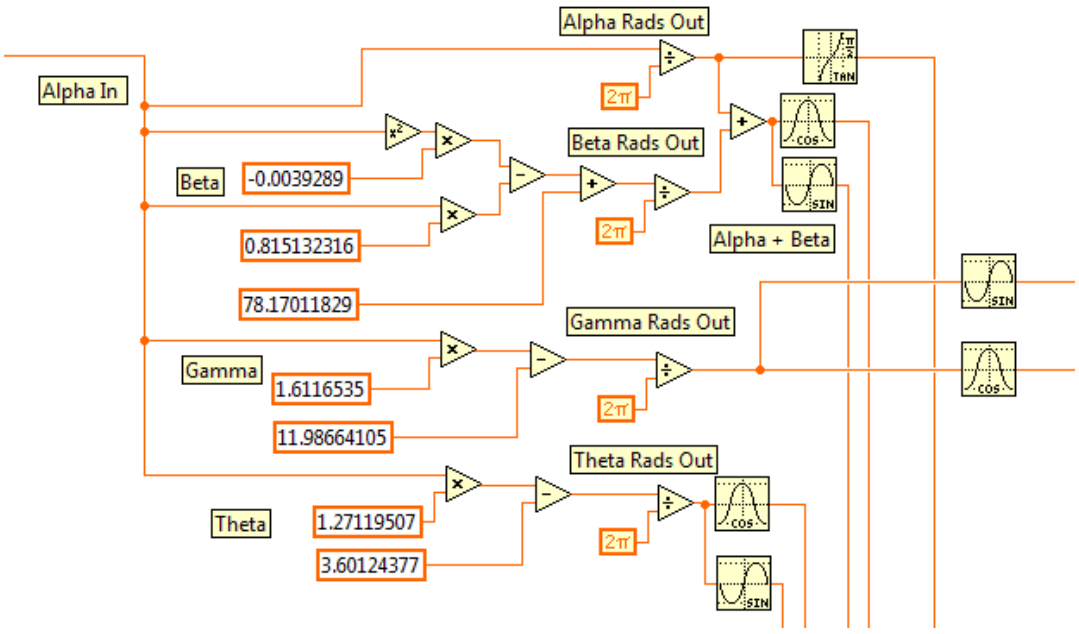

Figure 76: Block diagram code developed to incorporate equations to calculate linkage positional angular relationships α, β, γ and θ

(Source: This study)

Referring to Figure 76 the following lists comprises the actions completed within the code shown:

1. The output, α, from the linkage positional sensor (ELP) provides the input to the calculations;

2. Utilising Equations 3.14 to 3.16 the input α is manipulated to provide β, γ and θ as inputs to the force resolution elements of the control algorithm;

3. All of the calculated angles using Equations 3.14 to 3.16 are then converted into radians as LabVIEW can only process trigonometric functions in this way;

4. The sine and / or cosine of α, β, γ and θ are also calculated to provide the relevant data to input into linkage force resolution calculations.

Additionally the block diagram code developed to calculate the tractor dynamic kinematic parameters is shown below in Figure 77.

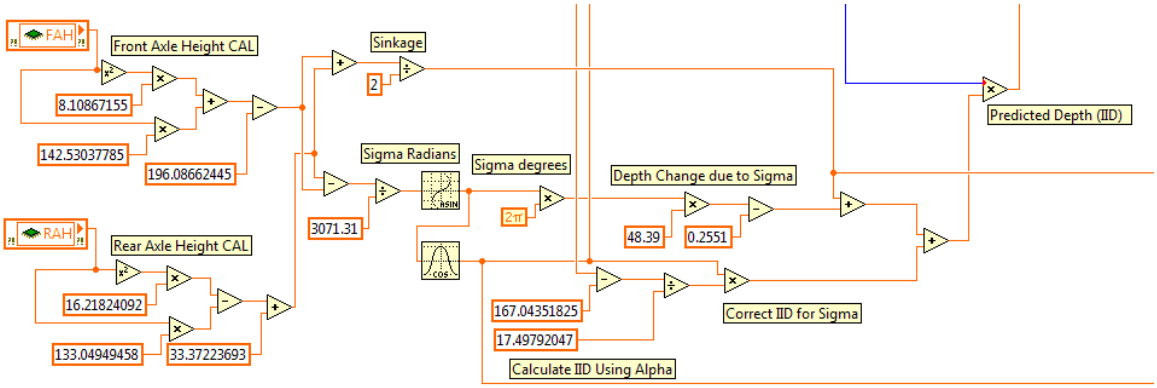

Figure 77: Block diagram code developed to calculate tractor dynamic kinematics

(Source: This study)

The purpose of performing the tractor dynamic calculations is such that in a final version of the control algorithm measured implement tillage depth (AID) will not be required as it is it

can be predicted (IID). The process employed within the code shown is Figure 77 is as follows:

1. Measure data from the front and rear axle height sensors and calibrate using trend line equations given in Figures 40 and 41 respectively;

2. Overall change in height of the tractor horizontal reference plane (i.e. tractor sinkage) in relation to the undisturbed surface (δRPS) is calculated using Equation 3.25;

3. Tractor attitude, σ, is calculated using Equation 3.24;

4. The predicted implement tillage depth (IID) is calculated using Equation 3.17 with respect to α;

5. A correction factor is then applied using the trend line equation given in Figure 21 to correct the predicted implement tillage depth (IID) and also the measured implement tillage depth (AID) with the data then logged for comparison to the measured implement tillage depth data recorded.

7.3.4 Linkage Force Resolution and Kinematics

The resolution of the generated linkage forces is a key aspect of the control algorithm as it allows calculation of energy usage and also informs wheel slip determination through the calculation of tyre deflections and hence rolling circumference. Shown below in Figure 78 is the code developed to complete the force resolution.

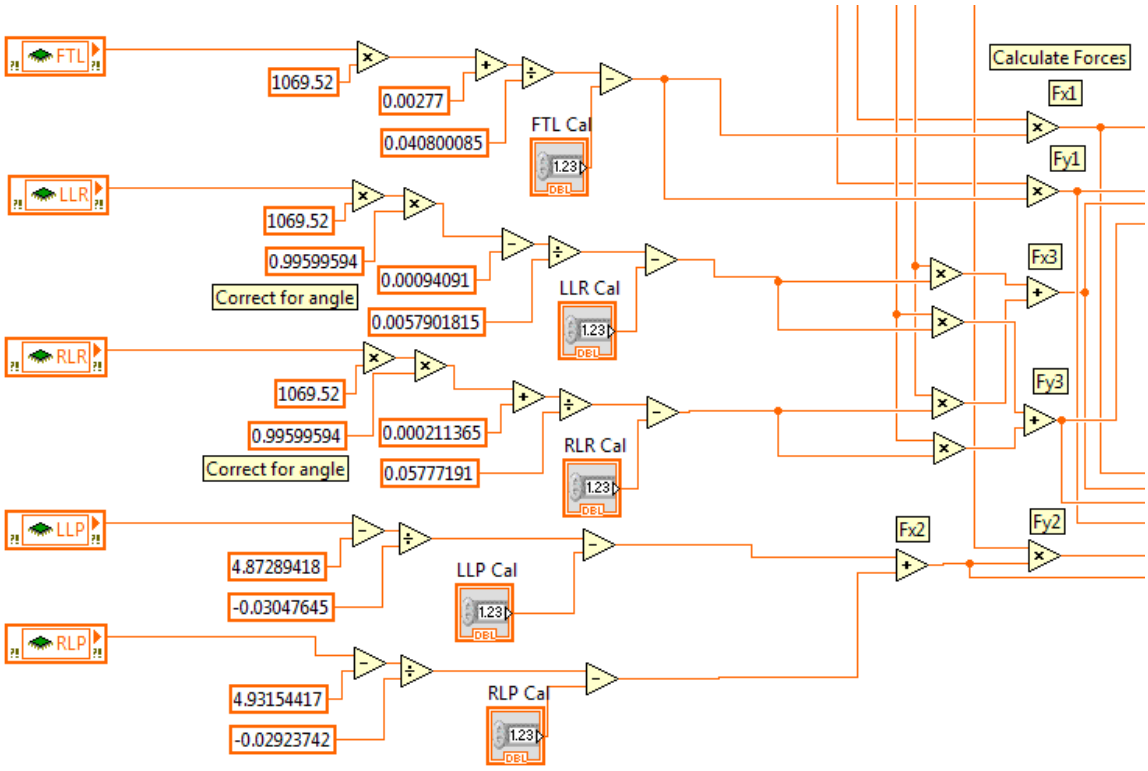

Figure 78: Block diagram code developed to incorporate linkage force input data and resolution of forces

(Source: This study)

The process employed in the code presented in Figure 78 is as follows:

1. Measure all voltage data from the top link, lift rods and draught force sensing pins;
2. Calculation of the tensions acting in the top link (FTL), the lift rods (LLR and RLR) and the draught force sensing pins (LLP and RLP) using trend line equations given in Figures 44 to 48 respectively;
3. Using angles α, β, γ and θ (Figure 76) the forces are then resolved into horizontal and vertical components using Equations 3.1 to 3.7;

4. The change in reaction force at each axle (δZF and δZR) is also calculated using Equations 3.12 and 3.13; the output is then used to calculate dynamic loaded rolling radii of the front (DLRF) and rear (DLRR) tyres.

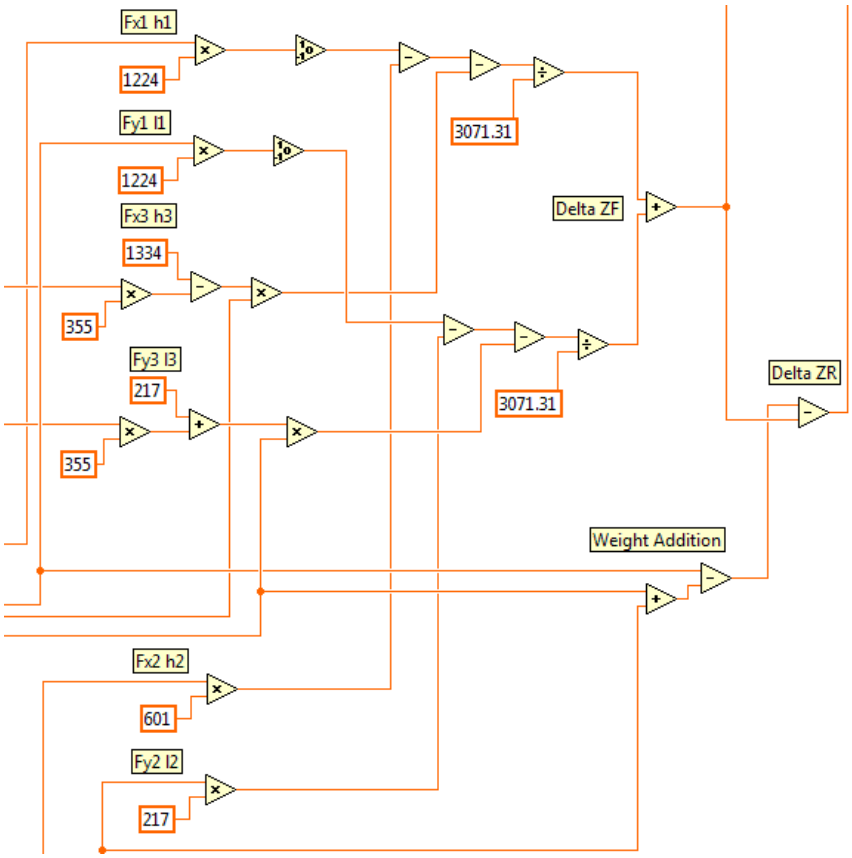

Figure 79: Block diagram code generated to calculate weight transfer

(Source: This study)

7.3.5 Current Tractor Implement Performance and Display

The display of current tractor/implement combination performance on the operator interface (shown in Figure 69) is displayed using various calculations performed in the control algorithm and also additional standalone measurements and calculations.

The following attributes are displayed on the operator interface and form the basis of the calculations shown in Figures 80 to 83:

- Actual implement tillage depth (AID) (mm);
- Power delivery efficiency (PDE) (%);
- Wheel slip (%);
- Drawbar power being used (kW);
- Fuel consumption (l h^{-1});
- Work rate (ha h^{-1});
- Recommendations for improvements to the field operation in terms of implement width and forward speed and the calculated effect on field work rate.

All performance measurements and calculations are in real-time and take into consideration the implement tillage depth corrections described in Section 7.3.2.

Shown below in Figure 80 is the block diagram code generated to calculate true forward speed using the 128 bit optical end encoder (Figure 49) fitted to the swinging arm front axle height sensor given in Figure 39. The data input to the code is based on the number of pulses per second and therefore knowing the radius of the wheel it is possible to calculate a forward speed (SOG) in both m s^{-1} and km h^{-1}.

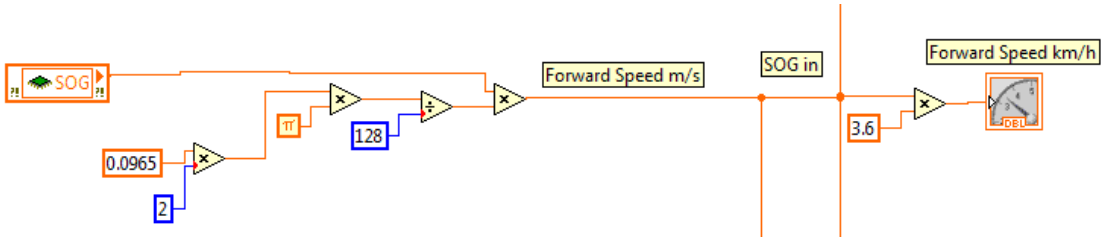

Figure 80: Block diagram code developed to calculate true forward speed (SOG)

(Source: This study)

Shown below in Figure 81 is the code developed to measure and calculate individual wheel speeds using the 128 bit optical end encoders (Figure 49) mounted into individual carries as given previously in Figures 50 and 51. The method for calculating the individual wheel speeds (FOS, FNS, ROS and RNS) deviates slightly from that of true forward speed. In these instances the dynamic rolling radii of the wheels are calculated using the tyre stiffness characteristics data supplied by the tyre manufacturers and the dynamic changes in axle loadings (δZF and δZR) calculated in Section 7.3.4. Thus changes in the static loaded wheel radii are calculated using Equations 3.28 and 3.29 and used for calculation of the individual wheel speeds.

Individual wheel slips are calculated employing Equation 2.6 as Wismer *et al.* (1974). Combined front wheel slip and rear wheels slip are displayed to the tractor operator on the interface screen.

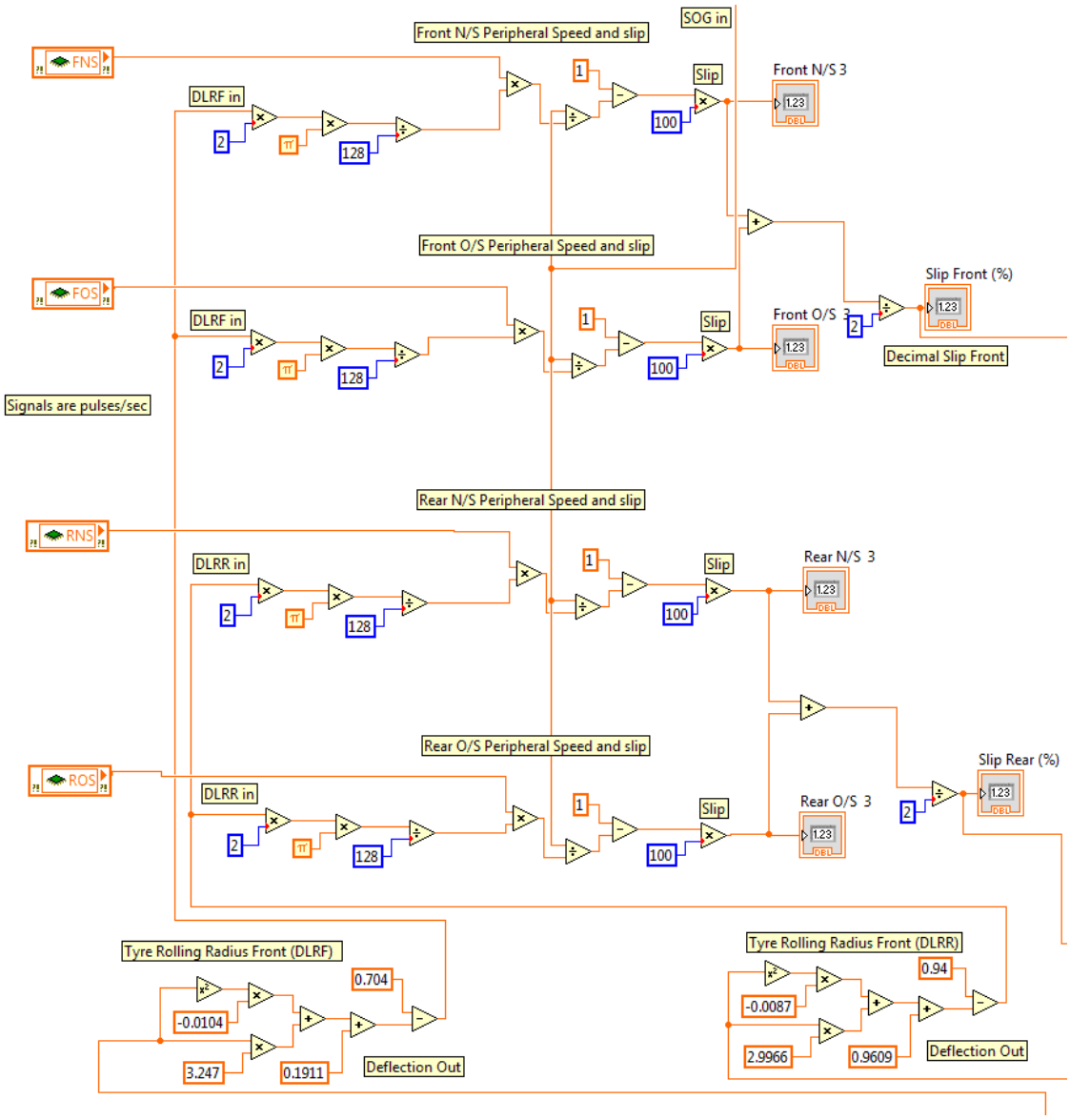

Figure 81: Block diagram code developed to calculate individual wheel speeds and tyre dynamic loaded radii

(Source: This study)

Shown below in Figure 82 is the LabVIEW code developed to calculate field work rate. Work rate is calculated using the true forward speed (SOG) of the tractor, the nominal width of the implement (3.3 m) and then converted into hectares per hour (ha h^{-1}) using Equation 7.1 below.

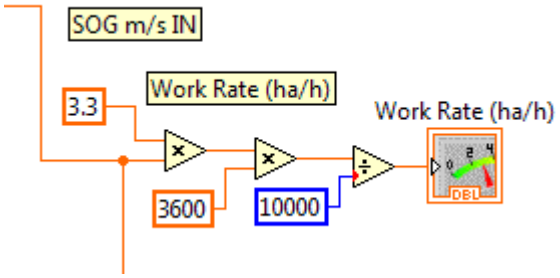

Figure 82: Block diagram code developed to calculate field work rate

(Source: This study)

Field Work Rate is defined as:

$$\text{Field Work Rate} = \frac{\text{Forward Speed (m s}^{-1}\text{) x Implement width (m) x 3,600}}{\text{10,000}} \text{ (ha h}^{-1}\text{)}$$

Equation 7.1

Shown below in Figure 83 is the block diagram code developed to measure fuel consumption in real-time.

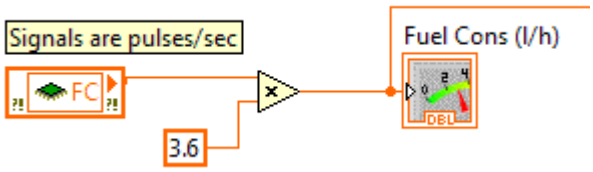

Figure 83: Block diagram code developed to calculate fuel consumption

(Source: This study)

The input data from the JPS fuel measurement system, given previously in Figure 52, is in pulses per second; the unit is set up such that one pulse is equivalent to one cubic centimetre of diesel fuel used. A simple calculation coverts the raw input data into real-time fuel consumption in litres per hour (l h^{-1}).

Shown below in Figure 84 is the code developed to display current tractor performance and potential set up improvements to the tractor operator.

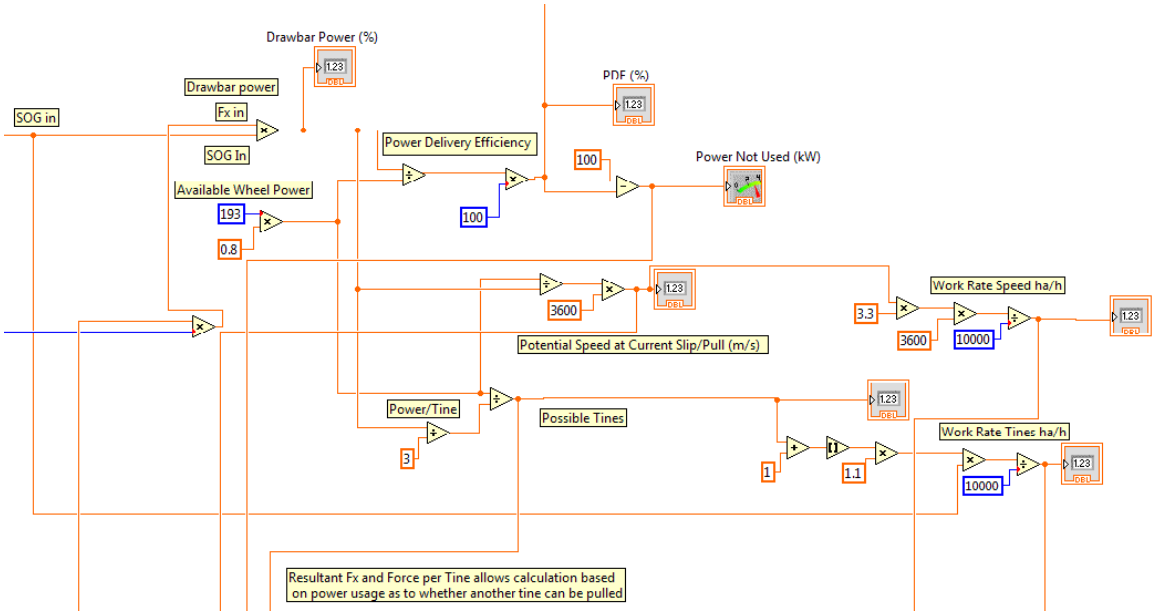

Figure 84: Block diagram code developed to calculate real-time performance

(Source: This study)

The performance calculations are based on the following assumptions included in the control algorithm:

1. The implement width is set within the system at 3.3 m (research sub-soiler);

2. The system is based on a fixed engine speed (1500 min^{-1}) set at the maximum torque of the engine and the flywheel power (kW) is known at this point - an estimated 80 % (Ryu *et al.*, 2003) of flywheel power is converted to wheel power.

Using the above two assumptions the following calculations of current tractor performance take place as the developed code shown in Figure 84 provides:

- Drawbar power (DBP) is calculated using Equation 4.1. Input data are the true forward speed (SOG) and the resolved draught force (Fx);

- Drawbar power is then used to calculate the following:
    - Power delivery efficiency using Equation 2.5 and additionally the available wheel power;
    - The amount of power not being currently used;
    - The amount of power consumed by each implement tine;
- Calculations are also then made to:
    - Establish how many more tines could be used and the potential effect on field work rate;
    - Establish if a faster forward speed could be employed and the potential effect on field work rate.

The above performance attributes and potential set up improvements are provided to the tractor operator to effect a manual change at this stage. It is perfectly feasible to automate these functions in a commercially developed system.

7.4 Control Algorithm Conclusions

The operator interface although simplistic provides real-time performance data with the ability to control the tractor. Whilst the system has only been tested in the laboratory it incorporates all of the parameters required to inform the operator of their current performance; the control algorithm is controlling the linkage position based on the work mode selected.

The real-time outcomes achieved by the system are:

1. Reduction in energy losses from poor tractor set up through reduction of implement tillage depth (AID) variation;
2. Providing the operator with current performance related information including current power delivery efficiency (PDE), available power not used, work rate, fuel consumption and wheel slip;
3. Provision of potential efficiency improvements through suggestions of forward speed or implement configuration changes and the effect these would have on work rate.

Whilst these are manual adjustments in the main the provision of performance to the operator may encourage more thought and attention employed in the tillage operation being conducted.

The system is currently designed to be a standalone add-on system to a standard tractor and does not require the use of a modern tractor ISO/CAN Bus electrical architecture. However, in a commercialisation of the entire system, the in-cab operator display could incorporate the control algorithm functionality and hence mathematical models developed within this study. The inclusion of the control algorithm within the tractor ISO/CAN Bus electrical architecture would allow automated input of implement parameters and control of engine speed, gear selection and implement configuration changes similar to Scarlett (2001). Shown below in Figure 85 is an artistic impression of how a commercial operator interface may appear.

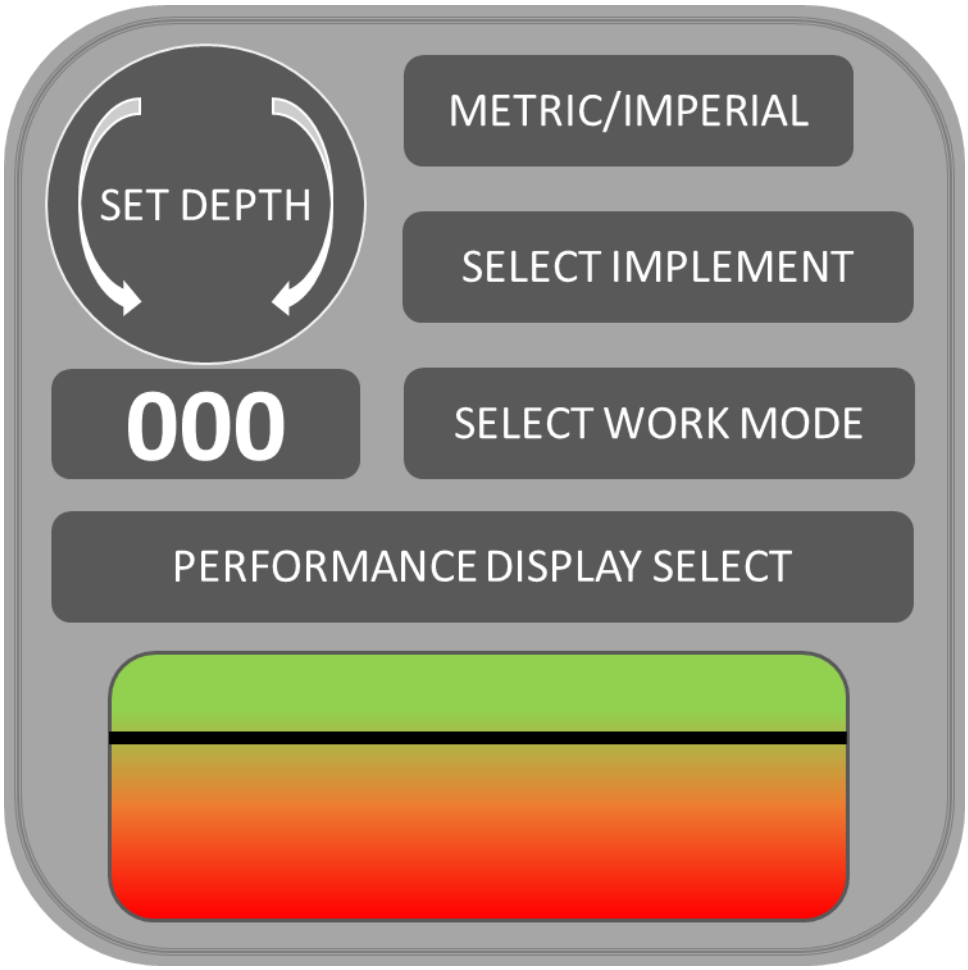

Figure 85: Proposal for a production in tractor operator interface

(Source: This study)

Referring to Figure 85 above the proposed production version of the operator interface consists of the following controls:

- **SET DEPTH** – Allows the operator to set the desired cultivation depth which is displayed numerically below the dial in display box;
- **METRIC/IMPERIAL** – The operator can choose whether to work in metric or imperial units with the current selection displayed;
- **SELECT IMPLEMENT** – The operator can choose what implement is fitted to the tractor. With an ISO/CAN Bus equipped implement or from an implement database

stored on the tractor the system could automatically calibrate the linkage and implement depth kinematics;

- **SELECT WORK MODE** – The operator selects the desired work mode from the available field work rate, tractor and fuel efficiency or consistent tillage depth and quality options. The current selection is then displayed;

- **PERFORMANCE DISPLAY SELECT** – The operator selects a specific performance option such as Field Work Rate, Power Delivery Efficiency, Fuel Consumption or a combined over all Operation Efficiency. The selected option is displayed and the slider bar moves within the red, amber green display below to provide real-time performance display.

The system developed in this study is versatile and has significant additional future applications. These consist of:

1. Measurement of field terrain and soil variation/resistance data in conjunction with weather data monitoring similar to Yahya *et al*. (2009);

2. Monitoring three point linkage vertical loading, e.g. fertiliser application rates, and integrate into a third party control system to ensure correct application rates reducing wastage (Auernhammer *et al*., 1988);

3. Monitoring of field terrain during linkage mounted or self-propelled spraying applications to control linkage or boom position to maintain accurate spray nozzle height above the field crop ensuring accurate application similar to Yahya *et al*. (2009).

CHAPTER 8 - Conclusions and Recommendations

8.1 Research Aim and Objectives

To accurately conclude the work completed here it is sensible to reproduce the aims and objectives that were defined at the outset and during this work.

8.1.1 Research Aim

'To develop a control algorithm for agricultural tractors conducting draught tillage operations with the aim of optimising tractor efficiency thereby minimizing fuel usage and operator time'.

8.1.2 Research Objectives

1. To develop a real-time computer based model to evaluate the critical soil/vehicle/implement parameters to efficiently control the tractor based upon the operator's preferred work modes of field work rate, tractor and fuel efficiency or consistent tillage depth and quality;
2. To create and develop an instrumentation system for the collection of the relevant parameters for the control algorithm and validate the performance of the control algorithm;
3. Develop an operator information interface to allow selection of work mode and display real time tractor/implement performance.

8.2 Context of Contribution to Knowledge

The objectives set out at the beginning of this study concentrated on deep tillage operations. As the study evolved the emphasis shifted towards tractor rather than tractive efficiency due

to the unavailability of wheel torque measuring equipment; centralising on the effects on tractor efficiency through more accurate three point linkage control. This study has demonstrated the following advances and potential in relation to those objectives:

1. Development of a full tractor kinematic model consisting of linkage force resolution and dynamic kinematic models within this study – incorporating weight transfer, tyre deflection and ground profile consideration;

2. Development of a specific instrumentation system to collect the relevant data input parameters;

3. A unique integration between linkage force resolution, dynamic kinematic tractor models and instrumentation system in a real-time tractor performance monitoring and linkage control algorithm with no reliance on previous pass or historical data;

4. A versatile system that can be installed as a standalone add-on to a simple tractor or the technology incorporated into an ISO/CAN Bus tractor electrical architecture.

8.3 Conclusions

8.3.1 Literature Conclusion

There is not a widespread volume of literature relating to tractor efficiency prediction and efficiency control systems with several key authors in the subject area (Scarlett, 2001) and Zoz and Grisso (2003). Much of the work looking at the tractive and tractor efficiency subject area is over twenty years old (Ward *et al.*, 2011) and was related to tractor systems that have long been superseded. More recent innovations have centred on tractor qualitative performance monitoring such functions as work rate, traffic pass to pass accuracy and seed rate application. SOYL recently developed an add-on controller to allow tillage depth variation depending on a field soil map. However the system relies on a mapping operation

of the field and adjusts a cultivator mounted depth wheel using a hydraulic control system; the system does not monitor efficiency performance in real time. A large body of International Patent review was required and forms the majority of the traditional literature review element of this study. Dr A J Scarlett claimed to have previously published research in the context of this study and was a prime author on the patents reviewed; this steered this towards the effects of three point linkages and its effects on energy usage. Whilst there are generic theoretical elements of this work in the filed patents, quite considerable differences are apparent. All elements of this study are in true real-time, taking into consideration full tractor kinematic force resolution and its effects such as weight transfer and tyre deflections without reliance on previous field pass calibrations or historical data. Therefore the work presented in this study advance previous work and makes a significant contribution to knowledge.

8.3.2 Kinematic Models

Linkage force resolution and dynamic kinematic models were developed in Chapter 3 and are sufficiently versatile to be considered for alternative applications. The methodology behind the integration of these models forms the unique elements of this study with the instrumentation system developed; reinvigorating earlier work and furthering knowledge in the subject area. The purpose of the models was to ensure that all dynamic parameters required for the control algorithm could be calculated and measured simply. The models furthered work conducted by Keen *et al.* (2009), Ward *et al.* (2009) and Ward *et al.* (2011). The integration of both models allowed versatile real-time resolution of measured three point linkage forces and weight transfer effects to be calculated. This is of high importance when considering real time efficiency performance monitoring as power usage is directly related to work done, which in this case is a function of draught force, rolling resistance, wheel slip and forward speed. Calculation of weight transfer uses the resolved linkage forces in

conjunction with the tractor wheel base dimension and the linkage geometry in relation to a quasi-static tyre/ground interaction patch. This was achieved using simple moments theory about the rear wheel tyre/ground interaction patch. Whilst not directly related to energy usage and performance this allows the tyre deflections to be estimated using tyre stiffness characteristics. It is therefore possible to correct the linkage geometry in relation to the tyre/ground interaction patch, effectively removing the quasi-static element of the force resolution present in previous works; closing the open-loop system. Whilst this feature was not utilised in the control algorithm developed here, although the calculation processes were, it would allow a further development of the control algorithm to monitor tractive performance of the wheels and potential variation of power to the wheels to achieve the optimum traction in the prevailing field conditions.

An additional element to the dynamic kinematic model centred on tractor attitude variations and linkage geometry. As discussed in Chapter 2 tractor ride dynamics can have a significant effect on the implement and ground interaction. Therefore a dynamic kinematic model of the MF8480 research tractor chassis was developed that allowed axle height variation and hence tractor attitude. It is then possible to calculate the attributed implement tillage depth and tractor sinkage variation. In conclusion the models developed within this study in their own right are relatively simplistic but allow a multitude of dynamic and force elements to be calculated in real-time.

8.3.3 Instrumentation System

The construct of the instrumentation system was dictated by the parametric requirements of the models developed in Chapter 3. Elements of the instrumentation system, detailed in Chapter 4, have previously been published by Keen *et al.* (2009), Ward *et al.* (2009) and Ward *et al.* (2011). The force measuring instrumentation on the top link and lift rods

consisted of a full Wheatstone Bridge constructed from 120 Ω strain gauges. These were calibrated using a tensile testing machine and demonstrated excellent linearity (typically R^2 of 0.99) in loading and unloading conditions with little hysteresis. The concept of using the on board tractor draught force sensing pins in place of strain gauges on the lower lift arms was proven successful and reduced potential instrumentation damage in field working conditions. There were two calibration activities of the on board Bosch draught force sensing draught pins. The first of these was to establish what forces were measured, purely draught in relation to the tractor or the actual tensile forces going the through the lower lift arms at the angle of action. It was found that the draught force sensing pins always measure the draught component (Fx2) of the force transmitted through the lower lift arm irrespective of the angle of action. The second element of calibration consisted of using a substitute lower lift arm to directly apply a horizontal load to the draught force sensing pins on the tractor. This was achieved using a 5 Tonne load cell attached to the boom of a telescopic handler and applying load through retraction of the boom. Whilst the data sheet for the draught force sensing pins (Appendix A) details the nominal calibration values it was important that these values were understood. The draught force sensing pins position is fixed in relation to the tractor with no rotation possible.

A simple depth wheel measures actual tillage depth (AID) using a commercially available string potentiometer. Linkage position was measured simply using a potentiometer attached to the lift arm which was calibrated using the known linkage geometry; an earlier prototype angular measurement system consisted of a top link and lower lift arm angular measurements, again using potentiometers. However these were found to be vulnerable to damage and were substituted with the lift arm potentiometer.

Additional elements have been added to the system developed by Keen *et al.* (2009), Ward *et al.* (2009) and Ward *et al.* (2011). These were driven by the desire to measure tractor

attitude changes due to field surface variations and the homogeneity of the soil causing variable weight transfer and sinkage (Ward *et al.*, 2011). This was achieved using swing arm depth wheels under both tractor axles with the arms swinging in the line of action with the tractor. Attached to the pivot point is a simple potentiometer where the change in resistance is proportional to the angle of swing seen which in turn is proportional to the change in axle height in relation to the ground surface. Whilst these additional elements were calibrated to form part of the control algorithm, in conjunction with the kinematic models, they only calibrated and proven in a controlled environment.

The final part of the instrumentation system consisted of a proprietary fuel measurement device manufactured by JPS Engineering (model FMS MK4). In conclusion a comprehensive instrumentation system was developed and proved generally reliable. However to completely satisfy the objectives of this research, torque measurements from the driving wheels were required to calculate tractive efficiency. A proprietary set of equipment exists to complete this task but was used on long term testing and due to the available power and torque of the tractor was beyond the manufacturing capabilities available.

8.3.4 Preliminary Experiments

The research within this study concentrated more on the effects of three point linkage control on energy used in field operations. To develop a control algorithm to control linkage dynamics and monitor in field performance it was necessary to understand how a typical linkage responds to draught force inputs. A typical linkage control system consists of three main controls; the mode of control – Position, Draught or Intermix, lift and lower speeds and a form of response control. It was found that existing systems, whilst allowing a multitude of variability in control strategy are too complex to set up consistently correctly for a given field tillage operation. The setup is completely controlled by the operator, where operator

skill levels vary. The ability to adjust for every small variation in field conditions either through soil type or undulations is compromised and therefore the tractor is usually set up for a particular implement type with little or no further adjustment. What suffers in this scenario is the consistency and quality of the tillage operation and the energy used.

A series of field experiments were conducted using three modes of tractor linkage operation, Position, Draught and an equal Position/Draught Intermix Control methods. The response and lift/lower speeds were set at the maximums available to ensure as rapid response as possible was available from the linkage controller. A constant forward speed of $3kmh^{-1}$ was used and it was found at a nominal tillage depth of 400 mm that tillage depth varied within a range of +49.61 mm to -45.46 mm. This is significant and considering the relationship between draught force and depth could account for significant power requirement fluctuations. In the same instance draught force varied within a range of +19.96 kN to -12.35 kN. It was demonstrated from the data collected in this experiment that in one instance a 7.13 mm increase in depth over a nominal 400 mm tillage depth results in a 3.5 % energy increase, justifying the development of an improved methodology for controlling tractor three point linkages.

A further series of experiments were conducted to estimate the performance of the standard MF8480 linkage control system with parameters such as response time, draught force ranges for given settings, three point linkage movement and implement depth start positions. It was designed to establish the sensitivity of draught force inputs and also how the Intermix control method functions. As predicted Intermix Control mixes the attributes of both Position and Draught Control. It was also found for a given tillage depth that a multitude of possible settings were available.

In conclusion the initial experiments proved the instrumentation and data logging system and confirmed that tillage depth variation, as described in the literature review, contributes significantly to energy wastage and therefore tractor inefficiency.

8.3.5 Control Algorithms

A control algorithm which includes tractor and implement parameters has been created. The algorithm integrates the key components of the linkage force resolution and dynamic kinematic models developed in Chapter 3 and the instrumentation system developed in Chapter 4. Parameters such as draught force, drawbar power, forward speed, wheel slip, wheel power usage, weight addition and tillage depth are calculated and allow the tractor implement combination performance to be displayed to the operator and automatic control of the three point linkage. Whilst the algorithm does not directly control all features such as engine speed and forward speed it does provide the operator with performance improvement information such as what forward speed could be achieved and also if a wider implement could be used in the current field conditions. The performance improvement attributes are based on a rolling average over the length of the tillage run; soil conditions will vary and tractor response to increases in forward speed are not fast enough to account for small variations in field conditions. The algorithm is based on a fixed engine speed of 1500 min^{-1}. Through analysis of the MF8480 engine map, at 1500 min^{-1} the engine is producing maximum torque of 1500 Nm (what is required for maximum drawbar pull) and power of 236 kW which equates to 88.4 % of maximum engine power (for a bare engine devoid of ancillaries).

The algorithm contains the work modes of field work rate, tractive and fuel efficiency or consistent tillage depth and quality and monitors the tillage depth set between limits dictated

by the work mode set. Should the tillage depth exceed the limits dictated an automatic three point linkage correction is actuated via an electronic link to the tractor control system.

Whilst only bench tested, mathematically, the algorithm will inform the operator of current performance and changes that could be made to improve the usage of the energy available. It also has the ability to calculate weight transfer which could be used in a further development where actual traction becomes part of the control system. Additional further developments would include the automation of engine speed and gear selection to best optimise the use of the power available in the current tractor conditions

8.4 Final Conclusion

The objectives set out for this study have been largely met with the creation of the real- time computer based models that has resulted in the creation of the control algorithm which incorporates the work modes originally set out with the exception of tractive and fuel efficiency. The control algorithm makes suggestions to the operator through an interface on potential set up changes to maximise the application of the available power at maximum engine torque making the most efficient usage of fuel; to quantify by using all of the energy available, whilst monitoring losses such as wheel slip, maximum fuel efficiency is implied. The study has highlighted that tillage depth variation impacts on energy usage significantly and this formed the basis of the control algorithm functionality. The integration of the mathematical linkage force resolution and dynamic kinematic models of both the tractor three point linkage in conjunction with an instrumentation system formed the back bone of the control algorithm and its ability to effect tractor control.

8.5 Recommendations for a Commercial Application

The scope of this study did not cover the commercial development of an instrumentation system but has centred on the research outcome; although some consideration has been made as to how the overall system and its components would be made commercially viable. This has been achieved through careful consideration of the instrumentation component functions and how the control algorithm might integrate with the tractor. Whilst the control algorithm is at present largely effected through the provision of performance and system settings information to the operator this can also be achieved through further integration with the tractor ISO/CAN Bus electrical architectures

8.5.1 Commercial Instrumentation Application

The force measurement system utilises the existing fitted draught force measurement pins with the addition of strain gauge bridges attached to the lift rods and top link all measuring both tensile and compressive forces. It is quite a realistic prospect to utilise directional force measurement pins at the pin joints between top link and gearbox casing and also at the pin joints between lift rods and lower lift arms. This solution offers the use of a known product with proven reliability to achieve the desired measurement requirement. A further enhancement of this commercial solution would be the use of a bi-directional force measurement pin as shown below in Figure 86 which is fitted at the lower lift arm / lift rod pin joint. This type of sensor was developed by the author throughout this study and potentially allows tensile forces to be measured in the lift rod and the lower lift arm simultaneously. However, there are cross sensitivity and durability implications in this location which may hinder its commercial development.

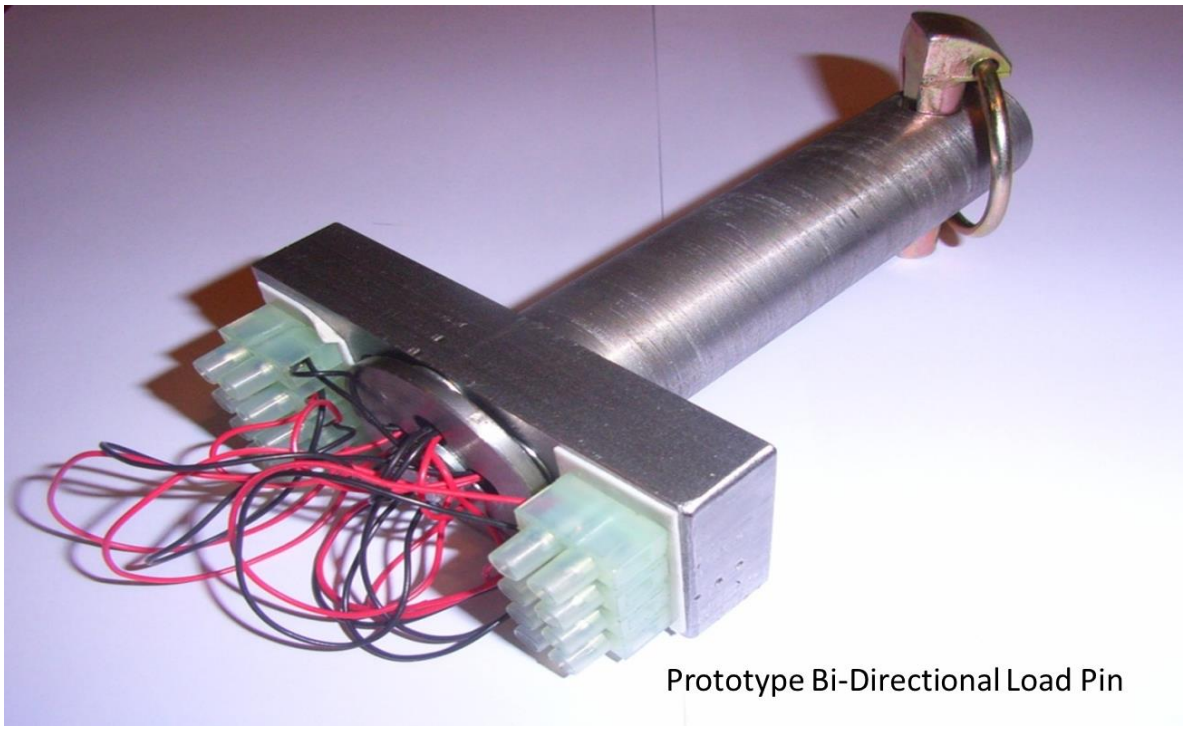

Figure 86: Bi-directional measurement device developed during this study

(Source: This study)

The instrumentation elements relating to kinematics consists of four key components: the front and rear tractor axle height measurement depth wheels, the linkage angle sensor attached to the cross shaft and the implement depth wheel. Firstly, the axle height measurement wheels could be substituted with laser or ultrasonic distance measurement devices Imou *et al.* (2001) and Scarlett (2001). These durable devices are commercially available and relatively inexpensive.. Secondly, fitted (but not used in this system) to the cross shaft of the tractor is an angular encoder; similar devices could also be utilised to measure the angle of the lower lift arm (α), the top link (θ) and the existing sensor being used for measuring the lift arm angle (γ). These angular measurements are critical to the instrumentation system and the function of the control algorithm. However, through some simple data entry by the operator it would be possible to reduce this sensor count to just one. To achieve this, the implement dimensions need to be inputted to the system (possibly with

draught tillage implements being fitted with an ISO/ CAN Bus *tag* which through an interface connection inputs the information or through a database of implements contained within the ISO/CAN Bus electrical information system). Also required would be the length of the lift rods, top link and the linkage attachment point geometry (contained with the control algorithm); with kinematic calculations the angle of the lower lift arm (α), the top link (θ) can be calculated with only the lift arm angle (γ) being measured. Whilst this is feasible, it may prove an unsuitable system for the operator to use on a daily basis with direct electronic measurement being the desired solution with potentially an integrated linear measurement device such as a Linear Variable Differential Transformer (LVDT). Thirdly the implement depth wheel measurement device has only been used as a confirmation of the linkage control algorithm's performance and therefore would not be required on a commercial system.

The dynamic element of the instrumentation system consists of independent wheel speed measurements, forward speed measurement and tyre deflection by calculation. Commercially this is easily achievable using shaft encoders at appropriate locations in the wheel drive line with the addition of, where needed, calculations to give actual wheel speeds. The algorithms within this study actually take into account tyre deformation where commercial slip systems do not and therefore are much more accurate. To achieve this the control algorithms use standard tyre deformation characteristics fitted to the tractor to ascertain, in conjunction with real-time weight transfer, tyre deflection; in reality it is possible to develop and integrated in wheel sensor that measures tyre deflection based on laser, ultrasonic or tyre pressure measurement.

8.5.2 Commercial Algorithm Application

The algorithms developed within this study have been created as a standalone system but are easily adapted to a commercial installation. The commercial application of these algorithms could either be through a third party micro controller, in the case of a retrofit system with a standalone display, a retrofit CANBus based ECU (which would require a major software upgrade to the tractor electrical system), or more likely through an ECU integrated within the tractor CAN/ISOBus system.

The linkage control and force resolution models effectively replace the generic tractor linkage control system. Most linkage control systems are very similar in their function with most coming from a single source manufacturer. There are two key advantages to the algorithms developed within this work, these being their simplicity of operation and the reduction in control parts required within the cab. In this study the function of the linkage positional control has been effected through application of voltages in place of the usual depth control selection wheel; in a commercial version this wheel would not exist with lift ram electrohydraulic valve being directly controlled. The tractor control components of the algorithms (which simply are calculations) again could be installed in a retrofit system or more suitably through an existing or additional ECU within the ISO/CAN Bus tractor electrical architecture.

The level of increased functionality depends heavily on the degree of tractor integration of the algorithms/system. Utilising a retrofit system the functionality is potentially more limited to linkage control and operator performance information; however this would lead to redundancy in tractor cab control components. Utilising a manufacturer ECU fitted within the tractor ISO/CAN Bus electrical architecture allows much greater degrees of control – such as forward speed control, engine power control, engine torque control, wheel torque

control through engine speed and gear selection and also implements width control maximising available drawbar power usage.

8.6 Recommendations for Further Research

The work conducted within this study advances to new levels work that has already been done by others such as Scarlett (2001) and Zoz and Grisso (2003). The linkage force resolution and dynamic kinematic models and control algorithms work in real-time with real-time performance attributes. To further this work, the incorporation of real-time wheel torque measurements and further control inputs such as engine speed and gear selection will allow, in conjunction with the existing control algorithm, full real-time control of the agricultural tractor with the aim of improving efficient use of fuel energy.

Additionally, the linkage force resolution model, tractor dynamic kinematic models and instrumentation system developed have significant future applications as retro-fits to existing tractors. The following are proposals for further research:

1. Investigate the integration of the real-time linkage force resolution models into solid or liquid fertiliser application control systems similar to Auernhammer (1988);

2. Investigate the potential integration of real-time field terrain measurement and linkage position correction into solid or liquid fertiliser application control systems;

3. Research the potential use of the linkage force resolution model to weigh items attached to the three point linkage;

4. Investigate the potential to use the linkage force resolution and the dynamic kinematic tractor models to map soil resistance and field undulations to produce a field soil map similar to Yahya *et al*. (2009).

REFERENCES

Al-Jalil, H.F., Khdair, A., and Mukahal, W. 2001. Design and performance of an adjustable three-point hitch dynamometer. *Soil and Tillage Research*, **62**, 153–156.

Al-Janobi, A. 2000. A data-acquisition system to monitor performance of fully mounted implements. *Journal of Agricultural Engineering Research*, **75**, 167–175.

Alimardani, R., Fazel, Z., Akram, A., Mahmoudi, A., and Varnamkhasti, M.G. 2008. Design and development of a three-point hitch dynamometer. *Journal of Agricultural Technology*, **4**(1), 37 – 52.

Auernhammer, H., Demmel, M. and Stanzel, H. 1988. Possibilities for weighing in the tractor's three point linkage. *Landtechnik*, Germany, **43(10)**, 414-418.

Bachche, S. G. 2009. *Performance evaluation of a three point hitch system of a tractor*. Asian Institute of Technology, Thailand. Master thesis (unpublished).

Bentaher, H., Hamza, E., Kantchev, G., Maalej, A. and Arnold, W. 2008. Three-point hitch-mechanism instrumentation for tillage power optimization. *Biosystems Engineering*, 100, 24 – 30.

Blackmore, S., Fountas, S. and Have, H., 2002. Proposed system architecture to enable behavioural control of an autonomous tractor. *Automation Technology for Off Road Equipment, Chicago Illinois,* 13-23.

BOSCH, R. 1988. *Arrangement for mechanical measurement and regulation of pulling force of tractor.* US4721001A

Brixius, W.W. 1987. *Traction prediction equations for bias ply tires.* ASAE Paper No. 87-1622, St. Joseph, MI: ASAE.

Bunting, E.V. 1965. *The Ferguson system – past and present*. ASAE Paper 65-133.

Chaplin, J., Lueders, M. and Zhao, Y. 1987. Three point hitch dynamometer design and calibration. *Applied Engineering in Agriculture*, **3**, 10–13.

Chen, Y., McLaughlin, N.B. and Tessier, S. 2007. Double extended octagonal ring (DEOR) drawbar dynamometer. *Soil and Tillage Research*, 93 (2), *462-471*

Clark, R. L. and Adsit, A.H. 1985. Microcomputer based instrumentation system to measure tractor field performance. *Transactions of ASAE*, **28**, 393-397.

Cowell, P.; Len, C. 1967. Field performance of tractor draught control systems. *Journal of Agricultural Engineering Research*, 12, 205.

Cowell, P.A. and Herbert, P.F. 1988. The design of a variable geometry linkage to improve depth control of tractor mounted implements. *Journal of Agricultural Engineering Research*, **39 (2)**, 85-97.

Crolla, D.A. 1975. *Implement control and its effect on the dynamic performance of tractor - implement combinations.* PhD Thesis, Loughborough University.

Crolla, D.A. 1975. The response of tractor draught controls to random inputs. *Journal of Agricultural Engineering Research*, 20, 181.

Crolla, D.A. 1975. *The dynamic performance of off-road vehicles under fluctuating load conditions*. Proc I Mech Engrs, Paper 206/75.

Culpin, C. 1992. *Farm machinery.* 12th ed UK. Blackwell Scientific Publications Ltd.

Davies, A. 2006. *Evaluation of weight transfer due to soil engaging implements on the tractive performance of an agricultural tractor.* Harper Adams University College, UK. Master Thesis, (Unipublished).

Dwyer, M.J. 1969 *The dynamic performance of tractor-implement combinations*. Proc I Mech Engrs, 184, part 3Q.

Gholkar, M., Keen, A., Ward, J., Salokhe, V. and Soni, P., 2009. Force measurement between a tractor and a three point linkage mounted tillage implement. *International Agricultural Engineering Conference 2009.* Bangkok.

Godwin, R.J., 1974 *An investigation into the mechanics of narrow tines in frictional soils.* Unpublished PhD, University of Reading & National College of Agricultural Engineering.

Godwin R. J. 1975. An Extended Octagonal Ring Transducer for Use in Tillage Studies. *Journal of Agricultural Engineering*, **20**, 347-352.

Godwin, R.J., Spoor, G. and Soomro, M.S. 1984. The effect of tine arrangement on soil forces and disturbance. *Journal of Agricultural Engineering Research*, **30**, 47-56.

Godwin R. J. , Reynolds, A.J., O'Dogherty, M.J. and Al-Ghazal, A. 1993. A triaxial dynamometer for force and moment measurements on tillage implements. *Journal of Agricultural Engineering Research*, **55**, 189–205.

Godwin, R.J. and O Dogherty, M.J. 2003. Integrated soil tillage force prediction models. *ISTVS 2003. Proceedings of the 9th European Conference Harper Adams September 2003.* England

Godwin, R.J. and O'Dogherty, M.J. 2007. Integrated soil tillage force prediction models. *Journal of Terramechanics,* **44**, 3-14.

Hesse, H. 1969. Reasons and scope for development of plough control systems. Grundl Landtech, 19, No.6, 197.

Hu, L., Lin, C., Luo, X.W., Yang, W.W., Xu, Y., Zhou, H. and Zhang, Z. 2015. Design and experiment on auto leveling control system of agricultural implements. *Transactions of the Chinese Society of Agricultural Engineering*, **31 (8)**, 15-20.

Imou, K., Ishida, M., Okamoto, T., Kaizu, Y., Sawamura, A. and Sumida, N., 2001. Ultrasonic Doppler sensor for measuring vehicle speed in forward and reverse motions including low speed motions. *Agricultural Engineering International: The CIGR Journal of Scientific Research and Development.* Manuscript PM 01 007. Vol 3.

Keen, A.P.C., Ward, J.L., Godwin, R.J., Hall, N., Cooper, S.E. 2009. Improvements to the Tractive Efficiency of Agricultural Tractors Carrying Out Cultivations. *ASABE Reno, Nevada.*

Khan, J., Godwin, R.J., Kilgour, J. and Blackmore, B.S. 2006. Design and calibration of a direct mounted strain gauged lower links system for measurement of tractor-implement forces. *APRN Journal of Engineering and Applied Sciences*, **1**(1) 22-25.

Kirisci, V., Blackmore, B.S., Godwin, R.J. and Blake, J. 1993. *Design and calibration of three different three-point linkage dynamometers.* ASAE paper No. 931009, American Society of Agricultural Engineering, St. Joseph, MI.

Lee, J,, Yamazaki, M., Oida, A., Nakashima, H. and Shimizu, H. 1998. Electro-hydraulic tillage depth control for rotary implements mounted on an agricultural tractor: Design and response experiments of control system. *Journal of Terramechanics*, **35**, No.4, 229-238.

McKeon, C.E. 1972. *Driveline torque coupling for tractor draft control*. SAE Paper 720710.

McLaughlin, N.B., Heslop, L.C., Buckley, D.J., St. Amour G.R., Compton, B.A., Jones, A.M., and Van Bodegom, P. 1993. A general purpose tractor instrumentation and data logging system. *Transactions of the ASAE*, **36**, 265–273.

Mouazen, A.M., Anthonis, J., Saeys, W. and Ramon, H. 2004. An Automatic Depth Control System for Online Measurement of Spatial Variation in Soil Compaction, Part 1: Sensor Design for Measurement of Frame Height Variation from Soil Surface. *Biosystems Engineering*, **89 (2)**, 139-150

Naaktgeboren, A., Paquet, B.J.F., Lowe, J.C., Scarlett, A.J. and Semple, D.A.2007. *Method and apparatus for controlling a tractor/baler combination*. EP1153538B1

Palmer, A.L. 1992. Development of a three point linkage dynamometer for tillage research. *Journal of Agricultural Engineering Research*, **52**, 157–167.

Reece, A.R. 1961. A three point linkage dynamometer. *Journal of Agriculture Engineering Research*, **6**, 45–50.

Reid, J. T., Carter, L.M. and Clark, R.L. 1985. Draught measurements with three-point hitch dynamometer. *Transaction of the ASAE*, **28**, 89–93.

Ryu, I.H., Kim, D.C. and Kim, K.U. 2003. Power efficiency characteristics of a tractor drive train. *Transaction of the ASAE*, **46 (6)**, 1481-1486.

Saeys, W. Mouazen, A.M. Anthonis, J. and Ramon, H. 2004. An automatic depth control system for online measurement of spatial variation in soil compaction, Part 2: Modelling of the depth control system. *Biosystems Engineering***, 89**, No.3, 267-280.

Sahu, R.K. and Raheman, H. 2008. A decision support system on matching and field performance prediction of tractor-implement system. *Computers and electronics in agriculture*, **60**, 76–86.

Scarlett, A.J., 2001. Integrated control of agricultural tractors and implements: a review of potential opportunities relating to cultivation and crop establishment machinery. *Computers and Electronics in Agriculture*, **30**, 167-191.

Scarlett, A.J. and Lowe, J.C. 2003. *A vehicle control apparatus and method.* EP0838141B1

Scarlett, A.J. and Miles, S.J. 2003. *A gravity actuated, moveable mounting*. EP0857408B1

Scarlett, A.J. and Lowe, J.C. 2003. *Improvements in or relating to tillage*. EP0838139B

Scarlett, A.J., Lowe, J.C. and Mackenzie, T.F. 2007. *A method and apparatus for controlling a tractor/implement combination.* EP1169902B1

Seifert, A. 1965. *Investigation of three systems of hydraulic depth control when ploughing on changing soil types*. Grundl Landtech, 15, No.4, 107.

Simalenga, T.E. and Kofoed, S.S. 1992. Development of a variable geometry three point hitch. *Agricultural Mechanization in Asia, Africa and Latin America*, **23 (2)**, 47-51.

Skalweit, H. 1963. *The ideal and actual in depth control via the hydraulic lift.* Grundl Landtech, 18, 574.

Spoor, G. and Godwin, R. J. 1978. An experimental investigation into the deep loosening of soil by rigid tines. *Journal of Agricultural Engineering Research*, **23 (3)**, 243-258.

Summers, J.D., Batchelder, D.G., and Lambert, B.W. 1986. Second generation tractor performance monitor. *Applied Engineering in Agriculture*. ASAE Paper No. 84-1080.

Tinker, D.B. 1993. Integration of tractor engine, transmission and implement depth controls: Part 1 Transmissions. *Journal of Agricultural Engineering Research*, **54,** No.1, 1-27.

Upadhyaya, S. K., Kemble, L.J., Collins, N.E. and Camargo Jr, F.J., 1985. Accuracy of mounted implement draught prediction using strain gages mounted directly on three-point linkage system. *Transactions of ASAE,* **28**, 40-46.

Vantsevich, V.V. 2010. *Driveline systems of ground vehicles: Theory and design*. CRC Press.

Ward, J., Gholkar, M., Keen, A., Godwin, R. J. and Crolla, D., 2009. Tractor – Implement force measurement. *ISTVS. 11th European Conference*. Bremen.

Ward, J., Crolla, D.A., White, D.R. and Godwin, R.J., 2011. The control of tractor 3 point linkage control systems. *ISTVS. 17th International Conference*. Blacksburg.

Wheeler, P.N. and Godwin, R.J. 1996**.** Soil Dynamics of Single and Multiple Tines at Speeds up to 20 km/h. *Journal of Agricultural Engineering Research*, **63**, 243-249.

Wismer, R.D., and Luth, H.J., 1974. Off road traction prediction for wheeled vehicles. *ASAE*. Paper No.72-619

Wong, J.Y. 2008. *Theory of ground vehicles.* 4th ed.USA: Wiley.

Wong, J.Y. 2009. Terramechanics and off-road vehicle engineering. 2nd ed: Terrain Behaviour, Off-Road Vehicle Performance and Design. Butterworth-Heinmann.

Xie, B., Li, H., Zhu, Z.X., and Mao E.R. 2013. Measuring tillage depth for tractor implement automatic using inclinometer. *Transactions of the Chinese Society of Agricultural Engineering*, **29 (4)**, 15-21.

Yahyaa, A., Zohadiea, M., Kheiralla, A.F., Giewa, S.K. and Boona, N.E. 2009. Mapping system for tractor-implement performance. *Computers and Electronics in Agriculture,* **69**, 2–11.

Zoz, F.M. and Grisso, R.D. 2003. Traction and Tractor Performance. *ASAE Distinguished Lecture Series*, Tractor Design No.27.

CITED WEBSITE REFERENCES

http://www.aghistoryproject.org/little-bit-tractor-history

http://www.boschrexroth.com/mobile-hydraulics-catalog/Vornavigation/VorNavi.cfm?Language=EN&PageID=m4444

http://www.icenta.co.uk/pdfs/FLOWMATE_micro_flow_meter_gbb340-8-e-ic.pdf

http://www.nationalmediamuseum.org.uk/voting/pastinnovations/three-point%20linkage

http://sine.ni.com/np/app/main/p/ap/daq/lang/en/pg/1/sn/n17:daq,n24:cRIO

http://www.rapidonline.com/netalogue/specs/78-1085.pdf

http://www.reading.ac.uk/merl/imagelibrary/steam.html

Appendix A – Bosch draught force sensing pin data sheet

(Source: http://www.boschrexroth.com/)

The Drive & Control Company

Rexroth
Bosch Group

Draft sensor
KMB series 30

RE 95170
Edition: 09.2013
Replaces: 04.2012

- Sensor for draft measurement

Features

- Draft sensor according to Category 3 rear three-point attachment (ISO 730-1)
- Sensor element with magnetoelastic measuring principle
- Integrated electronics
- Output signal ratiometric and proportional to draft
- Zero point and sensitivity are calibrated

Contents

RE 95170/09.2013, **Bosch Rexroth AG**

Ordering code

01	02	03	04	05		06		07
KMB					/	30	–	

Type

01	Draft measurement pin	KMB

Load range

02	±25 kN	025
	±40 kN	040
	±50 kN	050
	±60 kN	060
	±90 kN	090
	±110 kN	110
	±150 kN	150
	±160 kN	160

Supply voltage

03	5 ±0.5 V	05
	8 to 10 V	10

Cable version

04	Cable without protective sleeve	1
	Cable with spiral protective sleeve	2
	Cable with metal protective sleeve	3
	Cable with plastic protective sleeve	4

Connector

05	AMP connector; 3-pin	A
	DEUTSCH connector; 3-pin	B

Series

06		30

Cable length

07	800 mm	08
	965 mm	09
	1000 mm	10
	1500 mm	15
	1600 mm	16
	1800 mm	18
	2700 mm	27

Available variants

Type									Material number
KMB	025	05	1	A	/	30	–	15	R917007592
KMB	025	05	4	A	/	30	–	08	R917008079
KMB	025	05	4	A	/	30	–	15	R917008045
KMB	025	10	1	A	/	30	–	15	R917000161
KMB	025	10	4	A	/	30	–	08	R917000177
KMB	025	10	4	A	/	30	–	10	R917000158
KMB	025	10	4	A	/	30	–	15	R917000175
KMB	040	05	1	A	/	30	–	15	R917008099
KMB	040	05	3	A	/	30	–	15	R917008667
KMB	040	05	4	A	/	30	–	18	R917008003
KMB	040	10	1	A	/	30	–	15	R917000153
KMB	040	10	2	A	/	30	–	27	R917000160
KMB	040	10	3	A	/	30	–	15	R917000155
KMB	040	10	3	A	/	30	–	15	R917001320
KMB	040	10	4	A	/	30	–	08	R917000167
KMB	040	10	4	A	/	30	–	16	R917000159
KMB	040	10	4	A	/	30	–	18	R917000180
KMB	050	10	2	A	/	30	–	08	R917000157
KMB	050	10	2	A	/	30	–	08	R917000176
KMB	060	05	1	A	/	30	–	15	R917008098
KMB	060	05	3	A	/	30	–	15	R917008077
KMB	060	10	1	A	/	30	–	15	R917000154
KMB	060	10	1	A	/	30	–	15	R917000170
KMB	060	10	2	A	/	30	–	27	R917000164
KMB	060	05	3	A	/	30	–	15	R917008077
KMB	060	10	3	A	/	30	–	15	R917000156
KMB	060	05	4	A	/	30	–	18	R917008060
KMB	060	10	4	A	/	30	–	08	R917000166
KMB	060	10	4	A	/	30	–	15	R917000173
KMB	060	10	4	A	/	30	–	16	R917000165
KMB	060	10	4	A	/	30	–	18	R917000181
KMB	090	10	1	A	/	30	–	15	R917000168
KMB	090	10	1	A	/	30	–	15	R917000171
KMB	090	10	2	A	/	30	–	27	R917001969
KMB	090	05	3	A	/	30	–	15	R917008078
KMB	090	10	3	A	/	30	–	15	R917000163
KMB	090	05	4	A	/	30	–	18	R917008061
KMB	090	10	4	A	/	30	–	15	R917000172
KMB	090	10	4	A	/	30	–	18	R917000275
KMB	110	05	1	A	/	30	–	15	R917005142
KMB	110	10	1	A	/	30	–	15	R917000179
KMB	110	10	2	A	/	30	–	08	R917000162
KMB	150	10	2	A	/	30	–	08	R917000174
KMB	160	10	1	B	/	30	–	09	R917003021

Description

The draft sensor is designed as a bearing bolt. Shearing stress occurs at the bearing position, which is evaluated as a magnetoelastic effect.
In unloaded condition a symmetrical magnetic field is formed by the primary coil between the poles. If pulling or pressure drafts are induced, then the magnetic properties of the original isotropic material is altered. As a consequence, the magnetic field is rendered asymmetrical. This in turn induces a magnetic potential difference between the secondary poles. This causes a magnetic flux through the secondary circuit so that a voltage is induced in the secondary coils.
This voltage is proportional to the acting draft. It is amplified and rectified in an integrated evaluation circuit.
The sensor supplies a ratiometric voltage (25% to 75% of supply voltage). It is available with various measurement ranges and cable versions. This sensor is a typical part of an electro-hydraulic hitch control (EHC).

▼ **Function principle**

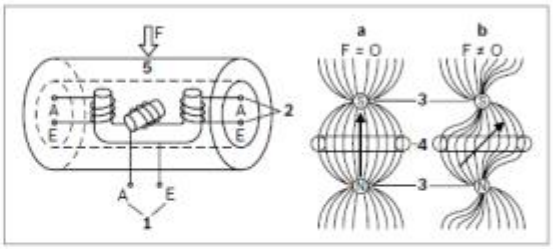

1 Primary coil
2 Secondary coil
3 Primary pole surface
4 Secondary pole surface
5 Steel sleeve
a Symmetrical magnetic field
b Asymmetrical magnetic field

▼ **Block circuit diagram**

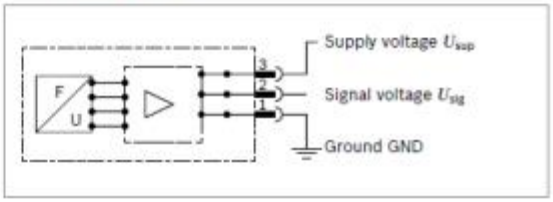

Technical data

Type		025	040	050	060	090	110	150
Load range F		±25 kN	±40 kN	±50 kN	±60 kN	±90 kN	±110 kN	±150 kN
Standard overload range		±80 kN			±160 kN			±220 kN
Electrically measurable overload		+1.2 $F_{pressure}$ to −1.5 $F_{tensile}$						
Supply voltage U_{sup}		8 to 12 V regulated voltage (no direct supply out of vehicle power (battery)) or 5 ±0.5 V						
Supply current I_{sup}		< 100 mA at 8 to 12 V; < 50 mA at 5 ±0.5 V						
Signal voltage U_{sig}		25% to 75% U_{sup} at 8 to 12 V; 15% to 85% U_{sup} at 5 ±0.5 V						
Load resistance		≥ 10 kΩ						
Characteristic		1			2			
Hysteresis		±0.01 U_{sup}			±0.005 U_{sup}			
Temperature coefficient of zero point		< ±0.25% U_{sup} / 10 °C			< ±0.5% U_{sup} / 10 °C			
Temperature coefficient of sensitivity		< 1% / 10 °C			< 1.25% / 10 °C			
Operating temperature range		−35 °C to +85 °C						
Storage temperature range		−40 °C to +125 °C (permanent); +130 °C (max. 2 h)						
Type of protection with installed mating connector	AMP DEUTSCH	IP67 and IP69K IP66K						
Vibration load		24 g						
Mating connector		3-pin connector with single-wire seal						
Electromagnetic compatibility EMC according to ISO 11452-5 2002-04 1 MHz to 2 GHz		150 V/m ≤ ±0.5% U_{sup}						

Characteristics

▼ **Characteristic 1 (load range up to 50 kN)**

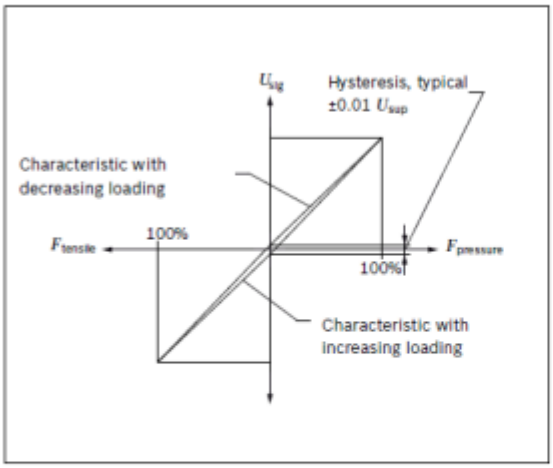

▼ **Characteristic 2 (load range up to 60 kN)**

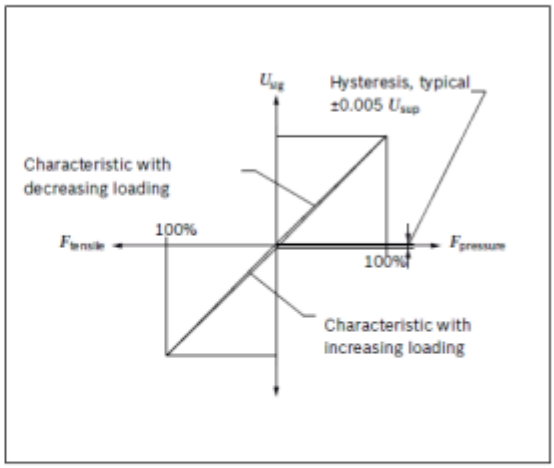

Dimensions [mm]

Dimensions

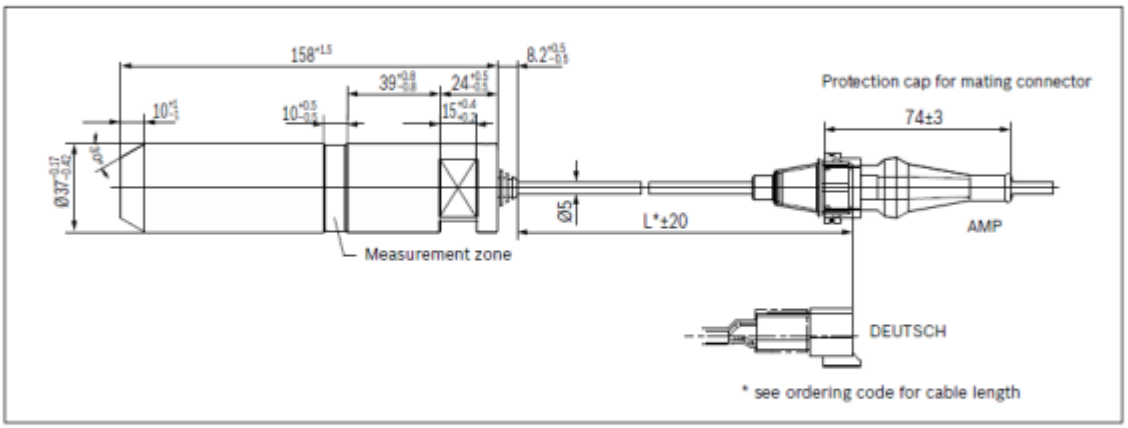

Connector

AMP

▼ **Pin assignment**

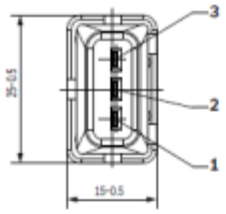

1 Ground GND
2 Signal voltage U_{sig}
3 Supply voltage U_{sup}

▼ **Mating connector**[1)]

Designation	Number	Material number
Housing	1	1928402579[2)]
Protection cap	1	1280703022[2)]
Contacts	3	929939[3)]
Single-wire seal (wire size: 0.5 to 1.0 mm²)	3 3	828 905-1[3)] for FLK cable type 828 904-1[3)] for FLKr, FLX cable

DEUTSCH

▼ **Pin assignment**

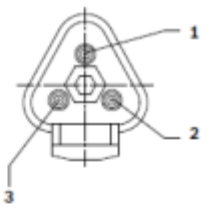

1 Supply voltage U_{sup}
2 Signal voltage U_{sig}
3 Ground GND

▼ **Mating connector**[1)]

Designation	Material number
Plug connector	DEUTSCH DT 04-3P[4)]
Wedge-lock	DEUTSCH W 3P[4)]
Contacts	DEUTSCH 0460-202-16141[4)]

1) The mating connector is not included in the scope of supply.
2) Available from Bosch
3) Available from AMP
4) Available from DEUTSCH

Cable versions

▼ **Cable without protective sleeve**

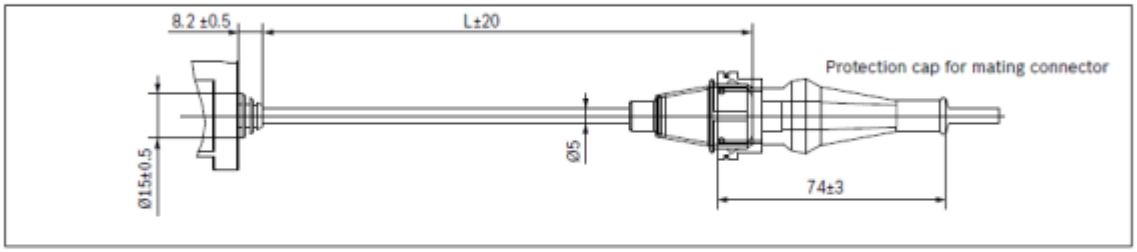

▼ **Cable with spiral protective sleeve**

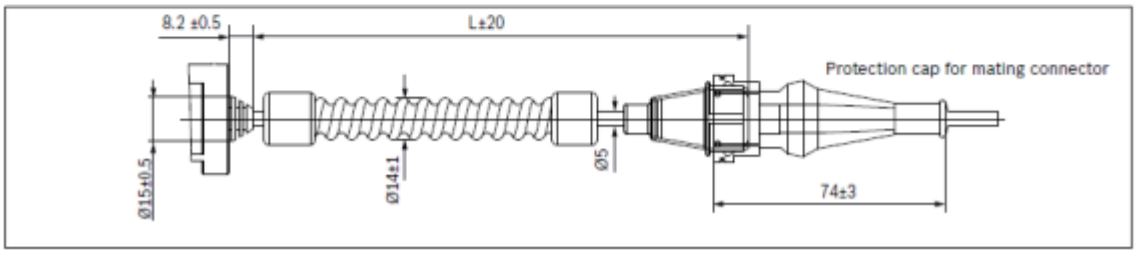

▼ **Cable with metal protective sleeve**

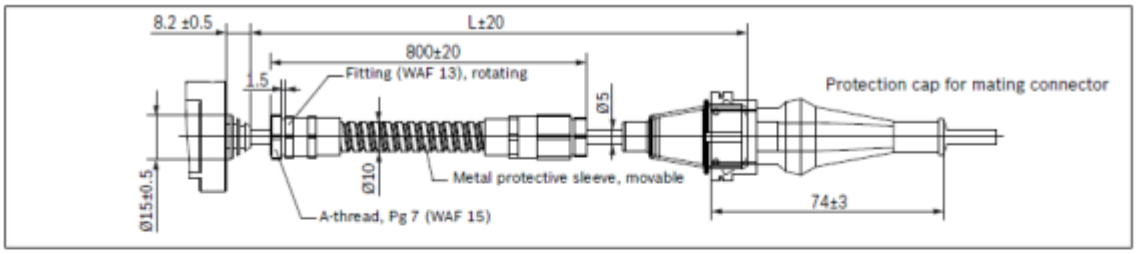

▼ **Cable with plastic protective sleeve**

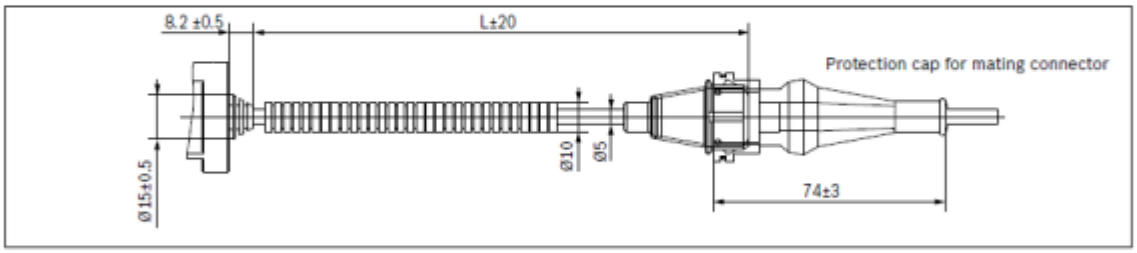

Installation instructions

- See installation drawing Y 830 304 223 to avoid measuring uncertainties
- Defined draft application, e.g., ball bushing
- Floating mount in radial direction with key plate

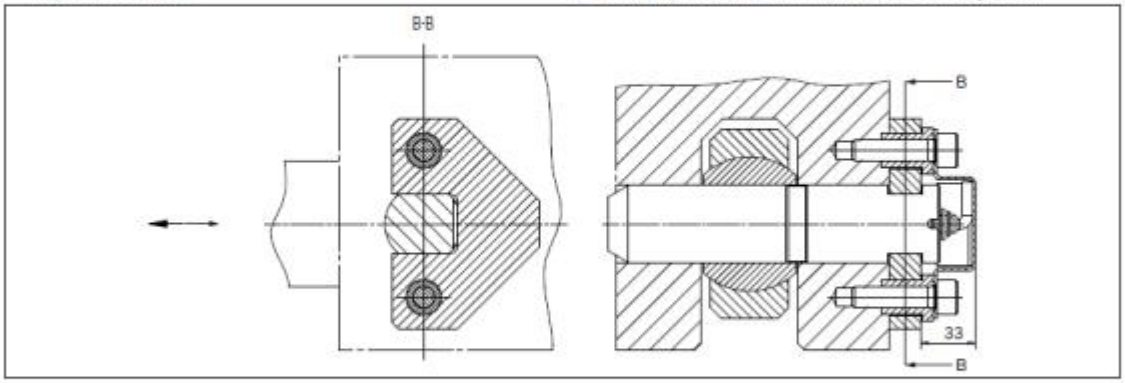

Safety instructions

General instructions

- The proposed circuits do not imply any technical liability for the system on the part of Bosch Rexroth.
- It is not permissible to open the KMB draft sensor or to modify or repair the KMB draft sensor. Modifications or repairs to the wiring could result in dangerous malfunctions.
- System developments, installation and commissioning of electronic systems for controlling hydraulic drives must only be carried out by trained and experienced specialists who are sufficiently familiar with both the components used and with the complete system.
- While commissioning the KMB draft sensor, the machine may pose unforeseen dangers. Before commissioning the system, you must therefore ensure that the vehicle and the hydraulic system are in a safe condition.
- Make sure that nobody is in the machine's danger zone.
- No defective or incorrectly functioning components may be used. If the KMB draft sensor should fail or demonstrate faulty operation, it must be replaced.

Notes on the installation point and position

- Do not install the KMB draft sensor close to parts that generate considerable heat (e.g. exhaust).
- A sufficiently large distance to radio systems must be maintained.
- The connector of the KMB draft sensor is to be unplugged during electrical welding and painting operations.
- Cables/wires must be sealed individually to prevent water from entering the device.

Notes on transport and storage

- If it is dropped, the KMB draft sensor must not be used any longer as invisible damage could have a negative impact on reliability.

Notes on wiring and circuitry

- Lines to the draft sensors are so short as possible and be shielded. The shielding must be connected to the electronics on one side or to the machine or vehicle ground via a low-resistance connection.
- The product should only be plugged and unplugged when it is in a de-energized state.
- Lines from the KMB draft sensor to the electronics must not be routed close to other power-conducting lines in the machine or vehicle.
- The KMB draft sensor and the connection line should be supported mechanically near the installation location.

RE 95170/09.2013, **Bosch Rexroth AG**

- If possible, lines should be routed in the vehicle interior. If the lines are routed outside the vehicle, make sure that they are securely fixed.
- Lines must not be kinked or twisted, must not rub against edges and must not be routed through sharp-edged ducts without protection.
- Lines are to be routed with sufficient distance from hot or moving vehicle parts.
- The sensor lines are sensitive to radiation interference. For this reason, the following measures should be taken when operating the sensor:
  - Sensor lines should be attached as far away as possible from large electric machines.
  - If the signal requirements are satisfied, it is possible to extend the sensor cable.

Intended use

- The KMB draft sensor is designed for use in mobile working machines provided no limitations/restrictions are made to certain application areas in this data sheet.
- Operation of the KMB draft sensor must generally occur within the operating ranges specified and released in this data sheet, particularly with regard to voltage, temperature, vibration, shock and other described environmental influences.
- Use outside of the specified and released boundary conditions may result in danger to life and/or cause damage to components which could result in consequential damage to the mobile working machine.

Improper use

- Any use of the KMB draft sensor other than that described in chapter "Intended use" is considered to be improper.
- Use in explosive areas is not permissible.
- Damages which result from improper use and/or from unauthorized, unintended interventions in the device not described in this data sheet render all warranty and liability claims with respect to the manufacturer void.

Use in safety-related functions

- The customer is responsible for performing a risk analysis of the mobile working machine and determining the possible safety-related functions.
- In safety-related applications, the customer is responsible for taking suitable measures for ensuring safety (sensor redundancy, plausibility check, emergency switch, etc.).
- Product data that is necessary to assess the safety of the machine can be provided on request or are listed in this data sheet.

Further information

- Further information about the KMB draft sensor can be found at www.boschrexroth.com/mobile-electronics.
- The KMB draft sensor must be disposed according the national regulations of your country.

Bosch Rexroth AG
Mobile Applications
Robert-Bosch-Straße 2
71701 Schwieberdingen, Germany
Tel. +49 711 811 430 80
info.bodas@boschrexroth.de
www.boschrexroth.com

© This document, as well as the data, specifications and other information set forth in it, are the exclusive property of Bosch Rexroth AG. It may not be reproduced or given to third parties without its consent. The data specified above only serve to describe the product. No statements concerning a certain condition or suitability for a certain application can be derived from our information. The information given does not release the user from the obligation of own judgment and verification. It must be remembered that our products are subject to a natural process of wear and aging.

Bosch Rexroth AG, RE 95170/09.2013

Appendix B – Cone index data from initial field experiments

Shown below are a set of Cone Index data taken from Block 1, Plot 1 and Treatment 6 during initial field experiments as an example.

Depth (cm)	Cone Index (Pa)				
	Point 1	Point 2	Point 3	Point 4	Point 5
0	753	565	376	403	350
1	753	780	484	403	538
2	887	1076	672	6588	1237
3	1103	1425	861	6588	1560
4	1318	1775	1049	6588	1613
5	1345	1855	1506	6588	1667
6	1345	1936	1694	6588	1694
7	1398	1990	1936	6588	1721
8	1506	2017	2124	6588	1667
9	1533	2017	2205	6588	1560
10	1533	1990	2232	6588	1506
11	1560	1963	2178	6588	1425
12	1613	1829	2178	6588	1345
13	1775	1829	1829	6588	1318
14	2044	1506	1829	6588	1264
15	1936	1506	1829	6588	1264
16	1936	1506	1829	6588	1103
17	1936	1506	1829	6588	1076
18	1479	1103	1829	6588	1103
19	1802	1103	1829	6588	1345
20	1802	941	1667	6588	1533
21	2286	941	1694	6588	1748
22	2689	861	1963	6588	1882
23	2850	887	2555	6588	2393
24	2850	1398	3308	6588	3711
25	2824	2528	3469	6588	4034
26	2850	2232	3684	6588	4034
27	3146	2958	0	6588	3899
28	3066	2689	0	6588	3953
29	2958	2689	0	6588	4114
30	3254	2689	0	6588	4464
31	3711	2555	0	6588	4410
32	3872	3066	0	6588	4329
33	4061	4222	0	6588	4303
34	4222	4571	0	6588	4168
35	4249	4222	0	6588	4195
36	4249	4222	0	6588	4168
37	4087	4356	0	6588	3657
38	4356	0	0	6588	3227
39	5324	0	0	6588	3227
40	0	0	0	6588	3227
41	0	0	0	6588	3173
42	0	0	0	6588	3980
43	0	0	0	6588	4087
44	0	0	0	6588	5943
45	0	0	0	6588	5997

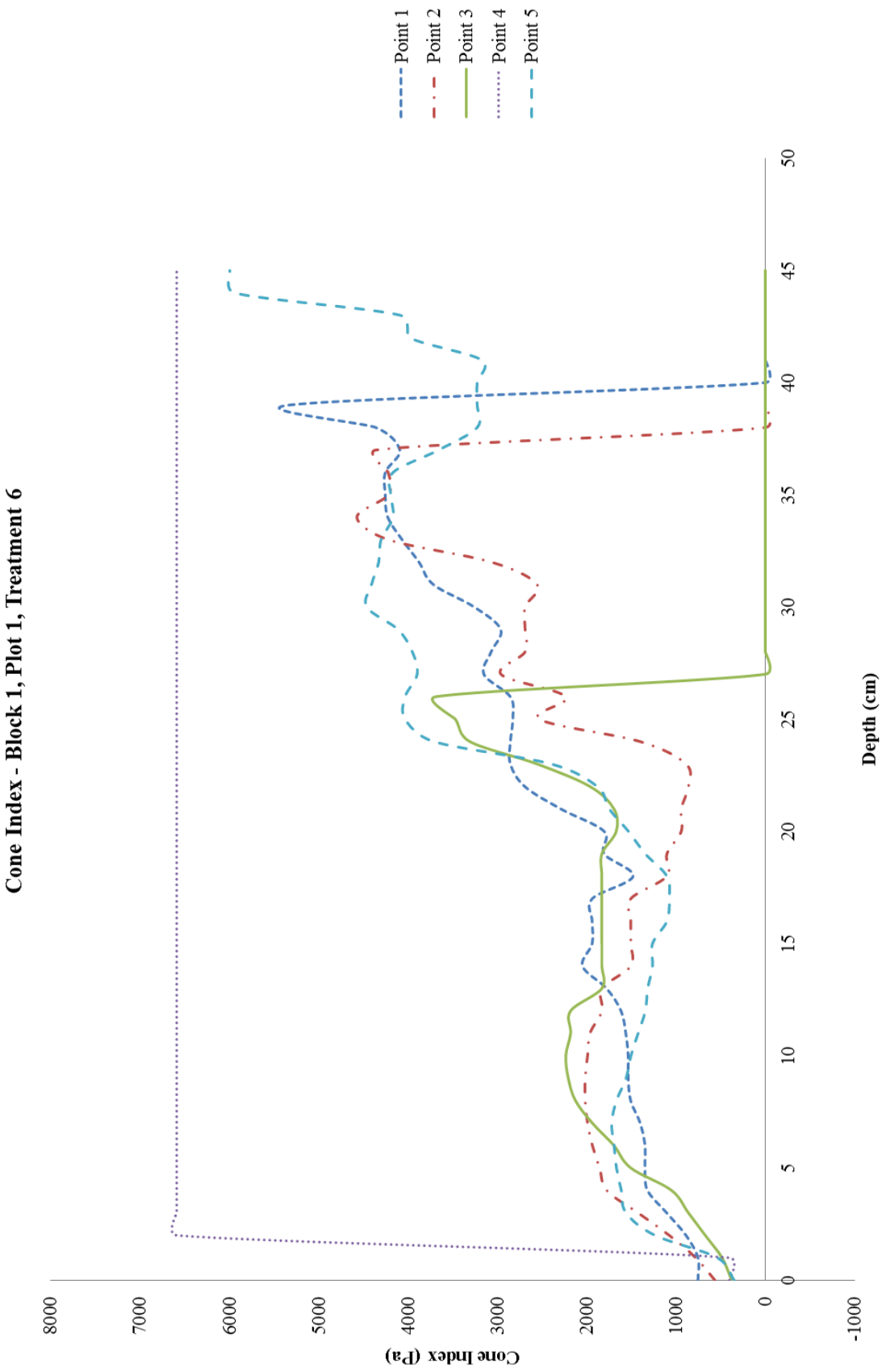
Cone Index - Block 1, Plot 1, Treatment 6
Point 1
Point 2
Point 3
Point 4
Point 5
Cone Index (Pa)
8000
7000
6000
5000
4000
3000
2000
1000
0
-1000
Depth (cm)
0
5
10
15
20
25
30
35
40
45
50

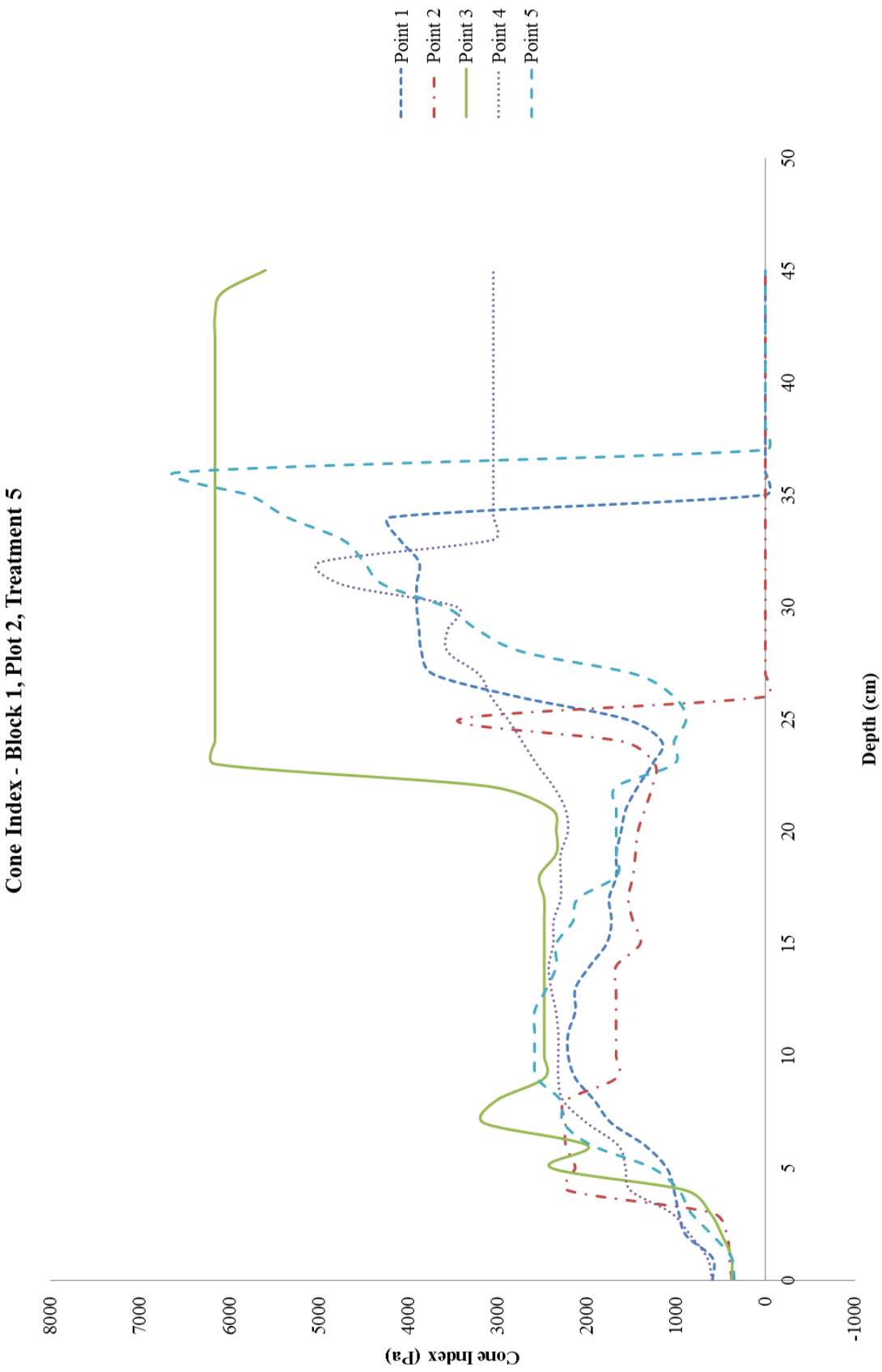
Cone Index - Block 1, Plot 2, Treatment 5
Point 1
Point 2
Point 3
Point 4
Point 5
Cone Index (Pa)
8000
7000
6000
5000
4000
3000
2000
1000
0
-1000
Depth (cm)
0
5
10
15
20
25
30
35
40
45
50

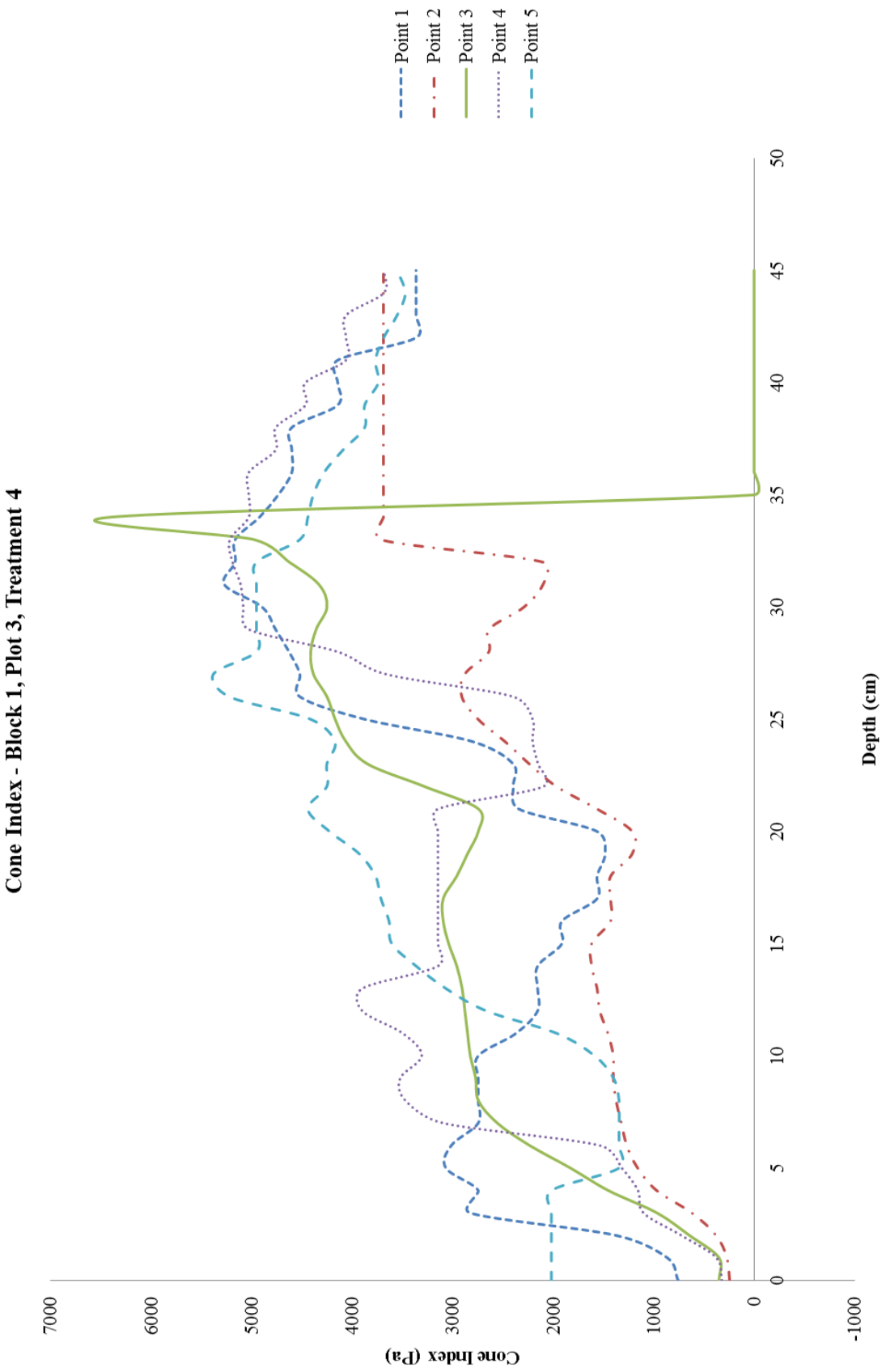
Cone Index - Block 1, Plot 3, Treatment 4
Point 1
Point 2
Point 3
Point 4
Point 5
Cone Index (Pa)
7000
6000
5000
4000
3000
2000
1000
0
-1000
Depth (cm)
0
5
10
15
20
25
30
35
40
45
50

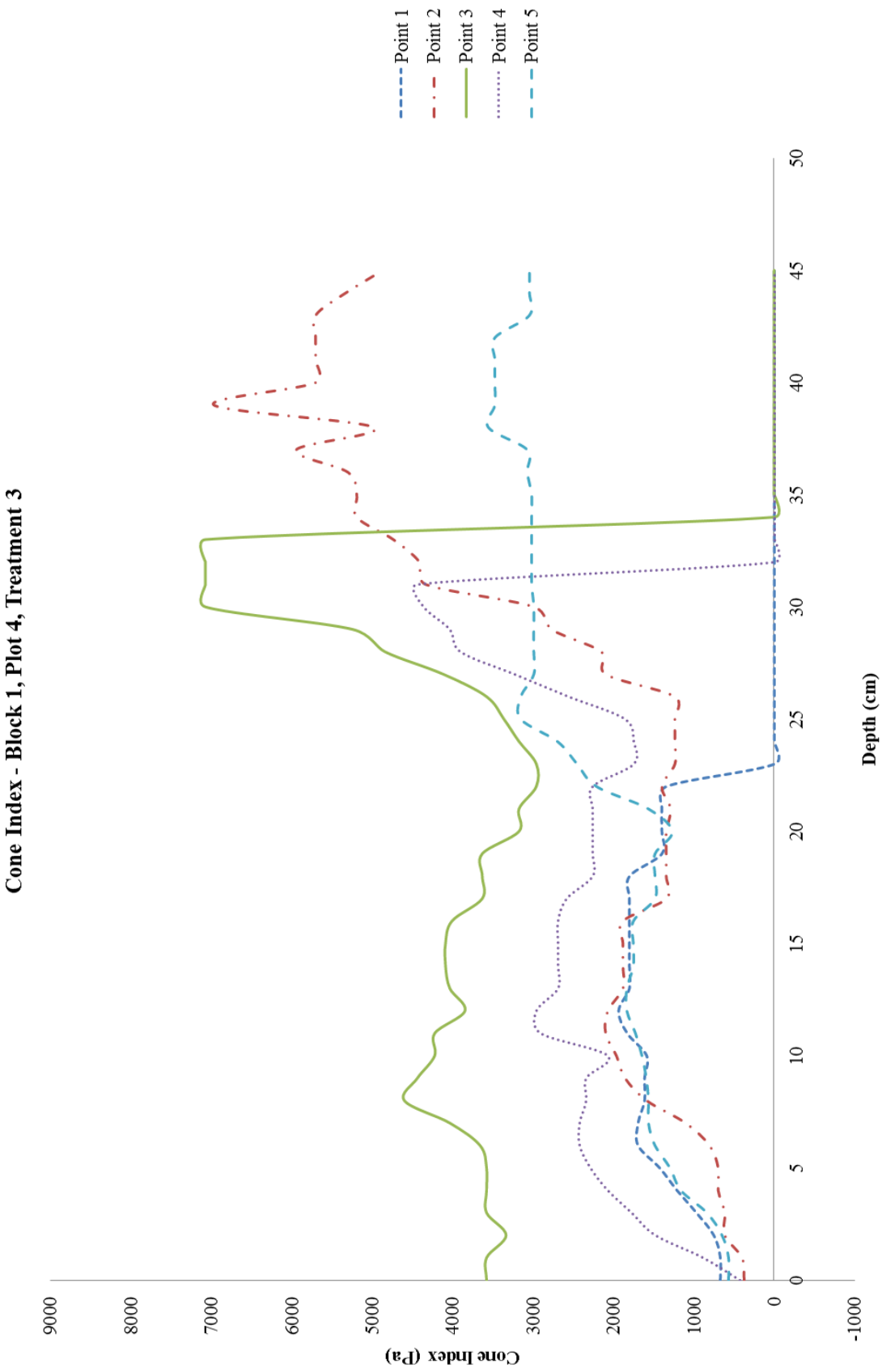
Cone Index - Block 1, Plot 4, Treatment 3
Point 1
Point 2
Point 3
Point 4
Point 5
Cone Index (Pa)
9000
8000
7000
6000
5000
4000
3000
2000
1000
0
-1000
Depth (cm)
0
5
10
15
20
25
30
35
40
45
50

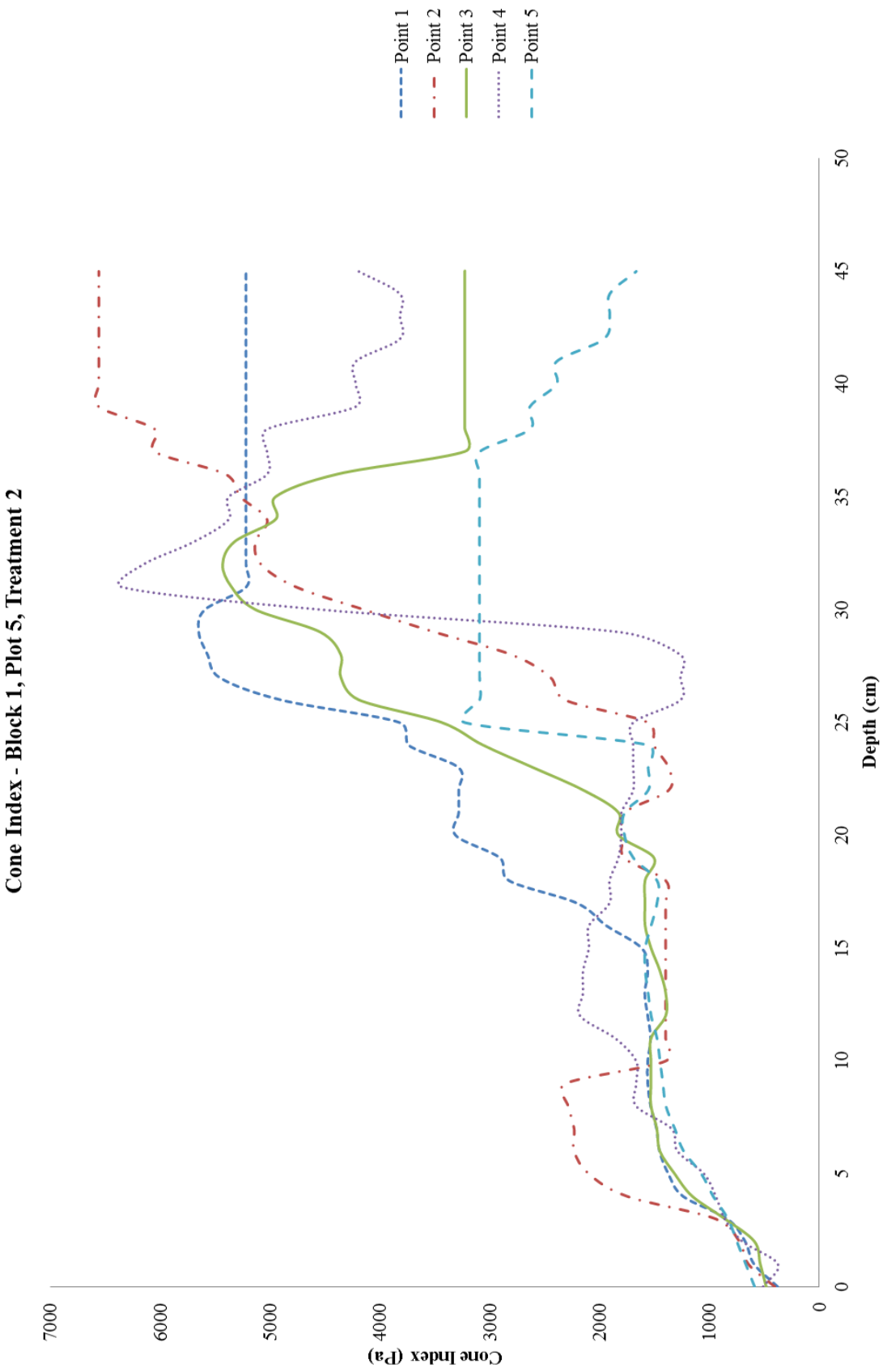
Cone Index - Block 1, Plot 5, Treatment 2
Point 1
Point 2
Point 3
Point 4
Point 5
Cone Index (Pa)
7000
6000
5000
4000
3000
2000
1000
0
Depth (cm)
0
5
10
15
20
25
30
35
40
45
50

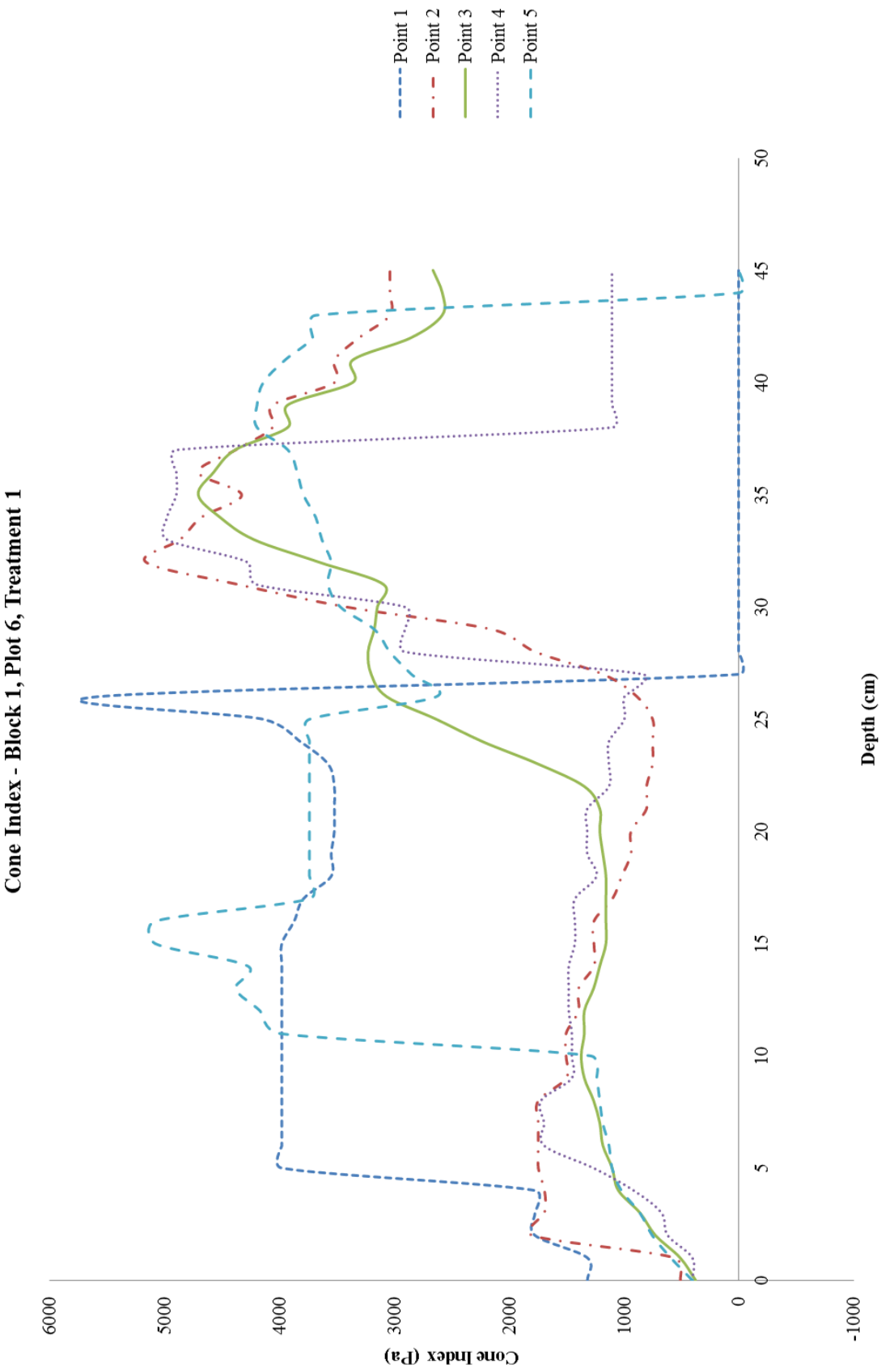
Cone Index - Block 1, Plot 6, Treatment 1
Point 1
Point 2
Point 3
Point 4
Point 5
Cone Index (Pa)
6000
5000
4000
3000
2000
1000
0
-1000
Depth (cm)
0
5
10
15
20
25
30
35
40
45
50

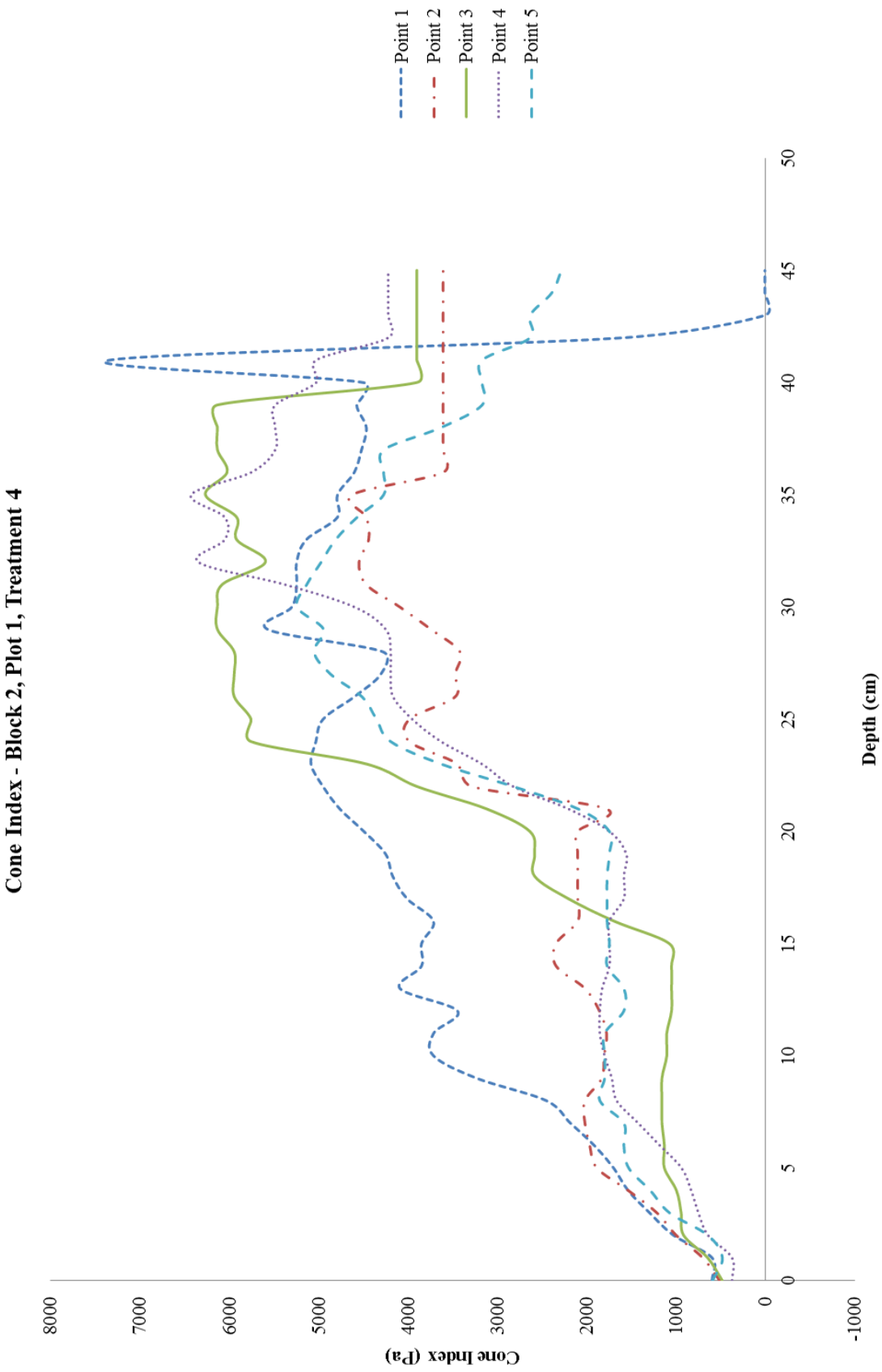
Cone Index - Block 2, Plot 1, Treatment 4
Point 1
Point 2
Point 3
Point 4
Point 5
Cone Index (Pa)
8000
7000
6000
5000
4000
3000
2000
1000
0
-1000
Depth (cm)
0
5
10
15
20
25
30
35
40
45
50

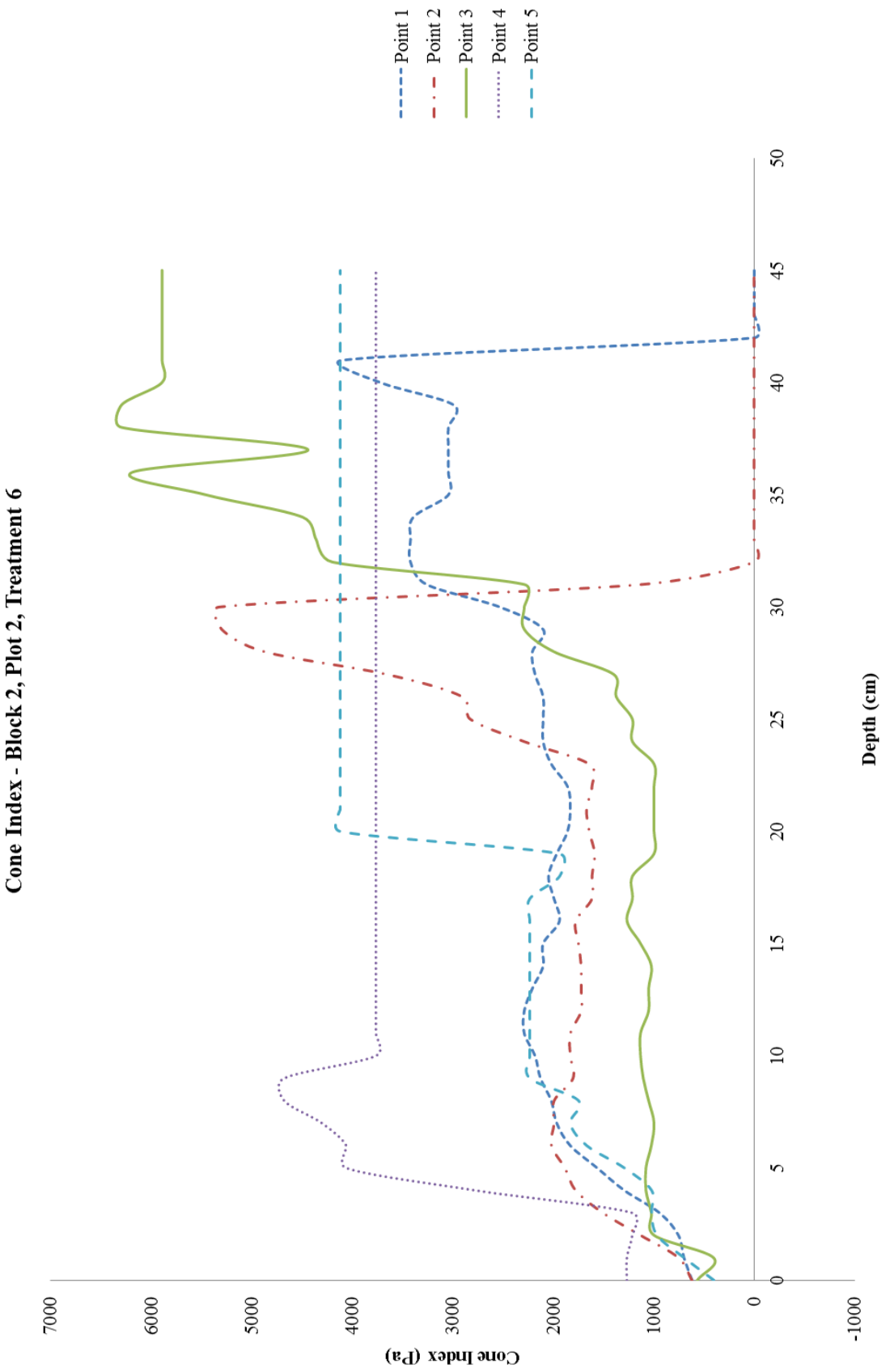
Cone Index - Block 2, Plot 2, Treatment 6
Point 1
Point 2
Point 3
Point 4
Point 5
Cone Index (Pa)
7000
6000
5000
4000
3000
2000
1000
0
-1000
Depth (cm)
0
5
10
15
20
25
30
35
40
45
50

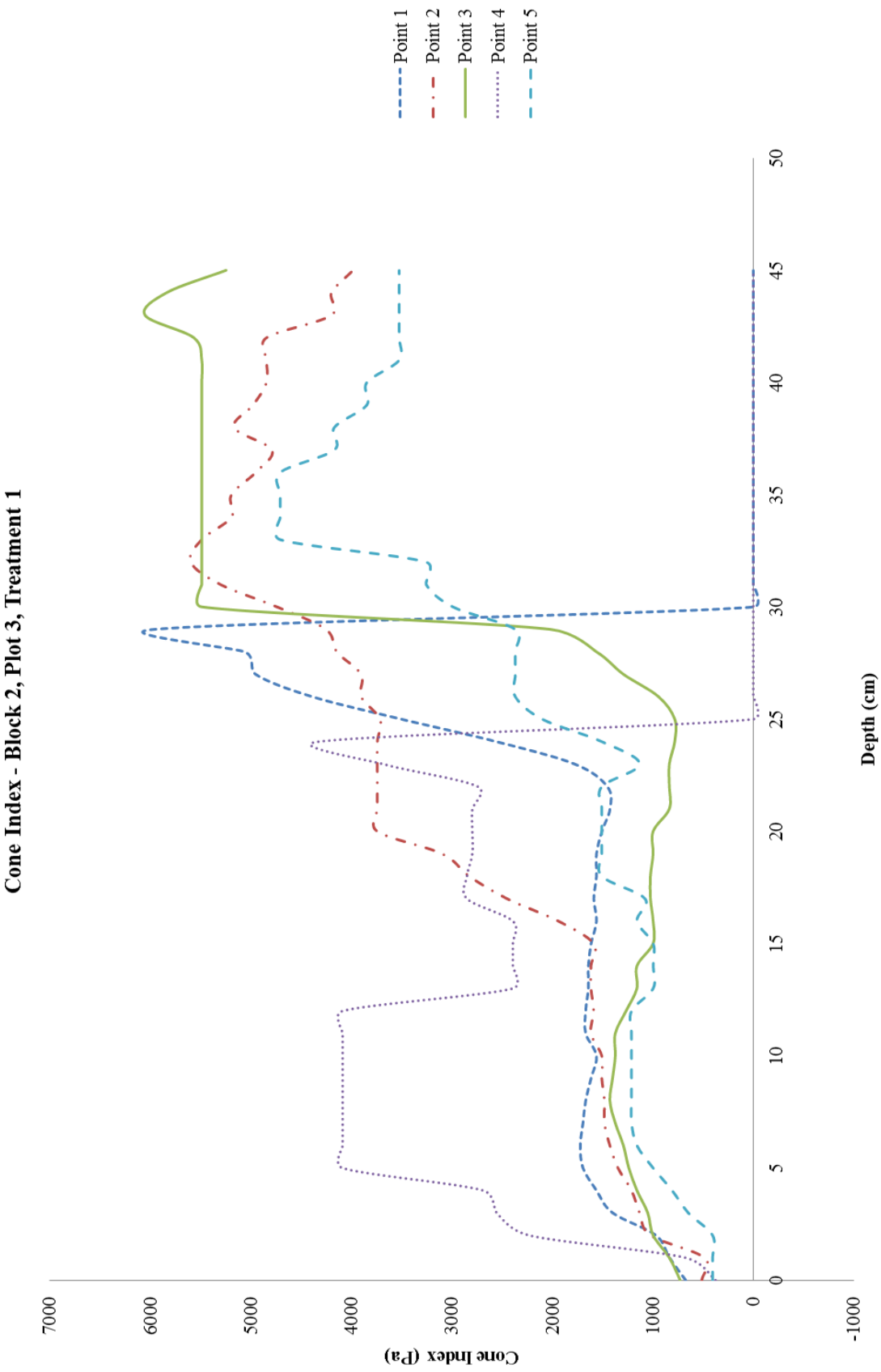
Cone Index - Block 2, Plot 3, Treatment 1
Point 1
Point 2
Point 3
Point 4
Point 5
Cone Index (Pa)
7000
6000
5000
4000
3000
2000
1000
0
-1000
Depth (cm)
0
5
10
15
20
25
30
35
40
45
50

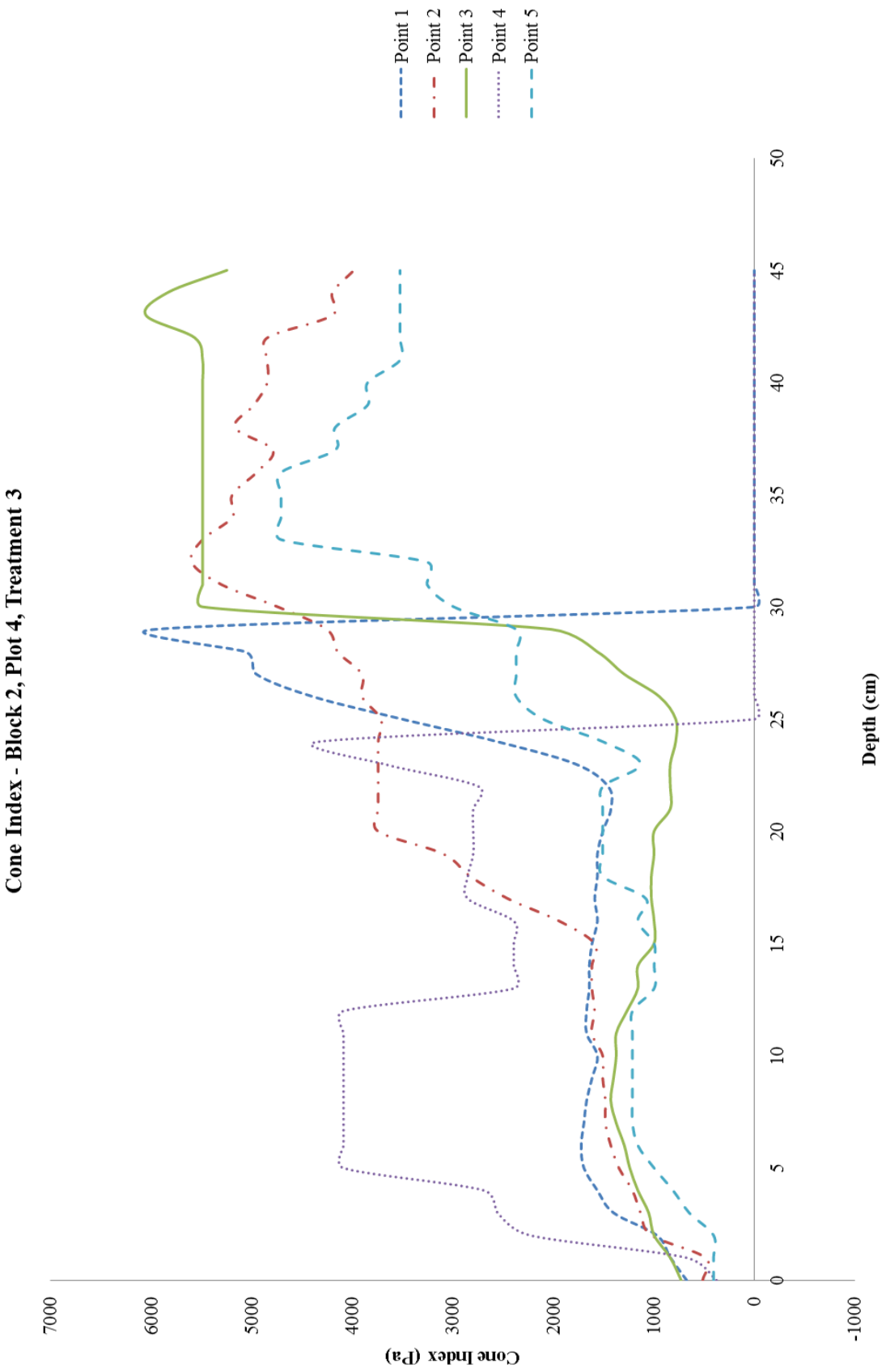
Cone Index - Block 2, Plot 4, Treatment 3
Point 1
Point 2
Point 3
Point 4
Point 5
Cone Index (Pa)
7000
6000
5000
4000
3000
2000
1000
0
-1000
Depth (cm)
0
5
10
15
20
25
30
35
40
45
50

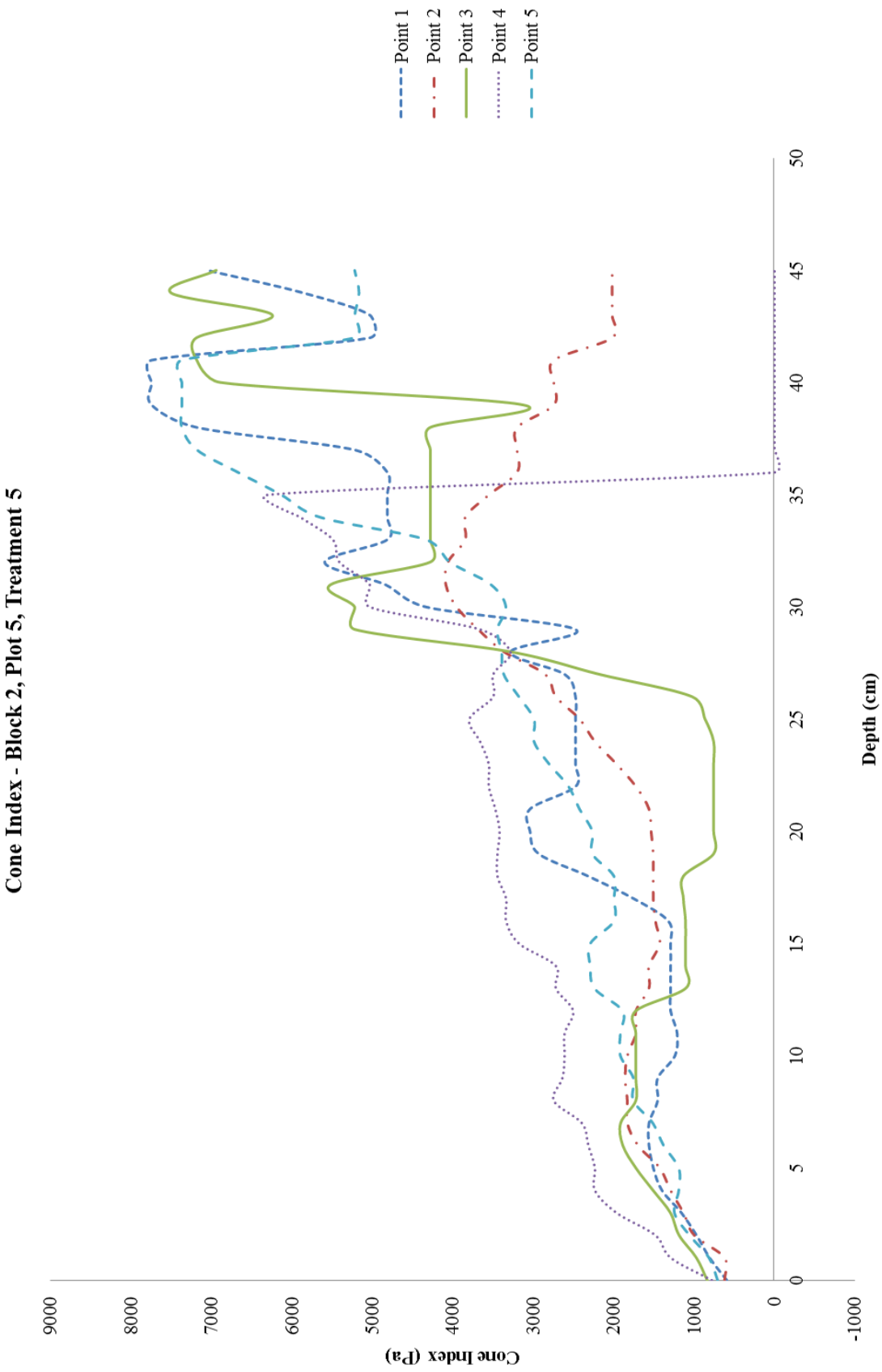
Cone Index - Block 2, Plot 5, Treatment 5
Point 1
Point 2
Point 3
Point 4
Point 5
Cone Index (Pa)
9000
8000
7000
6000
5000
4000
3000
2000
1000
0
-1000
0
5
10
15
20
25
30
35
40
45
50
Depth (cm)

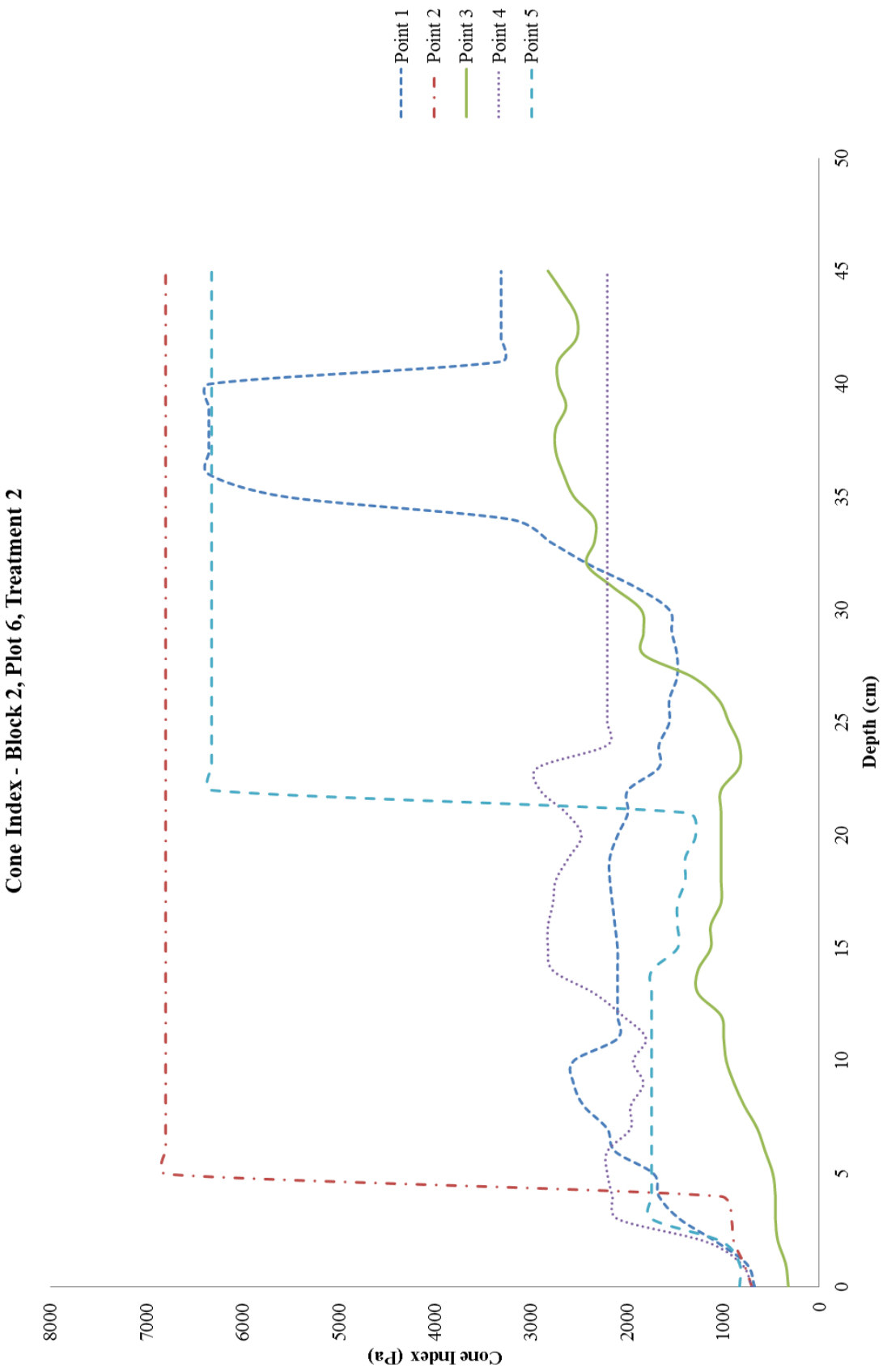
Cone Index - Block 2, Plot 6, Treatment 2
Point 1
Point 2
Point 3
Point 4
Point 5
Cone Index (Pa)
0
1000
2000
3000
4000
5000
6000
7000
8000
Depth (cm)
0
5
10
15
20
25
30
35
40
45
50

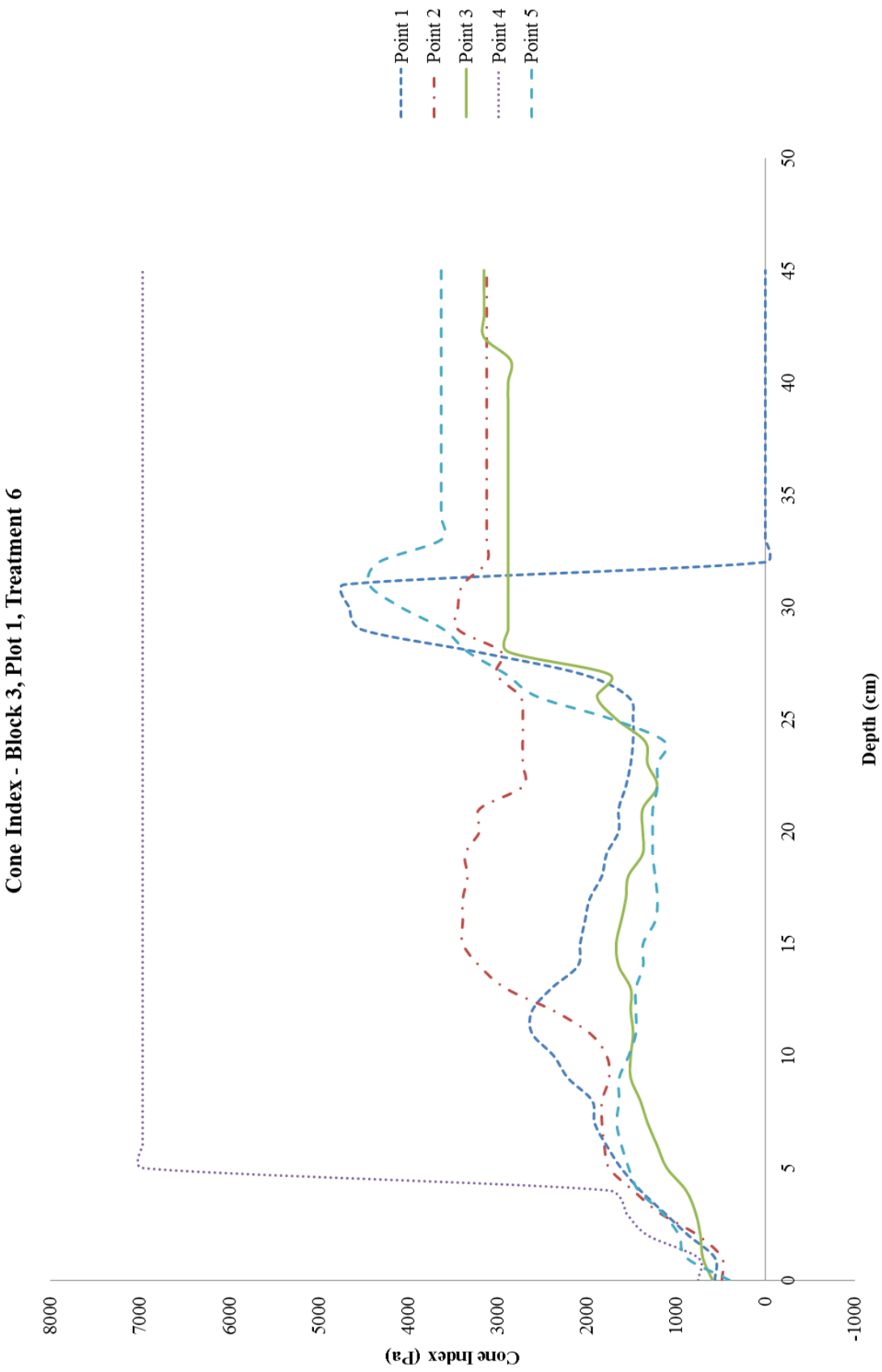
Cone Index - Block 3, Plot 1, Treatment 6
Point 1
Point 2
Point 3
Point 4
Point 5
Cone Index (Pa)
8000
7000
6000
5000
4000
3000
2000
1000
0
-1000
Depth (cm)
0
5
10
15
20
25
30
35
40
45
50

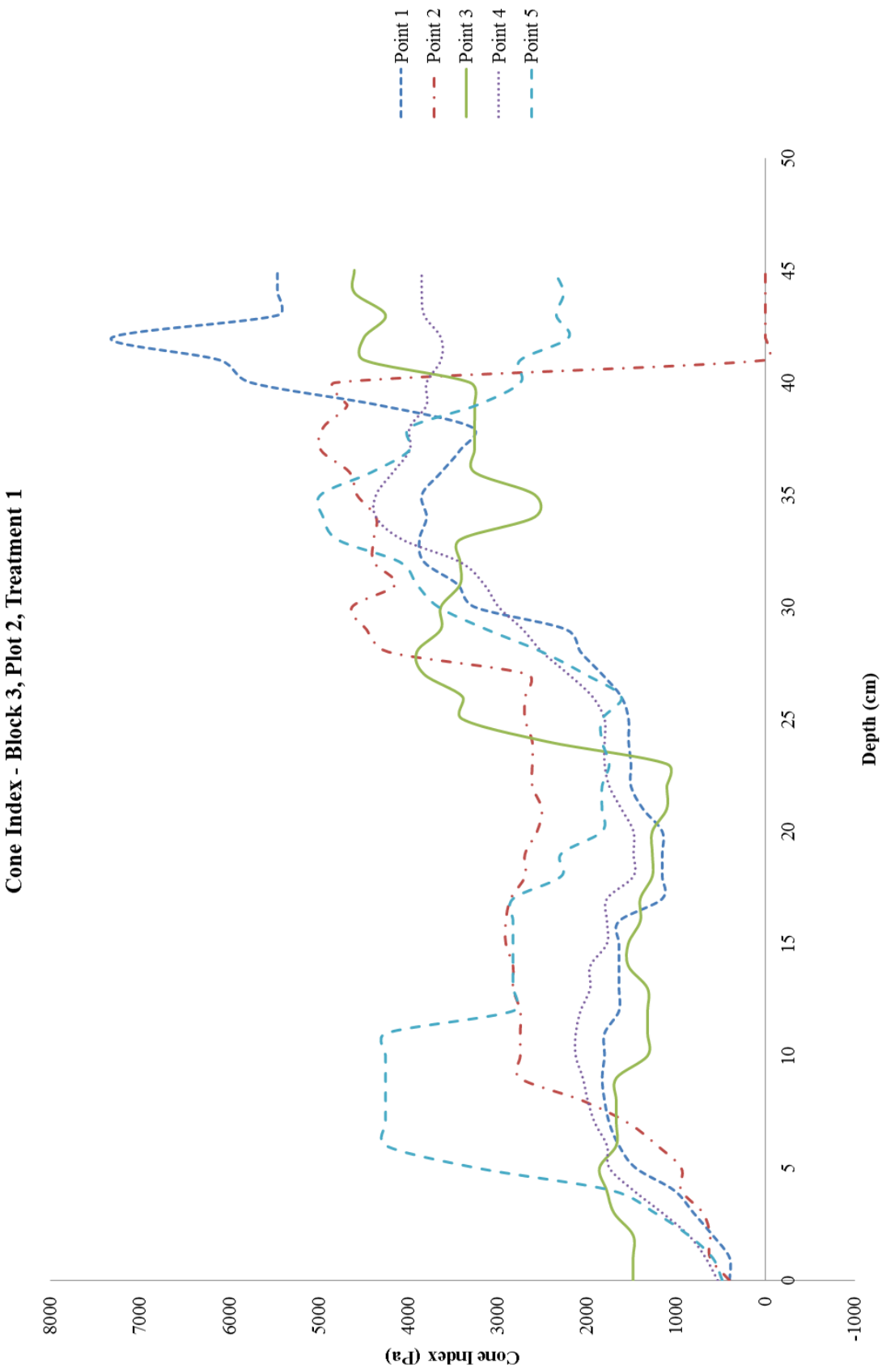
Cone Index - Block 3, Plot 2, Treatment 1
Point 1
Point 2
Point 3
Point 4
Point 5
Cone Index (Pa)
8000
7000
6000
5000
4000
3000
2000
1000
0
-1000
Depth (cm)
0
5
10
15
20
25
30
35
40
45
50

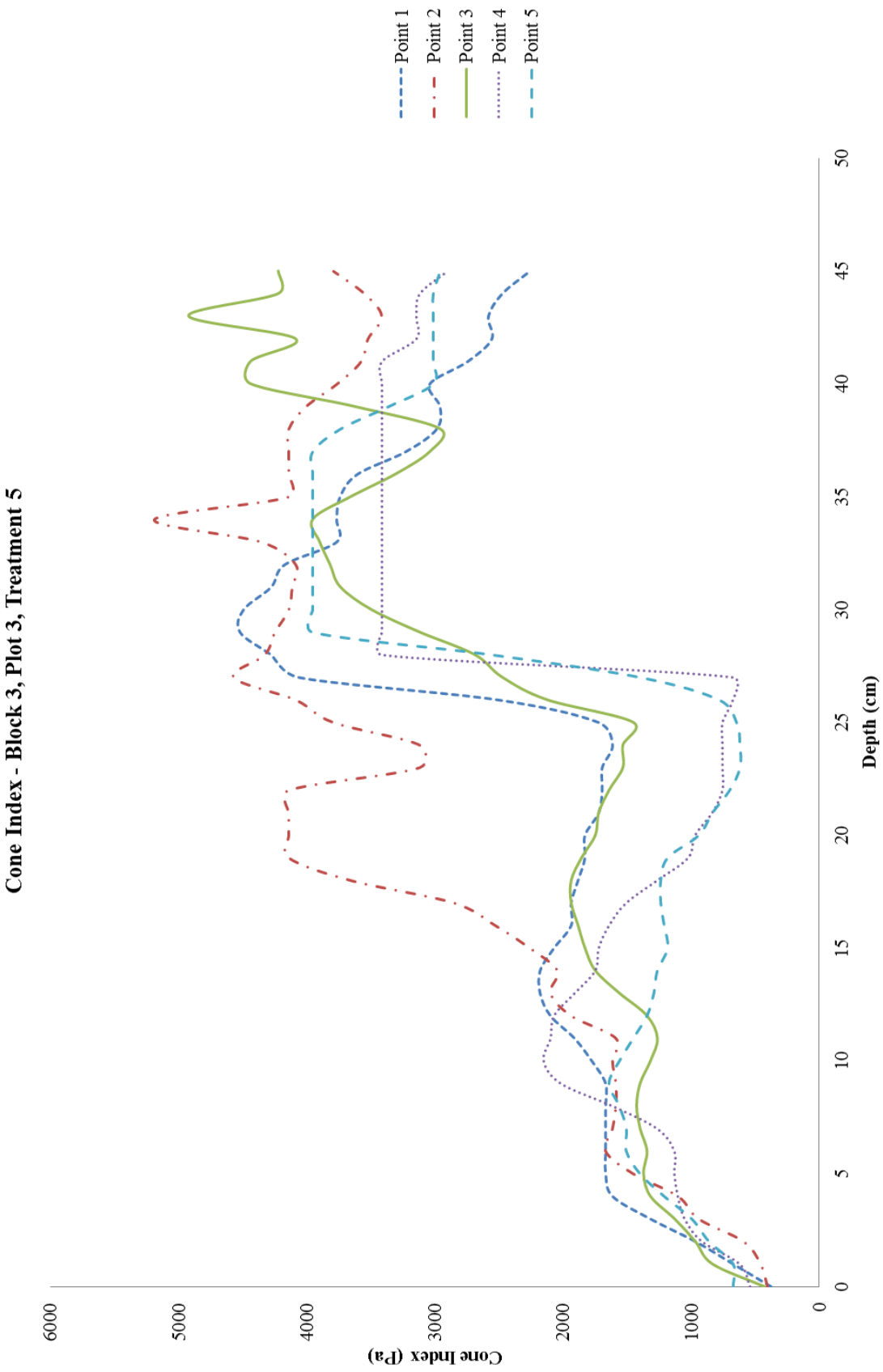
Cone Index - Block 3, Plot 3, Treatment 5
Point 1
Point 2
Point 3
Point 4
Point 5
Cone Index (Pa)
0
1000
2000
3000
4000
5000
6000
Depth (cm)
0
5
10
15
20
25
30
35
40
45
50

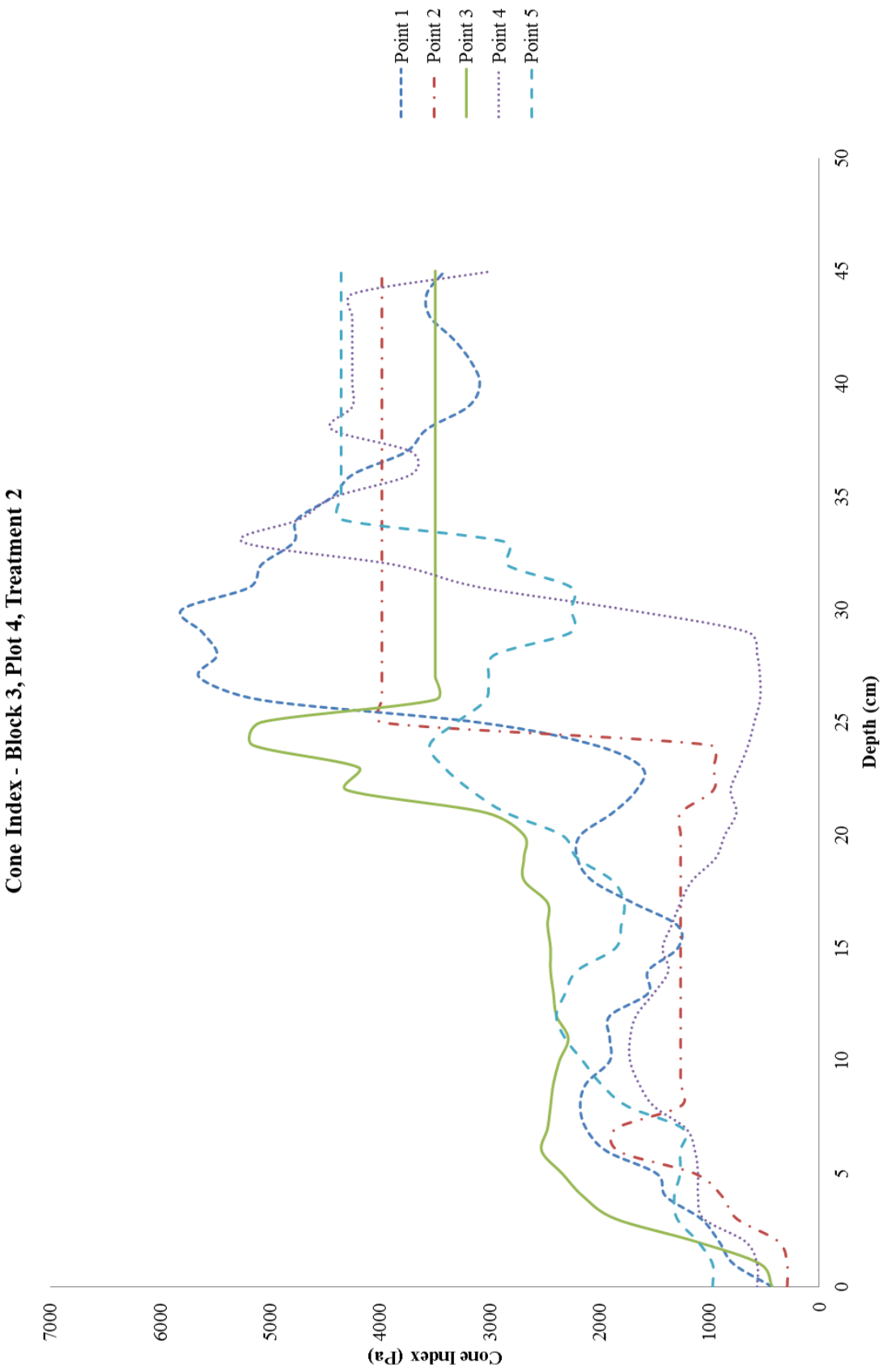
Cone Index - Block 3, Plot 4, Treatment 2
Point 1
Point 2
Point 3
Point 4
Point 5
Cone Index (Pa)
7000
6000
5000
4000
3000
2000
1000
0
Depth (cm)
0
5
10
15
20
25
30
35
40
45
50

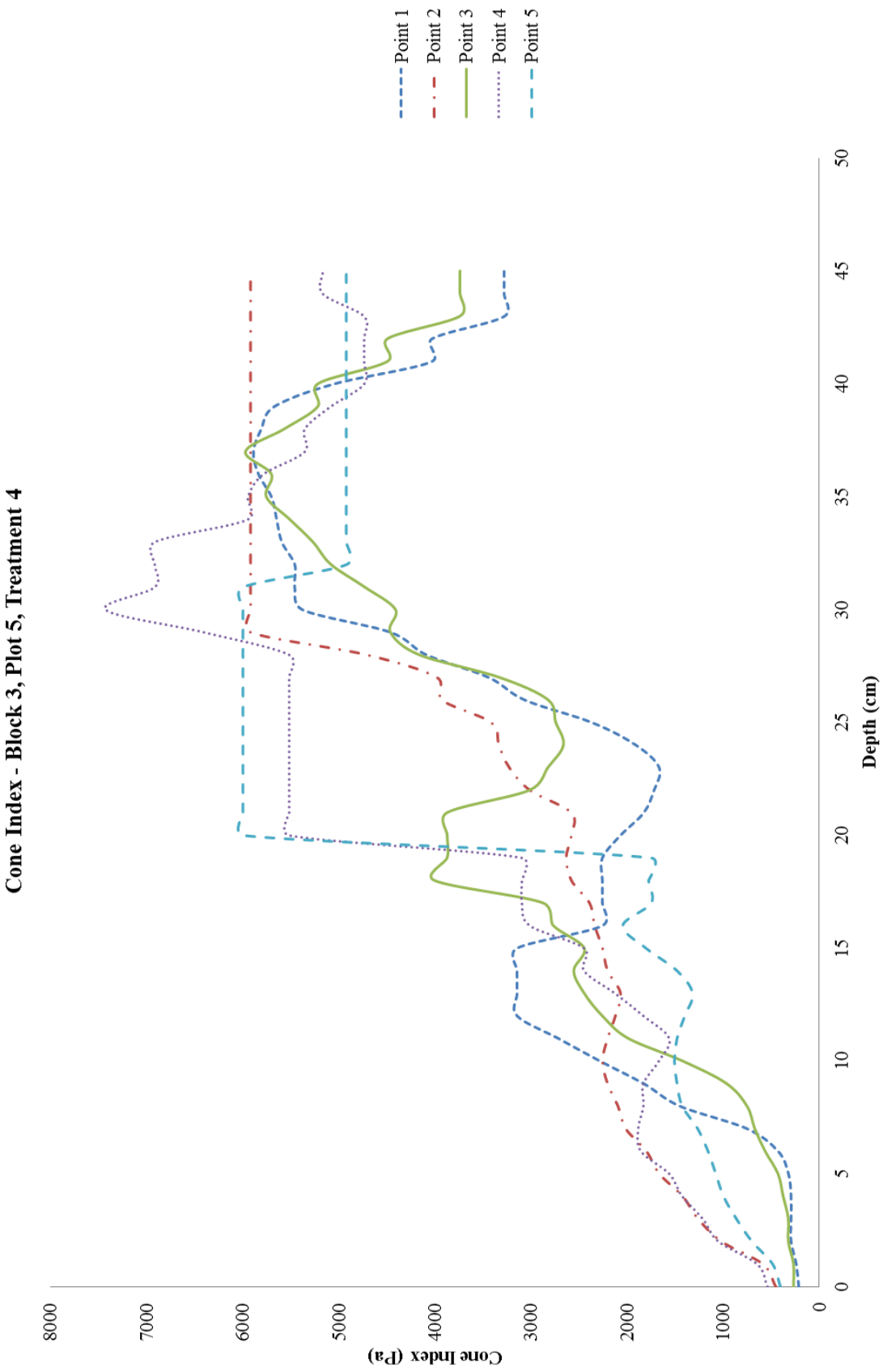
Cone Index - Block 3, Plot 5, Treatment 4
Point 1
Point 2
Point 3
Point 4
Point 5
Cone Index (Pa)
0
1000
2000
3000
4000
5000
6000
7000
8000
Depth (cm)
0
5
10
15
20
25
30
35
40
45
50

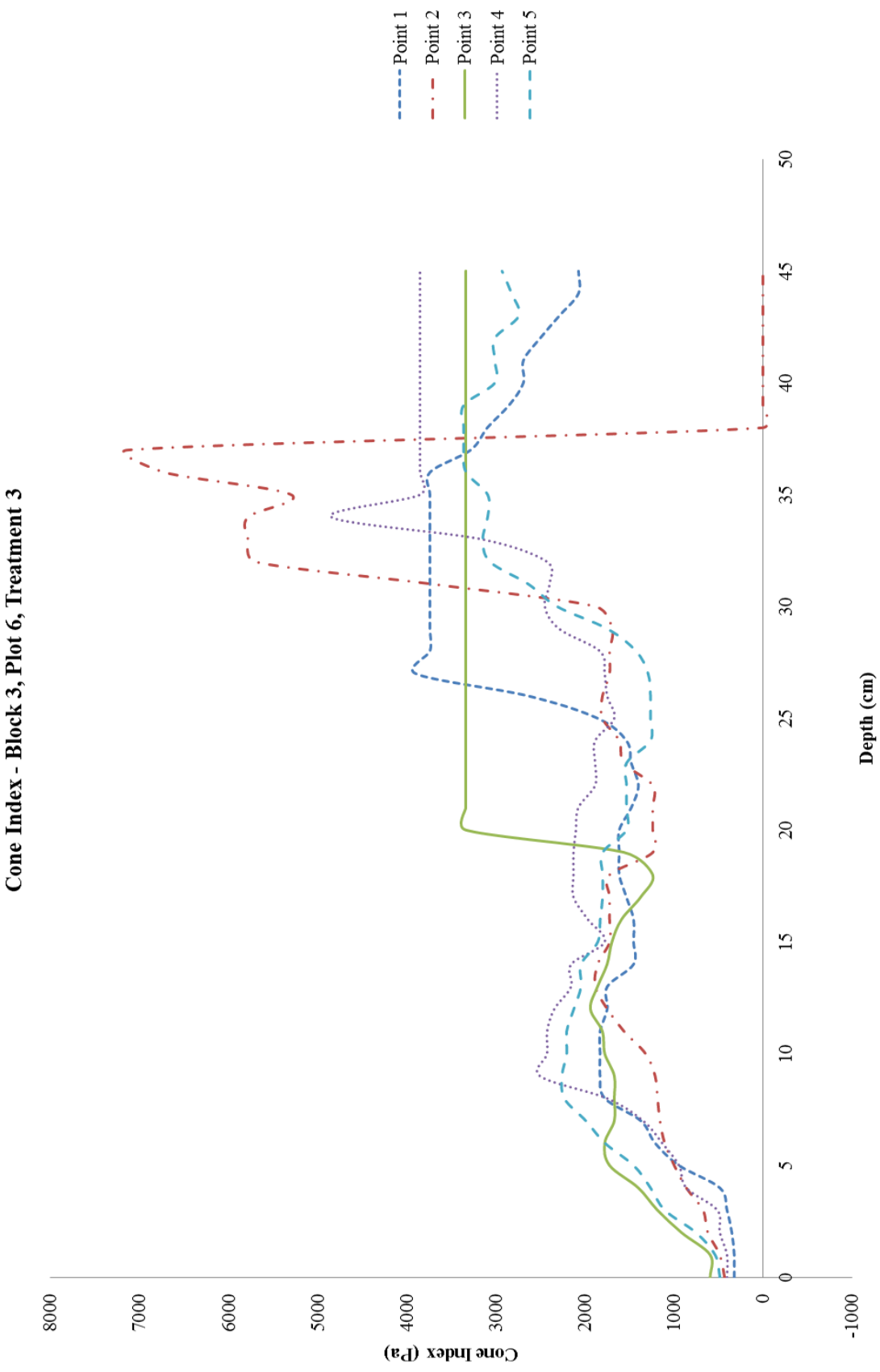
Cone Index - Block 3, Plot 6, Treatment 3
Point 1
Point 2
Point 3
Point 4
Point 5
Cone Index (Pa)
8000
7000
6000
5000
4000
3000
2000
1000
0
-1000
Depth (cm)
0
5
10
15
20
25
30
35
40
45
50

Appendix C – Initial field experiment summary of data

		Draught Control							Position Control							Mix Control						
		Treatment 1 (Block, Plot)			Treatment 4 (Block, Plot)				Treatment 2 (Block, Plot)			Treatment 5 (Block, Plot)				Treatment 3 (Block, Plot)			Treatment 6 (Block, Plot)			
		B1, P6	B2, P3	B3, P2	Mean	B1,P3	B2,P1	B3, P5	Mean	B1, P5	B2, P6	B3, P4	Mean	B1, P2	B2, P5	B3, P3	Mean	B1, P4	B2, P4	R3, P6	Mean	B1, P1	B2, P2	B3, P1	Mean
Weight Transfer (kN)	Mean δZR	16.36	16.97	24.05	16.66	37.42	37.15	34.23	36.27	8.61	8.18	7.28	8.02	33.93	37.16	36.19	35.76	13.37	13.66	13.11	13.38	36.58	33.90	34.71	35.24
	Max δZR	28.63	24.49	68.07	26.56	54.51	55.65	53.07	54.41	15.70	12.60	12.83	13.71	45.36	51.14	52.21	49.57	19.26	20.87	20.27	20.13	55.23	46.58	98.24	50.90
	Min δZR	9.68	11.33	9.07	10.50	26.66	25.29	22.87	24.94	2.87	4.25	3.93	3.68	22.66	26.50	25.14	24.77	6.99	8.48	6.64	7.37	25.94	23.90	21.61	24.92
	Stder δZR	3.13	2.53	17.76	2.83	5.30	5.34	5.78	5.47	2.54	1.62	1.56	1.91	4.67	5.30	6.10	5.36	2.43	2.26	2.45	2.38	5.24	4.91	6.92	5.08
	Mean δZF	-10.50	-10.70	-11.43	-10.60	-26.18	-26.19	-26.21	-26.19	-4.05	-3.88	-2.94	-3.62	-25.23	-26.33	-26.08	-25.88	-7.97	-8.15	-7.85	-7.99	-27.05	-25.05	-25.21	-26.05
	Max δZF	-7.19	-6.37	-6.24	-6.78	-20.97	-20.73	-19.20	-20.30	-1.19	-1.61	-0.80	-1.20	-19.91	-21.00	-20.28	-20.40	-5.01	-5.18	-4.40	-4.87	-20.70	-20.94	-19.13	-20.82
	Min δZF	-17.17	-16.24	-18.45	-16.71	-33.29	-31.73	-36.17	-33.73	-9.34	-7.29	-6.81	-7.82	-31.42	-34.64	-35.60	-33.89	-12.24	-12.50	-11.87	-12.20	-32.23	-33.51	-35.87	-32.87
	Stder δZF	1.81	1.68	2.66	1.74	2.23	2.18	3.05	2.49	1.58	1.14	1.03	1.25	2.47	3.07	3.22	2.92	1.34	1.29	1.42	1.35	2.62	2.42	2.49	2.52
Implement Depth Tillage (mm)	Stder AID	25.97	31.78	24.08	28.87	19.35	16.56	16.81	17.57	27.01	19.78	16.56	21.12	16.98	15.00	19.67	17.22	23.56	24.26	20.25	22.69	13.25	23.02	13.15	18.14
	Stder IID	16.70	28.66	18.31	22.68	41.45	38.50	28.06	36.00	15.68	18.63	23.40	19.24	25.25	17.31	45.71	29.42	19.41	18.88	22.78	20.36	49.42	62.54	44.33	55.98
	Mean AID	231.27	229.67	235.90	230.47	407.13	385.82	375.44	389.46	150.59	145.47	133.44	143.17	376.19	358.38	383.14	372.57	191.08	228.79	179.88	199.92	386.88	410.15	374.87	398.51
	Mean IID	241.57	197.22	212.29	219.40	450.20	407.97	392.27	416.81	161.74	151.34	141.68	151.58	420.30	403.91	408.49	410.90	123.46	179.90	182.14	161.83	424.31	405.74	437.17	415.03
	Max AID	293.29	286.56	277.13	289.92	453.51	425.24	403.70	427.48	240.78	188.27	172.11	200.39	402.35	398.31	421.20	407.29	250.21	273.09	224.62	249.31	421.20	475.06	409.08	448.13
	Min AID	174.81	116.91	176.15	145.86	360.61	349.84	321.57	344.00	100.75	95.37	95.37	97.16	318.87	322.91	328.30	323.36	139.80	165.38	118.26	141.15	356.57	360.61	344.45	358.59
	Max IID	266.81	232.12	243.56	249.46	597.05	525.13	483.39	535.19	187.50	176.64	176.64	180.26	539.28	442.70	525.13	502.37	176.64	266.81	232.12	225.19	553.55	567.93	597.05	560.74
	Min IID	187.50	144.77	176.64	166.13	377.24	351.88	326.99	352.03	113.95	103.91	93.99	103.95	377.24	364.50	326.99	356.24	93.99	144.77	134.38	124.38	364.50	326.99	377.24	345.74
Draught Force (Fx) (kN)	Mean Fx	8.02	8.15	9.14	8.09	36.90	36.54	35.27	36.23	-2.60	-2.79	-4.16	-3.18	33.05	35.92	36.03	35.00	4.51	5.26	4.65	4.81	36.30	24.14	34.64	30.22
	Max Fx	22.99	18.53	20.85	20.76	53.68	54.97	55.28	54.64	8.44	4.50	5.91	6.28	45.85	57.55	53.95	52.45	15.69	17.02	13.79	15.50	51.17	49.20	51.31	50.18
	Min Fx	-0.06	0.57	-0.48	0.25	24.45	25.60	21.61	23.89	-9.72	-8.66	-8.88	-9.09	21.07	23.81	23.99	22.95	-4.04	-2.19	-2.27	-2.83	24.52	25.06	21.22	24.79
	Stder Fx	4.45	3.79	4.58	4.12	5.42	5.53	6.30	5.75	3.08	2.55	1.97	2.54	5.11	6.52	7.19	6.28	3.55	3.18	3.29	3.34	5.59	5.08	5.30	5.33
Vertical Force (Fy) (kN)	Mean Fy	5.87	6.27	12.63	6.07	11.24	10.98	8.04	10.08	4.56	4.30	4.35	4.40	8.71	10.85	10.12	9.89	5.40	5.52	5.26	5.39	9.56	8.87	9.53	9.21
	Max Fy	12.48	10.07	30.73	11.27	24.09	24.80	17.34	22.08	8.54	7.72	7.06	7.77	15.30	19.53	17.59	17.47	8.76	10.08	9.18	9.34	23.71	17.36	62.56	20.53
	Min Fy	0.83	3.44	1.08	2.13	3.33	2.93	1.36	2.54	-1.06	0.55	1.64	0.38	1.32	4.13	1.73	2.39	0.41	1.68	0.48	0.85	2.79	2.67	1.50	2.73
	Stder Fy	1.76	1.36	15.52	1.56	3.63	3.90	3.34	3.62	1.60	1.08	0.96	1.22	2.75	2.60	3.35	2.90	1.46	1.35	1.43	1.41	3.40	3.25	5.25	3.33

KEY

Mean δZR Average change in rear axle ground reaction force (kN)

Max δZR Maximum change in rear axle ground reaction force (kN)

Min δZR Minimum change in rear axle ground reaction force (kN)

Mean δZF Average change in front axle ground reaction force (kN)

Max δZF Maximum change in front axle ground reaction force (kN)

Min δZF Minimum change in front axle ground reaction force (kN)

Stder AID Standard Deviation of actual implement depth

Stder IID Standard Deviation of indicated implement depth

Mean AI Mean actual implement depth (mm)

Mean III Mean indicated implement depth (mm)

Max AII Maximum actual implement depth recorded (mm)

Min AID Minimum actual implement depth recorded (mm)

Max IID Maximum indicated implement depth recorded (mm)

Min IID Minimum indicated implement depth recorded (mm)

Mean Fx Average draught force (kN)

Max Fx Maximum draught force (kN)

Min Fx Minimum draught force (kN)

Stder Fx Standard deviation draught force (kN)

Mean Fy Average vertical force (kN)

Max Fy Maximum vertical force (kN)

Min Fy Minimum vertical force (kN)

Stder Fy Standard deviation vertical force (kN)

Appendix D – Initial field experiment test data

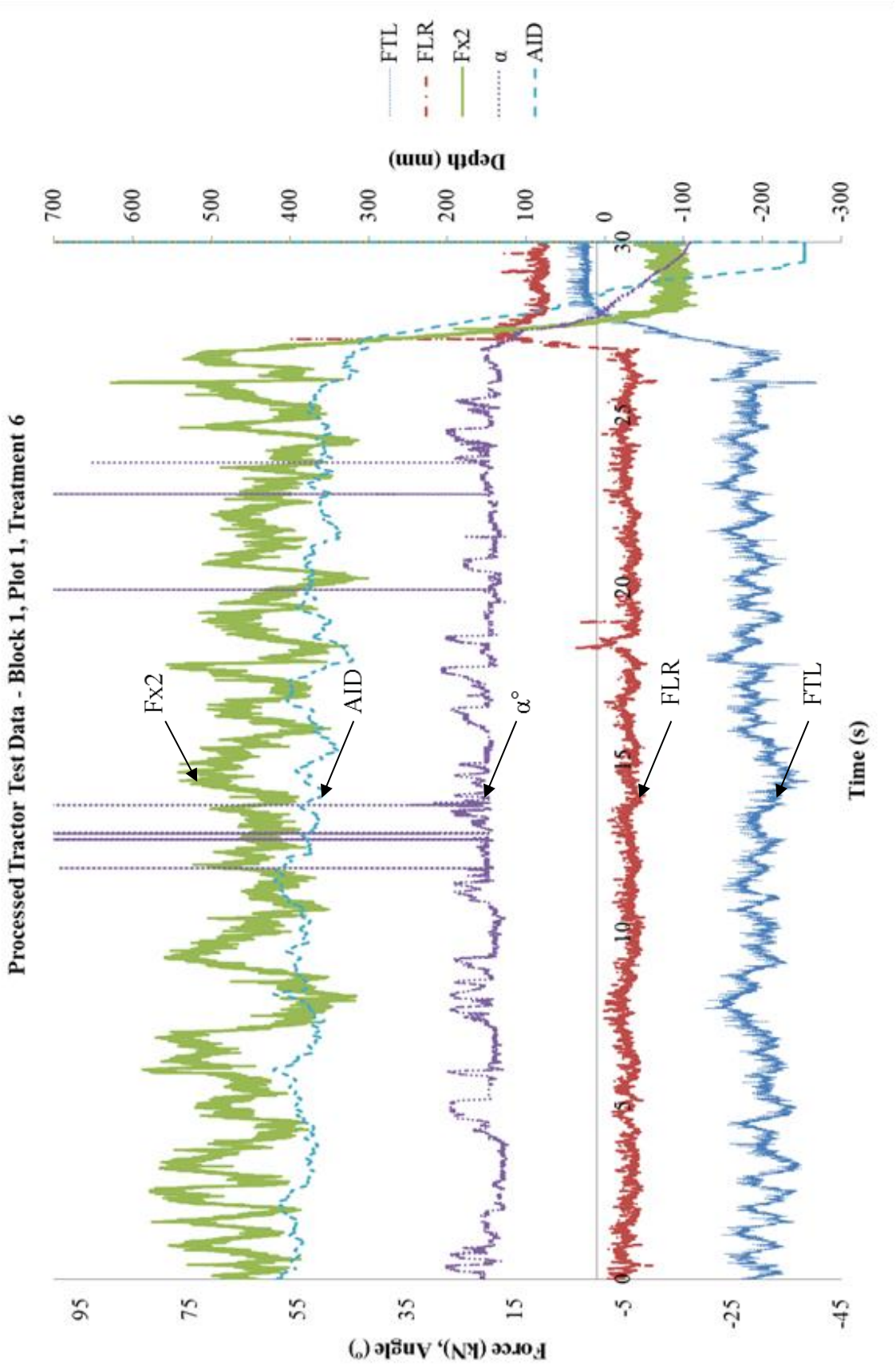

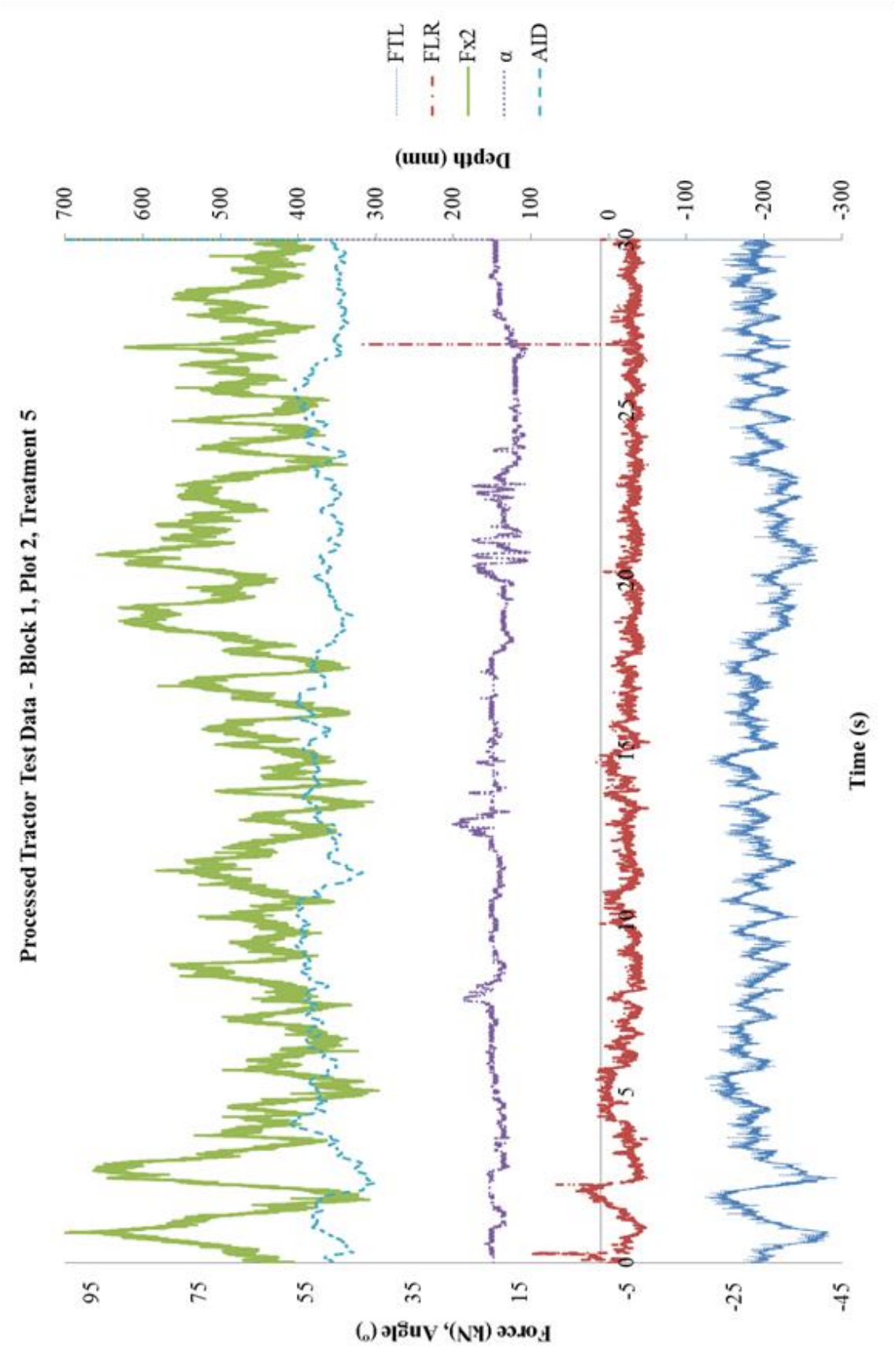
Processed Tractor Test Data - Block 1, Plot 2, Treatment 5
FTL
FLR
Fx2
α
AID
Depth (mm)
700
600
500
400
300
200
100
0
-100
-200
-300
Force (kN), Angle (°)
95
75
55
35
15
-5
-25
-45
Time (s)
0
5
10
15
20
25
30

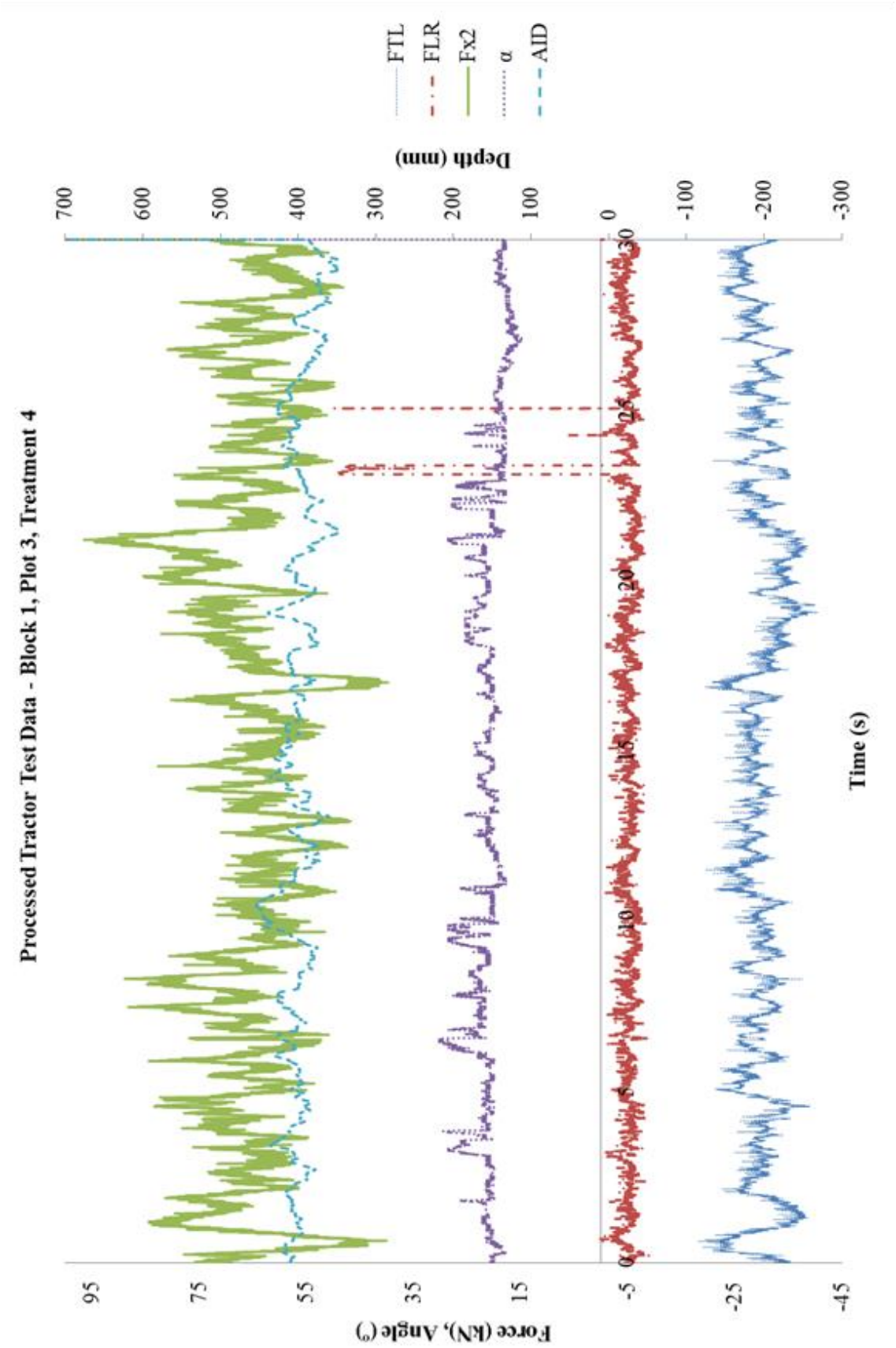
Processed Tractor Test Data - Block 1, Plot 3, Treatment 4
FTL
FLR
Fx2
α
AID
Depth (mm)
700
600
500
400
300
200
100
0
-100
-200
-300
95
75
55
35
15
-5
-25
-45
Force (kN), Angle (°)
0
5
10
15
20
25
30
Time (s)

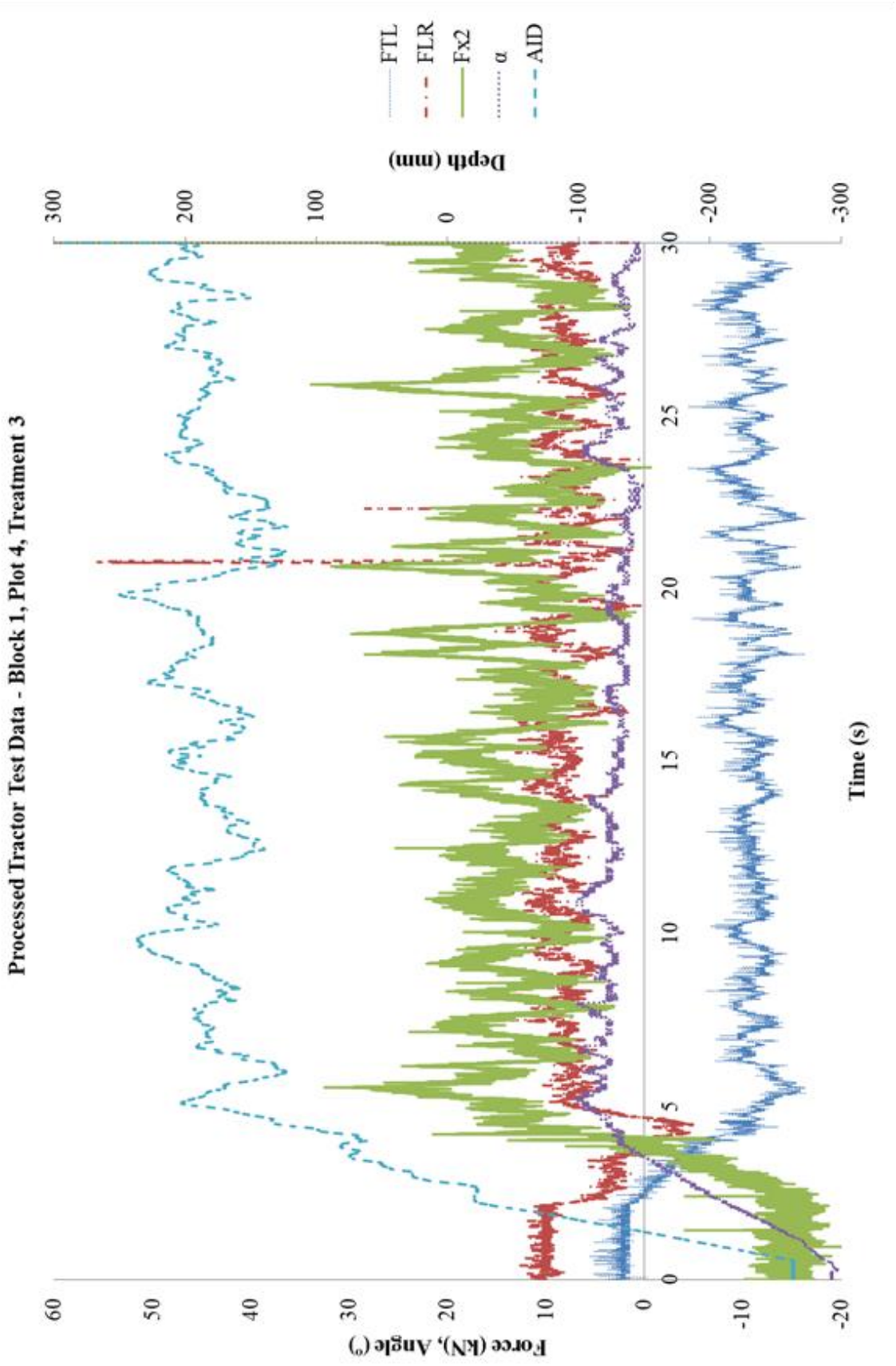
Processed Tractor Test Data - Block 1, Plot 4, Treatment 3
FTL
FLR
Fx2
α
AID
Depth (mm)
300
200
100
0
-100
-200
-300
Force (kN), Angle (°)
60
50
40
30
20
10
0
-10
-20
Time (s)
0
5
10
15
20
25
30

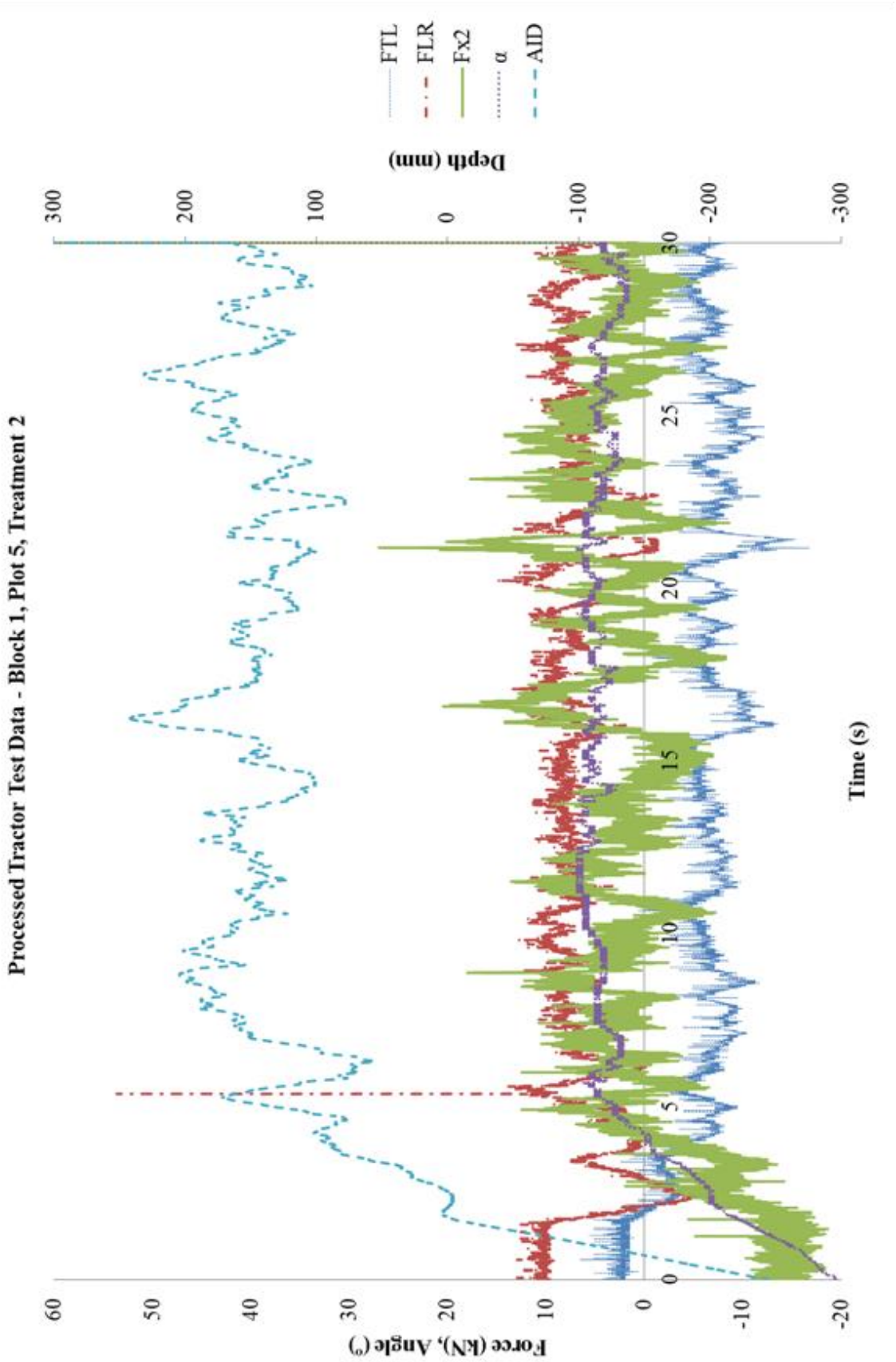
Processed Tractor Test Data - Block 1, Plot 5, Treatment 2
FTL
FLR
Fx2
α
AID
Depth (mm)
300
200
100
0
-100
-200
-300
Force (kN), Angle (°)
60
50
40
30
20
10
0
-10
-20
Time (s)
0
5
10
15
20
25
30

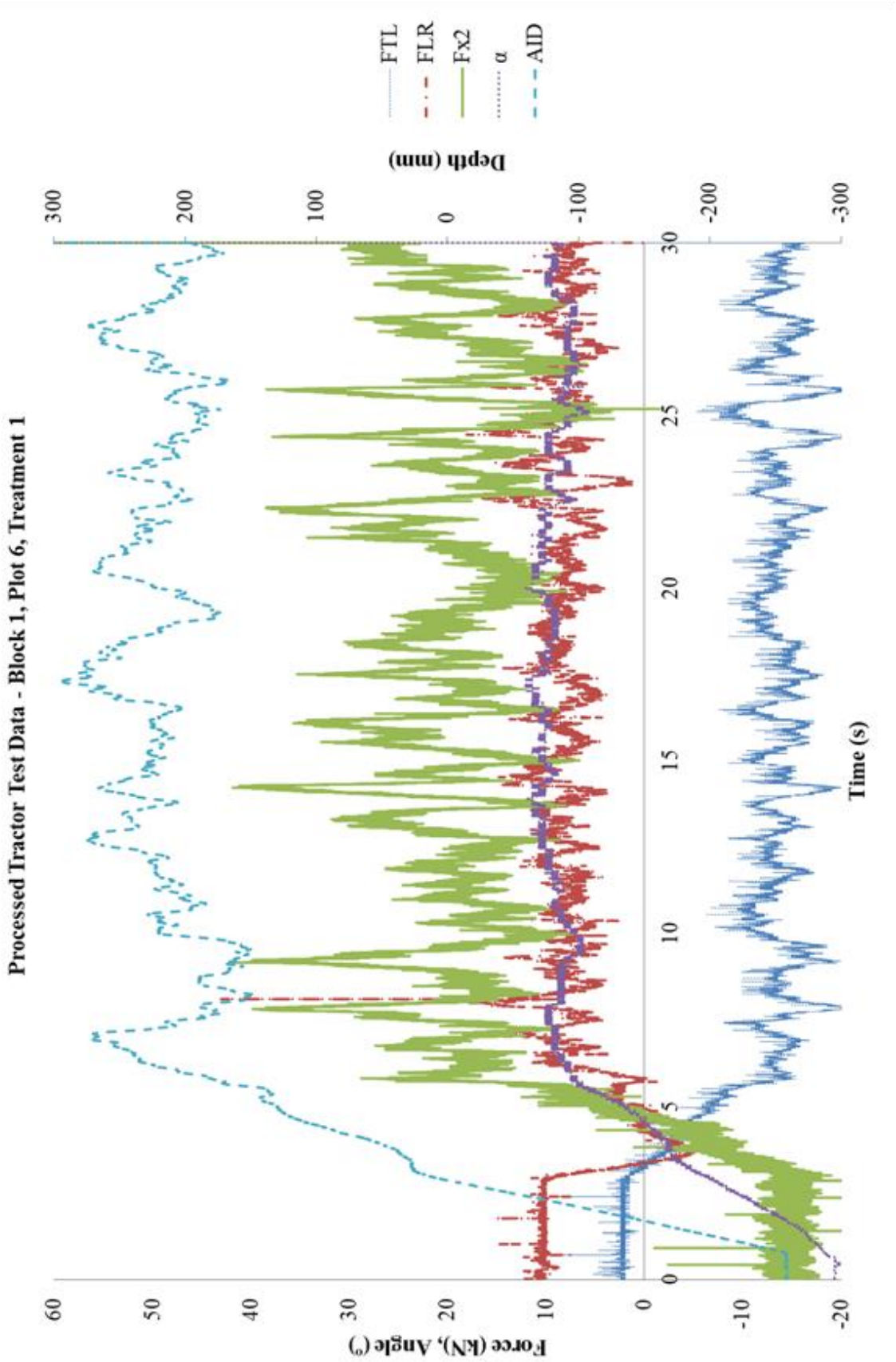
Processed Tractor Test Data - Block 1, Plot 6, Treatment 1
FTL
FLR
Fx2
α
AID
Depth (mm)
300
200
100
0
-100
-200
-300
Force (kN), Angle (°)
60
50
40
30
20
10
0
-10
-20
Time (s)
0
5
10
15
20
25
30

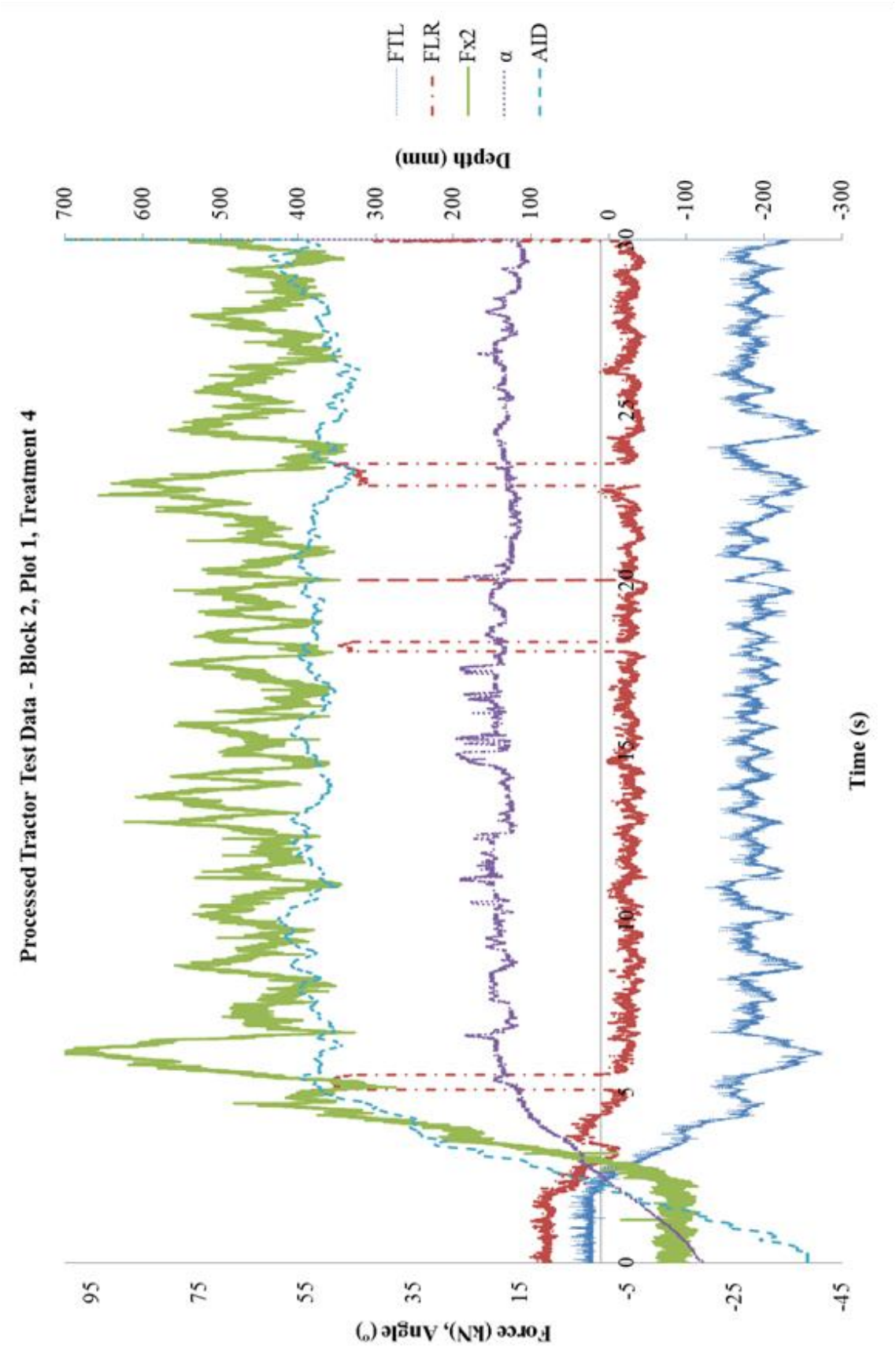
Processed Tractor Test Data - Block 2, Plot 1, Treatment 4
FTL
FLR
Fx2
α
AID
Depth (mm)
700
600
500
400
300
200
100
0
-100
-200
-300
Force (kN), Angle (°)
95
75
55
35
15
-5
-25
-45
0
5
10
15
20
25
30
Time (s)

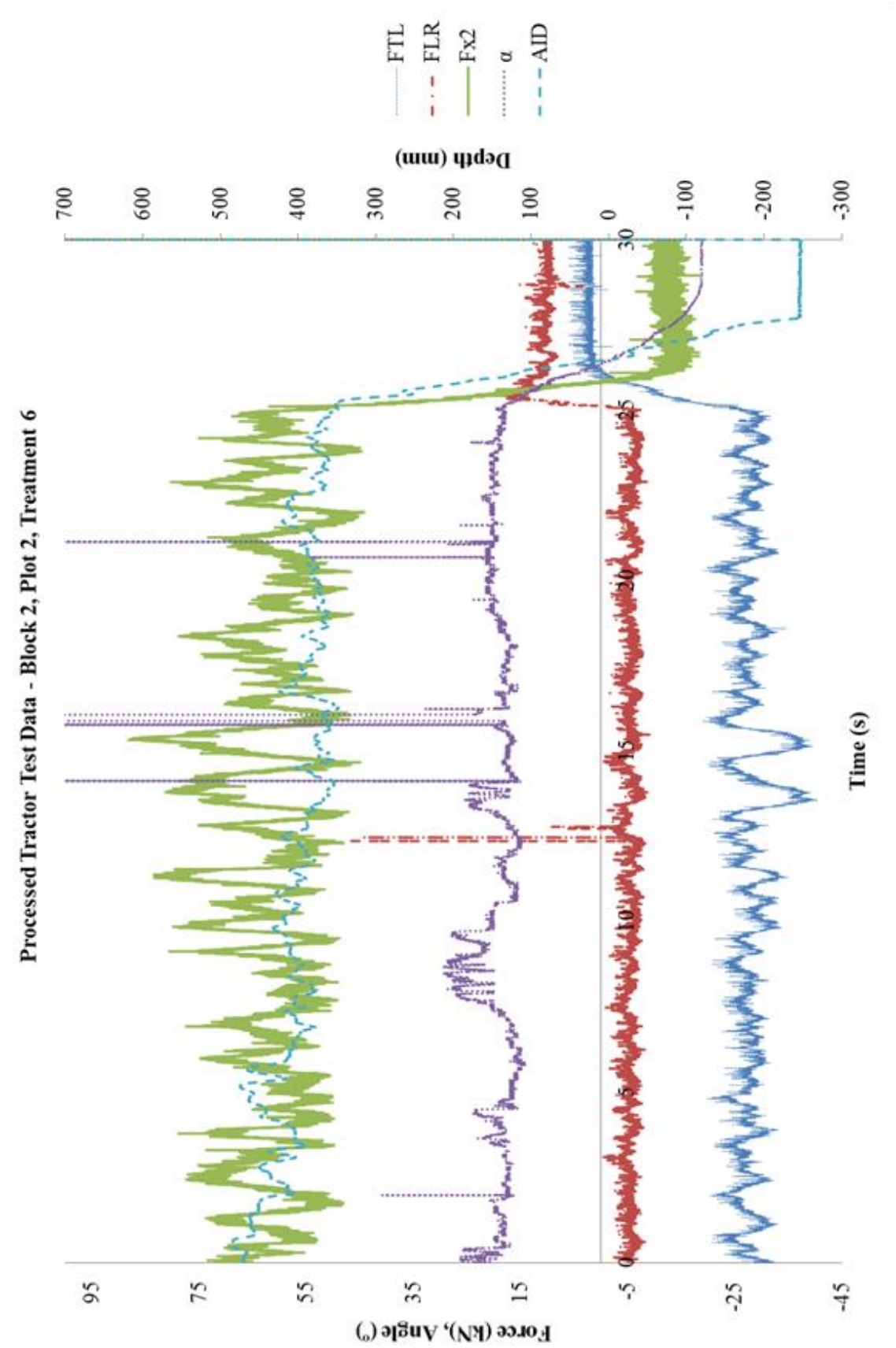
Processed Tractor Test Data - Block 2, Plot 2, Treatment 6
FTL
FLR
Fx2
α
AID
Depth (mm)
700
600
500
400
300
200
100
0
-100
-200
-300
Force (kN), Angle (°)
95
75
55
35
15
-5
-25
-45
Time (s)
0
5
10
15
20
25
30

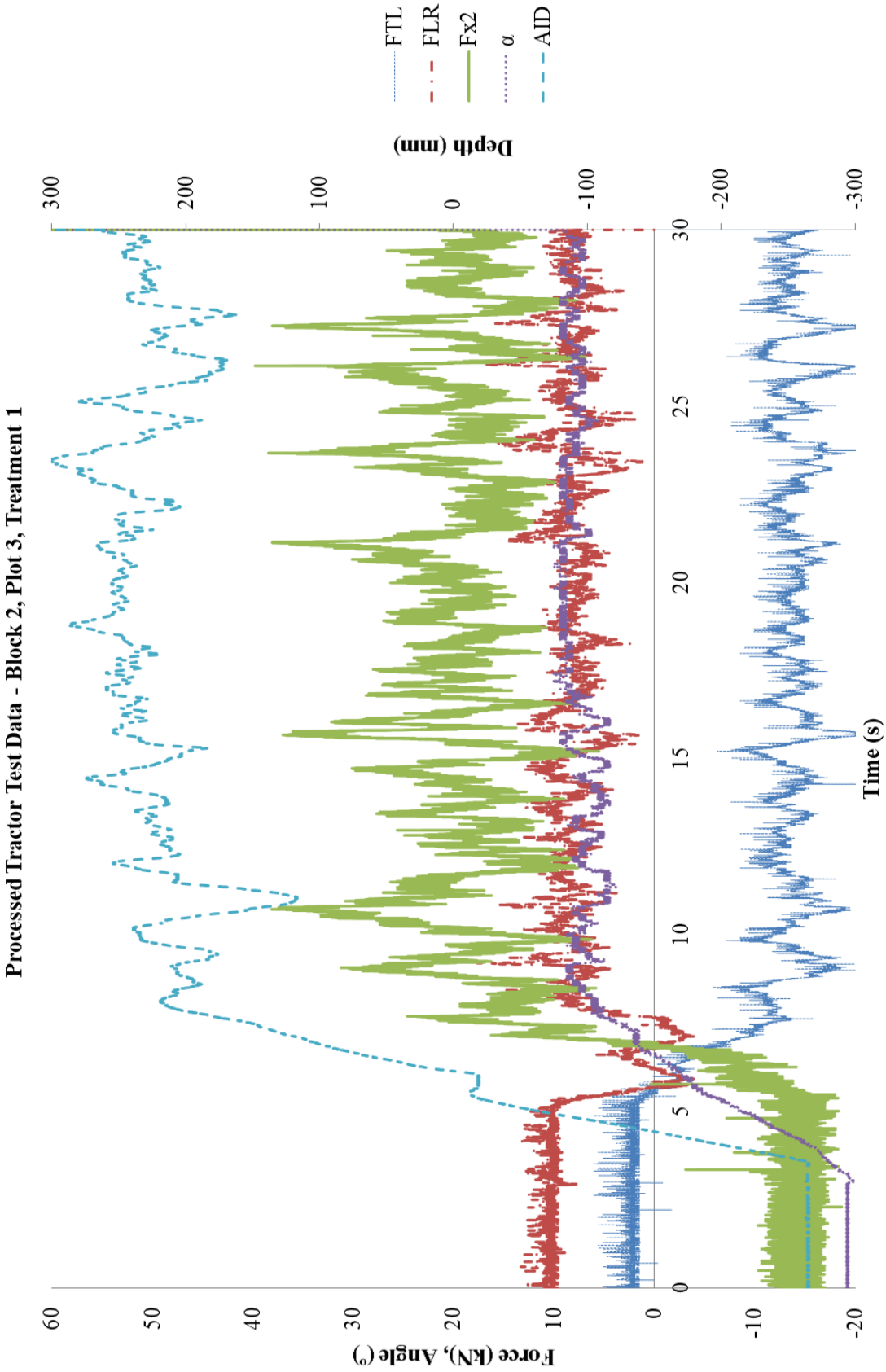
Processed Tractor Test Data - Block 2, Plot 3, Treatment 1
Force (kN), Angle (°)
Depth (mm)
Time (s)
FTL
FLR
Fx2
α
AID
60
50
40
30
20
10
0
-10
-20
300
200
100
0
-100
-200
-300
0
5
10
15
20
25
30

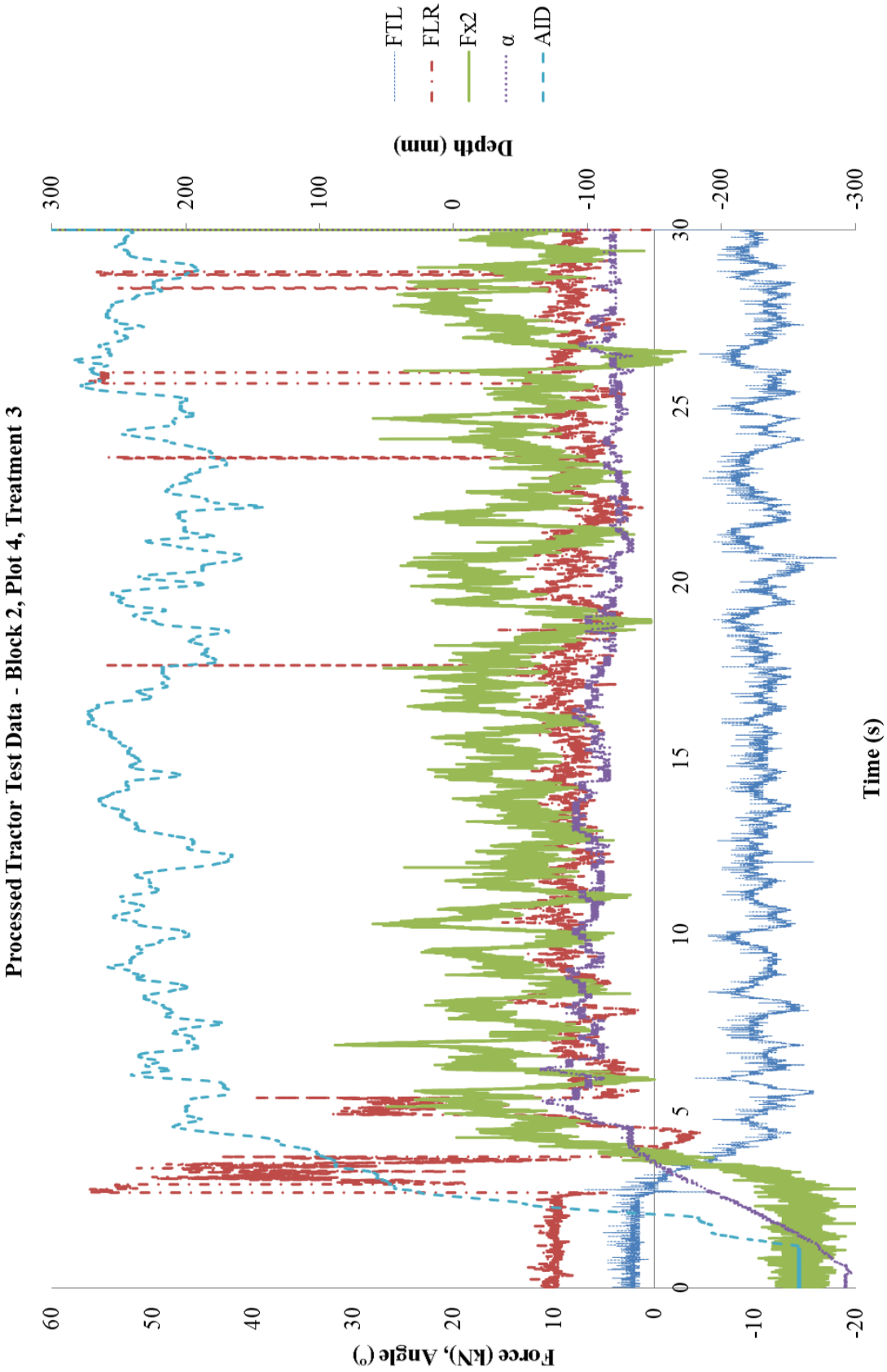
Processed Tractor Test Data - Block 2, Plot 4, Treatment 3
Force (kN), Angle (°)
Depth (mm)
Time (s)
FTL
FLR
Fx2
α
AID
60
50
40
30
20
10
0
-10
-20
300
200
100
0
-100
-200
-300
0
5
10
15
20
25
30

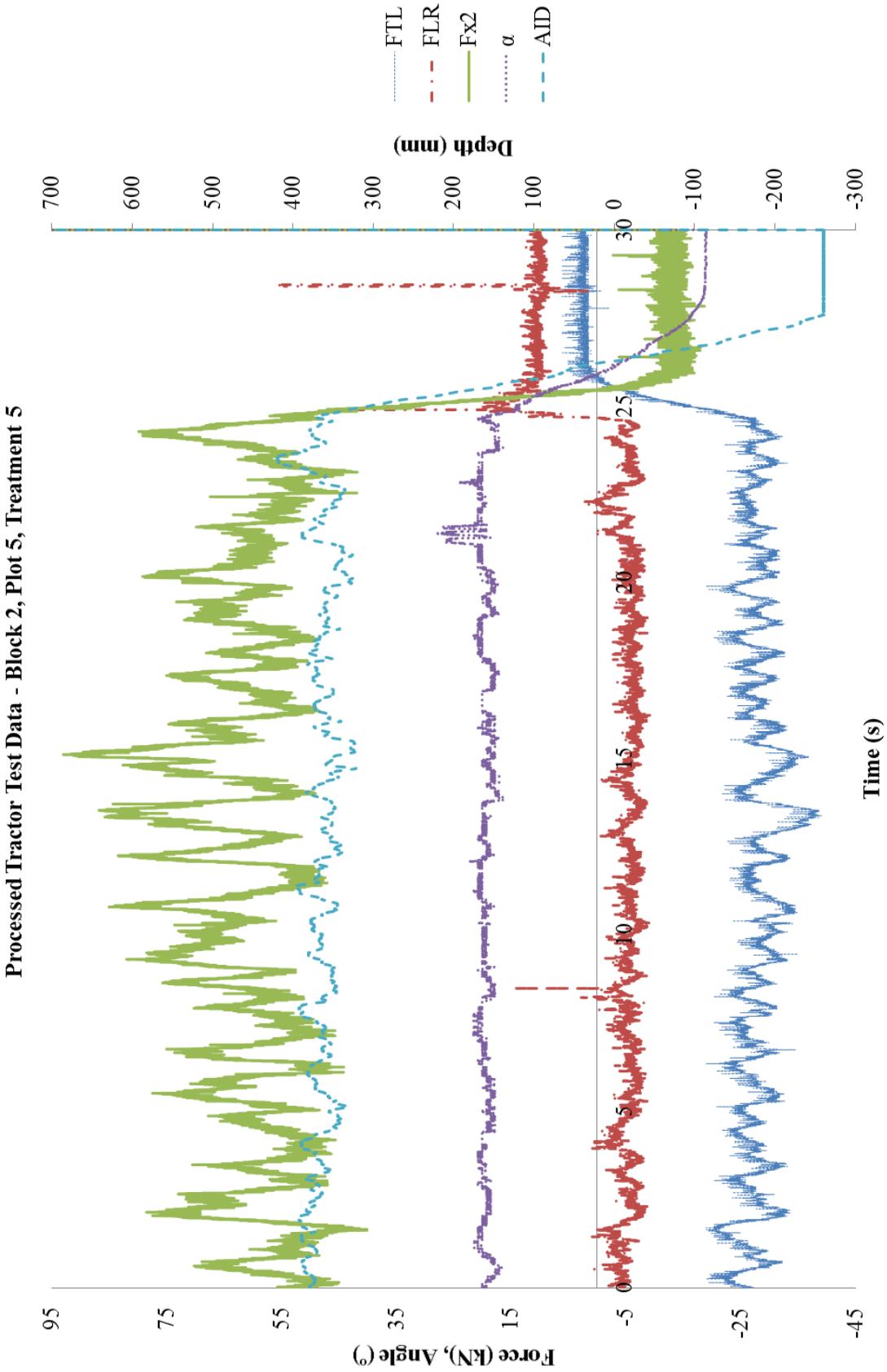
Processed Tractor Test Data - Block 2, Plot 5, Treatment 5
FTL
FLR
Fx2
α
AID
Depth (mm)
700
600
500
400
300
200
100
0
-100
-200
-300
Force (kN), Angle (°)
95
75
55
35
15
-5
-25
-45
0
5
10
15
20
25
30
Time (s)

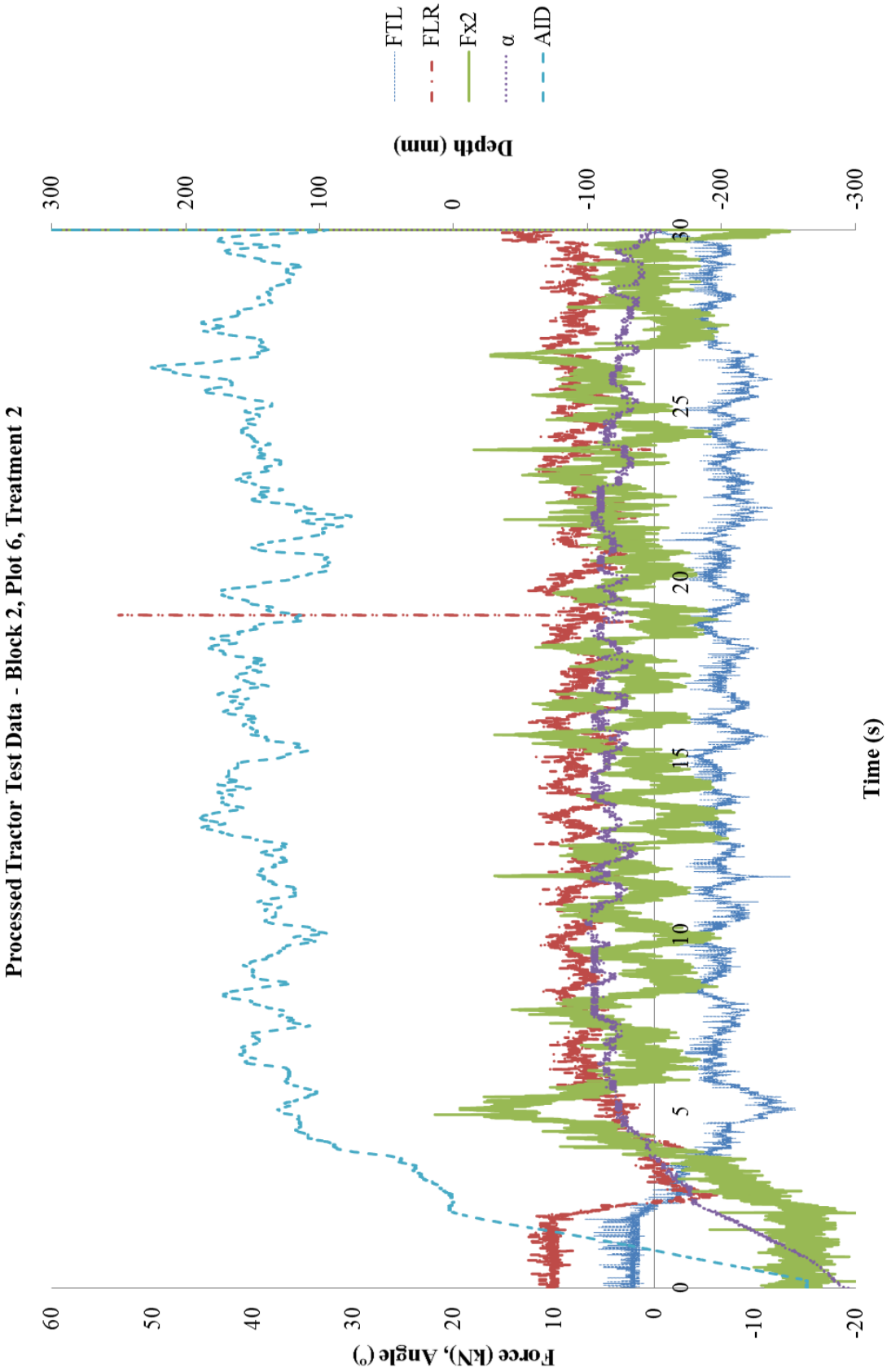
Processed Tractor Test Data - Block 2, Plot 6, Treatment 2
Force (kN), Angle (°)
Depth (mm)
Time (s)
FTL
FLR
Fx2
α
AID
60
50
40
30
20
10
0
-10
-20
300
200
100
0
-100
-200
-300
0
5
10
15
20
25
30

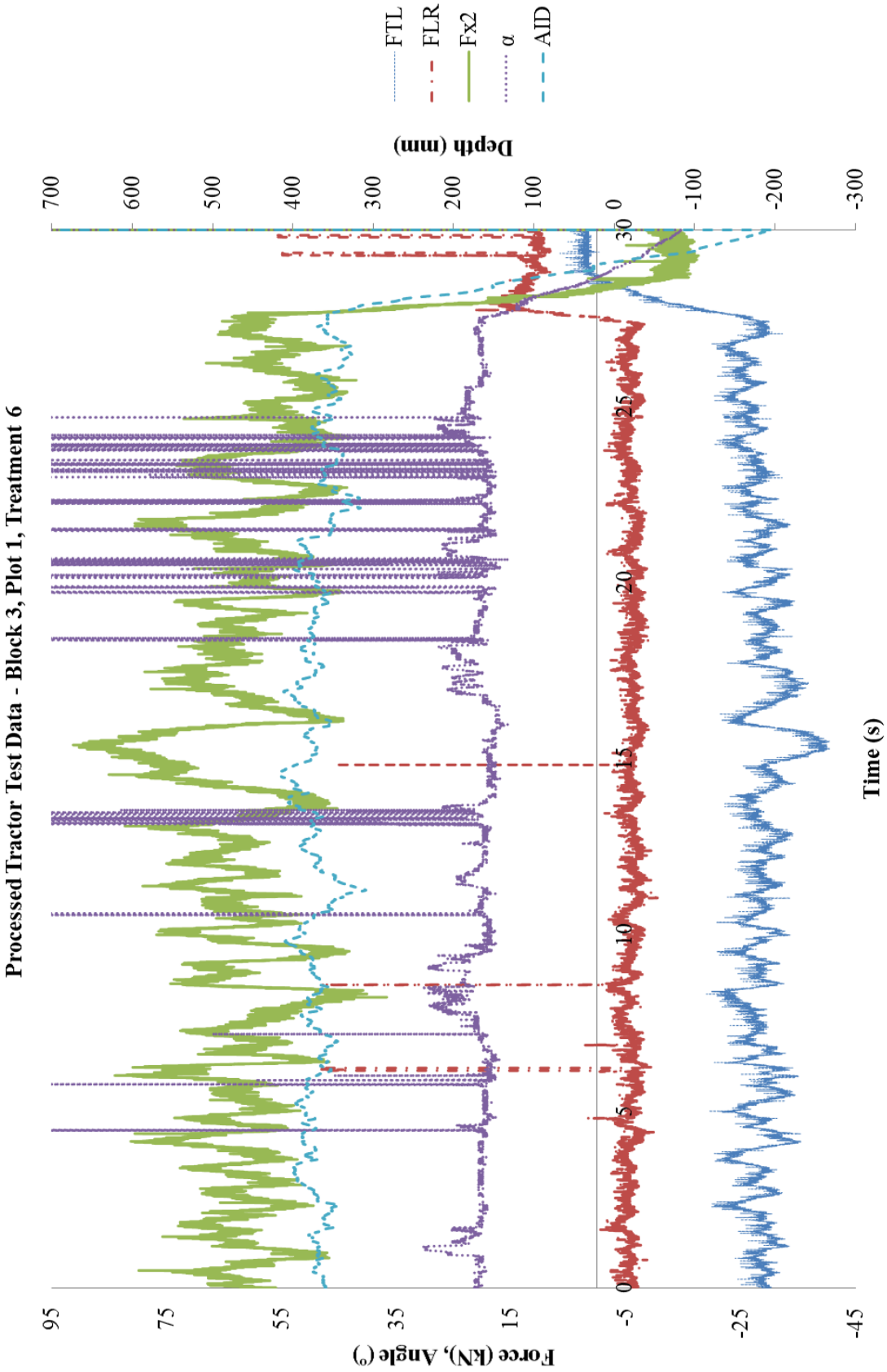
Processed Tractor Test Data - Block 3, Plot 1, Treatment 6
FTL
FLR
Fx2
α
AID
Depth (mm)
700
600
500
400
300
200
100
0
-100
-200
-300
Force (kN), Angle (°)
95
75
55
35
15
-5
-25
-45
0
5
10
15
20
25
30
Time (s)

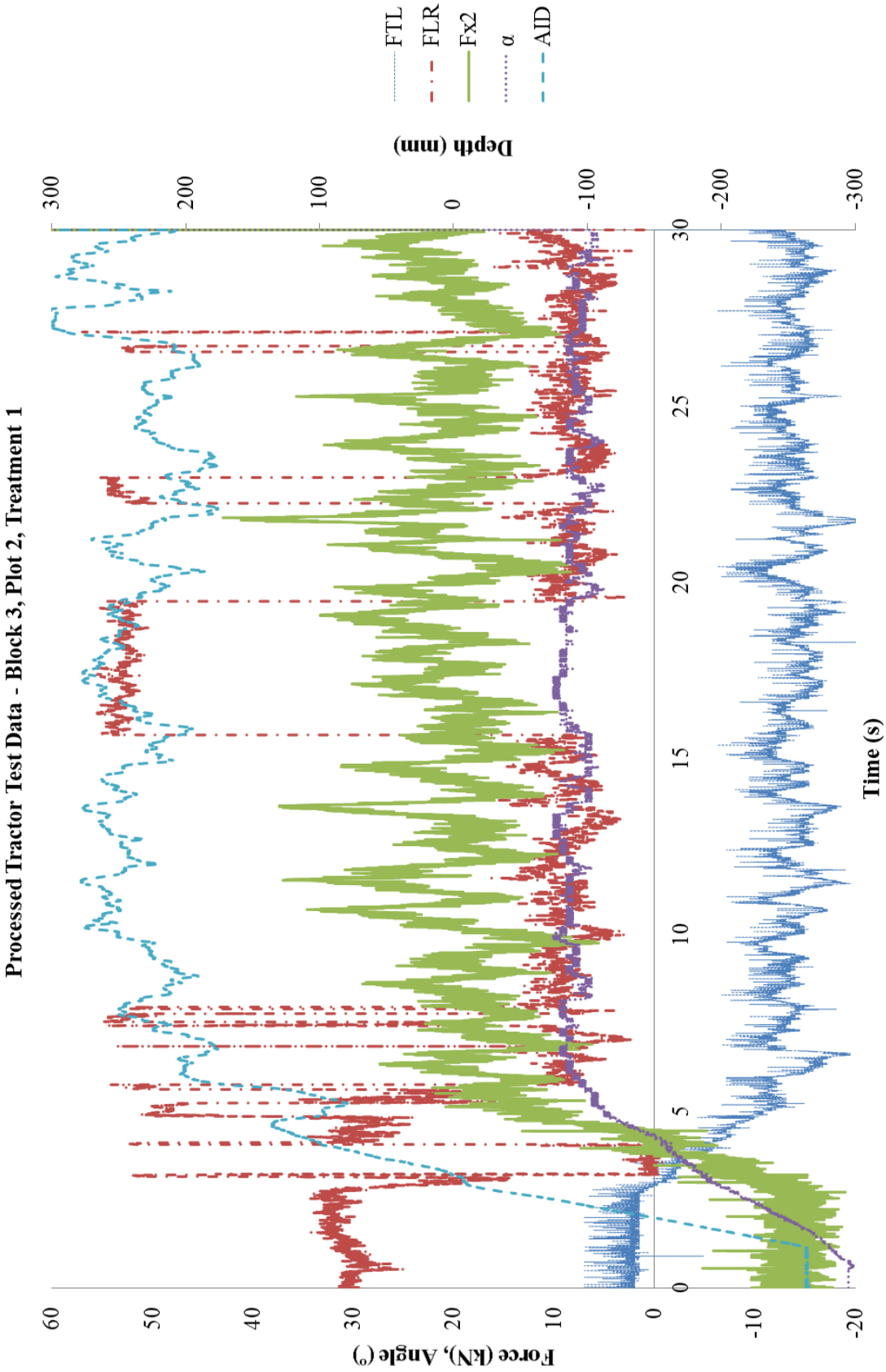
Processed Tractor Test Data - Block 3, Plot 2, Treatment 1
Force (kN), Angle (°)
Depth (mm)
Time (s)
FTL
FLR
Fx2
α
AID
60
50
40
30
20
10
0
-10
-20
300
200
100
0
-100
-200
-300
0
5
10
15
20
25
30

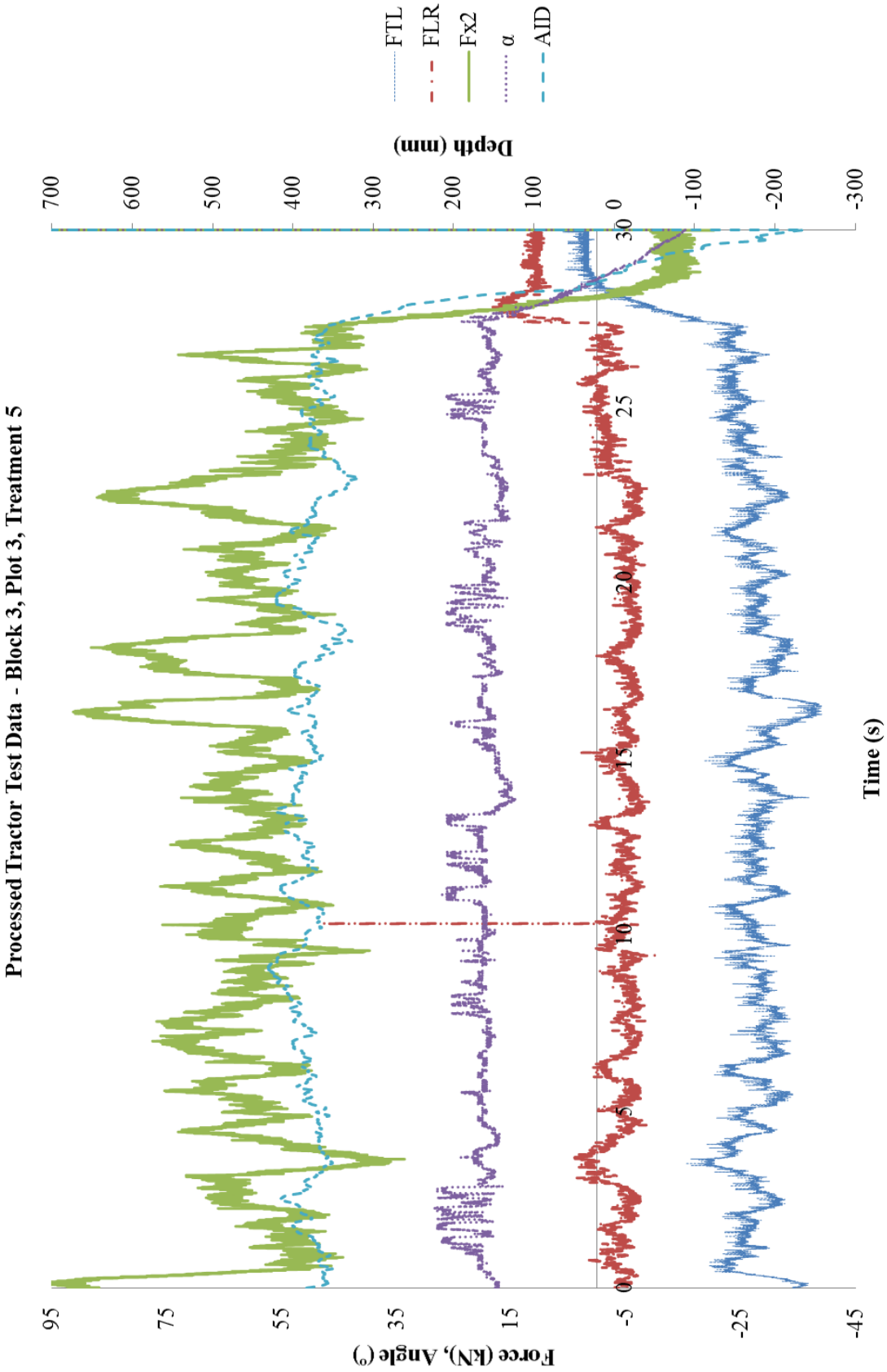
Processed Tractor Test Data - Block 3, Plot 3, Treatment 5
Force (kN), Angle (°)
95
75
55
35
15
-5
-25
-45
Depth (mm)
700
600
500
400
300
200
100
0
-100
-200
-300
Time (s)
0
5
10
15
20
25
30
FTL
FLR
Fx2
α
AID

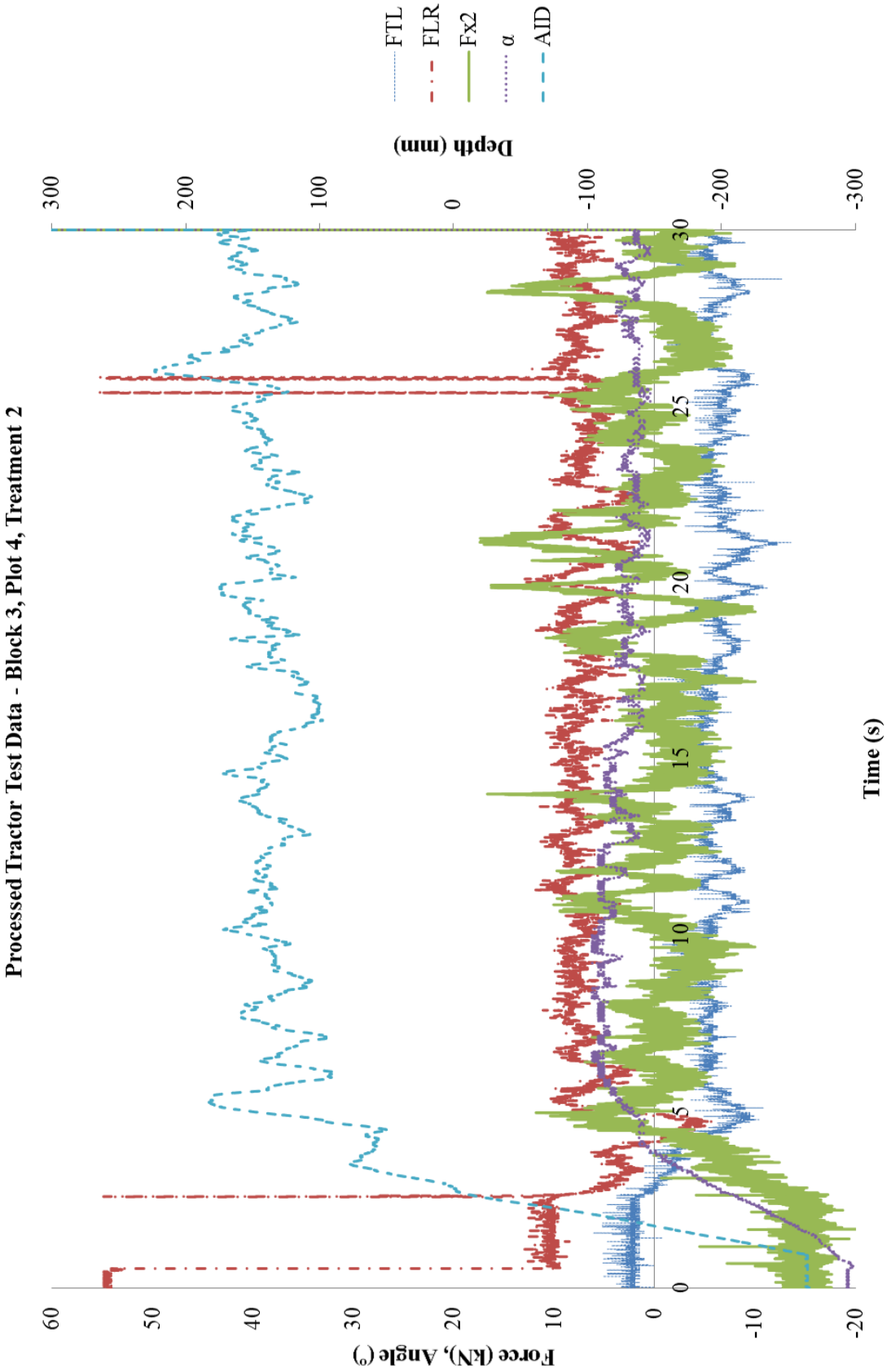
Processed Tractor Test Data - Block 3, Plot 4, Treatment 2
FTL
FLR
Fx2
α
AID
Depth (mm)
300
200
100
0
-100
-200
-300
Force (kN), Angle (°)
60
50
40
30
20
10
0
-10
-20
0
5
10
15
20
25
30
Time (s)

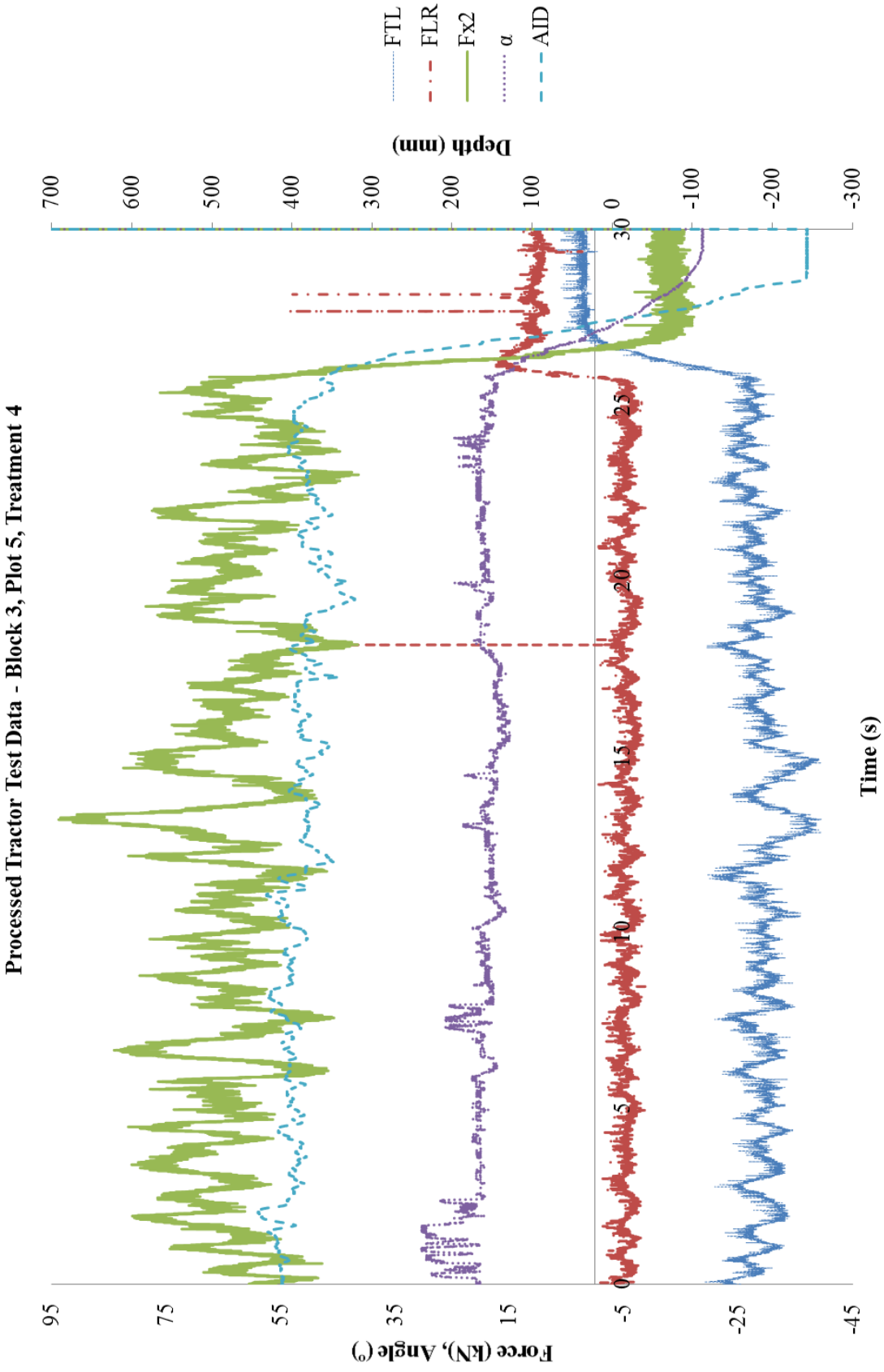
Processed Tractor Test Data - Block 3, Plot 5, Treatment 4
FTL
FLR
Fx2
α
AID
Depth (mm)
700
600
500
400
300
200
100
0
-100
-200
-300
Force (kN), Angle (°)
95
75
55
35
15
-5
-25
-45
0
5
10
15
20
25
30
Time (s)

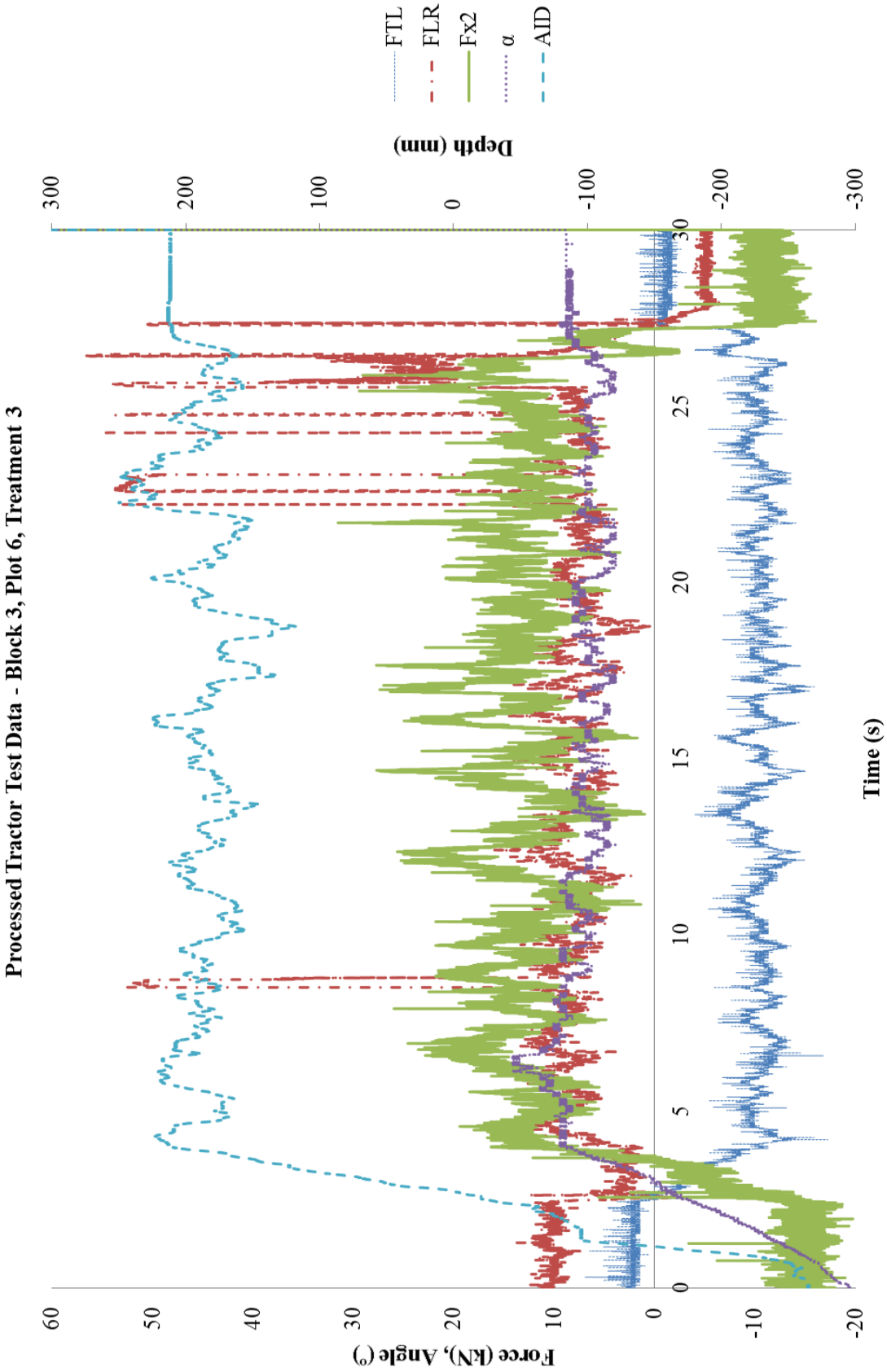
Processed Tractor Test Data - Block 3, Plot 6, Treatment 3
Force (kN), Angle (°)
Depth (mm)
Time (s)
FTL
FLR
Fx2
α
AID
60
50
40
30
20
10
0
-10
-20
300
200
100
0
-100
-200
-300
0
5
10
15
20
25
30

Appendix E - Three point linkage control response experiment data worksheet

Massey Ferguson 8480 Data Processing Sheet Linkage Response

Import Data

$A := READPRN("G:\Linkage Response Tests\Linkage Response 10 3 11\Raw Data\Depth 4\2Step\Test 22.lvm")$

$n := rows(A)$ $\quad n = 3.751 \times 10^3$

$i := 0..(n-1)$

$X_i := i$

Define Channels

Y1 LLAA
Y2 AID
Y3 RLPO
Y4 RLPS
Y5 LLPO
Y6 LLPS

Manipulate Data Using Calibrations and Data Logger Error

$$LLAA := \overrightarrow{\left[\left[\left(A^{\langle 1\rangle} \cdot A^{\langle 1\rangle}\right) \cdot 32.66445908\right] - \left(A^{\langle 1\rangle} \cdot 169.0981867\right) + 197.08859426\right]}$$

$$IID := \overrightarrow{\left[\left[\left(A^{\langle 1\rangle} \cdot A^{\langle 1\rangle}\right) \cdot 566.15795133\right] - \left(A^{\langle 1\rangle} \cdot 2942.2223179\right) + 3502.65246164\right]}$$

$$AID := \overrightarrow{\left[\left(A^{\langle 2\rangle} \cdot A^{\langle 2\rangle}\right) \cdot 0.93809122 + \left(A^{\langle 2\rangle} \cdot 136.52580439\right) + 694.69737144\right]}$$

$$\alpha := \overrightarrow{\left[\left(A^{\langle 2\rangle} \cdot A^{\langle 2\rangle}\right) \cdot 0.02544864 + \left(A^{\langle 2\rangle} \cdot 7.56036554\right) + 35.44775942\right]}$$

$$RLP := \frac{\overrightarrow{4.95 - A^{\langle 3\rangle}}}{0.0275} \qquad LLP := \frac{\overrightarrow{4.95 - A^{\langle 5\rangle}}}{0.0275}$$

$$Fx := \overrightarrow{(RLP + LLP)}$$

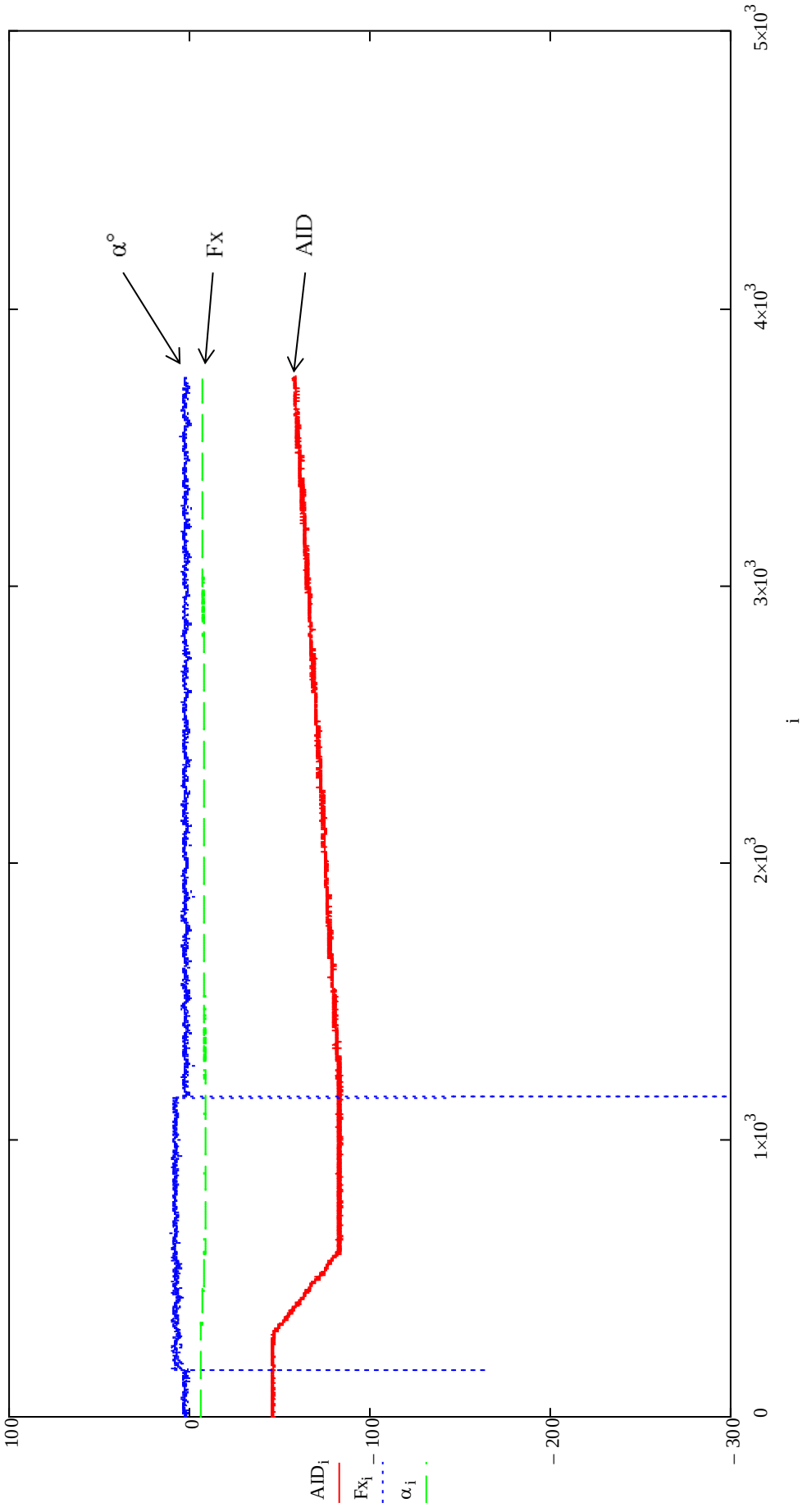
α°
Fx
AID
100
0
− 100
− 200
− 300
0
1×10^3
2×10^3
3×10^3
4×10^3
5×10^3
i
AID_i
Fx_i
α_i

Response Period

Define lift response period (Point 1 = Load Applied, Point 2 =Linkage Moves

$Point1 := 176$

$Point2 := 297$

$nn := Point2 - Point1$

$LiftResponse := \frac{nn}{250}$

$LiftResponse = 0.484$

Define Load Point and Load (Point 3 = End Point of Step load)

$Point3 := 1151$

$zz := 0.. Point3 - Point1$

$LoadRange_{zz} := Fx_{(zz + Point1)}$

$MeanLoad := mean(LoadRange)$

$MeanLoad = 7.658$

Define lower response period (Point 4 = Point load Removed, Point 5 = Linkage Moves Again)

$Point5 := 1248$

$pp := Point5 - Point3$

$LowerResponse := \frac{pp}{250}$

$LowerResponse = 0.388$

Linkage/Implement Movement

Define more points (Point 6 = AID At Linkage Movement Up, Point 7 = AID Motion Stopped, Point 8 = AID Motion Started, Point 9 = Point Linkage Stops again)

$Point7 := 596$

$Point9 := 374$

$AIDStart := AID_{Point2}$

$AIDStart = -46.457$

$AID_{Point7} = -83.629$

$AID_{Point5} = -83.629$

$AID_{Point9} = -58.011$

$qq := Point7 - Point2 \qquad LiftTime := \frac{qq}{250}$

$AIDMovedStep := AID_{Point7} - AID_{Point2}$

$AIDMovedStep = -37.172$

$AIDMovedAfterStep := AID_{Point5} - AID_{Point9}$

$AIDMovedAfterStep = -25.619$

$AIDFinish := AID_{Point9}$

$AIDFinish = -58.011$

$rr := Point9 - Point5 \qquad LowerTime := \frac{rr}{250}$

$AIDLiftSpeed := \frac{AIDMovedStep}{LiftTime}$

$AIDLiftSpeed = -31.081$

$AIDLowerSpeed := \frac{AIDMovedAfterStep}{LowerTime}$

$AIDLowerSpeed = -2.567$

Angular Movement

$AngleStart := \alpha_{Point2}$

$AngleMovedStep := \alpha_{Point7} - \alpha_{Point2}$

$AngleMovedStep = -2.149$

$AngleMovedAfterStep := \alpha_{Point5} - \alpha_{Point9}$

$AngleMovedAfterStep = -1.482$

$AngleFinish := \alpha_{Point9}$

$AngleFinish = -7.108$

$$AngleLiftSpeed := \frac{AngleMovedStep}{LiftTime}$$

$AngleLiftSpeed = -1.797$

$$AngleLowerSpeed := \frac{AngleMovedAfterStep}{LowerTime}$$

$AngleLowerSpeed = -0.148$

Output Data

$LiftResponse = 0.484$

$LowerResponse = 0.388$

$MeanLoad = 7.658$

$AIDStart = -46.457$

$AngleStart = -6.44$

$AIDMovedStep = -37.172$

$AngleMovedStep = -2.149$

$AIDLiftSpeed = -31.081$

$AngleLiftSpeed = -1.797$

$AIDFinish = -58.011$

$AngleFinish = -7.108$

$AIDMovedAfterStep = -25.619$

$AngleMovedAfterStep = -1.482$

$AIDLowerSpeed = -2.567$

$AngleLowerSpeed = -0.148$

Appendix F – Screen capture of the control algorithm